LOCALISATION OF UNDERWATER SENSOR NODES IN CONFINED SPACES

A thesis submitted to The University of Manchester for the degree of

Doctor of Philosophy

in the Faculty of Engineering and Physical Sciences

2012

MARK GERARD POTTINGER

SCHOOL OF ELECTRICAL AND ELECTRONIC ENGINEERING

Table of Contents

Main text word count including footnotes and endnotes 78310

List of Tables

List of Figures

List of Abbreviations

AASN4IP	Actuated Acoustic Sensor Networks for Industrial Processes
APA	Active Phased Array
APOS	Accurate Positioning Algorithm
AUV	Autonomous Underwater Vehicle
BER	Bit Error Rate
BPSK	Binary Phase Shift Keying
CVL	Correlation Velocity Log
DAQ	Data Acquisition Card
EIT	Electrical Impedance Tomography
FCC	Fluid Catalyst Cracking
FFVS	Free Field Voltage Sensitivity
FPGA	Field Programmable Gate Array
GOSP	Gas Oil Separation Plant
GPS	Global Positioning System
LOS	Line Of Sight
LPS	Local Positioning System
LWA	Light Weight Aggregate
MEMS	Micro Electro Mechanical Systems
MEO	Medium Earth Orbit
MRI	Magnetic Resonance Imaging
MSPS	Million Samples per Second
NBFF	Neutrally Buoyant Flow Follower
OOK	On-Off Keying
PVDF	Polyvinylidene Fluoride
RDOA	Range Difference of Arrival
RF	Radio Frequency
RMSE	Root Mean Square Error
RTT	Round Trip Time
TDOA	Time Difference of Arrival
TOF	Time of Flight
UWB	Ultra Wide Band
UWSN	Underwater Wireless Sensor Networks
WSN	Wireless Sensor Networks

Abstract

The aim of the project is to explore 3D localisation of a sensor “pill”, contained in an enclosed vessel, using multiple acoustic transducers mounted on the pill’s surface. The thesis suggests strategies for placement, excitation and synchronisation of the transmitters on the pill and receivers on the vessel wall to deliver 3D localisation.

Motivation for the project has emerged from the desire to develop wireless sensor networks to monitor the internals of industrial processes. A major challenge relates to the ability to accurately determine the location of the pill within the vessel, in the presence of multipath reflections.

The main challenges relate to the determination of suitable transmission methodologies and synchronisation strategies to allow accurate localisation. The pill has to be a finite size in order to contain the required sensor hardware and transducers must be mounted on the surface of the pill such that signals are able to propagate directly to receivers on the vessel wall. This presents challenges in optimising the transmitter and receiver layout to maximise signal strength and also to determine how the separation of multiple transmitters on the pill impacts localisation accuracy.

Time-Difference-of-Arrival (TDOA) has been investigated as a localisation technique, with simulations revealing that the separation of transmitters on the pill influences the accuracy. By modifying the standard TDOA equations with offset knowledge it has been demonstrated, in simulation, that this error can be reduced and by uniquely coding transmitters it is possible to resolve rotation of the pill in the vessel allowing further reduction in localisation error. Simulations have investigated how the location of receivers on the vessel wall influences the localisation error when the TDOA values are compromised by noise. It has been demonstrated that by mounting receivers at the extremities of the vessel the localisation error of the pill can be reduced.

Work has also been undertaken to characterise both the vessel reflection properties and also the transmitter beam profile to allow a suitable transmitter layout on the pill to be determined. Simulations, supported by experimental results, have shown that a curved vessel surface can focus the reflected signals and therefore compromise peak detection signal methodologies. As a result amplitude thresholding is suggested for detecting received signals.

The research is substantiated with a simple demonstrator that suggests, for both Time-of-Flight (TOF) and Time-Difference-of-Arrival techniques, that the location of the pill can be determined with an accuracy of ± 5 cm throughout a 250 litre vessel.

This is the first time that underwater localisation in a confined space using multiple transmitters on the surface of a sensor “pill” has been reported.

Declaration

No portion of the work referred to in the thesis has been submitted in support of an application for another degree or qualification of this or any other university or other institute of learning.

Copyright Statement

i. The author of this thesis (including any appendices and/or schedules to this thesis) owns certain copyright or related rights in it (the "Copyright") and s/he has given The University of Manchester certain rights to use such Copyright, including for administrative purposes.

ii. Copies of this thesis, either in full or in extracts and whether in hard or electronic copy, may be made **only** in accordance with the Copyright, Designs and Patents Act 1988 (as amended) and regulations issued under it or, where appropriate, in accordance with licensing agreements which the University has from time to time. This page must form part of any such copies made.

iii. The ownership of certain Copyright, patents, designs, trade marks and other intellectual property (the "Intellectual Property") and any reproductions of copyright works in the thesis, for example graphs and tables ("Reproductions"), which may be described in this thesis, may not be owned by the author and may be owned by third parties. Such Intellectual Property and Reproductions cannot and must not be made available for use without the prior written permission of the owner(s) of the relevant Intellectual Property and/or Reproductions.

iv. Further information on the conditions under which disclosure, publication and commercialisation of this thesis, the Copyright and any Intellectual Property and/or Reproductions described in it may take place is available in the University IP Policy (see http://www.campus.manchester.ac.uk/medialibrary/policies/intellectualproperty.pdf), in any relevant Thesis restriction declarations deposited in the University Library, the University Library's regulations (see http://www.manchester.ac.uk/library/aboutus/regulations) and in The University's policy on presentation of Theses.

Acknowledgement

I would like to take this opportunity to express my gratitude to all of the people who have helped me and provided their support and time through my PhD studies.

I would firstly like to thank my supervisor Professor Trevor York for providing me with this opportunity. You have provided me with continual support and wisdom, allowing me the freedom to pursue my research in the method I thought best while still being there to provide a sensible word of advice when required. I cannot thank you enough for the support and commitment that you have shown to me during my studies.

I am grateful to all of the staff both within the Sensing, Imaging and Signal Processing group and further a field who have provided their time to support my work. This includes Dr. Peter N Green, Mr. Peter R Green and Dr John Davidson and Dr. Paul Wright.

I would also like to thank all of the supporting staff in the School of Electrical and Electronic Engineering, in particular Danny in the Mechanical Workshop who has always been able to construct something useful out of my loose ideas and usually at short notice. Can I also thank both Steve in stores and Ms. Marie Davies at the administration office.

I have made many friends during my studies, Dr. Rebecca Robinson, Will Carr, Simon Watson, Dominic Crutchley and Liam Marsh. We had laughs both in and out of University and the friendships that have been formed during my studies have always kept me going even during the hard times, particularly during our insightful Friday lunches. Of all of the people I have met during my time I must offer the biggest thank you to Dr. Renee Chin who has been a cubicle colleague for the duration of my studies. Going through the same process as me you have always had a wise word and some useful research advice. I will miss our discussions on solving the world's problems from our desks but never quite putting them into practice. You have been a constant source of fun and laughs in my life and we shall always remain great friends.

To my parents and brother I cannot offer thanks enough. You have always instilled in me the desire to strive for success in my life and have supported me whatever my decisions. You have been there through both my successes but more importantly in my failures with unwavering support and for that I will be eternally grateful.

I have left the most important thank you to last, that for my fiancée Tracey O'Halloran. Of all the people who have been there for me during my studies you have been the

most important. You have been my constant, dealing with the daily highs and lows that this process brings, understanding to a fault when I have not seen nor spoken to you for days on end, and being a source of continual cups of tea during my writing. I hope that in our future I am able to repay in some small way all of the love and support you have given me.

List of Publications

Pottinger M.P and York T.A 2011 "Modified algorithm for localisation of wireless sensors in confined spaces" *IEEE Topical Conference on Wireless Sensors and Sensor Networks, WiSNet 2011, Phoenix, United states,* pp 29-32

1.0 Introduction

1.1 Aim

The aim of the project has been to explore 3D localisation of a sensor “pill” that is contained in a confined space.

The specification for the pill requires underwater operation, up to several centimetres in size and able to function in an optically opaque medium. Localisation is to be achieved by low cost, low power and small ultrasonic transducers. Transmitters are to be located on the surface of the pill and receivers on the inside wall of the vessel.

The main challenge has been to identify optimum strategies, for placement, excitation and synchronisation of the transducers to deliver 3D localisation. This has been achieved by a combination of modelling and experimentation and the results are substantiated in a simple demonstrator.

1.2 Motivation

This research into wireless sensor pills is motivated by a desire to determine the distribution of materials and optimum operating parameters, such as temperature and pressure, in industrial process vessels. For instance, the oil industry is continually seeking improved methods for determining the proportions of oil, gas, water and sand in a pipeline (Achour, M. et al, 2008). Alternatively, knowledge of the evolution of products during mixing can inform improvements in, for instance, impeller design leading to greater efficiencies in processing. Realisation of sensor pills with the ability to determine their position and to acquire, store and transmit measurements of important parameters has the potential to deliver previously inaccessible mapping of industrial processes.

Typically industrial processing can consist of any or all of 4 distinct actions, mixing, separation, reactions and transport.

Mixing

Mixing problems encountered in industry can take many forms however ‘*In all of these problems, there is global progress from a segregated state toward a more homogeneous state, but the physical phenomena vary widely’* (Aubin, J. et al, 2009).

For different applications substantially different methods of agitation are required. In order to mix most materials correctly it is necessary to maintain movement of the reactants. Viscosity of liquids,

settling rates of solids, corrosive characteristics, and other important physical properties of the mixing process are all key to determining suitable rates of agitation[1]

Mixing applications within industry vary greatly; a typical application is the mixing of concrete. The properties of concrete such as strength, durability or density can vary greatly depending on the ratio of input materials. The frost-resistance of concrete for example can be greatly improved through the addition of Light Weight Aggregate (LWA) in specific quantities, (Zhang, B-S. et al, 2009). The ability to monitor the specific quantities of ingredients during mixing for example can help to provide a reliable and repeatable product.

Separation

The term separation is typically used in the industrial context to describe the ability to retrieve two or more specific products from a mixture. There are many possible forms of separation which depend entirely on the substances to be separated. Typical examples include distillation; the process of separating liquids via different boiling points or sedimentation; the process of separating particulates due to different densities.

One specific common application in industrial processing is the separation of water and crude oil in a pipeline. In general *'Most of the crude is commingled with water and produced in the form of emulsions that are separated at the gas/oil separation plant (GOSP) using demulsifiers'* (Kokal, S. et al, 2008). Through separation the desired product, in this case crude oil, can be obtained from the emulsion.

Reactions

In industrial processing a reaction is the transformation of one or a group of elements to another, possibly through a process of exciting through heat, or the creation of a new product through the combination of two elements.

An example of such a reaction is the contact cracking process used in gasoline production, *'Fluid catalytic cracking (FCC) catalysts are used to produce high-quality petroleum from residual oil by the contact cracking process in the petroleum refinery'* (Zhao, T. et al, 2007). Approximately 45% of worldwide gasoline production is generated through the FCC process and its ancillary units (Chen, Y-M, 2006). The FCC process vaporizes and breaks the long-chain molecules of the high-boiling hydrocarbon liquids into much shorter molecules by mixing the feedstock, at high temperature and moderate pressure, with a fluidised powdered catalyst[2].

[1] http://www.industrialmixer.net/industrial-mixer/13/
[2] http://en.wikipedia.org/wiki/Fluid_catalytic_cracking

Transport

Transport relates to the movement of reactants or products from one area to another. This might typically include the movement of the reactants from storage containers to the reaction chamber. For instance this might be a blast furnace or a mixing vessel containing an impeller. It also includes the transportation of the resulting products away from the reaction chamber in their mixed or combined state.

Multiphase flow in a pipeline is a typical example of such transport. *'Multiphase flow is widely encountered in the petroleum industry. It is expected that a significant part of the future production of oil and gas in offshore will come from deeper water and in many cases from marginal fields. Rigid fixed platform system with production and processing facility located in the same field may not be economical in such cases. Many oil companies are investing heavily to develop multiphase technology, with the ultimate goal to transport unprocessed multiphase well fluid for a long distance'* (Rai, R. et al, 1991). This application exemplifies a situation in which monitoring would allow the design of better systems to control the flow.

1.3 Overview of Monitoring Techniques - Tomography

It is not uncommon for monitoring of industrial processes to comprise only simple single point measurements of, for instance, temperature and pressure. Alternatively samples may be taken, for instance from an oil pipeline, and analysed remotely. These approaches have limited usefulness and techniques are desired for delivering on-line, distributed measurements. Tomography has emerged as an important technique that goes some way to satisfying the requirements (Chin, R et al, 2010). Possible modalities include – X-ray, MRI, ultrasound, microwaves, gamma ray, optical, and electrical (Williams R.A and Beck M.S, 1995). Despite the successes of, for instance, X-ray and MRI in the medical arena, electrical tomography has emerged as a leading contender for industrial process applications primarily due to mobility of equipment and versatility of the measurements (York, T et al, 2011).

Tomography is a method of injecting an energy signal into a vessel and using this to image the contents of the vessel. The technique is typically non-intrusive but can be non-invasive. In general electrode plates are placed around the outside of the vessel and signal is injected into the vessel. In EIT (Electrical Impedance Tomography) for instance electrical current is injected into the vessel, which contains conducting materials, and voltages are measured around the periphery of the vessel on electrode plates. Through knowledge of the interaction of the exciting signal with the materials it is possible to solve the inverse problem to determine the distribution of the contents of the vessel.

Figure 1-1 displays a typical electrical tomogram (Murphy S.C et al, 2008). The tomogram displays two metal and two plastic rods contained in a water solution. The metal rods are the red images in the centre of the vessel while the plastic rods are the blue images at the edge of the vessel. The

image demonstrates some of the main problems with electrical tomography, that of poor resolution and the inclusion of artefacts, as shown by the blue image in the centre of the vessel. For a single object which has a substantially different material composition to the surrounding medium the image resolution is poor and the exact shape of the object is difficult to determine. With multiple objects in the vessel it becomes more difficult to resolve separate objects and the inverse problem becomes more complex.

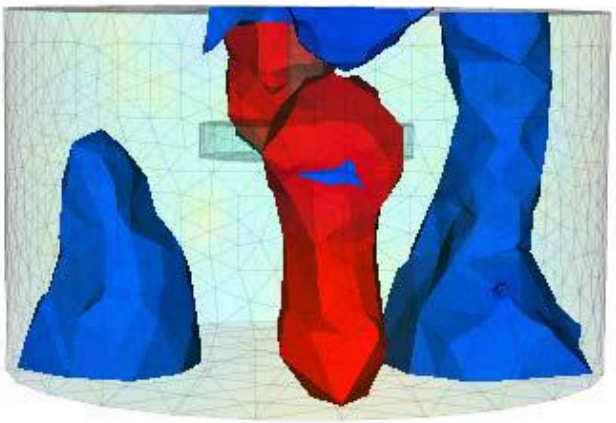

Figure 1-1: Typical Electrical Tomogram (Murphy S.C et al, 2008).

Despite the success of tomography it is essentially limited to determining distributions of physical properties such as density or electrical impedance. Some efforts have been made to exploit chemically specific measurements in tomography, for instance by measuring infra-red absorption (Wright, P et al, 2010) but examples are limited. In addition monitoring of industrial processes using tomography typically requires significant installation costs, either for new vessels or retrofitting, to accommodate the electrodes and wiring and this is often impracticable. For instance, using electrical tomography it is usually necessary to use at least 16 electrodes and, for 3D imaging, numbers in excess of 100 are not uncommon (York, T.A, 2001).

For the reasons discussed above it is desirable to find new techniques for monitoring industrial processes and a major programme of work is underway at the University of Manchester to explore the use of wireless sensor networks[3] (Antoniou, M. et al, 2009, Nawaz, S. et al, 2009). The vision is to deploy a cluster of wireless sensor pills within a process vessel to measure localised parameters. For instance, desirable parameters might include temperature, pressure, humidity, pH and dissolved oxygen. The pills should be able to determine their position in 3D and to communicate with others in the cluster in order to broadcast measurements to the control room. A representative schematic of such an arrangement is shown in Figure 1-2.

[3] http://wsn4ip.aasn4ip.org.uk/mainPage.php

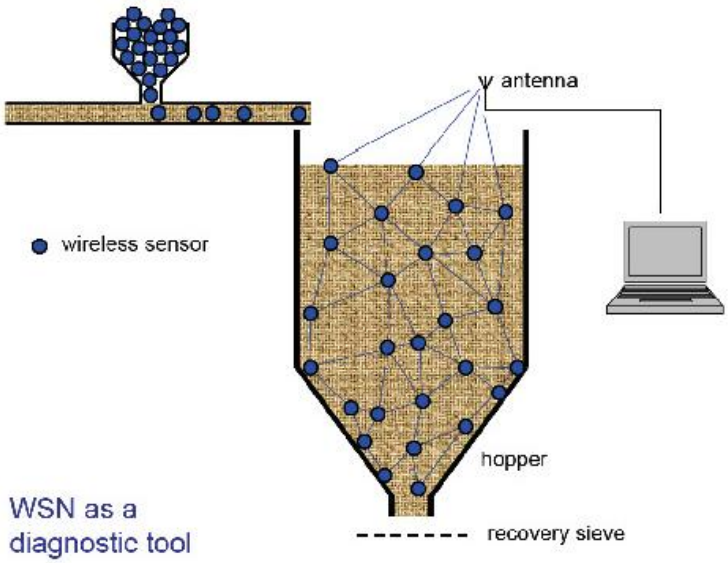

Figure 1-2: Schematic Representation of a Wireless Sensor Network in an Industrial Process Vessel, WSN4IP[4]

Figure 1-2 illustrates the use of wireless sensor nodes in a grain hopper. The desire is for each sensor to take reading of the local environment and then communicate back both its position and environmental readings to an external control station. From here it is possible to monitor the local conditions in the grain silo to monitor, for example, the build up of explosive gases.

There are many challenges associated with realising such a network including localisation, power minimisation, acquiring measurements from sensors and data communication. The target for the present work is to address the first of these challenges, namely how to determine the location of the sensor pills, in three dimensions, in the restrictive environment of a small, enclosed, process vessel?

1.4 Previous Related Work

Previous work at the University of Manchester was undertaken to develop a Local Positioning System (LPS) to track a Neutrally Buoyancy Flow Follower (NBFF) in a metallic vessel containing an opaque conductive fluid (Burnett-Thompson A, 2007). To achieve this, a wired, "omnidirectional", ultrasonic transmitter was used as the object to be located. Four transducers that are mounted on the internal walls of the vessel detect the ultrasonic signal. The Time of Flight (TOF) for the acoustic signal is calculated for each receiver and used to determine the range. Least error calculations subsequently derive the position of the transmitter.

The project considered a small, wired omnidirectional transmitter whose position in 3D could be accurately recorded to within $\pm$ 2 cm in a vessel of the order of 1m in dimension. Significantly, if low

[4] http://wsn4ip.aasn4ip.org.uk/schematic.php

power sensor pills are to be realised, results were achieved using a drive voltage of only 10 V peak to peak. The limitations of the system included the wired nature of the transmitter, together with its size and cost. The omnidirectional unit costs in excess of £400 and its size and construction is not conducive to implementation on a realistic sensor pill.

A typical result for localisation with the system, using the optimum threshold technique with a transmit frequency of 100 kHz is shown in Figure 1-3. The value in each square shows the localisation error of the transmitter between the actual and calculated location.

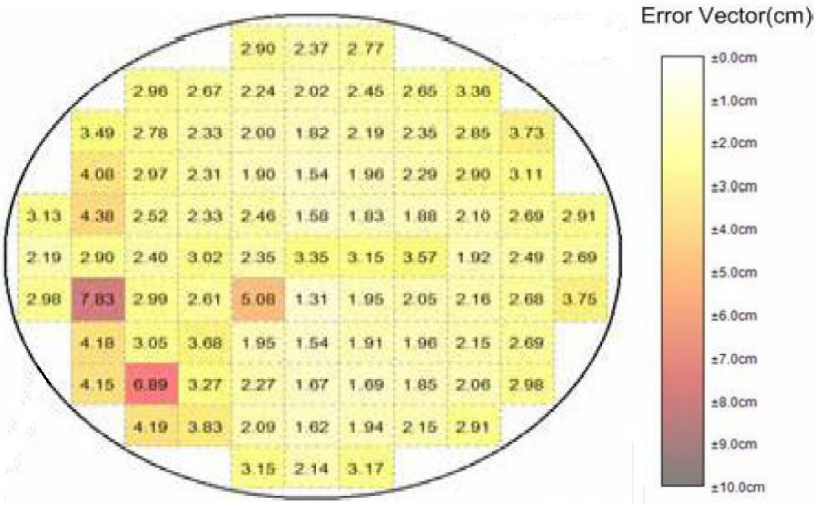

Figure 1-3: Typical positional accuracy of system (Burnett-Thompson A. et al, 2007)

A subsequent project within the University of Manchester further developed the work on the LPS. The single omnidirectional transmitter was replaced with a rudimentary transducer array mounted around the surface of a spherical pill which contained control hardware. Magnetic coupling was also considered for synchronisation. Results established that in principle this system could provide a solution for synchronisation but it was found to be unreliable and have limited operational range.

The work reported in this thesis extends that undertaken by (Burnett-Thompson A, 2007). While the previous research produced a small omnidirectional transducer which was wired and utilised TOF localisation this thesis extends this work by developing a realistic pill, with size sufficient to contain internal hardware and investigates low cost transducers which need to be mounted to the surface of the pill to achieve localisation. Additionally this thesis investigates the localisation technique of TDOA to allow a wireless pill to be developed.

1.5 Current Related Work

A significant ongoing project, Actuated Acoustic Sensor Networks for Industrial Processes (AASN4IP)[5], was begun in 2008 at the University of Manchester with the aim to develop a network of sensor pills, with buoyancy and propulsion control, for surveying large nuclear storage ponds.

[5] http://www.aasn4ip.org.uk/

These nodes will have the capability to locate their position within the environment, to take measurements and communicate these to the outside world and to replenish power at charging stations. Motivation for the nuclear industry in this work concerns the ability to map storage environments that are used to store radioactive waste, to inform the decommissioning process.

Modern facilities are well developed and very safe to allow the storage of long-term radioactive material. Key concerns for the modern nuclear industry are sustainability and maintainability, the process is designed such that easy access to the waste is possible and the waste can be transported safely and processed as required. This situation has not always prevailed. When the nuclear industry was in its infancy substantially less emphasis was placed on long-term issues such as safely storing and discarding nuclear waste[6]. For this reason the first generation of nuclear storage consists of large containers of waste stored in ponds haphazardly with no concern for future processing. With the current political emphasis to reduce carbon emissions and the closure of substantial coal fired power-generating facilities in the near future[7] nuclear energy is again in the spotlight as a potential low carbon replacement for future power generation. For this reason the problem of old radioactive waste needs to be addressed to press the safety and green credentials of nuclear power generation.

Within the old facilities little is known about the location of material in the ponds. Containers have decomposed and waste has leaked into the facility. Containers have possibly fallen and become dislodged from their initial placements. A final concern is that a radioactive “sludge” of an unknown consistency has formed on the bottom of the ponds which needs to be investigated such that the most appropriate removal method can be devised.

The objective of the AASN4IP project is to produce a network of nodes which are able to move through the environment and map the layout of containers in the pond. The nodes should also be able to take chemical readings of the environment with a final task to investigate the “sludge” at the bottom of the ponds and ascertain its “hardness”.

The largely unknown nature of the storage ponds means that the AASNIP project has many complex challenges to overcome. One of the primary concerns is the ability to navigate within the environment. The nature of the task with a survey “mission” requires the node to be capable of moving in 3 degrees of freedom. This means a vertical displacement system and propulsion are required. The radioactive nature of the environment imposes the constraint that human retrieval of the nodes from the pond is unfeasible. As the “mission” is envisaged to be longer than a single battery charge capacity some form of in-situ charging is required which is compatible with the aqueous nature of the medium. The current preferred method for this application is electromagnetic inductive charging. The final challenge for AASN4IP relates to locating the position of the nodes

[6] http://www.no2nuclearpower.org.uk/reports/waste_disposal.php
[7] http://www.decc.gov.uk/assets/decc/publications/energy_rev_06/file31890.pdf

and transmitting this information to the external system, along with data from the node. This thesis aims to inform the design of an ultrasonic transducer arrangement for the AASN4IP nodes

1.6 PhD Challenges

The central challenge of the present project relates to the ability to accurately locate the 'pill' within an enclosed vessel. The ability to locate the pill wirelessly underwater within a small confined metallic space encompasses a number of challenges. The most obvious consideration relates to the method of transmission of signal. This project uses ultrasound for localisation.

One of the key motivations for the use of acoustic signals is the propagation speed in water. Over the relatively short distances envisaged in the target environment, 0 – 1m a typical TOF measurement will be in the order of milliseconds, allowing the signal to be accurately timed with relatively inexpensive equipment. A further motivation for acoustics is its excellent propagation through water. The attenuation of low frequency acoustic signals is relatively small and is dependent upon frequency. By maintaining a low frequency substantial signal can be received even with minimal drive voltage.

Radio Frequency (RF) signals are extensively utilised in standard methodologies such as Global Positioning System (GPS). However, for underwater applications RF has a number of constraints. Firstly attenuation of RF is substantial in water (Chakraborty, U. and Tewary, T. 2009). For a vessel size such as the proposed target application this is not necessarily a problem however at a frequency of 10 MHz the attenuation of RF is 100 dB over 10 m in fresh water (Rhodes, M. 2007). Another challenge relating to RF is due to the high speed of propagation. The short distances in the proposed environment make the ability to accurately record the TOF difficult without expensive timing equipment. With an orbit range of approximately 20200 kms[8], as used with GPS Medium Earth Orbit (MEO) satellites accurate timing is possible with a TOF of approximately 67 ms. With a diameter of 0.5 m for the target demonstrator this would produce a TOF of 2.17 ns assuming a refractive index of 1.3 in water.

A further possibility for localisation is the use of trilateration of optical signals from knowledge of the direction of propagation. A proposed constraint within the project is that the fluid medium could be optically opaque. For this reason optical positioning is not considered further.

As the eventual pill is intended to monitor and record information from the environment a finite amount of hardware is required to take sensor readings and store data, along with battery storage to provide power to these devices. Some form of transmitting hardware is also required for localisation. This imposes a minimum size for the pill sufficient to contain all the necessary

[8] http://www.kowoma.de/en/gps/orbits.htm

hardware. Therefore an imposed constraint of the project is that the pill will be assumed to be larger than the transducers.

Transmission from the pill to the external host allows localisation information to be collected at the receiver and reduces the demands on processing hardware required on the pill. However, it also places greater demands on the power required to transmit signals. The alternative is to transmit from the external host to the pill. Both arrangements have their merits but for this project transmission from the pill to the host is assumed.

As the use of transmitters mounted on the pill places greater demand on the power required to transmit signals there is a limitation on the driving voltage for the transmitters. For this project a transmission voltage of 10 V peak to peak has been imposed, based on the work undertaken in (Burnett-Thompson A. 2007). A one second positional update rate has also been imposed.

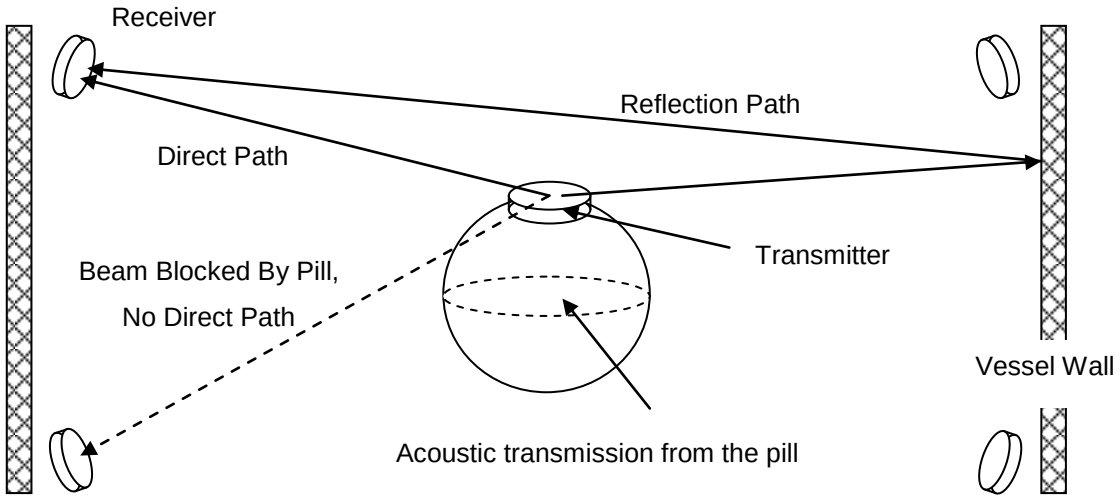

Figure 1-4: Challenges of Project

Based on the specification Figure 1-4 illustrates some of the major challenges of the project. The use of a finite sized pill creates a number of challenges for the project which primarily relate to the optimum placement of transmitters on the pill to provide signal coverage to all receivers and prevent any potential beam blocking by the body of the pill itself.

One of the key concerns for the project is the ability to provide adequate signal coverage throughout the vessel, such that all receivers can detect a signal. A signal of uniform intensity would be desirable irrespective of angle of transmission such that regardless of the pill's location within the vessel receivers are able to detect good signal strength. To achieve this, an attractive solution is to create an omnidirectional beam profile.

A challenge therefore for the project is to investigate potential transmitter options for the pill, regarding size and transmission pattern, together with investigating the most suitable locations to mount single or multiple transmitters to maximise the signal at any receiver. Potential options for investigation include the use of a single omnidirectional transmitter or the use of multiple

transmitters to approximate an omnidirectional profile. From research conducted in this thesis, [Chapter 4.0, section 4.1] the decision to use multiple transmitters on the surface of the pill has been selected.

The option to use multiple transmitters mounted to the periphery of the pill thus providing unobstructed coverage to receivers creates its own challenges for localisation. In a conventional system a single transmitter broadcasts a signal which is detected by multiple receivers. This allows the transmitter's location to be pinpointed. With multiple transmitters the signal arriving at different receivers will not have originated from the same transmitter and therefore an important consideration is how the localisation accuracy of the system is affected and how the centre of the pill can be accurately determined. A key research question is, how accurately the pill's location can be determined as a function of transmitter layout?

Coinciding with this work is the effect that receiver position has in relation to optimum transmitter layout and if by careful selection of receiver position errors on localisation measurements can be accommodated while maintaining an accurate location of the pill. Feedback from the previous work (Burnett-Thompson A. 2007) was that the optimum position of the receiver locations should be considered.

The target vessel for this application was a vessel with dimensions 1.0 m in height by 0.6 m in diameter. The vessel wall was metallic with a high reflection coefficient. Throughout this thesis the vessel is referred to as the "250 litre" vessel. The vessel was chosen as its small size and high reflection coefficient make it a "typical" process environment and create a challenge for localisation due to multipath. Due to the construction of the vessel and small size, reflections within the vessel are substantial. This creates complexity differentiating the direct path received signal from reflected signals. Incorrect signal acquisition leads to incorrect range information and subsequently incorrect position. Peak detection methodologies fail in such an environment due to non-line of sight signals arriving with larger amplitude that direct path signals. For this reason a key interest is why this occurs and if it can be predicted and therefore compensated for, or else determining an alternative detection strategy which negates these reflection issues.

A typical method to allow the location of a transmitter to be determined is to synchronise the transmitter and receivers to achieve TOF measurements. Due to the low propagation speed of signals in the underwater medium typical synchronisation techniques are difficult to implement. The highly reflective coefficient of the vessel surface also creates a challenge for acoustic localisation techniques. Therefore another key research challenge is to investigate possible synchronisation techniques for application in the target environment.

The aim of the project was to focus on the 3D localisation of a sensor "pill" that is contained in a confined space. As such the project focused on a small-enclosed metallic vessel. The medium used was tap water. Although small size has always been a consideration the challenges of

localisation and power supply have not been compromised by a high priority for miniaturisation. It was intended that the pill can be viewed as a “particle” such that it is significantly smaller than the dimension of the containing vessel.

The key areas of research covered were the selection of small, low cost, and low power transmitters for use on the pill. The challenge was to determine how adequate vessel coverage can be achieved, through the use of multiple transmitters mounted to the periphery of the pill. It was also of interest how the transmitters’ locations and corresponding receiver locations influence the positional accuracy of the pill, not only as a function of received amplitude but also how transmitter separation from a single point influences the positional accuracy of the system using traditional positioning methodologies. The work conducted within this research concentrated on the wireless localisation strategy and the transmitter layout of a single pill to achieve optimum vessel coverage while preserving spatial resolution

1.7 Thesis Outline

The structure of the thesis is as follows: Chapter 2 presents a detailed literature review with the main focus being on methods for localisation. A general overview of available sensor network technology is presented before more detailed consideration of localisation. This includes acoustic transmission of signals, underwater positioning systems, transducer array design and also positioning methodologies such as TDOA.

Wireless localisation options are presented in chapter 3. This chapter considers possible synchronisation options and preliminary experimental work on electrical synchronisation is discussed along with localisation through the use of TDOA where no synchronisation between the transmitter and receiver are required.

In chapter 4 a detailed discussion of the application of TDOA for use within this project is presented. This chapter investigates the impact that separation of the transmitters on the pill has on the localisation accuracy of the system through simulation. The impact of receiver location on localisation error is also considered.

Chapter 5 presents research into possible transmitter options to create a low cost pill. Testing of a suitable transmitter is conducted as both a single unit and multiple transmitter layouts. Modelling of the reflection properties of the vessel was undertaken to confirm experimental results and allow understanding of reflection issues to develop suitable solutions.

The design of a transmitter array on the pill is discussed in chapter 6. This includes the theory behind the array, along with transmitter and receiver profiling to allow the development of a model concerning optimum transmitter and receiver placement for vessel coverage. This information was

used to simulate possible transmitter layouts and optimise the layout to maximise received signal strength and vessel coverage.

Chapter 7 presents the localisation results for the wireless prototype pill. This details localisation strategies for the pill before presenting experimental testing results comparing localisation using TDOA and TOF techniques.

2.0 Literature Review

This chapter discusses the topics which are relevant to the development of an underwater wireless sensor network (UWSN), with specific interest in the desire to develop a pill for underwater localisation in confined spaces. The chapter investigates the current 'state of the art' technology in a number of fields applicable to the development of an underwater pill for utilisation in confined spaces and is divided into six subsections.

In section 2.1 an introduction into wireless sensor networks (WSNs) is presented detailing the principle behind their operation, techniques which are employed to realise them and the current state of the art technology developments within the field.

From the overview of WSNs, section 2.2 investigates the development of wireless sensor networks developed specifically for underwater use, and the development of sensor nodes which have applications in the underwater medium, highlighting the challenges which this medium creates. This section also details current applications within the underwater wireless networks field with special interest in wireless sensor networks which are concerned with confined spaces.

Possible signal modalities for transmission through the underwater medium are discussed in section 2.3. This section investigates the "typical" transmission method of acoustics along with a critique of other possible options due to the short range nature of the application. The limitations of each method are evaluated and a suitable transmission method selected. The techniques which are considered include optical, RF and acoustic transmission.

In section 2.4 the primary challenges for underwater localisation are investigated. This section discusses existing synchronisation methodologies applied to achieve underwater localisation. Techniques such as localisation by time synchronised clocks, bearing measurements, round trip times (RTTs) and time difference of arrival measurements (TDOA) are considered. Synchronisation techniques using electrical and electromagnetic properties are also investigated.

Section 2.5 discusses acoustic transducers from a theoretical design perspective, as well as considering commercially available options, which are used as a transmission source for localisation signals. The section will look into the different construction methodologies of acoustic transducers before specifying in detail the transducer requirements for the work of this thesis. The limitations of available technologies are detailed before a discussion of commercially available transducers suitable to the project is presented, and a final selection made.

In section 2.6 transducer arrays are discussed with the aim to investigate the design of current transmitter arrays and the techniques used to determine the suitable placement of transmitters. This section also investigates the technique of beam forming to create the desired beam profile both through the use of electrical excitation techniques and transmitter placement methods.

2.1 Wireless Sensor Networks

Wireless sensor networks (WSNs) consist of spatially separated sensors which are used to monitor information about the surrounding environment in which they are located. Through the use of a large number of inexpensive sensors it is possible to obtain distributed data over wide areas which can then be communicated back to a base station for processing and interpretation.

In recent years WSNs have gained worldwide attention due to the development of micro-electro-mechanical systems (MEMS) technology. This has allowed the development of smart sensors which are able to sense, measure and gather information and relay this back to the user (Yick, J. et al, 2008).

Applications of WSNs span many areas which include military, environmental, health, home and commercial (Akyildiz, I.F. et al, 2002). For example, environmental applications of WSNs include tracking the movement of animals, monitoring weather patterns and conditions and pollution monitoring.

The advancement of WSNs in recent years means that there are now commercial companies supplying wireless technology solutions as platforms to develop WSNs. A leading company in this field is Crossbow[9] which has developed numerous platforms for sensor node technology; the most developed being the mica2[10] motes platform.

There are typically two types of WSN: structured and unstructured networks (Yick, J. et al 2008). An unstructured network consists of nodes which are placed at random and usually in a dense format in the location to be monitored. Once deployed the nodes are left unattended and remain operative until their battery source becomes depleted at which point they disconnect from the network.

In contrast, the node deployment in a structured network is done strategically such that the node's placements are chosen to maximise the data which can be obtained, for the minimum number of deployed nodes. Structured networks are able to contain significantly fewer nodes to monitor the same area.

The decision to deploy a structured or unstructured network is usually dependent upon the environment to be monitored. For example, in order to monitor forest habitats over significant areas nodes may be deployed by aircraft which leads to an unstructured network layout.

[9] http://www.xbow.com/index.html
[10] https://www.eol.ucar.edu/rtf/facilities/isa/internal/CrossBow/DataSheets/mica2.pdf

In comparison to traditional networks, WSNs have significant resource constraints which are directly related to their intended deployment for long term monitoring applications, potentially in locations where retrieval is not possible. The devices have a very limited power supply and the storage capacity and processing power of the nodes is small. Therefore, the devices should be designed to be as efficient as possible in terms of processor throughput and power usage. To put the challenge into perspective the sensors used by (Vardhan, M. et al, 2000) are operated from a lithium ion coin cell battery. The average current consumption in this application is less than 30 µA.

While the longevity of the sensor nodes can be increased through the use of power scavenging techniques such as solar cells or vibration, these techniques are not always suitable for all applications and only offer a modest amount of energy. The modality of choice for power harvesting is solar energy due to its high power density. However, the use of these techniques is complex due to the task of managing different voltage-current characteristics (Raghunathan V. et al, 2005). In most applications, power scavenging is not implemented. Therefore, once the battery source becomes depleted, the node ceases to function.

A typical single sensor node for WSNs consists of a sensor for environmental monitoring, a processor, memory, power source and a radio to allow communication with other nodes or the user (Yick, J. et al, 2008). One of the key requirements to make WSNs suitable for operation is that the number of nodes over a given area should be dense. To accomplish this, there is the requirement that sensor nodes must be small, extremely low power, have a low production cost, be autonomous and be adaptive to the environment (Kahn, J.M. et al, 1999)

In WSNs three of the primary issues for application are communication, localisation and time synchronisation. Communication between nodes is usually made possible through Radio Frequency (RF) signals, infrared or optical (Akyildiz, I.F. et al, 2002). However, most of the current development is based upon RF technology.

For localisation of sensor nodes, common techniques used include Global Positioning System (GPS), beacon nodes or proximity based systems (Yick, J. et al 2008). While the task of localisation becomes trivial if each node is equipped with a GPS receiver this is a costly implementation which has lead to the development of beacons as demonstrated by (Sichitiu M.L. and Ramadurai V. 2004), whereby a single node is equipped with a GPS receiver, which is utilised to assist in the localisation of nodes without GPS.

The final key issue in WSNs is time synchronisation. In order to allow nodes to transmit in a scheduled manner there is the requirement for time synchronisation across the network. To achieve this there are numerous protocols currently in use, from estimating clock drift (Ganeriwal S. et al, 2005) to conventional sender receiver synchronisation (Ganeriwal S. et al, 2003) and clock sampling techniques (Rentel C.H. and Kunz T. 2005).

2.2 Underwater Wireless Sensor Networks and Nodes

Underwater wireless sensor networks (UWSNs) share many similar traits with their non-underwater based counterparts in terms of the design and structure of the network (Lee, K.H. et al, 2008). The transmission medium however leads to differences in the communication methodology which complicates issues such as time synchronisation and localisation. UWSN nodes are also significantly more expensive than nodes intended for operation above ground which leads to a sparser node deployment (Yick, J. et al, 2008).

UWSNs and underwater sensor nodes have applications in numerous fields of research, such as oceanographic data collection, pollution monitoring, offshore exploration, disaster prevention, assisted navigation and tactical surveillance applications (Akyildiz, I. F. et al, 2005). A typical UWSN consists of multiple sensor nodes which are located underwater with communication to an external structure which is based out of the water medium, such as an oil platform or monitoring station. Figure 2-1 displays such a configuration.

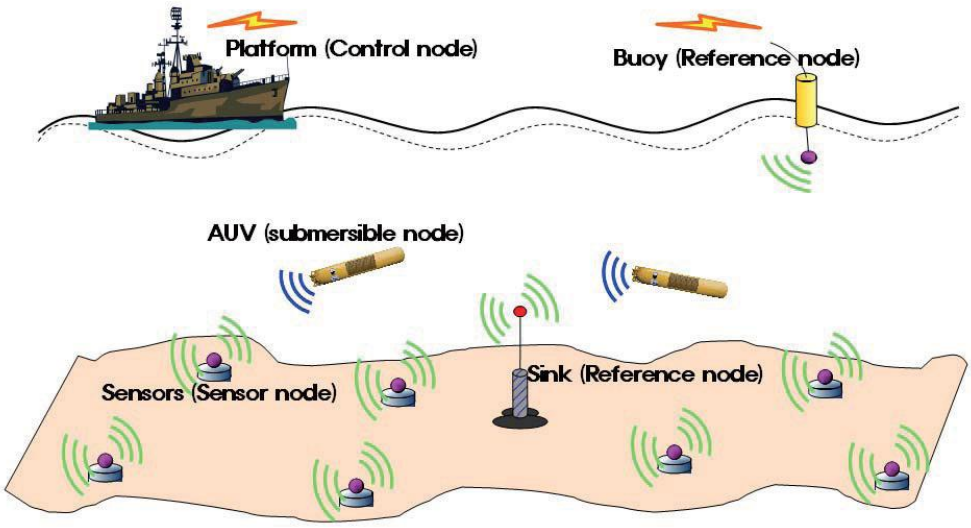

Figure 2-1: Typical underwater sensor network configuration (Lee K.H. et al, 2008)

In comparison to the above ground sensor networks in section 2.1, which have many commercial applications and whose design has advanced considerably in recent years, the development of networks where communication is considered underwater is in its infancy and significantly more limited (Heidemann, J. et al 2006).

While many of the design principles which apply to sensor networks above ground can also be adopted for use underwater, there are significant differences in their implementations, resulting in a number of unique challenges. The primary difference between their implementation relates to the transmission medium.

In conventional above ground networks communication between nodes is conducted through RF techniques, (Pandya, S. et al 2005) however the underwater medium cannot support RF

communication due to poor transmission of RF signals through water, and the strong attenuation of the signal (Anguita, D. et al, 2009).

To overcome this limitation, acoustics are considered as an alternative strategy for communication underwater. This, however, brings its own challenges due to the construction of standard acoustic modems which have large power requirements and are designed for long range communication rather than the dense set up anticipated for WSNs (Heidemann, J. et al 2006).

The second significant challenge relates to the speed of transmission underwater due to the use of acoustics rather than RF techniques. In above ground networks the propagation delay for short range RF is negligible; this is not true for acoustics underwater. As such this significantly impacts both time synchronisation and localisation (Heidemann, J. et al 2006).

These two significant differences from air-based wireless sensor networks make the challenge of designing and implementing an underwater sensor network significantly more complex. Current developments in underwater sensor networks and underwater communication systems are considered over large ranges with high power requirements and significant costs. The focus of the majority of literature therefore is on networks and communication over these ranges. A selection of relevant publications is given below:

Stojanovic, M. et al, (1994) considered acoustic communication for applications over ranges of 40 – 140 nautical miles (74 km – 259 km) with a 1 kHz carrier frequency. Experimental work over a 2 mile range (3.7 km) demonstrated the ability to transmit acoustic signals at a rate of 10kb/s with no errors in 10000 symbols. This paper demonstrated the feasibility of acoustic communication underwater over large ranges at low frequency.

Faugstadmo, J.E et al, (2010) discusses the development of an underwater wireless sensor network employing acoustic communication. A sea trial was undertaken with a system comprising 5 sea floor nodes and 1 master node at the surface. Experimentation was undertaken when both direct node to master communication was possible and when multi-hop communication was necessary. Flood algorithms were used to establish network routing.

Tests demonstrated the ability to gather 1 kB of data from 2 separate nodes with a data rate of 500 bps for direct node to master communication. Using multi-hop communication, with a sensor node communicating with the master via a second sea floor node, a communication rate of 500 bps was achieved; the link to the master took place with a communication rate of 200 bps. Both of these data rates were selected by the nodes autonomously through measurement of SNR in the flooding algorithm. The depth of the nodes in this test was 190 m.

Adams, A.E and Acar, G. (2005) discussed the development of new protocols for acoustically linked sub-sea sensors. Sea trials were conducted using a network which consisted of 1 master

and 3 slave nodes. Due to problems with the experimental conditions, communication between the master and two of the slaves was not possible. The data retrieval success rate for the working slave node was 80%. However, communication between nodes experienced extended outages due to nearby shipping activity. The problems experienced with this network demonstrate some of the difficulties in maintaining reliable underwater communication in networks, especially with external activity such as shipping creating acoustic noise in the channel.

In situations with confined spaces where severe multipath propagation from the walls of the vessels compromises measurements, only a modest amount of previous work has been reported into such applications.

Ong K.G. et al, (2003) presented developments on a small scale sensor application. In this instance, small scale relates to a sensor node separation of less than 20 m. The project developed an underwater sensor node capable of taking temperature and pH measurements, which then relays the data through an acoustic transducer to a base station. Experimentation was conducted in a swimming pool of dimension 40' x 40' x 18', (12.2 m x 12.2 m x 5.5 m) were data was collected from 3 stationary nodes and transmitted to a base station node over a 2 hour period monitoring the pH and temperature levels in the pool. The paper demonstrated the feasibility of networking multiple nodes using acoustic communication to relay information in an underwater environment within a reasonably confined space.

While communication using acoustics between underwater nodes has been demonstrated to be possible, the establishment of a sensor network in confined spaces is extremely limited, with only one application found detailing such a layout (Ong K.G. et al, 2003). In this the nodes are stationary and their locations are not anticipated to alter during the duration of the experiment. This is unlike the challenge envisaged in this thesis, whereby the position of the pill is dynamic.

2.3 Underwater Transmission Modalities

From the research conducted in section 2.2 it can be observed that existing UWSNs primarily consider acoustic transmission methods. One of the driving factors for this is that the typical application of UWSNs is over large ranges (Heidemann, J. et al. 2006), where low frequency acoustic signals show excellent propagation characteristics.

In contrast, this project anticipates localisation over small ranges, in confined spaces. This creates the possibility of using other transmission methodologies underwater. For this reason this section investigates possible underwater transmission methods and discusses their merits and limitations for application in this project.

2.3.1 Optical

One possible technique to allow transmission of signal underwater is through optics. Optical localisation uses light to transmit signals through a medium which must be optically translucent. Typically a light source and reception device are attached to the target and receiver respectively. A significant advantage of using optical transmission is that, since the speed of transmission is large, achievable data rates are extremely high over short distances. The main disadvantage of optical localisation is that the working medium must be translucent. Therefore, even though the speed of transmission is large, the system can only be used over short ranges as the underwater medium absorbs much of the signal as the range increases.

Bellin M. et al, (1990) considered the use of optical means for underwater localisation. Two cameras were used to pinpoint a specific point on a target image. As the target moved, the cameras were able to stay locked onto this point and track the target. For operation up to a range of 2 m, a stationary target was able to be located within an accuracy of 5 mm of its true location. Once the target began to move, the accuracy of the system decreased with an error of approximately 1% of the vessel volume (dimensions of the vessel are not given in the paper). This paper showed that over a short range, provided the medium is translucent, optical means can be used to determine the location of a target with good accuracy.

While the anticipated demonstrator will use water it is possible that process vessels could contain materials which make the aqueous solution opaque. For this reason optical transmission methods have been ruled out for use in the present project.

2.3.2 Radio Frequency (RF)

For underwater localisation however, the use of RF signals is very limited. This is typically because the signal degradation of RF is substantial in water and the amplitude of the received signal quickly diminishes with range (Anguita, D et al, 2009). While for application in systems with ranges from hundreds of metres to kilometres this is a problem, this project only envisages use in small process vessels, up to a few metres in diameter.

Chakraborty, U. and Tewary, T. (2009) exploits the limited propagation of RF signals through water by investigating how the transmission frequency alters the propagation depth. The paper investigates the penetration depth of electromagnetic waves in sea water, also referred to as “skin depth” which is the distance through which the amplitude decreases by a factor of 1/e, where “e” is Euler’s number. The results demonstrate that for a 1 MHz operating frequency the skin depth in sea water is only 25 cm and 7.1 m in fresh water. As the frequency is reduced the penetration depth increases. For an operating frequency of approximately 1 kHz the penetration depth is 7.5 m in sea water. The results show that provided the operating frequency is low, short range penetration of RF signals underwater is possible.

While the range of RF propagation for this project is not a concern, the limitation of RF for application is this work relates to the speed of transmission of the signal. With a large propagation speed, the short distances in the proposed environment make the ability to accurately record the TOF difficult without nanosecond timing equipment. With a diameter of 0.5 m for the target demonstrator this would produce a TOF of 2.17 ns accommodating for a refractive index of 1.3 in water. To achieve accurate localisation results there is the requirement for a timing system accurate to nanoseconds. For this reason RF has been ruled out as a suitable transmission option for localisation signals.

2.3.3 Acoustic

From a review of UWSNs in section 2.2 it has been demonstrated that the preferred signal modality for underwater networks is acoustic. The long range propagation of the signal at low frequencies makes is ideal when there is the requirement for signal transmission over large ranges underwater.

The excellent propagation characteristics of acoustics underwater mean that over the short ranges envisaged within this project it is possible to have high transmission frequencies, 100 kHz and above, and still have minimal signal attenuation. At 100 kHz for example at a range of 400 m the attenuation of the signal is only 15 dB relative to the signal at 1 m (Preisig J. 2006). It is also possible to reduce the transmission frequency to increase the received signal strength, for 50 kHz the attenuation drops to approximately 8 dB. This allows a reduction in drive voltage while maintaining received signal levels which is important for a pill which must be battery powered.

A further benefit of acoustic signal propagation underwater for use in this project relates to its transmission speed. In contrast to RF signals, acoustic signals propagate at only 1500 ms^{-1} in water. Over the relatively short distances in the target environment this gives typical TOF measurements in the order of milliseconds, allowing the signal to be accurately timed with relatively cheap timing equipment.

The challenge for the use of acoustic signals in the anticipated target environment is due to multipath reflections (Woosuk C. et al, 2008). The target vessel is to have a metallic wall which will have a high reflection coefficient, approximately 0.88 for steel[11]. As such it can be anticipated that multipath reflections in the vessel will cause multiple receptions of the transmitted signal at receivers making detection of the signal difficult.

While the reflection properties of acoustic signals present a challenge deciphering the correct signal at the receiver the excellent signal strength through water with minimal attenuation and the relatively slow transmission speed make acoustic transmission an ideal candidate for use. For this reason the transmission method in this project is to be acoustic.

[11] http://www.ndt-ed.org/EducationResources/CommunityCollege/Ultrasonics/Physics/reflectiontransmission.htm

2.3.4 Underwater Transmission Modalities Summary

While the research in section 2.2 on UWSNs has demonstrated that the typical transmission method used underwater is acoustics, the unusual short range application of this project means that other transmission modalities are possible. This section has therefore investigated potential transmission modalities for underwater application.

Optical transmission techniques have been demonstrated for use in underwater localisation. Previous work has demonstrated that over short ranges, up to 2 m, it is possible to locate a stationary object to an accuracy of 5 mm. The limitation of this method is that the transmission medium must be translucent. This project has already defined that the medium may be opaque and therefore optical transmission can be ruled out.

While RF transmission cannot be utilised over long ranges underwater due to signal degradation, over the short range in this project it has been shown that RF signals can propagate with low attenuation loses. The transmission speed of RF underwater over the short range however means timing equipment must be accurate to nanoseconds, which means expensive timing equipment beyond the scope of this project.

Acoustics are the typical method of choice underwater as seen in section 2.2 due to their excellent propagation characteristics. The transmission speed, $1500ms^{-1}$ also means that over short ranges timing is possible with relatively inexpensive equipment. The confined space of the process vessel does however present a challenge due to acoustic reflections. Of the methods available however acoustics shows the most promise for application.

2.4 Underwater Synchronisation Options

As discussed in section 2.2, the challenge of establishing reliable communication underwater is increased due to the high latency of the transmission medium when acoustic signals are considered. The challenges associated with establishing reliable communications are further complicated when localisation is considered and the requirement for time synchronisation between transmitter and receiver (Lu C. et al, 2009).

As presented in section 2.3 signals transmitted in the vessel to allow the location of the pill to be determined, are anticipated to be acoustic, due to the propagation of the signal through the water and the low speed. To determine the Time-of-flight (TOF) of the signal there must be some form of synchronisation between the pill and external system (Chaczko Z. et al, 2007) such that the arrival of the signal is referenced in relation to when it was transmitted. While it is also possible to implement synchronisation via acoustic means the slow propagation of acoustic signals means that for the synchronisation task, acoustic signals are not well suited.

For this reason this section investigates possible synchronisation options for underwater applications, along with investigating current techniques which are utilised to achieve localisation underwater. This includes techniques which avoid the need for synchronisation of the pill while still allowing the location of the transmitter to be determined.

2.4.1 Time Synchronised Clocks

A common technique employed to achieve localisation over significant distances, is through the use of time synchronised clocks. On both the transmitter and receiver, clocks are used which, ideally, have a very small drift. The clocks on the transmitter and receiver are synchronised before deployment, which allows accurate time stamps to be transmitted with signals. Upon reception of a signal at the receiver, the receiver has knowledge of when the signal arrived through referencing its own clock, as well as when the signal was transmitted from the time stamp in the signal. This information allows the TOF and subsequently the range between the transmitter and receiver to be determined.

The main advantage of this technique is that it does not require any form of synchronisation during operation. The synchronisation between the transmitter and receiver can be completed before deploying the instruments into the target environment. The significant disadvantage of this method is that to ensure the clock drift between the clocks is minimal, expensive timing equipment must be used. Even with expensive equipment, there is always some drift between clocks which introduces error into the measurements and this increases with the duration of the mission.

Garcia J.E, (2005) relied on the use of synchronised clocks to achieve synchronisation between transmitter and receiver to achieve localisation of nodes. The ‘accurate positioning’ algorithm (APOS) was presented, in which nodes estimated their distance to neighbouring nodes using acoustic velocity and signal delay. In order to achieve this, the nodes were synchronised before they were deployed, such that TOF information could be obtained.

Baker J. and Thomas H. (1999) used an acoustic beacon as a “pinger”, which was time-synchronised with receivers via the use of precision clocks. This system was used for applications over a range of approximately 750 m underwater. Through the use of precision quartz clocks, the time drift between the transmitter and receiver was found to result in a drift of 5 cm/hr in the localisation result. Considering the range of the targeted applications for their work, the drift was deemed to have a minimal impact on the accuracy of the localisation.

2.4.2 Acoustic Round Trip Time Measurements

Another technique which is used to allow TOF measurements to be obtained underwater and the use of trilateration localisation techniques is Round Trip Time (RTT) measurements. RTT methods determine the range of an object by measuring the time a transmission signal takes to reach the object and return to the transmitter. This time can then be halved to obtain the relevant TOF

information. Such systems typically utilise reflections from the object to be located, such as radar[12], to determine range. However, it is also possible to interrogate a target such that the target responds acoustically upon reception of the transmitted signal.

The advantage of using this technique is that synchronisation is not required between the target and receiver to obtain TOF measurements. The disadvantage is that extra computation is required from the monitoring systems' perspective, as it must both transmit and receive signals. As the implementation of this technique also requires acoustic signals to travel in multiple directions, to and from the target, interference between the signals due to reflections is increased.

Typically, acoustic RTT methods underwater are used for profiling of the seabed (Creuze, V. et al 2001, and Lygouras J.N et al, 1994). Reflections from the surface of the seabed are obtained by an Autonomous Underwater Vehicle (AUV), which allows the range to the seabed from a known depth to be determined. As the AUV moves on a pre-determined path, a map of the seabed can be established from the changing range measurements from reflections off the seabed. The depth of the AUV is typically known with (prior knowledge) through the use of pressure sensors.

Stokey R.P and Austin T.C. (1999) discussed the development of a long baseline navigation system for an AUV. The system was intended to guide the AUV in shallow water situations. The system employed a moored pair of acoustic transponders, whose coordinates were determined using GPS. The AUV acoustically "pings" these transponders, which responded accordingly to allow RTTs to be determined, and the range between transponder and AUV to be calculated. The system employed two transponders which provided two range measurements. Conventionally, to localise in 3D, four range measurements are required to identify the location of the target. To eliminate the depth variable a pressure sensor was used while the 4^{th} variable was eliminated through knowledge of the approximate location of the target. The developed system was intended for application in large-scale environments, such as tracking and monitoring pipelines. A track line experiment conducted at sea showed that the AUV was able to follow a box of length 400 m with a root mean square error of ±3.1 m on true position over multiple runs.

2.4.3 Bearing Measurements

Localisation through the use of bearing measurements is a technique which determines the location of a transmitter through the knowledge of the angle at which the received signal intersects a receiver. By using multiple receivers in an array format and from the varying intersect angle at each receiver, it is possible to localise the direction of the signal. Assuming that the transmitted signal travels in a straight line, it is possible to use these bearing measurements to determine a signals path. From this point, the intersection of multiple paths to different receivers allows the location of the target to be determined.

[12] http://en.wikipedia.org/wiki/Radar

The main advantage of this technique is that no synchronisation is required between the transmitter and receiver. Upon reception of the signal at a receiver, the origin path can be calculated. Subsequently, through multiple receptions at different receivers, the target location can be determined. The main disadvantage of this technique is that it relies on a large number of receivers, such that small variations in incident angle can be detected. This makes it costly with respect to the number of receivers which are required. The technique also relies on the assumption that received signals travel in straight lines to allow the location of the target to be calculated.

Mian J.T et al, (2000) investigated the use of the bearing calculation method to determine the position of a transmitter. The system employed both Round Trip Time (RTT) measurements and the use of multiple receivers mounted to the bottom of a ship to measure the phase difference between the transmitted and received signals. By knowing the phase difference, the direction of the signal can be obtained, and through the use of 3 receivers it is possible to locate the target in 3D.

2.4.4 Electrical

A recent technique which has seen application for short range communication through water is the use of electrical signals (Joe J. and Toh S.H. 2007). This technique utilises the conductive properties of water to allow communication. At the transmitter end, a pair of electrodes is used, and a voltage difference established between them, allowing the flow of current. At the receiver end, a second set of electrodes is used to detect the voltage potential established on the first pair of electrodes.

The advantage of this method is that the propagation speed of this signal is negligible over short ranges due to a propagation speed of 2.3×10^{8} ms^{-1} (due to the refractive index of water) and the communications are not prone to interference from movement or noise. This means that the achievable data rates for communication are significantly higher over short ranges. The main disadvantage of using electrical communication is that the medium of transmission must be electrically conductive. The orientation of transmit and receive electrodes is also crucial in determining the received signal strength.

While no references were found to demonstrate the application of this technique for localisation, the ability to transmit and receive electrical pulses through water presents the possibility to use electrical signals as a trigger for a timing system, which allows accurate TOF measurements to be determined. Such a system utilises the relative difference in speeds of the acoustic and electrical signals through the medium. For this application, the speed of electrical signals through water is much larger than the speed of an acoustic signal though water. Consequently the TOF for electrical pulse is negligible in comparison to the acoustic signal.

The simultaneous transmission of both electrical and acoustic pulses from the pill, results in essentially, a zero transmission time for the electrical pulse relative to the acoustic signal. The

arrival of the electrical signal at the external hardware allows timing to commence. The negligible electrical transmission time means the arrival of an acoustic signal represents the TOF from pill to receiver.

The use of electrical pulses as a communication method through water is demonstrated by (Joe J. and Toh S.H. 2007). In this experiment, 2 sets of copper plated electrodes were used in a fibreglass aquarium of dimensions 12 ft x 6 ft x 4 ft (3.7 m x 1.8 m x 1.2 m), filled with seawater. Using a simple On-Off Keying (OOK) methodology, results demonstrate the ability to determine received signal pulses at a range of 2.2 m and with transmission rate of 100 kbps at the receiver electrodes.

(Wu Z. et al, 2010) also investigated high speed underwater communication through the use of the electric current method. In this experiment, similarly, an OOK methodology of transmission is considered. Experiments were conducted in a tank of dimension 130 cm x 40 cm x 80 cm, filled with water at 3.5 % salt intensity to mimic that of seawater. Zinc electrodes were used with dimensions 3 cm x 5 cm. The separation between the transmit electrodes is 20 cm, as are the receive electrodes. Results demonstrated that over a range separation between transmit and receive electrodes of 50 cm; a transmission rate of 1 Mbps was achievable with a Bit Error Rate (BER) of 100 %. As the range was increased up to 1 m at 1 Mbps transmission rate, the BER reduces to 90.3 %.

2.4.5 Electromagnetic Induction

Another method to allow synchronisation between transmitter and receiver to obtain TOF information is through the use of electromagnetic synchronisation. Electromagnetic induction relies on the ability to establish an electromagnetic field at a primary coil and use a secondary coil to detect this field (Kojiya, T. et al 2005). Through changing the excitation at the primary coil, these changes can be detected and monitored in the secondary coil, allowing the transmission of information between the coils. The speed of transmission of the signals is negligible relative to the acoustic signals.

For application underwater, synchronisation through electromagnetic field detection has distinct advantages, similar to those of electrical communication. Like electrical signals, electromagnetic signals are not subject to interference from acoustic noise in the vessel and they have a high propagation speed.

The main disadvantage of electromagnetic signals is also similar to those of electrical signals. The orientation of the primary and secondary coil is crucial to detect good signal strength. The strength of the received signal is also proportional to a number of factors, including the radius of transmit and receiver coils, the number of turns on the coils and the excitation frequency on the primary coil along with coil misalignment, (Babic S.I. and Akyel, C. 2008).

Commercial applications for this technique revolve around the use of electromagnetic induction for communication at high data rates over small distances underwater. WFS's[13] Seatooth short range broadband electromagnetic communications device is an example application of this technology. Seatooth allows the transfer of data between autonomous underwater vehicles (AUVs) and underwater sensors at data rates up to 100 kbs over distances up to 10 m without the requirement for docking between the AUV and sensor node[14].

Feezor M.D et al, (2001) discussed the development of AUV homing via electromagnetic guidance. The system used electromagnetic signals to determine both range and orientation of the AUV in relation to the docking station. The dock consisted of two coils mounted at the top and bottom of the AUV entry point, with diameter 64 cm and 24 turns of #12 wire. The dock acted as the transmitter, with power input of 15 W. On the AUV, 3 receiver coils, each of which was 9 cm in diameter and with 25 turns of #18 gauge wire were used. Field trials conducted in a shallow water environment showed that after completing an execution path using compass control, the AUV was able to detect the magnetic field from the dock and switch to the electromagnetic homing system to allow docking. Of 8 trials carried out under varying sea current conditions, 5 tests were completed successfully with the AUV correctly entering the docking station. The operating range of the present system is 25 – 30m.

2.4.6 Time Difference of Arrival

A 'Time Difference of Arrival' (TDOA) localisation[15] system utilises the relative time difference in the arrival of signals at multiple receivers rather than the absolute TOF measurements to determine the location of a target. Such systems typically consist of a single roaming transmitter of unknown origin with 4 fixed position receivers, which are synchronised in relation to each other. It is however possible to also implement systems with multiple transmitters to locate an unknown receiver.

For a single transmitter to multiple receivers implementation, the first arrival of a signal at any receiver allows a 'zero' time reference point to be established. Subsequent receptions of the single transmitted signals at other receivers can then be referenced with respect to this zero time. Using the known locations of the receivers and the TDOA values obtained, a set of non-linear differential equations can be populated and these can be solved to give the (x, y, z) location of the transmitter.

TDOA has many advantages for wireless localisation; one of the key advantages is that the technique does not require any form of synchronisation between the transmitter and receiver as no TOF signals are required. The technique is therefore particularly relevant for use underwater where synchronisation is difficult. Another distinct advantage is that signals are only required to be

[13] http://www.wfs-tech.com/
[14] http://www.wfs-tech.com/index.php/products/seatooth/
[15] http://en.wikipedia.org/wiki/Multilateration

transmitted in a single direction, from the target (transmitter) to the receivers, this minimises both reflections and acoustic interference.

The main disadvantage of using TDOA is that the use of non-linear equations presents multiple candidate positions for the transmitter. From these candidate positions the actual location of the transmitter must be deciphered. This imposes a significant processing requirement for a PC to be able to achieve real-time processing of the location of the target. A further issue with the technique is that because no synchronisation is used between the transmitter and receiver, the detection of the acoustic signal at the receiver must be done through thresholding. This means that the technique is susceptible to false triggers from noise resulting in a misleading TDOA reading and therefore incorrect target location.

Parkinson G. et al, (2009) investigated the use of a TDOA based system for localising pills stored in grain. The technique used employed pulse edge detection and triggering of RF signals combined with time of flight trilateration to achieve TDOA measurements. The system demonstrated that within the medium of grain, position resolution of up to 5 cm is achievable in a vessel 1.1 m diameter and 1.27 m in height.

Bakhoum E.G. (2009) discussed the solution to the TDOA equations which is closed form and does not depend on any knowledge of range data. The paper demonstrated that assuming multipath is non-existent; it is possible to precisely locate the transmitter coordinates in 3D.

Xu, J. et al, (2011) investigates the use of TDOA measurements using Ultra wideband (UWB) for indoor localisation. The paper investigates localisation using 3 receivers with a single transmitter using a 4 GHz UWB pulse. Measurements are considered in an indoor environment with dimensions of 15 m x 15m. The receivers are located at fixed locations with 12 m separation between them. The paper uses cross correlation to calculate and select the arrival of an RF signal at the receivers. The results demonstrate that when line of sight (LOS) measurements are possible the root mean square error (RMSE) on the localisation is 0.0811 m.

Caudal, F. and Glotin, H. (2008) discusses real time underwater tracking of whales using TDOA localisation. The paper presents results for only typical speed and depth of the whales however this is over long ranges, with whales located between 1 km and 5 km from four receive hydrophones. The paper uses a widely space bottom mounted array in deep water to track the whales. To detect the signal cross correlation is used. As the actual location of the whales is unknown it is difficult to compute the accuracy of the system.

Shatara, S. et al, (2008) discusses the use of TDOA localisation for underwater robotic fish. The paper demonstrates TDOA through acoustic measurements and evaluates four different detection strategies, threshold-crossing, tone detection, correlation integral and sliding window. Underwater location experiments were conducted in a swimming pool of dimension 25 yards by 10 yards (22.9

m x 9.1 m), with depth varying from 4 yards (3.7 m) at one end of the pool to 10 yards (9.1 m) at another. The robotic fish has dimensions 14.8 cm by 6.3 cm by 5.2 cm and contains a buzzer and microphone for signal transmission and reception. Fixed receivers within the target environment also contain both a buzzer and microphone. The transmission frequency is 2.8 kHz. The results demonstrate ranging using TDOA with results using thresholding showing a maximum error of 90 cm over a 5 m range.

2.4.7 Underwater Synchronisation Options Summary

This section has investigated potential synchronisation options between transmitter and receiver to allow underwater localisation. The use of time synchronised clocks is a common technique to achieve synchronisation. High precision clocks are used to keep the transmitter and receiver synchronised, results have shown that a typical clock drift results in a positional drift of 5 cm/hr. For application in this project over short ranges this clock drift will lead to large positional errors.

Another common technique utilised underwater is the use of RTT measurements. This method does not require synchronisation between transmitter and receiver. The method is implemented either by measuring reflections, for example off the sea bed, or by interrogating an object which responds acoustically. The technique is widely used over large ranges. It is anticipated that due to the confined spaces of the target vessel a large number of reflections will be present which could make detecting the correct signal a challenge.

Bearing measurements localise the transmitter through knowledge of the impact angle of the transmitted signal at the receiver. This method does not require synchronisation; however a receiver array is required to determine small differences in the impact angle to allow accurate localisation results. The technique is not widely used from research into the literature and therefore detailed information on its positional accuracy or computational impact is unknown.

Electrical synchronisation utilises the conductive nature of the underwater medium to allow the transmission of an electrical pulse between a transmitter and receiver. While no references were found demonstrating electrical synchronisation for underwater localisation the technique of electrical communication underwater was demonstrated. This allows the development of a system which utilises the electrical signal as a trigger for acoustic transmission. Such a system utilises the relative difference in speeds of the acoustic and electrical signals through the medium to allow a TOF to be calculated. Results have observed electrical communication over a range of up to 2.2 m with a transmission rate of 100 kbps. The short range application of the project means that electrical synchronisation should be possible making this technique an ideal candidate.

Similar to electrical synchronisation electromagnetic induction utilises the ability to establish an electromagnetic field in a primary coil and detect it at a secondary coil. As this technique utilises RF properties, the speed of transmission of the signals is negligible relative to the acoustic signals and

therefore synchronisation and TOF measurements can be obtained. Research has demonstrated the use of electromagnetic synchronisation in docking stations for AUVs. The system utilised a transmission coil with diameter 64 cm with 3 receiver coils on the AUV of 9 cm diameter. The system operates up to a range of 30 m. The orientation and sizes of the primary and secondary coil is crucial to achieve good signal transmission which could present a problem for insertion into the target vessel.

TDOA does not require synchronisation but instead utilises the relative time difference in the arrival of a signal at multiple receivers to determine the location of the transmitter. To locate the transmitter there are complex calculations which utilise non-linear equations which must be solved. While no literature was found for TDOA localisation in 3D underwater, techniques utilising TDOA for grain applications have demonstrated that positional resolutions of up to 5 cm are possible in a vessel 1.1 m by 1.27 m. The short range application and excellent localisation results along with the method not requiring synchronisation make it a prime candidate for application in this project.

2.5 Acoustic Transducers

To allow the location of the pill to be determined, there is a requirement for the pill to be able to communicate with the external system. As the work for this thesis is based in water, the use of acoustics has been selected for this communication due to its low propagation speeds and penetration through the medium. To achieve this, an acoustic transducer, which is a device that converts electrical energy into acoustic output or detects an acoustic signal and converts this into an electrical output, is used. There are two construction methodologies for acoustic transducers, namely piezoelectric crystals and piezoelectric film. The active element of most acoustic transducers is piezoelectric ceramic[16].

2.5.1 Construction Method

The construction method, materials and dimensions of an acoustic transducer heavily determine its properties. Typically, for ceramic crystals, maximum acoustic power is delivered to the load when the thickness of the piezoelectric material is half of the acoustic wavelength of the material. However, because of the large acoustic impedance mismatch between the ceramic (typically, 30 MRayl) and the propagation medium (approximately 1.5 MRayl), a significant part of the acoustic wave generated in the ceramic material is reflected (Lewin P.A. 1988). The required frequency of the transducer determines the thickness of the active element; a thin wafer element vibrates with a wavelength twice its thickness[16].

To transfer the maximum amount of energy from the transducer, an impedance matching layer is inserted between the active element and the transducer face. This element should be sized such

[16] http://www.ndt-ed.org/EducationResources/CommunityCollege/Ultrasonics/EquipmentTrans/piezotransducers.htm

that its thickness is a quarter of the desired wavelength. This ensures that the waves which are reflected in the matching layer are kept in phase when they exit the layer. To achieve the maximum bandwidth from a transducer, the backing material for the active element should have impedance as closely matched to the active element as possible[17].

Piezoelectric film consists of numerous interlocking crystal domains which have both positive and negative charge. Upon compression of the film, a voltage which is proportional to this compression is produced. Piezoelectric film is typically made from polyvinylidene fluoride (PVDF). Piezoelectric film has a wide frequency range (from 0.001 Hz to 10^9 Hz), and typically has an output voltage 10 times higher than piezo ceramics for the same force input[18]. One of the major disadvantages of piezoelectric film is that it makes a relatively weak electromechanical transmitter in comparison to ceramics, particularly at resonance and at low frequencies[18].

The fabrication and characterisation of $PbZrTiO_3$ (PZT) thin film acoustic devices for application in underwater robot systems is detailed by Chang C-C. et al (2000). Results for both transmission and reception sensitivities are evaluated over frequencies ranging from 100 kHz to 4 MHz. For transmission, a driving voltage of 10 V pk-pk is utilised. The highest transmission and reception sensitivities are observed at 4 MHz, and are 76 dB and 75 dB respectively. It can be observed that at lower frequencies, such as 100 kHz, the transmission sensitivity is particularly low (less than 10 dB). An element of piezoelectric film can be observed in Figure 2-2.

Figure 2-2: An example of piezoelectric film[19]

The characteristics of piezoelectric film, such as its lightweight construction and thin film design, present interesting properties for use within the project. One option might be to coat the pill's surface in piezoelectric film to investigate the beam shape produced and see if it has omnidirectional properties. The film's low transmission sensitivity at lower frequencies however means that it is not suitable to be used as a transmitter in its basic form as a thin film. While the development of this film through careful backing materials could lead to an effective acoustic transmitter, this is beyond the scope of this research. Therefore piezoelectric film in thin sheet form has been ruled out for the work of this thesis. Transducers constructed using thin film technology, with the required transmission properties will however be considered for the purpose of this work.

[17] http://www.ndt-ed.org/EducationResources/CommunityCollege/Ultrasonics/EquipmentTrans/characteristicspt.htm
[18] http://www.media.mit.edu/resenv/classes/MAS836/Readings/MSI-techman.pdf
[19] http://www.imagesco.com/catalog/sensors/piezo.html

2.5.2 Transducer Requirements

To achieve localisation, one of the key requirements for the project is that acoustic transducers must be mounted to the pill in order to transmit signals to external receivers. To allow research to be concentrated onto appropriate transducers the requirements of the transducers must be defined. The construction of the pill, with multiple transmitters, and the expected target environment restrict the choice of transducers in a number of categories.

One requirement of the project is to produce a wireless pill which has the smallest size possible. It is intended that any pill which is inserted into a process should be of a size such that it does not interfere with or alter the process due to its insertion. This limits the available space onboard the pill to house batteries required to power the transducers. It is therefore essential that the transducers are low power. The driving voltage in this project has been limited to 10 V peak – peak, [Chapter 1.0, section 1.6].

One of the main target applications for the project is for insertion into mixing vessels. The duration of these processes can vary from a few minutes to a number of hours depending on the process. As the pill is intended to update its position regularly, nominally once per second, [Chapter 1.0 section 1.6] such that it can be tracked accurately there is the requirement for a battery source which is able to power the transducers over the maximum intended processing time. The transmitters are intended to be driven with a 10 V peak to peak signal. The use of small coin batteries has been ruled out as they contain limited charge and are low voltage; typically between 1.5 V and 3 V[20]. An example 15 V lithium ion battery with 2200 mAh has dimensions of 70 mm x 37.5 mm x 37.5 mm[21]. For this reason a pill size of 0.1 m diameter has been selected such that it has sufficient internal space to store a battery with a capacity suitable to operate for the length of the process. Therefore any transmitter which is to be mounted on the pill needs to be physically small. This relates to both the size of the transmitter face and the body of the unit which is inside the pill. A nominal transmitter size has been specified in relation to that of the anticipated pill size with maximum transmitter face diameter and depth of 0.02 m.

One of the key motivations for the project is that the construction of a single pill should be low cost, allowing the deployment of multiple pills in the future target environments. In order to achieve this, the target cost of each individual pill is in the region of £100.

To minimise the cost of each pill, the objective is to utilise the minimum number of transmitters feasible to provide the required signal coverage. To achieve this, the transmitter should provide flat signal strength over the widest possible beam angle. A transmission beam angle of 180º with uniform intensity would be desirable, minimising the number of transmitters required on the pill.

[20] http://uk.rs-online.com/web/p/coin-button-batteries/0597194/
[21] http://uk.rs-online.com/web/p/lithium-rechargeable-battery-packs/5306347/

However, this is an unreasonable expectation for low cost transmitters. A practical approach is to select a transmitter which is capable of providing the widest possible beam angle.

The final consideration for selecting the appropriate transmitter is the frequency of operation. As discussed in section 2.5.1 the optimum driving frequency depends on the individual transmitter construction and the piezoelectric crystal used; it therefore varies greatly between different transmitters depending on their application. To minimise the error on the localisation accuracy, there is a desire to have a transmitter with a high operating frequency which minimises the wavelength of the signal. The relationship between the speed of transmission (v), the frequency of transmission (f) and the wavelength of the signal (λ) is displayed in equation (2.1).

$$\lambda = \frac{v}{f} \tag{2.1}$$

To allow detection of the acoustic signal at the receivers the technique of thresholding is considered as a potential candidate. This technique relies on setting a threshold level at the receiver to allow the detection of the signal. When the signal impinges on the receiver above the threshold the point at which is the signal reaches the threshold is used to calculate the TOF of the signal. With this technique however the frequency of operation naturally introduces a small localisation error. This is due to the difference between the absolute first arrival of the signal and the threshold level which is set to detect the signal. This idea is illustrated in Figure 2-3.

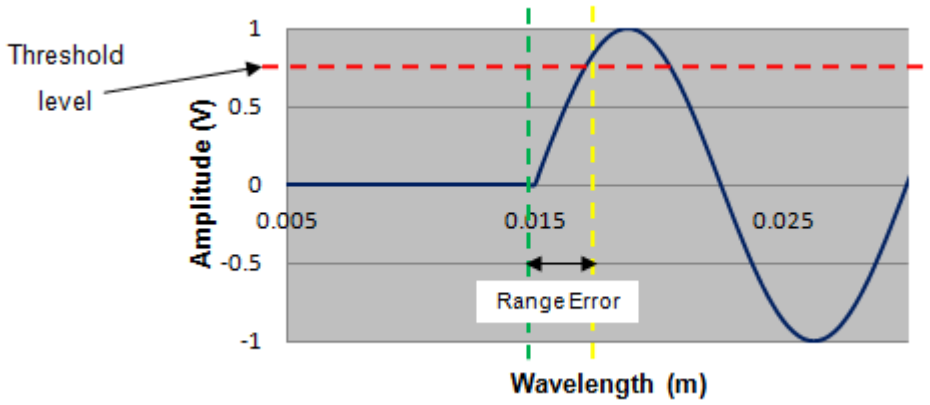

Figure 2-3: Error on localisation due to wavelength, 100 kHz signal

Figure 2-3 illustrates the reception of a 100 kHz sine wave at the receiver. It can be observed that assuming a transmission speed in water of 1484 ms^{-1} at 20°C[22], the wavelength of the signal is 0.015 m (3dp). The green line represents the absolute first arrival of the signal which should be used to calculate the TOF. As this point however the amplitude is just above 0 V, using this threshold level would leave the system vulnerable to false triggers due to noise. To alleviate this a threshold level is selected, illustrated by the red line. This threshold is selected such that noise will

[22] http://en.wikipedia.org/wiki/Speed_of_sound

not exceed this threshold level, removing the problem of false system triggers. By using this threshold however the point on the signal which is referenced has shifted as illustrated by the yellow line. Using this point to calculate the TOF means that the TOF is marginally larger than the absolute TOF.

As the maximum amplitude of the signal is unknown, the 'rise time' between the absolute first arrival of the signal (green line) and the point at which the signal passes the threshold level (yellow line) is unknown. The absolute first arrival of the signal at the receiver refers to the "perfect range" between transmitter and receiver. For signals which arrive with different amplitudes, the difference in range between the absolute first arrival and threshold point changes accordingly. This results in an error which cannot simply be eliminated. As a result of applying the thresholding method, there is always a range error. This can be improved by increasing the frequency of transmission, as this decreases the wavelength of the signal and therefore the 'rise time' of the signal.

The influence of frequency of transmission also becomes apparent when the amplitude of the first peak of the sine wave that arrives is below the threshold level. As a result, the next peak that meets the threshold level is mistakenly read as the first peak. This idea is illustrated in Figure 2-4.

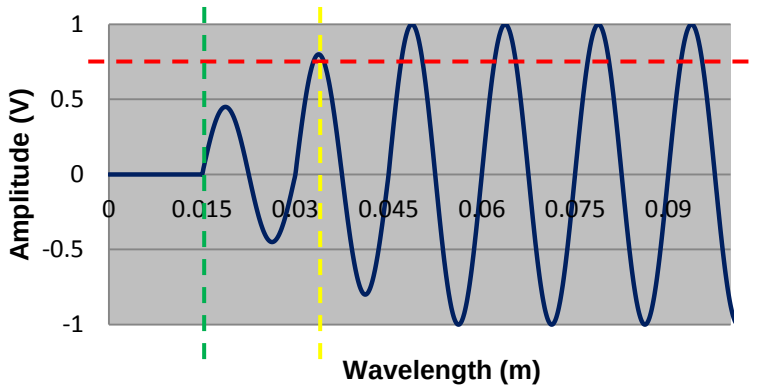

Figure 2-4: Error on localisation due to weak signal arrival

Figure 2-4 displays the arrival of a signal where the amplitude increases as the sine wave arrives. It can be observed that the first peak of the sine wave is below the threshold, and therefore is not detected. In this instance, it is the second peak which is detected, which is over a full wavelength behind the absolute first arrival. With a 100 kHz sine wave this means there will be a minimum error of one full wavelength on the ranging result, which is 0.015 m, in this case.

By increasing the frequency, the wavelength is reduced. If for example, the frequency of the signal is increased to 200 KHz. This, in turn, reduces the wavelength to 0.0075 m. As a result, the error on the range calculation is halved.

While it is desirable to select a transmitter with a high operating frequency to minimise localisation offset, there is a direct link between the operating frequency and the beam width of the

transmitter[23], where the beam width of the transducer is inversely proportional to the transmission frequency. Therefore, there is a trade off between the two requirements. Using a very narrow beam width, the pill becomes expensive due to the number of transmitters required.

2.5.3 Choice of Commercially Available Transducers

As presented in section 2.2, underwater applications for acoustic transmitters typically operate over large distances, typically in the order of hundreds of metres to kilometres. The applications cover fields of research such as oceanographic data collection, pollution monitoring, assisted navigation and tactical surveillance. The majority of commercially-available transmitters designed specifically for underwater applications are large, with high power requirements, and expensive. A selection of these is presented as follows.

Neptune Sonar's T204 transmitter[24] is a transmitter designed for deep operation and long range; it has dimensions of 48 mm diameter by 56 mm length, transmission sensitivity of 150 dB with reception sensitivity 190dB and an operating depth of 1500 m. The cost for the device is £450. Ashtead technology's Sonardyne 7656 Omni Transponder[25] is rated to a depth of 1000m with a transmission sensitivity of 188 dB and a receive sensitivity of 100 dB. The device is 72 mm diameter with length 357 mm. The device costs £600.

From the research into underwater transducers severe limitations of the available technology have been realised. While research was initially conducted into underwater transducers, the cost and power of these devices quickly eliminated them for consideration for this work. The search range was therefore broadened to investigate transmitters which are not designed specifically for underwater operation. Of the transmitters researched the most suitable options are presented in this section.

Airmar Technology[26] produces a wide range of transducers for multiple applications. Considering the requirements for this project, the AT range, which are small acoustic transmitters with high frequency operation, are best suited. The transducers of interest are the AT300, AT225, ATK200 and the AT200. A summary of these transducers are given in Table 2-1.

[23] http://www.bats.ac.nz/resources/physics.php

[24] http://edition.pagesuite-professional.co.uk/launch.aspx?referral=other&refresh=M0g81m6FB1i7&PBID=f7b8707c-94bb-4338-a20e-8c65734dcb87&pnum=50&skip

[25] http://www.ashtead-technology.com/us/Offshore/Content/131_S.html

[26] http://www.airmartechnology.com/2009/air/ultrasonic-search-results.asp

	AT300	AT225	ATK200	AT200
Transmission Frequency (kHz)	300	228	200	200
Transmit sensitivity @ 1m (dB)	95	101	102	105
Receive Sensitivity (dB)	-180	-180	-180	-174
Minimum sensing range (m)	0.04	0.08	0.1	0.1
Maximum sensing range (m)	1	2.5	3	3
Beam width –3dB (degrees)	10 ± 2	15 ± 2	10 ± 2	14 ± 2
Weight (grams)	4	4	6	6
Diameter (mm)	12	13	16	25
Length (mm)	10	19	19	25
Cost (USD$)	35.00	30.00	37.50	30.00

Table 2-1: Comparison of Airmar's AT transducer range

As shown in Table 2-1, all of the devices have a high frequency of operation. The AT300 has the shortest maximum range of operation at 1 m, which is sufficient for the expected vessel size. However, the specification is for operation in air. The dimensions and weight of the units makes them all suitable for use in the pill. The narrow beam angle of the transmitters means that there is a need for a large number of transmitters to be mounted on the pill, in order to provide sufficient coverage. With the cost of USD$30.00 per unit for the AT225 transmitter, which provides the widest beam angle, the use of multiple units on a pill is an expensive solution. For 360º coverage in only the x and y plane using the beam angle of 15°, there is a requirement for 24 transmitters (USD$720). As previously established the high frequency of operation for the devices means that the beam angle is relatively narrow.

An alternative choice of low-cost transmitters is the range of transmitters from Senscomp[27]. Similarly, these transmitters are not designed for operation underwater but could be adapted to allow underwater use. A comparison of the transmitters is displayed in Table 2-2.

[27] http://www.senscomp.com/products.htm

	S 9000	40KT08	40KPT18A	40LT10	40LT12	40LPT16
Frequency (kHz)	45	40	40	40	40	40
Transmit sensitivity @ 30cm (dB)	108	100	108	112	115	117
Receive sensitivity (dB)	-75	-80	-75	-70	-67	-65
Beam width –6 dB (degrees)	17 ± 2	125	85	72	85	55
Diameter (mm)	36	9.1	14.8	9.7	12.7	16.2
Length (mm)	12.7	4.6	13	6.7	10	12
Cost (£)	15.13	6.33	7.71	4.42	5.91	7.67

Table 2-2: Comparison of Senscomp's transducer range

Excluding the S9000 model, all the devices have an acceptable size for use on the pill with dimensions of less than 20 mm x 20 mm. In comparison to the devices by Airmar the beam widths of these devices are also substantially larger, with a maximum – 6dB angle of 125º for the 40KT08 transmitter. All of the available models are also relatively cheap; with a majority of devices costing less than £10 per unit.

While the transmit sensitivities specifications for both the Senscomp and Airmar devices are similar, the transmit sensitivity specified for the Senscomp devices are for a 30 cm range, while the Aimar devices are for 1 m. This suggests that the signal strength from Senscomp devices will be significantly less. It is however worth noting that the stated performances for both cases are for operation in air, and as such the change in the transducers characteristics when operated underwater is unknown.

The primary concern with the Senscomp transmitters relates to the relatively low transmission frequency of operation at 40 kHz. This will impact on the theoretical localisation accuracy of the system as the signal at this frequency has substantially longer wavelength. While the nominal frequency of operation is 40 kHz, there is the option to experiment with the transmitter at a higher frequency. However, it would be envisaged this would reduce the received signal amplitude.

The transmitter selected for experimentation for the purpose of this work is the Senscomp 40KT08. While the products from Airmar have better suited operating frequency range, the narrow beam width and the cost of the transmitters means that for this project the cost to provide full beam coverage from the pill is above a reasonable level, as one of the aims of this work is to produce a low cost pill for localisation. Of the Senscomp devices available, the 40KT08 has the widest transmit beam width at – 6 dB, making it the preferred option to achieve omnidirectional beam coverage.

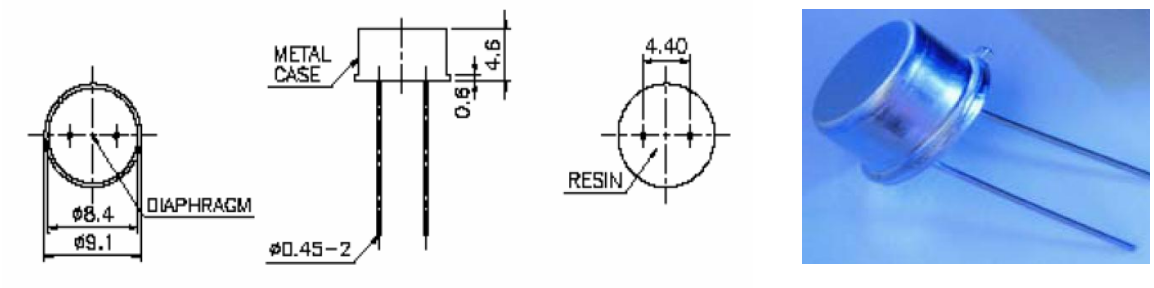

Figure 2-5: Transmitter encapsulation diagram[28]

Figure 2-5 displays the transmitter layout and its encapsulation. The transmitter face, with diameter 8.4 mm and depth of 4.6 mm, makes the size ideal to be mounted on a pill with diameter 100 mm. The encapsulation of the transducer in a water resistant housing and with an external flange presents the option to mount the transducer through the pill housing. This maximises the internal space within the pill as the intrusion of the transmitter is minimised. It should also maximise the transfer of signal from the transmitter as it is not attenuated and reflected at the transmitter/pill housing interface. The closed face construction of the device prevents water ingress meaning it should be suitable for insertion directly into the water.

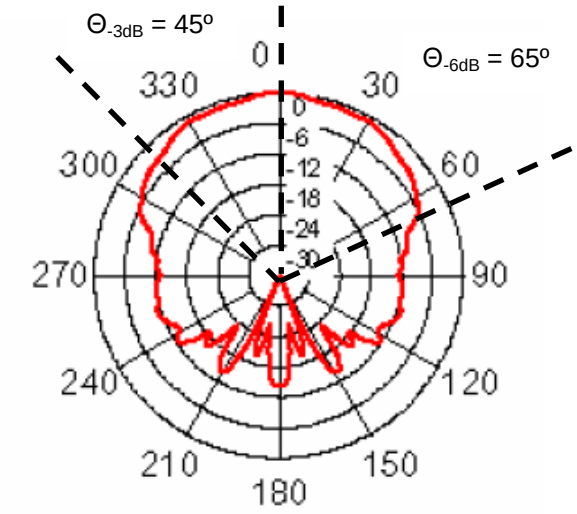

Figure 2-6: Senscomp specified transmitter beam profile[28]

Figure 2-6 displays the beam profile of the transmitter for operation in air at a transmission frequency of 40 kHz, as specified by Senscomp. The specified θ_{-6dB} angle is just over 60º, giving a full beam width of approximately 130º. From Figure 2-6, it is shown that the θ_{-3dB} angle observed at approximately 45º is able to provide a full beam width of 90º.

2.5.4 Acoustic Transducers Summary

This section has investigated the properties of acoustic transducers and defined requirements for this project to allow research into suitable commercially available transducers. The transducer

[28] http://www.senscomp.com/specs/40KT08%20%20spec.pdf

construction method has been found to heavily determine its properties. Two main methods of transducer construction exist, the use of ceramic piezoelectric crystals and piezoelectric film.

Piezoelectric film works excellent as a receiver, without output approximately 10 times higher than piezoelectric crystal for the same input. Research has shown however that at low frequencies, it makes a relatively weak transmitter, with less than 10 dB sensitivity at 100 kHz. In its natural form piezoelectric film is not usable due to its requirement for a suitable backing material, the development of which is beyond the scope of this project.

To select appropriate transducers the transducer requirements were defined. The intended small size of the pill means that battery space is limited onboard, hence the transducers must be low power, with driving voltage of 10 V peak to peak suggested. The intended pill diameter of 100 mm means that any transducer on the pill must be physically small, nominal dimensions for depth and face width were defined as 20 mm.

Transducers must also be low cost, the target pill cost to allow the insertion of multiple pills is £100 per pill. To minimise cost and reduce transducer numbers transducers should have a wide transmission beam angle with uniform intensity. The final consideration for transducers is their operating frequency. Low operating frequencies travel further in water however a higher operating frequency offers better localisation accuracy. With a target accuracy of 10 mm in the vessel an operating frequency in the region of 100 kHz has been suggested.

Based on the transducer requirements established, section 2.5.3 has investigated commercially available transducers which meet the requirements of the project. Research has been undertaken into both underwater and non-underwater transducers. The typical application for underwater transducers, over large distances, means that research has shown underwater transducers to be unsuitable. They have large power requirements, in the order of hundreds of watts, large physical size and weight and are also expensive, in the region of hundreds of pounds.

Therefore, research has concentrated on transducers not designed for underwater operation. From the commercially available options the 40KT08 transducer has been selected for use. The devices show good transmission properties with wide beam angles, -3 dB of 45° and small physical size, depth and face dimension less than 20 mm. They are also a cost effective option at £6.33 allowing multiple units on the pill. For this reason the Senscomp 40KT08 has been selected as the transmitter for mounting on the pill.

2.6 Transducer Array Design

As detailed in Chapter 1.0, one of the main objects for the project is to develop a pill which is able to be localised irrespective of its location in the vessel. To achieve this, there is a requirement for the pill to produce signal in all directions and with as near as possible uniform amplitude. From the

research conducted into small low cost acoustic transducers and the associated beam coverage achievable from a single unit, in order to create uniform coverage, there is a requirement for multiple units on the pill in an array format.

A transducer array is a configuration of multiple transmitters such that the beam patterns of the individual transducers interact in a manner that produces the desired beam shape and amplitude profile for a specific application. Through the use of multiple transmitters, it is possible to create a beam profile which cannot be achieved by a single unit alone and tailor the beam profile to best suit the requirement of the application.

To create the desired beam profile, there are two methods of configuring the structure of the transmitter array. The first method is through strategic placement of the transmitters. The desired beam profile is then created through simultaneous excitation of the transmitters. The second method is through sequential excitation of an array of transmitters aligned adjacent to each other. This method is termed an active phased array (APA).

With a transmitter array which relies on the placement of the transmitters to create the desired beam profile, one of the main advantages is the simplicity of implementation, as all of the elements of the transmitter are excited simultaneously. The main disadvantage of this technique is that as the transmitter locations are fixed, the beam pattern is also fixed.

APAs do not have the limitation of a fixed beam pattern. These systems rely on a group of transmitters in which the phases of the signals are altered such that they can create the desired beam pattern of the application[29]. The main advantage of this technique is that by changing the sequence in which the transmitters are excited, it is possible to produce multiple different beam patterns and also actively scan the beam across a wide area. This technique is commonly used in radar applications. The disadvantage of using a phased array is that there is the requirement for complex electronics to control the excitation sequence of the transmitters to produce the desired beam profiles.

The majority of the literature focuses on the development of transmitter arrays utilising electronically scanned arrays. A selection of the literature is detailed below:

Harput S. and Bozkurt A. (2008) discussed the use of an ultrasonic phased array for acoustic imaging in air. Two linear transducer arrays were constructed from commercially available transducers to perform the acoustic imaging. The paper investigated how to eliminate grating lobes from the system by having different element spacing for the transmitter and receiver arrays. The transmitter array was made up of 6 individual transmitter elements and the receiver array was made up of 4 elements. Both the transmitter and receiver arrays used beamforming to sweep the

[29] http://en.wikipedia.org/wiki/Phased_array

acoustic beam to detect objects, the system performs imaging by determining the acoustic reflectivity of objects. The paper demonstrated how the array was able to determine the location of multiple separated wooden blocks up to a range of 2 m without the formation of ghost images. The resolution of the system was approximately 4.5°.

Boltryk P. et al, (2004) investigated the use of transducer arrays for velocity measurements in underwater vehicles. The paper investigated the system of Correlation Velocity Log (CVL) to determine the speed of an underwater vehicle. Typical CVL consists of an ultrasonic transmitter and an array of receiver elements. Two short duration signals with a known time separation were transmitted to the seabed and the receiver was used to detect the reflections of these signals. In trials in a reservoir environment, results indicated that the developed system closely tracked the data observed from GPS measurements. The system described in this paper utilised a receiver array rather than a transmitter array.

Alkoy S. et al, (2001) discussed the construction of a directional transducer array from piezoelectric ceramic hollow spheres. The individual elements were created into arrays of (2x2), (4x4) or (6x6) elements. Results showed that through the use of multiple receivers in a (4x4) array connected in series, the free field voltage sensitivity (FFVS) of the array was increased by 12 dB over a single receiver. From a transmitting perspective, it was observed that the transmitting response for a 4x4 array was 22 dB higher than for a single element. The paper also investigated the effect that element size had on the transmitting sensitivity of the array. The results demonstrated that by increasing the element radius from 1.15 mm to 1.35 mm, a 12-15 dB increase in transmitting sensitivity was possible due to the increased radiating area.

From a review of the literature, the majority of work on the design and creation of transducer arrays for application above ground or for underwater are concerned with the design of a receiver array rather than a transmitter array. To this end, no work has been located with respect to the design of a transmitter array for deployment on a sensor node to allow localisation of the node. As such the development of a transmitter array to allow localisation of a moving sensor node is of interest to this thesis.

2.7 Literature Review Summary

This chapter has conducted research into areas related to the development of an underwater pill for localisation in confined spaces. Section 2.1 has investigated WSNs, providing background information on their typical applications, structures and limitations. The development of WSNs is progressing with commercially available sensor nodes available. For localisation, systems typically utilise RF localisation, with many using GPS to localise.

Based on the research on WSNs section 2.2 has specialised in the area of UWSNs. Research has demonstrated that the development of UWSNs is at an earlier stage in comparison to WSNs. The

transmission medium limits the choice of transmission method, which is typically acoustic, complicating the issues of localisation and communication. UWSNs are employed for monitoring over large ranges, usually from hundreds of metres to kilometres which means that typical acoustic transducers are physically large with large power requirements. The literature search has found only one application of an UWSN in a small space of 40' x 40' x 18' (12.2 m x 12.2 m x 5.5 m). In this application nodes were stationary and localisation was not considered. No previous examples of localisation of underwater nodes in confined spaces were found.

The research into underwater transmission modalities is summarised in section 2.3.4. While optical, RF and acoustics have all been considered the most appropriate option is acoustics which has the advantage of low propagation speed and low attenuation in aqueous media.

Research into underwater synchronisation options has been investigated in section 2.4. To allow localisation of the pill it is crucial that the pill can be synchronised with an external system, allowing TOF measurements and localisation. The result of this research is summarised in section 2.4.7. Typical underwater localisation techniques such as the use of precision clocks for synchronisation or RTTs to calculate TOFs have been ruled out for use within the project due to positional error and transmission receiver complexity respectively. Two techniques have been selected for further consideration namely, electrical synchronisation of TOF measurements and TDOA, a technique which allows localisation without the requirement for synchronisation.

In section 2.5 acoustic transducers are researched, selecting a transducer appropriate for mounting to the pill. The research is summarised in section 2.5.4. Research has demonstrated two construction techniques for acoustic transducers, with the use of piezoelectric ceramic crystals deemed the most suitable for use in the project. The requirements for acoustic transducers in the project have been defined, allowing research into commercially available transducers. The key requirements are size, power, beam width and cost. Underwater acoustic transducers do not meet these requirements and therefore acoustic transducers not designed for underwater operation have been considered. Of the available choices the Senscomp 40KT08 has been selected, with a key area of research being how operation underwater affects the signal strength and beam pattern produced.

Finally in section 2.6, research has been conducted into current strategies for transducer array design. The research has demonstrated that typically active phased arrays are utilised which use beamforming. This uses multiple active transducer elements which are activated in sequence to allow the beam shape from the array to be altered or zones to be swept. The advantage of this is that the array is able to create multiple different beam patterns. The disadvantages relate to the complexity of the excitation system. The design of an active phased array is beyond the scope of this research. The shaping of beam patterns through the placement of transducers alone has not been observed in the literature. This creates an opportunity for research to investigate how the location of transducers on the pill influences the beam shape.

3.0 Wireless Localisation

This chapter discusses the work undertaken regarding wireless localisation and underwater synchronisation options for the project. From the literature search conducted in [Chapter 2.0, section 2.4], numerous possible underwater synchronisation techniques are available. To allow the location of the pill to be derived knowledge of the transmission time of the signal is required. This allows the time of flight (TOF) and therefore range between the transmitter and receiver to be determined. From this information it is possible to localise the pill. Therefore a key challenge within this project is to determine a suitable technique to allow synchronisation between the pill and external receivers or to investigate localisation techniques which do not require TOF information in order to localise the pill.

From the research conducted in [Chapter 2.0, section 2.4] two potential methods have been selected for investigation. The first is the use of electrical signals between the pill and receiver to allow a TOF to be determined. The transmission speed of electrical signals through water is significantly higher than that of acoustic signals; this makes it possible to send an electrical to trigger timing of the acoustic signal. Upon reception of the electrical signal at the receiver timing can begin allowing the TOF of the acoustic signal to be determined.

The second technique is to utilise time difference of arrival (TDOA). Unlike techniques which utilise TOF measurements, there is no requirement to synchronise the transmitter and receiver using TDOA. Instead, the location of the transmitter is determined through knowledge of the time difference of arrival of the transmission signal at multiple receivers.

This chapter details the evaluation of both techniques to determine their suitability for this project. In section 3.1 the technique of synchronisation through electrical means is explored. This section discusses the background and principles of operation before detailing experimental work undertaken to test its validity for use within the target environment. This includes work discussing the impact that electrode sizes have on the received signal strength and the influence of electrode orientation.

In section 3.2 the technique of time difference of arrival (TDOA) is investigated. This section discusses the theory of operation from first principles followed by simulation to explore the feasibility of this technique for localisation of a single transmitter.

3.1 Exploration of Electrical Synchronisation

3.1.1 Background

From the literature review and the work conducted by Joe J. and Toh S.H (2007) the ability to transmit an electrical pulse between two sets of underwater electrodes was demonstrated providing supporting evidence for the suitability of this method for electrical synchronisation.

The limitations of their research for application within this thesis relate to the set-up of their experiment. The transmitting electrodes are driven from a commercial power supply and signals are detected by receiving electrodes connected to an oscilloscope. In the present project the transmitter or receiver is anticipated to be mounted on the pill. Hence, the power source is provided by a battery. Therefore, it is necessary for this work to include an investigation into the feasibility of using a low voltage battery for transmission.

A secondary area of research, which is also related to the fact the power source has an isolated ground is the directionality of electrical synchronisation, where two distinct modes of operation present themselves. The first is transmission from vessel to pill whereby a synchronisation pulse is generated at the host system and transmitted through the medium; reception of this pulse by the pill would trigger the pill to respond acoustically. Due to negligible transmission time of electrical pulses through water, timing of acoustic signals can commence on reception of the electrical pulse. This method allows high driving voltage for the electrical pulse due to external power supplies but creates more processing requirements on the pill as the pill must detect the electrical signal, process it and respond acoustically.

Similarly, the second option is transmission of the electrical and acoustic signals simultaneously by the pill. This method reduces the computational load on the pill as it is only required to transmit signals. However, the maximum possible electrical drive voltage is limited as this comes from an onboard battery supply, which could limit the operational range of the pill.

Electrical synchronisation has the advantage that as the localisation system is triggered from an electrical signal it should be less susceptible to false triggers due to noise in the vessel, as acoustic timing does not commence until the detection of an electrical pulse.

3.1.2 Preliminary Testing

As a test set-up for the work on electrical transmission through water with an isolated power supply a monostable-timer circuit was constructed producing a clock output at a preset frequency. A 12 V battery source is used to drive this circuit. (Joe J. and Toh S.H 2007) demonstrated the transmission of a 100 kbps signal through water for communication purposes. The results however show low pass filtering of the signal due to the medium which distorts the received signal shape. As the electrical signal is in this instance to be used for synchronisation and not communication there is not the requirement for such a high transmission rate. The pill's location is anticipated to be

updated approximately once per second, however, to allow for a more regular update, a transmission rate of 100 Hz was tested. This provides the opportunity to increase the localisation rate but is still sufficiently low such that the received signal shape is not distorted.

The initial experimental set-up utilised the timer with single core wire connected to the output pin and the 0 V rail of the board. These wires were used as the transmission outputs and placed within a plastic container of dimensions 8 cm diameter and 10 cm in height filled with tap water. Two receive wires were connected to the positive and negative oscilloscope terminals.

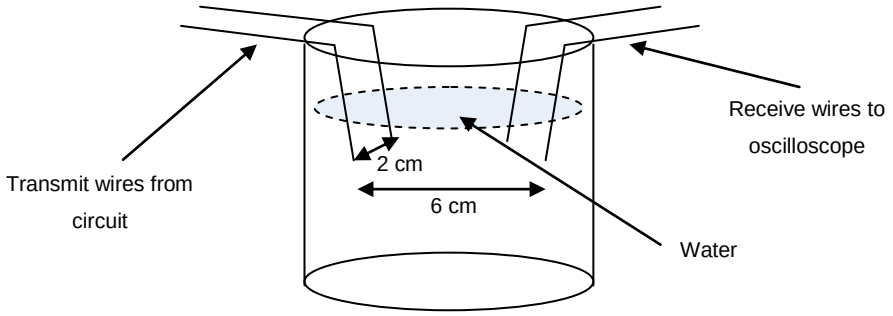

Figure 3-1: Initial testing set-up

Figure 3-1 shows the experimental set-up. A separation distance between transmit wires of 2 cm was maintained with the receive wires being positioned with the same separation. A 6 cm range between transmit and receive pairs was initially tested, with transmission voltage set at 12 V.

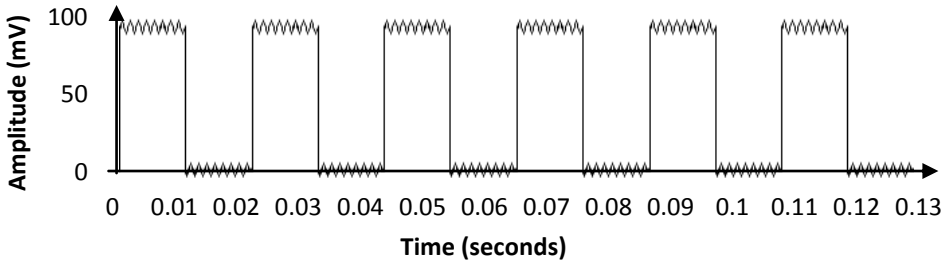

Figure 3-2: Received signal transmitted through water

Figure 3-2 is an illustration of the received signal as observed at the oscilloscope when transmitted through the aqueous solution. A relatively clean square wave can be observed with some high frequency noise. The amplitude of the signal has been reduced substantially to 100 mV; the outline of the received signal however remains distinguishable in relation to the transmitted signal with minimal distortion due to noise. The amplitude of the high frequency noise is approximately 5 mV.

3.1.3 Electrode Size Testing

The use of specific electrodes to influence both the size of the signal received and the shape of the receive field by altering the shape of the transmit electrodes, effectively creating directional electrodes, was demonstrated by Joe J. and Toh S.H (2007) Results demonstrated how electrodes could be used to enhance the received signal strength of a signal while minimising noise.

Opportunities for scale up mean that the requirements for transmission across distances of the order of metres are an important consideration. To increase the signal strength of the underwater channel the optimisation of the electrodes was explored. As discussed in Joe J. and Toh S.H (2007) the size of electrodes has been demonstrated to have an effect on the received signal strength. Therefore, for initial tests 4 electrodes, each 1 cm square, were utilised. This small electrode size was selected such that the results obtained can be used as reference results for further tests with larger electrodes. The initial testing set-up described above was maintained to allow a fair comparison for results, with separations of 2 cm between electrode plates from the edge of each electrode plate and 6 cm between transmitter and receiver pairs as observed in Figure 3-3**.**

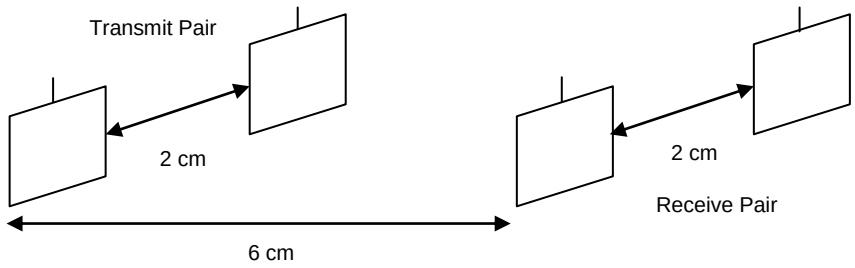

Figure 3-3: Electrode testing set-up

The received signal strength for this experiment was 750 mV, a 7.5 fold improvement on the original 100 mV received with only bare wires (negligible electrode size). Noise observed on the signal is approximately 2 mV, an improvement on the test using bare wires as electrodes. Results confirm those described in the literature with a substantial improvement in received signal strength due to the use of electrodes at the transmitter and receiver.

To investigate the effect that electrode size has on the received signal strength, a set of electrodes was produced with dimensions 5 cm square. In this case, the surface area for each electrode is 25 times greater than for the 1 cm square electrodes. Maintaining the same electrode separations measurements were acquired using the 5 cm^2 electrodes only. It was observed that the large increase in electrode size has negligible effect over the received signal strength, with the received signal strength being maintained at approximately 750 mV. This result suggests that the use of larger electrodes within this environment has little impact upon the received signal strength and that an increase in receiver and transmitter surface area relates to a minimal increase in received signal strength. The result suggests there is a limit on the improvement in received signal strength which is possible through purely increasing the electrodes size.

Due to the encouraging results work was undertaken to determine the most suitable transmission direction for the synchronisation pulse. Two options are available, transmission of the synchronisation pulse from external electrodes to the pill or transmission of the electrical synchronization pulse from the pill to the external electrodes.

3.1.4 Vessel to Pill Transmission of the Electrical Synchronisation Pulse

In order for the synchronisation pulse to be detected via the pill receive circuitry is required onboard the pill and must be powered from a battery source. To determine the viability of this method the oscilloscope was replaced by a battery powered receive circuit. This consisted of a high impedance operational amplifier (op amp) used to drive an LED on detection of a synchronisation pulse. An AD623 op amp with adjustable gain of 1 K and input impedance 2 GΩ was selected to allow the detection of a small difference in electric field set up between the two receive electrodes.

The small test environment was again utilised with tap water as the medium for conduction and electrodes of 1 cm by 1 cm. The output of the op amp with gain of 1 during test was between 0.2 and 0.4 V. With the gain set to 10 results demonstrated the correct detection of a synchronisation pulse due to the illumination of the LED. To test the effective range of this synchronisation set-up a test was undertaken in the anticipated target vessel. The target vessel is a metallic vessel with diameter 0.6 m and height 1 m. For this thesis it will be referred to as the 250 litre vessel.

The battery powered receive unit was encased in a floating container to allow free movement throughout the 250 litre vessel. The separation of the transmit and receive electrode pairs was set at 5 cm. The transmission electrodes were mounted to a strip of plastic to reduce the possibility of the transmission signal going straight to the ground of the vessel rather than through the water to the receiver. This can be seen in Figure 3-4. They were also mounted 5 cm from the vessel edge. The range of the receiver unit from the transmitter electrodes was manually adjusted.

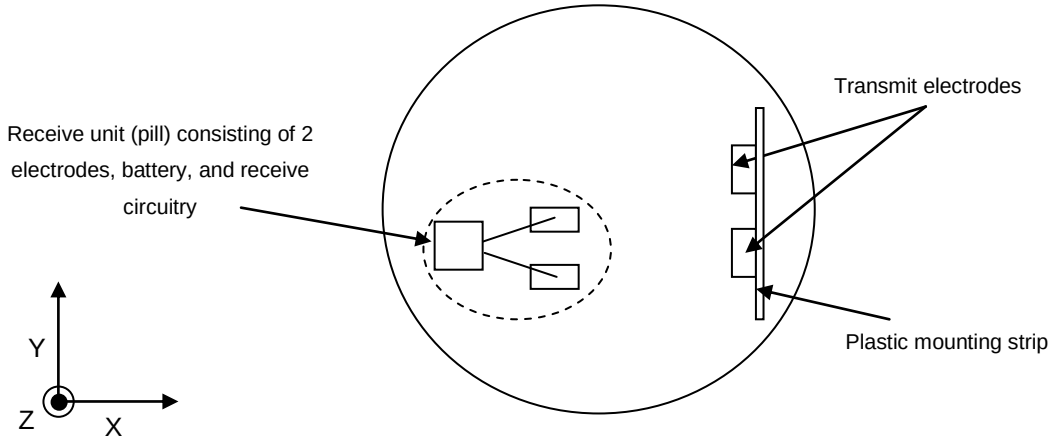

Figure 3-4: Transmission from vessel to pill set-up

With range between transmitter and receiver electrodes of less than 5 cm detection of the synchronisation pulse is possible however as the range is increased beyond 5 cm the received signal strength is no longer sufficient to illuminate the LED. In order to double the operational range from 5 cm to 10 cm the gain of the receiver op amp needs to be significantly increased from 10 to 150. To allow reception across the 60 cm diameter of the vessel the gain required on the op amp needs to be increased to such a point that noise within the vessel is sufficient to trigger a false reception result at the receiver. For this reason transmission of the signal pulse from the vessel to the pill can be eliminated for use within this thesis.

3.1.5 Pill to Vessel Transmission of the Electrical Synchronisation Pulse

An alternative arrangement to allow synchronisation between the pill and vessel is to transmit the electrical synchronisation signal from the pill to electrodes on the vessel wall along with the acoustic signal allowing TOF data to be obtained. An experimental set-up exploiting the battery powered transmission hardware with 50 Hz transmission frequency and 12 V driving voltage was used as the drive circuitry, electrodes of 1 cm square were used for both transmit and receive pairs. Transmitter electrodes were mounted 5 cm apart with receiver electrodes 5 cm apart and mounted 5 cm away from the vessel wall. The experiment is conducted in the 250 litre vessel.

Results demonstrated that reception of the pulse was possible over the full dimension of the vessel for this set-up. In comparison to pilot scale tests the noise level observed increased from approximately 5 mV to 10 mV. The received signal strength is observed to be inversely proportional to the range between transmitter and receiver electrodes. Results also demonstrated that for a fixed range between transmitter and receiver electrodes, increasing the separation between the receive electrodes increases the received signal strength.

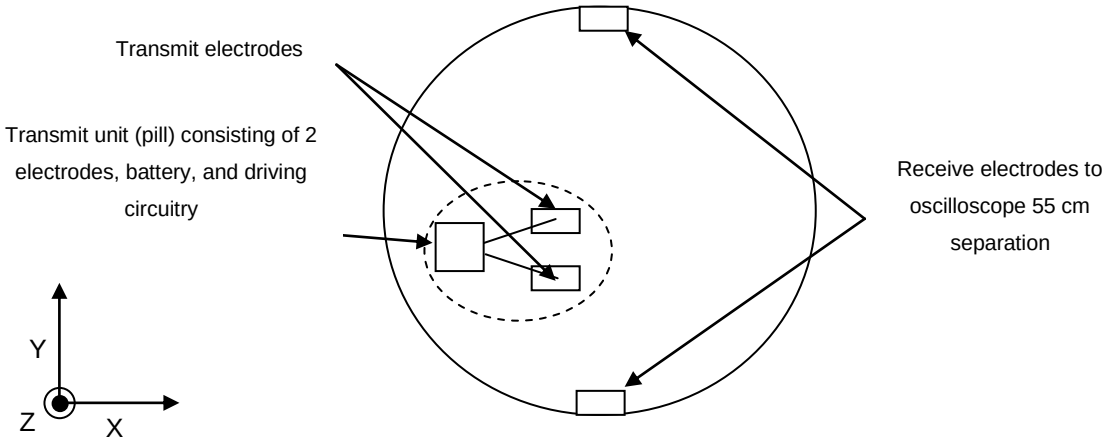

Figure 3-5: Vessel set-up testing maximum electrode separation

Figure 3-5 shows the configuration for testing the maximum receiver electrode separation within the vessel. The separation between transmission electrodes will be limited due to the size of the pill however the separation for the receive electrodes can be up to the maximum vessel diameter. With this test set-up it was observed that the received signal strength at the receiver for a 12 V driving voltage is approximately 750 mV.

Testing also identified a relationship between electrode orientation and received signal strength. With transmit and receive electrodes perpendicular no signal is received, in all other directions a signal is received however this varies in relation to the relative angle of transmit and receive electrodes; the strongest signal is witnessed when the transmit and received electrodes are parallel.

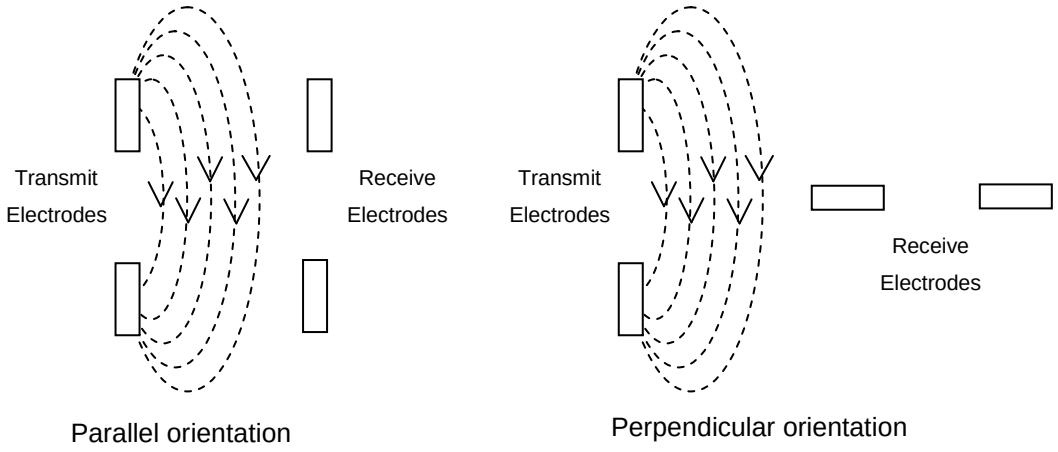

Figure 3-6: Receive electrodes parallel and perpendicular to transmit electrodes

Figure 3-6 displays the layout for parallel and perpendicular receive electrode orientations. The influence orientation has upon the level of received signal can be attributed to the electric field within the vessel and the manner in which the receive electrodes intercept this field. The transmit electrodes set up an electric field between the positive output pin and the 0 V pin. When the receive electrodes are perpendicular to the transmit electrodes then the field lies perpendicular to the receive electrodes. As such, at the point which the field lines cross the electrodes each electrode detects a signal which has approximately the same potential, therefore no potential difference is detected. For the parallel case field lines cuts through both receive electrodes with the field line having a different potential at each electrode, hence an electric potential is observed between the receive electrodes and displayed by the oscilloscope.

3.1.6 Electrode Orientation

The orientation of both transmit and receive electrodes has been shown to be a crucial factor in the received signal strength. To maximise received signal strength and therefore vessel coverage exploratory work on the use of multiple electrodes was conducted. To negate the problems associated with electrode rotation, a second set of receive electrodes were added perpendicular to the original receive electrodes to cover all possible transmit electrode orientations.

Using four receivers connected to two separate channels on an oscilloscope the system is able to constantly track a signal. When the transmit electrodes lie parallel to the receive electrodes connected to channel 1 of the oscilloscope a signal is detected on channel 1. As the receive electrodes connected to channel 2 of the oscilloscope lie perpendicular to the transmit electrodes at this point channel 2 detects no signal. The inverse is true when the pill is rotated such that the transmit electrodes lie parallel to the receive electrodes connected to channel 2. In this instance a signal is detected on channel 2 however channel 1 no longer detects a signal. The option of using 4 transmitter electrodes is also possible to compensate for coverage however by using the receiver set-up power usage can be minimised on the pill.

3.1.7 Electrical Synchronisation Summary

This section has investigated the technique of electrical synchronisation, with the aim being to determine if it is a viable option to allow TOF localisation. This section has been a brief investigatory study into electrical synchronisation to substantiate information obtained through the literature review. While experiments have been completed to determine its viability in the vessel alternative methods are proposed within this research for localisation and therefore only preliminary experiments were conducted.

Initial testing was undertaken to determine if using a battery power transmitter a received signal could be detected at the receiver. Testing demonstrated that using a four wire set-up it was possible to detect a potential difference at the receiver over a short range. To enhance the signal strength and reduce noise electrodes were considered at both the transmitter and receiver. With a 1 cm square electrode the received signal strength was seen to improve by a factor of approximately 8 over bare wires.

From initial testing, work was undertaken to determine in which direction electrical signals should be transmitted to maximise received signal strength and also minimise complexity. Testing signal transmission from the vessel to the pill was conducted with receive circuitry designed for the pill. Results showed that the electrical signal could only be received up to a range of 10 cm between the transmitter and receiver. To increase the range further the gain on the receiver must be increased to a point such that it is susceptible to false triggers due to noise. For this reason it is not possible to transmit the electrical signal from the vessel to the pill.

Experiments to explore transmission of the electrical signal from the pill to external receivers utilised a battery power transmission source with a driving voltage of 12 V. Results demonstrated that the electrical signal can be detected at the receiver over the diameter of the vessel, at a range of 0.5 m. It was also observed that the received signal strength can be increased by maximising the separation of the receive electrode pairing. With the receivers mounted on opposing walls of the vessel the detected received signal level was 750 mV over the 0.5 m range.

Through testing, the orientation of transmit and receive electrodes with respect to each other have been demonstrated to have a large impact of the received signal strength. With transmit and receive electrodes perpendicular it has been shown that no signal is detected. The rotation of the pill means that to ensure signal reception regardless of the pill's orientation there is a requirement for 4 receive electrodes mounted perpendicular to each other. From the results observed electrical synchronisation between the pill and external receivers is a viable option to allow TOF localisation. Based on the limitations of the vessel diameter it has been shown that for a 12 V driving signal, electrical synchronisation is a viable option over 0.5 m, with a 750 mV received signal strength. As alternative strategies for localisation were also researched the experimentation was concluded at this preliminary stage,

3.2 Time Difference of Arrival

Time Difference of Arrival (TDOA) localisation systems utilise the relative time difference in arrival of signals at multiple receivers rather than absolute TOF measurements to determine the location of a target, (Exel R. et al, 2010, Xu, J. et al, 2011). As such this technique, unlike electrical methods, does not require synchronisation between the pill and external system. For the test environment chosen this presents a substantial advantage, reducing unwanted signals and requiring only four acoustic receivers to be mounted to the vessel wall. Due to the nature of the vessel and the difficulty synchronising the transmitter and receiver underwater TDOA suggests itself as a prime candidate to alleviate synchronisation issues.

3.2.1 Theory

For techniques which rely on synchronisation between transmitter and receiver a TOF for the signal can be determined. This TOF means that for a single receiver a sphere of possible locations for the origin of the signal can be established. With multiple receivers then each receiver has a sphere where it believes the transmitter could lie and the common point of intersection identifies the transmitter location.

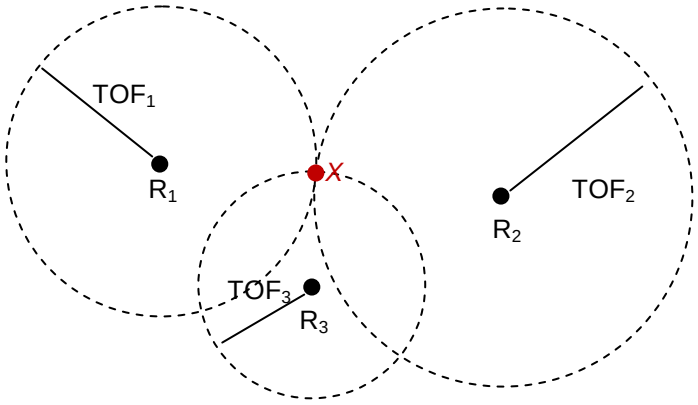

Figure 3-7: TOF localisation through intersecting spheres

Figure 3-7 illustrates the localisation of a transmitter in 2D with the use of 3 receivers. In this instance 3 TOFs, one for each receiver is established with creates 3 spheres where the transmitter could lie. Point X is the only point in which all of the spheres intersect and therefore is the only point where the transmitter could be located to produce the TOF values obtained. When noise is introduced to the measurements the spheres do not intersect perfectly and a region of uncertainty is created where the spheres overlap (Grosicki, E. and Abed-Meraim, K. 2005). In this instance techniques such as least mean squares can be used to calculate the target location which minimises any error.

In contrast to techniques which utilise TOF and therefore intersecting spheres to determine position, TDOA does not use absolute TOF data but relative time of arrival in comparing the arrival time of a signal at multiple receivers. The TDOA information therefore does not create a sphere

around the receiver on which the transmitter location lies, but rather it creates one half of a two sheeted hyperboloid (Exel, R. et al, 2010). This idea is illustrated in 2D in Figure 3-8.

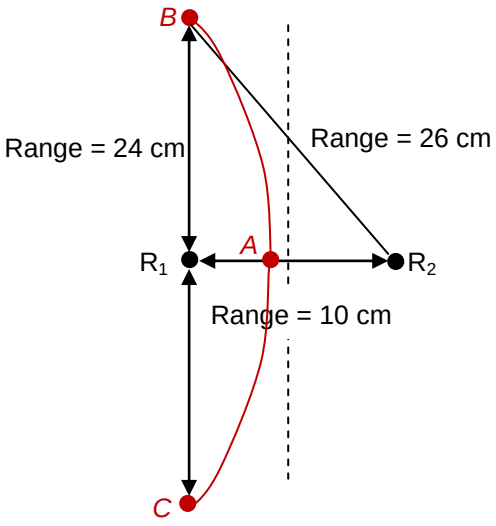

Figure 3-8: One half of two sheeted hyperboloid shape in 2D due to TDOA

Figure 3-8 considers two receivers R_1 and R_2 located 10 cm apart. If we consider that the TDOA between these receivers, from an unknown transmitter location gives us a range difference of 2 cm then there are multiple points at which the transmitter can lie. Point A lies directly in-between receivers R_1 and R_2, the range to R_2 is 6 cm and the range to R_1 is 4 cm therefore the range difference between them is 2 cm. It is also possible for the transmitter to be located, for instance, at point B. In this instance the range to R_1 is 24 cm and the range to R_2 is 26 cm which again gives us a range difference of 2 cm. Therefore for this TDOA value and subsequent range difference both of these potential transmitter locations are valid. The same is true for location C and all of the locations highlighted by the red line.

When this discussion is extended into 3D then there are possible transmitter locations which lie above and below the plane of the page. The possible solutions to the 3D localisation problem using TDOA lie on one half of a two sheeted hyperboloid such as the example in Figure 3-9.

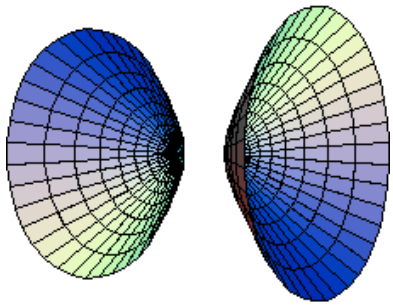

Figure 3-9: Two sheeted hyperboloid[30]

[30] http://mathworld.wolfram.com/Hyperboloid.html

With the use of two receivers it is possible to locate a transmitter onto a hyperboloid (Xu, J. et al, 2011). With the use of 3 receivers then it is possible to locate a transmitter in 2D at the intersection of 2 separate hyperboloids. If 4 receivers are used then 3 hyperboloids are created and it is possible to locate a unique point in 3D space. This is illustrated, in 2D, in Figure 3-10.

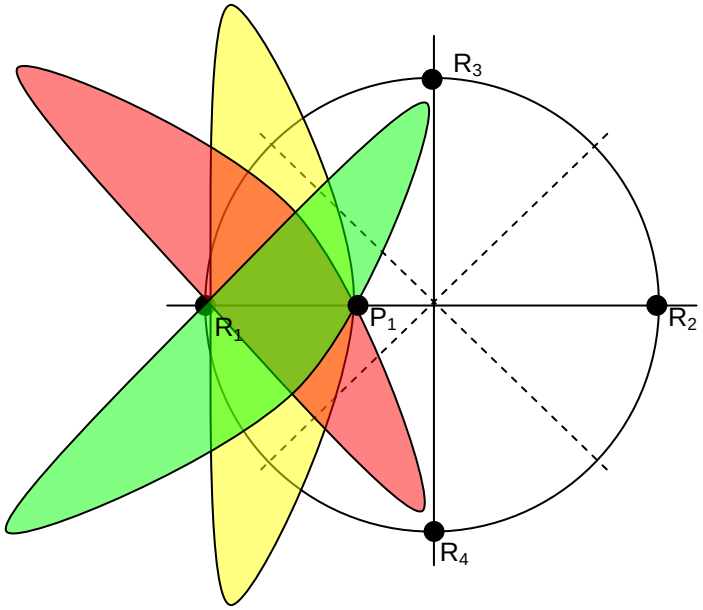

Figure 3-10: Schematic Representation of the Intersection of 3 hyperboloids

Figure 3-10 shows the intersection of 3 hyperboloids in 3D. If the yellow hyperboloid represents a TDOA between receivers R_1 and R_2 as has been illustrated in Figure 3-8 then the transmitter must lie on that hyperboloid. For a TDOA between receivers R_1 and R_3 a second hyperboloid is created, shown in the red in Figure 3-10. If the TDOA between receivers R_1 and R_4 is considered then the green hyperboloid is created. Remembering that these hyperboloids are sheets and not solid objects then the only single point of intersection is at the point P_1 which is the unique transmitter location.

The solution to TDOA can be derived as follows. With an unknown transmitter location represented as *x, y, z* and 4 known receiver locations *A, B C* and *D* then for each a TOF can be considered as follows,

$$T_A = \frac{1}{c}\left[\sqrt{(x - x_A)^2 + (y - y_A)^2 + (z - z_A)^2}\right] \quad \textbf{(3.1)}$$

$$T_B = \frac{1}{c}\left[\sqrt{(x - x_B)^2 + (y - y_B)^2 + (z - z_B)^2}\right] \quad \textbf{(3.2)}$$

$$T_C = \frac{1}{c}\left[\sqrt{(x - x_C)^2 + (y - y_C)^2 + (z - z_C)^2}\right] \quad \textbf{(3.3)}$$

$$T_D = \frac{1}{c}\left[\sqrt{(x - x_D)^2 + (y - y_D)^2 + (z - z_D)^2}\right] \quad \textbf{(3.4)}$$

Where x_A, y_A and z_A are the coordinates of receiver *A* and *c* is the speed of sound. If the location of receiver *A* is taken to be the coordinate system origin (0, 0, 0) then

$$T_A = \frac{1}{c}\left[\sqrt{(x)^2 + (y)^2 + (z)^2}\right] \quad \textbf{(3.5)}$$

To calculate the TDOA values the TOF values must be subtracted. Subtracting equation (3.5) from (3.2) gives,

$$\Delta_{BA} = T_B - T_A = \frac{1}{c}\left[\sqrt{(x - x_B)^2 + (y - y_B)^2 + (z - z_B)^2} - \sqrt{x^2 + y^2 + z^2}\right] \quad \textbf{(3.6)}$$

Subtracting equation (3.5) from (3.3) creates,

$$\Delta_{CA} = T_C - T_A = \frac{1}{c}\left[\sqrt{(x - x_C)^2 + (y - y_C)^2 + (z - z_C)^2} - \sqrt{x^2 + y^2 + z^2}\right] \quad \textbf{(3.7)}$$

Subtracting equation (3.5) from (3.4) creates,

$$\Delta_{DA} = T_D - T_A = \frac{1}{c}\left[\sqrt{(x - x_D)^2 + (y - y_D)^2 + (z - z_D)^2} - \sqrt{x^2 + y^2 + z^2}\right] \quad \textbf{(3.8)}$$

Equations (3.6), (3.7) and (3.8) then represent the unknown transmitter coordinate *x, y, z* with respect to the receiver locations and the TDOA values obtained (Bakhoum, E. 2006). These three non-linear equations can then be solved using a non-linear equation solver in order to calculate the unknown transmitter location. The three TDOA values are converted into range differences by knowing the speed of transmission through the medium. These range differences along with the receiver coordinates are then input into the non-linear equation solver in order to compute the root (zero) of the equations which represent potential transmitter locations in *x, y* and *z.*

As the equations are non-linear then more than one possible solution is returned via the solver, which depends on the starting condition implemented. All of the solutions calculated via the solver are valid for the three TDOA values, however as the equations are non-linear, solutions which fit both the positive and negative TDOA values are returned. Therefore for a TDOA Δ_{BA} = 0.062 m for example, the solution calculated by the solver could be for either ±0.062 m. The implementation of the solver for this thesis is discussed in section 3.2.2.

Provided that the TDOA values have no error due to noise then the solution returned by the non-linear equation solver, assuming that the correct starting parameters are applied will be a location which has negligible error against the true position. The impact of noise however will cause the TDOA values to contain error. Unlike TOF localisation, which utilises techniques such as least

mean square to minimise the error in the region of uncertainty where the spheres overlap, the non-linear equation solver in this instance will instead converge to a different transmitter location due to the impact of noise. As the TDOA values change then the solution given by the solver also changes such that the solution is still a root of the 3 equations. In [Chapter 4.0, section 4.4] work investigating the impact that noise has on the localisation accuracy of TDOA for different receiver locations is investigated.

In the present work a "typical" TDOA environment utilises a single transmitter communicating with multiple receivers and therefore the solution derived from equations (3.6), (3.7) and (3.8) can be used to obtain the transmitter location. The inverse problem can also be solved, where multiple transmitters having known positions can be used to find an unknown receiver location.

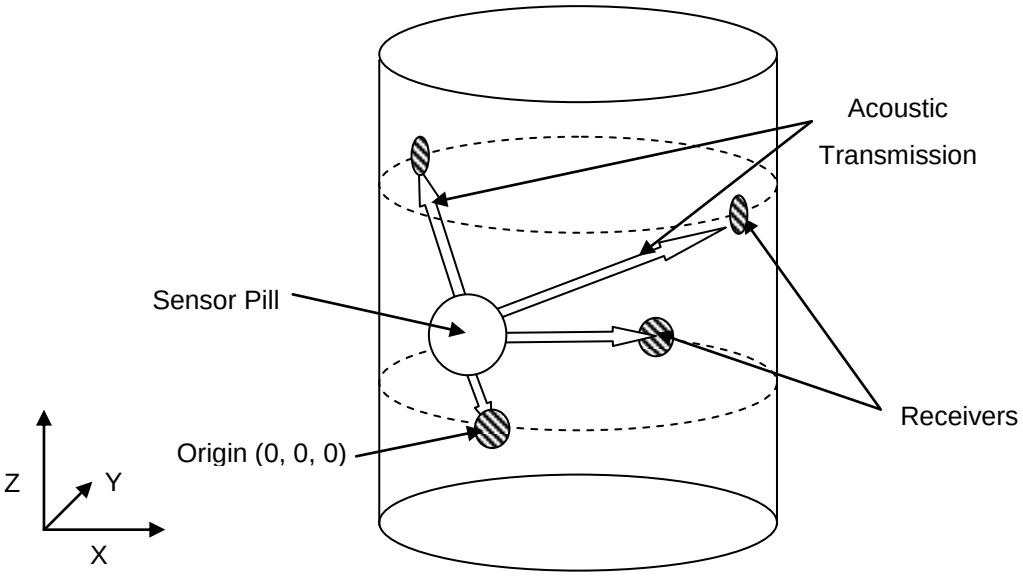

Figure 3-11: Example vessel layout

Figure 3-11 displays representative positions for the receivers and the sensor pill in the vessel. Receivers are mounted to the vessel wall with known locations. Signals transmitted from the pill are received at these known locations and the TDOAs between the arrivals of the signal are calculated. From this information the location of the transmitting pill can be derived.

3.2.2 Single Transmitter Simulation

To test the feasibility of using TDOA as a localisation technique and to allow a comparable starting point a single transmitter MATLAB model was constructed to calculate the appropriate TDOAs and solve the non-linear equations established in section 3.2.1 to locate an unknown transmitter. To solve the non linear equations MATLAB's *fsolve*[31] function was considered. *Fsolve* is a predefined non-linear equation solver specified in MATLAB, it attempts to find the root (zero) for a system of non-linear equations. The solver employs an iterative approach to solving non-linear equation

[31] http://www.mathworks.it/access/helpdesk/help/toolbox/optim/ug/fsolve.html

problems. The solver takes input arguments of the equations to be solved and also requires a starting point, x0, to attempt to solve the equations. This point is a first guess approximation of the solution to the equations. From this starting point *fsolve* iteratively converges to a root of the equations.

Fsolve calculates the solution f(x) to the non-linear equations specified for the initial starting condition, x0. The solver compares the function returned, f(x), to the desired result, which is a root or zero value. Modifications are then made within the solver to the starting condition x0, and the function f(x) recalculated. This continues until the function f(x) is within a specified tolerance of a zero value. The number of iterative attempts made by *fsolve* and the tolerance can both be specified within the function.

Fsolve was selected for use within this thesis as it is a predefined non-linear equation solver already defined with the simulation tool MATLAB. The solver is part of the library of tools within MATLAB and is therefore a tested tool to solve non-linear equations. The non-linear equation solver is only a small part of the algorithm required to locate the pill, as the solutions output by the solver must be evaluated to determine if they are the solution required. Due to the nature of non-linear equations there are multiple solutions to each possible set of TDOAs. The algorithm described in this research uses an iterative approach to selecting the correct solution from *fsolve*. From the TDOA values obtained, range differences are calculated and these along with the receiver coordinates are input into *fsolve*. As the location of the transmitter is unknown the initial starting condition for the transmitter's location is always specified as (0, 0, 0) m and *fsolve* is used to return the proposed transmitter location in *x, y, z*.

The validity of the returned transmitter location is then investigated to determine if the solution selected via *fsolve* is the solution required as described below. For a given set of TDOA values *fsolve* calculates a possible transmitter location in x, y and z. The algorithm used in this thesis then calculates what the TDOA values will be if this transmitter location is the correct location of the transmitter. The magnitude of the TDOA values will always be correct, however as the equations specified are non-linear then both positive and negative roots are valid. If for example a TDOA value was 0.01 seconds between receivers then a TDOA of -0.01 seconds would also give a valid solution for *fsolve*.

The algorithm therefore compares the polarity of the TDOA values for the solution suggested by *fsolve* with the values which were actually recorded for the unknown transmitter location. If the magnitude and polarity of the values is correct then it is known that the solution returned via *fsolve* is the correct transmitter location. If the polarity of one of the TDOAs is incorrect, then while the calculated location via *fsolve* is a valid solution to the non-linear equations it is not the true transmitter location. The starting condition can be modified and *fsolve* will tend to a different valid solution which again can be compared to the true TDOA values.

Assuming 3 decimal places to give millimetre accuracy, if a single transmitter at (0.200, -0.100, 0.300) m within the vessel is the transmitter location and the location of four receivers in metres are, R_A = (0.00, 0.00, 0.00), R_B = (0.500, 0.00, 0.00), R_C = (0.250, 0.250, 0.500) and R_D = (0.250, -0.250, 0.500) then the range values to each receiver can be calculated as follows,

$$Range_A = \left[\sqrt{(0.200 - 0.000)^2 + (-0.100 - 0.000)^2 + (0.300 - 0.000)^2}\right] = 0.374\ m\ (3dp)$$

$$Range_B = \left[\sqrt{(0.200 - 0.500)^2 + (-0.100 - 0.000)^2 + (0.300 - 0.500)^2}\right] = 0.436\ m\ (3dp)$$

$$Range_C = \left[\sqrt{(0.200 - 0.250)^2 + (-0.100 - 0.250)^2 + (0.300 - 0.500)^2}\right] = 0.406\ m\ (3dp)$$

$$Range_D = \left[\sqrt{(0.200 - 0.250)^2 + (-0.100 - -0.250)^2 + (0.300 - 0.500)^2}\right] = 0.255\ m\ (3dp)$$

This gives range difference of arrival (RDOA) values of Δ_B = 0.062 m (3dp), Δ_C = 0.032 m (3dp) and Δ_D = -0.119 m (3dp). Using *fsolve* the solution returned is (0.200, -0.100, 0.300) m and the error on this location is calculated as $6.8663e^{-10}$ m. This result suggests that TDOA is a viable method with a single transmitter and that the MATLAB model correctly operates and is able to locate the transmitter to a high degree of accuracy.

Using TDOA the detection system is triggered from the reception of the acoustic signal. This leaves the system vulnerable to noise which could cause false triggers. The non-linear TDOA equations must also be solved in real time to allow the location of the transmitter to be determined. This presents a significant computational load, albeit at an external processing system.

3.2.3 TDOA Exploration Summary

This section has investigated the technique of localisation through TDOA. The aim has been to investigate how the technique is able to localise a transmitter without synchronisation and to construct an algorithm which is able to accurately locate the transmitter utilising TDOA.

In section 3.2.1 the theory of TDOA has been investigated. The section has shown how TDOA differs in localisation in comparison to TOF and how the method utilises hyperboloids to localise the transmitter. The TDOA equations required to localise the transmitter in 3D have been derived from first principles and an explanation of the requirements to solve the equations detailed.

From this work section 3.2.2 has described MATLAB simulations to allow the unknown location of a transmitter to be derived using TDOA values at 4 receivers. The algorithm utilised within this thesis has been explained and an example localisation using range difference information derived from TDOA has been given. Results suggest that for noise free TDOA values it is possible to localise a single transmitter in 3D with negligible error using 4 receivers. This section has shown the validity of the TDOA technique and also the validity of the model to solve the equations. This allows work

to be undertaken to determine how the separation of multiple transmitters on the pill will impact the localisation error.

3.3 Summary of Wireless Localisation

The ability to localise the pill within the target environment is a key research challenge for the project. Within the intended process vessel environment it is crucial that the pill is able to freely move without being connected to the outside world via a cable or cord which could become tangled or even severed by potential impellers. To satisfy these requirements a wireless pill is the most suitable option. This creates the requirement for synchronisation between transmitter and receiver, such that range and location of the transmitter can be determined.

TOF localisation synchronisation using electrical signals has been considered in section 3.1. This section has shown that electrical synchronisation is possible using a transmitter on the pill over the intended vessel size of 0.5 m. With a 12 V battery it is possible to detect the synchronisation pulse at the external receivers making electrical synchronisation a viable option for the project.

As a technique which does not require synchronisation to achieve localisation TDOA has been investigated in section 3.2. An algorithm to locate the transmitter using TDOA has been developed, with simulations suggesting that it is possible to localise the transmitter with negligible error for noiseless TDOA values.

For application in this project TDOA has been selected for implementation. TDOA provides the “cleanest” solution for implementation, with only acoustic signals required and four receivers. In comparison electrical synchronisation requires the use of additional transmit and receive electrodes and injects electrical signal into the vessel, this also imposes the condition that the medium must be electrically conductive, which is not a constraint for TDOA. The use of TDOA also reduces the complexity of the pill and reduces battery consumption as only acoustic signals are transmitted. Experimental localisation results will therefore focus on TDOA localisation, with TOF localisation results used for comparison.

4.0 TDOA Simulation

In [Chapter 3.0, section 3.2] the localisation strategy of time difference of arrival (TDOA) was investigated, with a single transmitter localised using four receivers. Results demonstrated that the single transmitter could be localised with negligible error for noiseless TDOA values. This chapter discusses the implementation introduced in this project, with the use of multiple transmitters located on the pill and the challenges which arise due to this.

Section 4.1 outlines the challenges associated with the project which lead to the requirement for multiple transmitters on the pill and how this in turn creates the TDOA implementation challenge. In section 4.2 simulations are conducted in MATLAB for pill layouts with multiple transmitters, focusing on the localisation errors due to the transmitter separation from the centre of the pill and the problems which arise due to the pill's rotation in the vessel.

To overcome pill localisation errors section 4.3 introduces a method of modifying the TDOA equations to accommodate the transmitter separation. Suggestions for negating the effects of rotation of the pill by utilising individual transmitter coding are also presented with the desire to minimise the localisation error. Optimisation of the receiver layout is considered in section 4.4, with the aim of exploring how different receiver layouts accommodate error on TDOA values due to noise and how this impacts the localisation accuracy.

4.1 TDOA Implementation Challenge

To facilitate localisation throughout the vessel, one of the key requirements of the project is that the pill must be able to provide signal coverage in all directions. The intended environment for operation, within the confines of a steel vessel, creates a localisation challenge due to the high reflection coefficient (0.88) of the vessel wall[32], which makes differentiating between direct and reflected signals a challenge at the receiver.

To assist in the differentiation of reflected and direct path signals, a transmission signal of uniform intensity is desired, irrespective of the angle of transmission from the pill. This ensures that for a single pill, the strongest received signal will correspond to the direct path. To achieve this, the desirable transmitter is one with an omnidirectional beam profile allowing the signal to radiate in all directions with uniform intensity, reaching the required receivers from any location in the vessel.

There are however obstacles regarding the implementation of an omnidirectional transducer within the project. The pill is intended to be wireless, which means that hardware to allow generation and transmission of signals is required onboard, imposing a minimum pill volume sufficient to contain

[32]http://www.ndt-ed.org/EducationResources/CommunityCollege/Ultrasonics/Physics/reflectiontransmission.htm

the hardware. One option is to utilise an omnidirectional transducer as the pill and contain the hardware inside. Inherently transducers are sized to allow the natural resonance of a signal at a specific frequency, for example Neptune Sonar's D/140 transmitter[33] has a resonant frequency of 150 kHz with a diameter of 20 mm. For devices with lower resonant frequency such as Neptune Sonar's T204[34] and D/60[35] at 54 kHz and 60 kHz respectively it can be observed that the size of the device increases, with diameters of 48 mm and 42 mm. The small size of these transducers and therefore the limited internal space eliminates the option of using of an omnidirectional transmitter as the pill.

To alleviate this issue two possible options present themselves. The first is to mount a small omnidirectional transmitter inside a larger diameter pill housing such that the beam from the transmitter is able to resonate through the housing. The second is to mount the omnidirectional transmitter below the pill and attach it via a cable or cord.

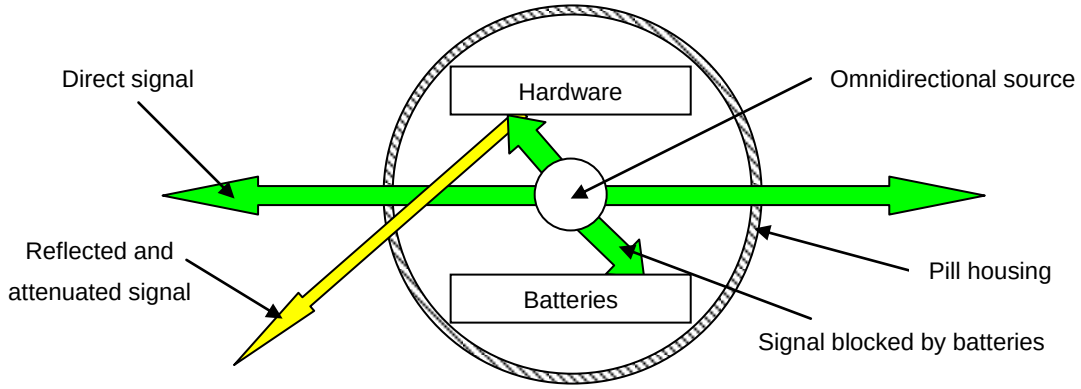

Figure 4-1: Omnidirectional beam pattern blocking due to hardware

Figure 4-1 displays the pill with an omnidirectional transmitter mounted in the centre. Electronic hardware must also be mounted inside the pill to allow signal generation to create a wireless unit. The insertion of these items prevents the beam from the transmitter leaving the pill in an omnidirectional pattern. Signals are either reflected by objects in the pill, pass through them but are attenuated, or are completely blocked. This problem means that while the transmitter produces an omnidirectional beam pattern the pattern actually radiating from the pill is no longer omnidirectional. This negates the original purpose of using an omnidirectional transmitter and is therefore not a viable solution.

[33] http://edition.pagesuite-professional.co.uk/launch.aspx?referral=other&refresh=Nx807K1my9D0&PBID=f7b8707c-94bb-4338-a20e-8c65734dcb87&pnum=12&skip=

[34] http://edition.pagesuite-professional.co.uk/launch.aspx?referral=other&refresh=M0g81m6FB1i7&PBID=f7b8707c-94bb-4338-a20e-8c65734dcb87&pnum=50&skip

[35] http://edition.pagesuiteprofessional.co.uk/launch.aspx?referral=other&refresh=J1t69zH0F0w5&PBID=f7b8707c-94bb-4338-a20e-8c65734dcb87&pnum=12&skip=

To alleviate the problem of “beam blocking” due to hardware, an alternative option is to suspend the omnidirectional transmitter from the base of the pill. This method allows the majority of the signal from the transmitter to propagate in an omnidirectional pattern.

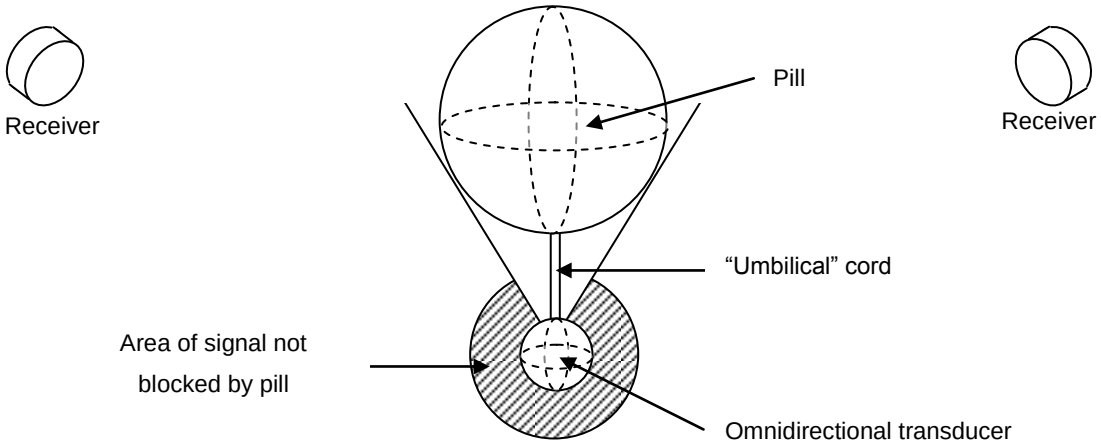

Figure 4-2: Arrangement with transducer suspended from pill

Figure 4-2 illustrates the arrangement with an omnidirectional transmitter suspended from the pill. With this arrangement a significant amount of signal is able to propagate in an omnidirectional pattern as the pill blocks only a small area of signal from the top of the transducer. The angular region of signal which is blocked by the pill is related to the length of the cord between the transmitter and the pill. By lengthening the cord the angular region which is blocked by the pill can be reduced. For all angles not blocked by the pill the signal propagated is on uniform intensity.

As discussed in [Chapter 1.0, section 1.2] one of the intended applications for the pill is in process vessels which may contain impellers for mixing. The use of impellers mounted inside a vessel raises questions over the robustness of a design with a transmitter suspended from the pill. There is a high probability of the transmitter cable becoming damaged or even severed due to the impellers. For this reason the design is considered insufficiently robust for implementation within the project.

Due to the limitations of using a single omnidirectional transmitter with the pill but the desire to create an omnidirectional beam pattern the construction of a transmitter array has been proposed. In this instance it is envisaged that multiple small, low cost transmitters can be mounted to the pill’s surface in order to create the desired beam shape. As the transmitters are mounted on the surface of the pill and the hardware is mounted inside it is proposed that beam blocking can be eliminated. To allow sufficient vessel coverage multiple transmitters are required; the use of a single transmitter would create a beam-blocking problem due to the pill body itself.

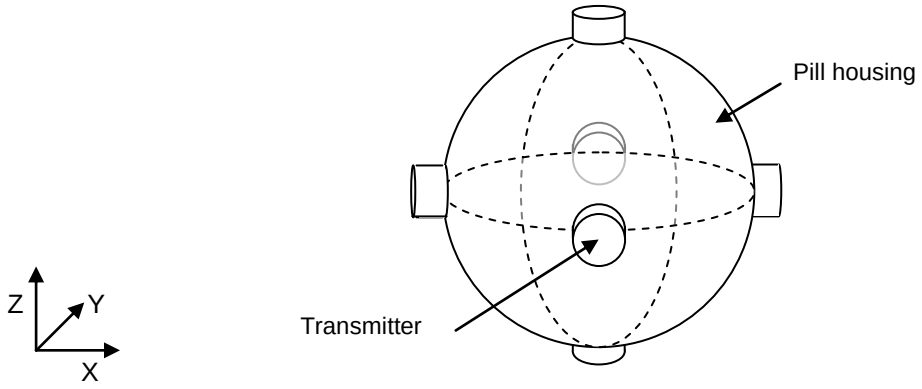

Figure 4-3: Example transmitter layout

Figure 4-3 illustrates a possible transmitter layout with 6 transmitters mounted to the pill's surface. The desire in this instance is to locate multiple transmitters on the surface of the pill such that they approximate the omnidirectional beam pattern desired. The challenge is to use the beam profiles from multiple individual transmitters to approximate that of an omnidirectional transmitter. This is discussed in more detail in [Chapter 6.0, section 6.4].

However, for localisation using TDOA the placement of multiple transmitters on the outside of the pill creates a specific design challenge, identifying the location of the pill from multiple transmission sources. Standard TDOA methodology involves locating a single transmitter with multiple known receivers or locating a single receiver from multiple transmitters (Xu, J. et al, 2011). When locating a single transmitter, the transmitter is considered a point source and the TDOA algorithms are used to determine its location. For the design considered in this project the pill is not a point source as it has multiple transmitters distributed over its surface. Unlike the standard TDOA methodology, where signals arriving at different receivers originate from the same location, with multiple transmitters signals arriving at different receivers will have different points of origin. This creates the challenge of using TDOA to solve for the centre of the pill rather than any specific transmitter location.

The challenge which therefore presents itself is how do the TDOA values for the pill's location alter due to offsetting the transmitters from the centre of the pill, and what impact does this have on the ability to localise the position of the pill accurately?

4.2 Simulation of a Multiple Transmitter Array

4.2.1 Multiple Transmitter Condition

With the standard TDOA methodology, by solving the three non linear equations a single transmitter can be located with minimal error under the constraint of ideal TDOA values [Chapter 3.0, section 3.2.2].

Two areas of research encompass the design of the transmitter array. The primary purpose of the transmitter array is to provide uniform signal coverage within the vessel, this means that regardless

of the pill's location the array should be able to transmit signals which reach the receivers and allow the TDOAs and subsequent location of the pill to be calculated. This section of research relates to the individual transmitters selected and their respective beam profile and signal strength and is covered in [Chapter 6.0, section 6.4].

The second area of research regarding the transmitter array is whether TDOA is a viable technique to allow localisation when transmitters are distributed from a single location on the pill. For localising a transmitter with TDOA multiple receivers are required, however this is used to localise a single transmission point. In this thesis the transmitters are separated and therefore the transmission point is not a single unique point in space. It is therefore crucial to discover if error is observed on the localisation due to the transmitter separation and if this is the case, can the level of error be tolerated? This work will be covered in this chapter.

To determine a suitable transmitter layout for testing it is first crucial to understand the desired profile of a single transmitter, as this profile influences the number of transmitters required and their subsequent placement on the pill. Characteristically a signal transmitted from an angle of 0º (perpendicular to the transmitter's face) is the strongest signal. As the angle of transmission increases, the signal strength decreases (Chupyra, A.G et al, 2006). To maintain uniform signal strength over the entire pill, there is the requirement for transmitters to be mounted adjacent to each other.

Therefore, to create uniform beam coverage with multiple transmitters from the pill the theoretical desired profile of a single transmitter is one which provides uniform intensity over a given angular divergence. With this transmission profile it should be possible to create uniform coverage from the pill via spacing the transmitters adjacent to each other. This idea is illustrated in more detail in [Chapter 5.0, section 5.1] when considering the use of multiple transmitters to maximise beam coverage. To minimise the number of transmitters required and therefore the cost of the pill this uniform intensity should be over a wide angular region, Figure 4-4 illustrates this idea.

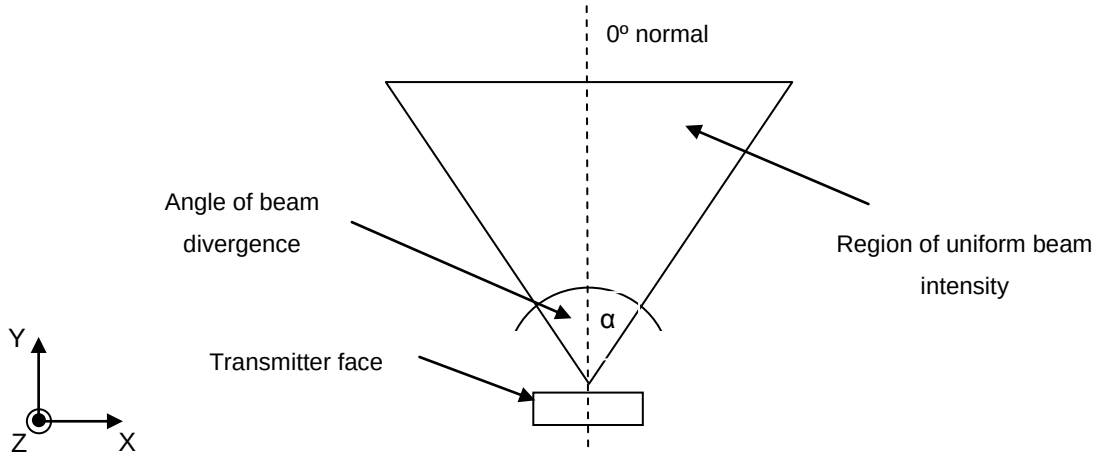

Figure 4-4: Desired single transmitter profile

Figure 4-4 shows the desired beam profile for a single transmitter. With this profile there is a single region of uniform signal intensity with beam divergence α from the 0º normal, this is both in the horizontal and vertical plane. To minimise cost a large beam divergence angle is desired as this increases the vessel coverage possible from a single transmitter. In theory a beam divergence angle α, of 90º would give 180° coverage and allow any region in front of the transmitter to be reached in 2D. Expanding this into 3D then if a sphere measures 4π steradians then the desired beam profile for a single transmitter is 2π steradians.

To simulate the influence that transmitter layouts have on the localisation accuracy of TDOA a receiver layout in the vessel must first be established. To determine the location of the pill in 3D there is the requirement for 4 receivers as this allows the calculation of 3 TDOA values [Chapter 3.0, section 3.2.2]. The receivers cannot be located in a coplanar manner, if all receivers are mounted at the same *x, y*, or *z* coordinate then it is not possible to localise a transmitter in 3D. With the target environment of a cylindrical vessel it has therefore been decided to consider the receivers on opposing sides of the vessel at two different heights. This layout can be seen in Figure 4-5.

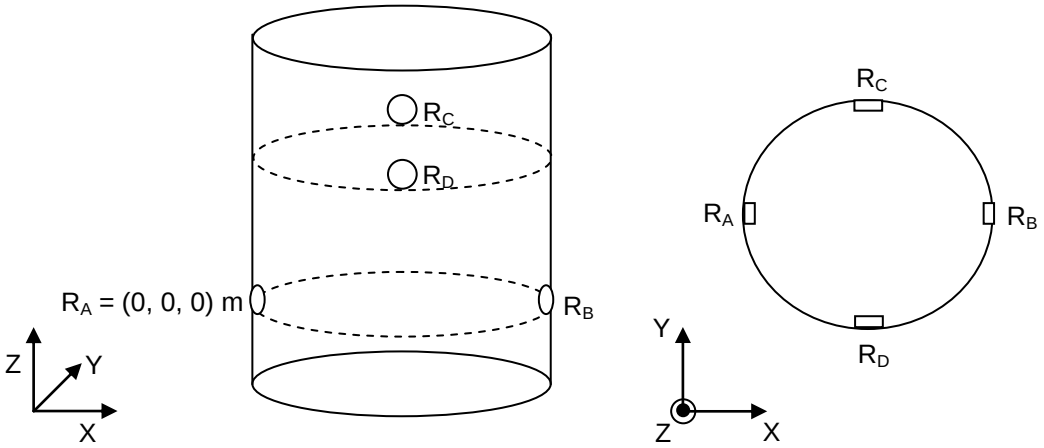

Figure 4-5: Vessel receiver layout

The receiver locations are the same as those in [Chapter 3.0 section 3.2.2] these are, R_A = (0.000, 0.000, 0.000), R_B = (0.500, 0.000, 0.000), R_C = (0.250, 0.250, 0.500), and R_D = (0.250, -0.250, 0.500). All values are in metres. Coordinates are considered to 3 dp which is mm accuracy. For mounting in the vessel this is the highest level of accuracy which can be achieved in practice. The initial separation of the receivers in the *z* direction is selected due to experimental validation completed by Burnett-Thompson A. (2007) however one of the targets for this project is to determine the optimum receiver layout which is discussed in section 4.4 of this chapter.

Assuming that the beam pattern from a single transmitter is likely to be less than the theoretical ideal of 2π steradians then a single transmitter is able to provide signal to only a single receiver. To provide coverage to all receivers 4 transmitters are required on the pill. To maintain an even spacing between transmitters on the pill these should be mounted at 90º to each other. This layout

is illustrated in Figure 4-6. In this instance 4 transmitters are mounted around the equator of the pill, with a separation of 90º.

To allow a comparison between the simulations with a 4 transmitter arrangement and the single transmitter case, the same transmitter location is maintained as in [Chapter 3.0, section 3.2.2]. In this instance however the position refers to the centre of the pill which is (0.200, -0.100, 0.300) m.

For this arrangement the time of flight (TOF) measurements to each receiver can be simulated which allows the TDOAs to be derived. The origin of the signal detected at each receiver is dependent upon the pill's location and its orientation in the vessel. When multiple signals from different transmitters reach a specific receiver the first signal to arrive is selected as the TOF measurement.

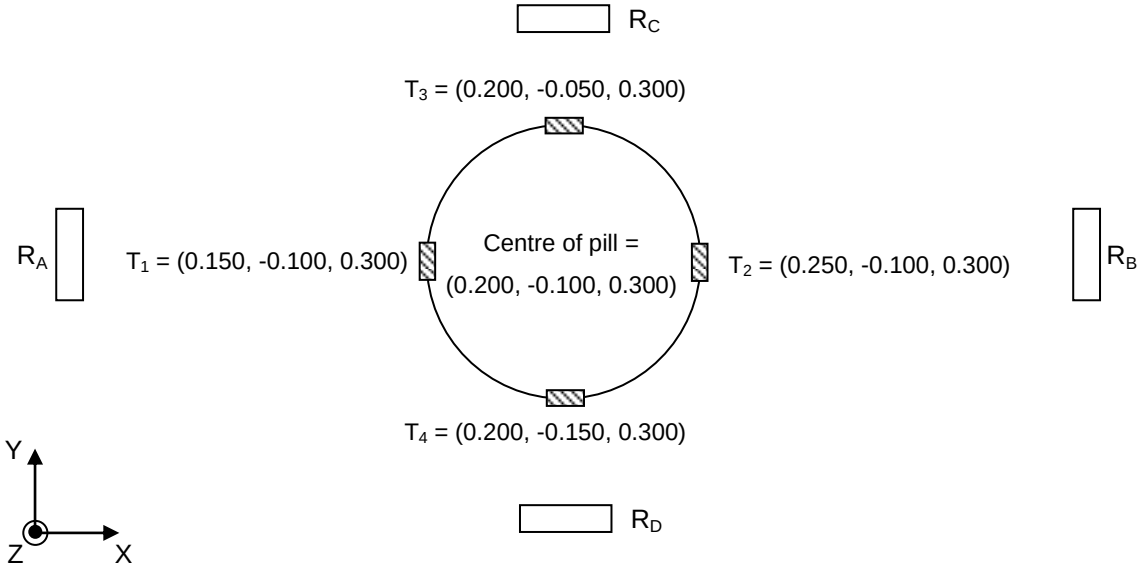

Figure 4-6: Pill layout with 4 transmitters

Figure 4-6 displays the locations of each transmitter for the 4 transmitter arrangement with centre of pill location (0.200, -0.100, 0.300) m. In each instance the transducers are mounted 0.05 m from the centre of the pill in either the *x* or *y* component depending upon the transmitter. With this layout and orientation all the transducers are mounted closer to their respective receivers than if a single transmitter was mounted in the centre of the pill. Therefore, the TOFs when compared to a single transmitter in the centre of the pill will be reduced, altering the TDOA values between receivers. This pill orientation is defined as 0° rotation.

For localisation this thesis investigates TDOA through a range difference approach. That is to say that because the speed of sound is assumed to be the same for each received signal this is removed from the equation and the range and therefore range difference to each receiver is used to calculate the location of the transmitter. The influence on noise on range measurements leading to localisation error is considered in section 4.4.

The range values at each receiver for the pill location in Figure 4-6 can be seen below. The range equations are labelled representing the transmitter origin of a signal and the receiver at which it arrives. Therefore R_{1A} is the range of signal from transmitter T_1 to receiver R_A.

$$R_{1A} = \sqrt{(0.150 - 0.000)^2 + (-0.100 - 0.000)^2 + (0.300 - 0.000)^2} = 0.350\ m\ (3dp)$$

$$R_{2B} = \sqrt{(0.250 - 0.500)^2 + (-0.100 - 0.000)^2 + (0.300 - 0.000)^2} = 0.403\ m\ (3dp)$$

$$R_{3C} = \sqrt{(0.200 - 0.250)^2 + (-0.050 - 0.250)^2 + (0.300 - 0.500)^2} = 0.364\ m\ (3dp)$$

$$R_{4D} = \sqrt{(0.200 - 0.250)^2 + (-0.150 + 0.250)^2 + (0.300 - 0.500)^2} = 0.229\ m\ (3dp)$$

From the individual range values it is possible to calculate the difference in range; Δ_{BA} is the difference in arrival between receiver R_B and receiver R_A.

$$\Delta_{BA} = 0.403 - 0.350 = 0.053\ m\ (3dp)$$

$$\Delta_{CA} = 0.364 - 0.350 = 0.014\ m\ (3dp)$$

$$\Delta_{DA} = 0.229 - 0.350 = -0.121\ m\ (3dp)$$

The algorithm used to determine the location of the pill is discussed in [Chapter 3.0, section 3.2.2] and uses the *fsolve* function in MATLAB. The location calculated for the centre of the pill is (0.207, -0.088, 0.305) m. This is an error of 0.015 m on the actual centre of the pill.

The distribution of transmitters on the pill means that different range difference values are obtained in comparison to those when only a single transmitter is used. For a single transmitter in the same vessel location as seen in [Chapter 3.0, section 3.2.2] the difference values are Δ_{BA} = 0.062 m (3dp), Δ_{CA} = 0.032 m (3dp) and Δ_D = -0.119 m (3dp).

The result suggests that the separation of transmitters from a single point induces error into the localisation. To investigate how the transmitter separation impacts the localisation accuracy throughout the vessel three test locations were selected. These test locations were selected for two reasons. Firstly their separation across the vessel in *x, y* and *z* provides a good cross section of potential pill locations. The second reason relates to how the layout of the transmitters on the pill affects the shortest range to each receiver. For locations 1 and 3 the location of the pill means that the shortest range from transmitter to receiver is T_1 to R_A, T_2 to R_B, T_3 to R_C and T_4 to R_D. For location 2 however the pill's location means that the shortest range to R_A is actually from transmitter T_3 rather than T_1. These locations therefore allow observations on how the origin point

of a signal affects the localisation accuracy, specifically when the pill is rotated. The localisation error for each location is presented in Table 4-1.

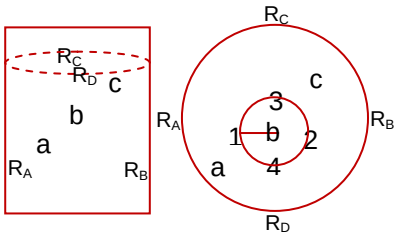

	Actual Location (m)	Calculated Location (m)	Error (m)
a	(0.200, -0.100, 0.300)	(0.207, -0.088, 0.305)	0.015
b	(0.080, -0.180, 0.150)	(0.094, -0.161, 0.144)	0.024
c	(0.400, 0.050, 0.500)	(0.376, 0.045, 0.518)	0.030

Table 4-1: Actual and calculated centre of pill positions for three test locations

Table 4-1 displays the actual centre of pill location, the location calculated by fsolve and the error between the actual and calculated location. The diagram displays the receiver locations along with the three simulated pill locations, which are represented as *a, b* and *c*. The orientation of the pill and therefore the position of the transmitters are also illustrated where 1 equals T_1, 2 equals T_2 and so forth. The results show that the magnitude of the localisation error is not consistent but varies for different pill locations within the vessel. In this instance the largest observed error is 0.030 m which is approximately 6% of the vessel size for a 0.5 m by 1 m vessel.

The result suggests that even though error is induced due to the spatially separated transmitters on the pill the centre of the pill can still be approximated with reasonable localisation accuracy. While the largest observed error of 0.030 m is relatively small in terms of absolute error this result is for a simulation where range values are ideal and not subject to error due to noise. It might be anticipated that with the addition of noise and therefore non-perfect range values this error would increase.

4.2.2 Pill Rotation Issues

The design of the pill and the expected target environment creates another challenge for localisation due to rotation. The pill is intended to move freely in the vessel, which means any rotational force applied onto it due to, for example, an impeller may cause the pill to rotate.

The design of the pill allows rotation around the *x* and *y* axes to be negated through the careful placement of ballast. To provide vertical motion (Watson S.A and Green P.N. 2011) proposes the use of propellers mounted to the equator of the pill. This system requires the pill to be neutrally buoyant in order to minimise the thrust required from the propellers. The volume of the pill however means that extra ballast is required to achieve this neutral buoyancy. By mounting the ballast in the bottom of the pill rotation around the *x* and *y* axes can be minimised and thus this effect is negligible on the orientation of the pill. Rotation around the *z* axis however cannot be ignored.

This rotation around the *z* axis means that for a fixed centre of pill the transmitters' locations can change relative to the receivers in the *x* and *y* coordinates. This idea is illustrated in

Figure 4-7 for the centre of pill location (0.200, -0.100, 0.300) m with a 45º pill rotation. This rotation raises two questions. Firstly, does the rotation of the pill allow more than one set of TDOA values to represent the same centre of pill location? Secondly, does rotation of the pill mean that for a given receiver, the first arrival of a signal at that receiver originates from a transmitter adjacent to the one expected, and if so what impact does this have on the accuracy of the localisation?

The effect that rotation has on localisation accuracy is a consequence of using a transmitter array and is not observed for the case of a single transmitter. For a single transmitter point source if the transmitter rotates on its axis it will not change coordinates. If it rotates around another point then this is purely a shift in one or multiple directions, *x, y* and *z*, and is therefore in a new location which is represented by a new set of TDOA values. To observe the influence rotation has on the calculated accuracy of the localisation the condition where the pill is rotated but with the same centre of pill location is considered.

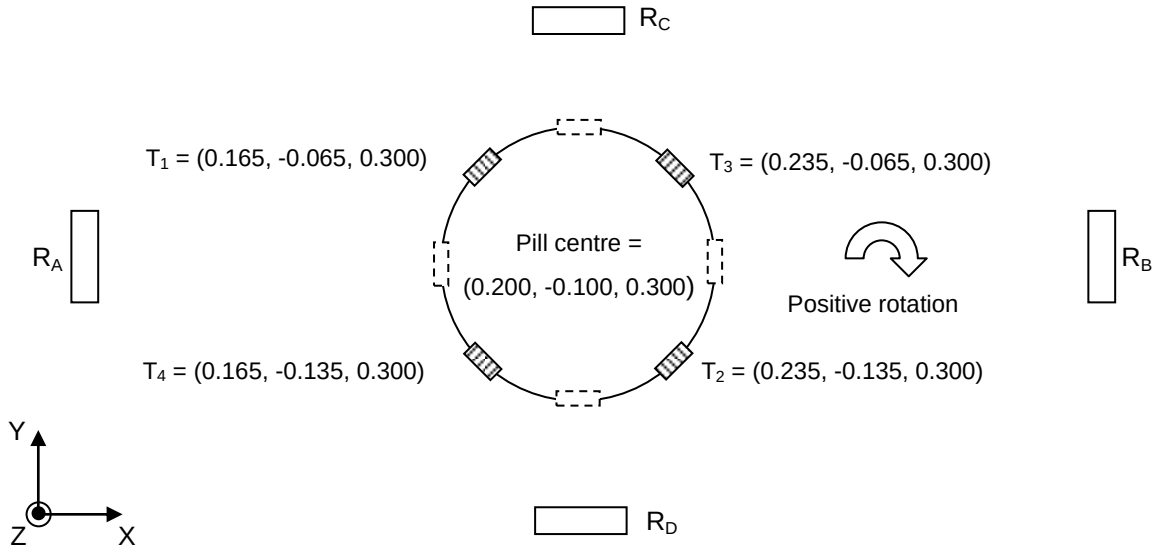

Figure 4-7: Pill centre (0.200, -0.100, 0.300) m, rotation angle 45º

Figure 4-7 displays the same centre of pill location as Figure 4-6, (0.200, -0.100, 0.300) m. In this instance however the pill has been rotated 45º and therefore the locations of the transmitters on the surface of the pill have changed relative to the receivers in the *x* and *y* coordinates. Rotation clockwise is considered positive in this instance. As discussed, for a given receiver this pill rotation raises the question of whether the origin position of a signal can change. If for example the pill is able to rotate such that the range from transmitter T_4 to receiver R_A is less than the range from transmitter T_1 to receiver R_A then the first signal to arrive at receiver R_A will originate from T_4. As such the origin of the signal will have switched between adjacent transmitters, from T_1 to T_4.

For a rotation of 45º the shortest range between transmitter and receiver to 3dp are, R_{1A} = 0.348 m, R_{3B} = 0.405 m, R_{3C} = 0.373 m and R_{2D} = 0.231 m. This gives range difference values for 45º pill rotation of Δ_{BA} = 0.057 m, Δ_{CA} = 0.025 m and Δ_{DA} = -0.117 m all to 3dp. It can be observed that for

this rotation of the pill the transmitter origin for certain receivers has altered in comparison to the 0° pill rotation. The first signal to arrive at receiver R_B now originates from transmitter T_3 rather than T_2 and for receiver R_D the first signal arrival originates from T_2 rather than T_4.

For 0º pill rotation the range difference values were Δ_{BA} = 0.053 m, Δ_{CA} = 0.014 m and Δ_{DA} = -0.121 m all to 3dp. The maximum effect of this change in transmitter origin is therefore observed for Δ_{CA} and is 0.009 m. As the change in the values between 0° and 45° pill rotations are very small it could be expected that the error on positional calculations would be relatively similar to those observed for 0° rotation. The result also highlights that for a fixed centre of pill location multiple sets of TDOA values can be used to represent this single location. While the difference between values for 0° and 45° pill rotation has been shown to be relatively small, the TDOA technique is unable to resolve the rotation of the pill, as each pill location does not have a unique set of TDOA values which represent it.

To observe the influence that the pill rotation angle has upon the accuracy of the localisation, rotation angles of 10°, 45° and 60º are simulated for the three test locations.

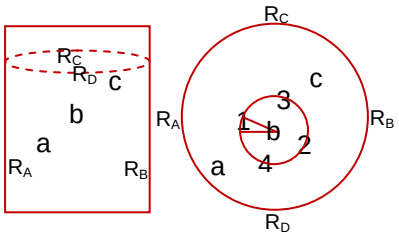

	Actual Location (m)	Calculated Location (m)	Error (m)
a	(0.200, -0.100, 0.300)	(0.203, -0.086, 0.304)	0.015
b	(0.080, -0.180, 0.150)	(0.093, -0.159, 0.149)	0.025
c	(0.400, 0.050, 0.500)	(0.379, 0.040, 0.519)	0.030

Table 4-2: Calculated centre of pill location and error for 10º rotation, 4 transmitter layout

Table 4-2 displays the actual and calculated locations of the centre of pill along with the error for a 10º positive rotation. The error on location 2 shows a 0.001 m increase over the 0º rotation however locations 1 and 3 are identical to the 0º condition to 3dp.

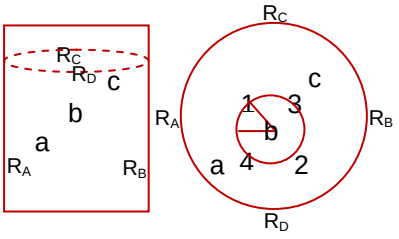

	Actual Location (m)	Calculated Location (m)	Error (m)
a	(0.200, -0.100, 0.300)	(0.204, -0.093, 0.300)	0.007
b	(0.080, -0.180, 0.150)	(0.094, -0.162, 0.143)	0.024
c	(0.400, 0.050, 0.500)	(0.389, 0.051, 0.536)	0.037

Table 4-3: Calculated centre of pill location and error for 45º rotation, 4 transmitter layout

Table 4-3 displays the actual and calculated locations for the centre of pill along with the error for a 45º positive rotation. The error in location 1 is approximately halved when compared to the 0º condition; the error in location 2 is identical however there is a 0.007 m increase in location 3. This result highlights that the most accurate approximation of the centre of the pill is not always obtained for 0° rotation.

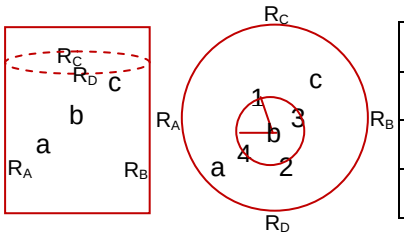

	Actual Location (m)	Calculated Location (m)	Error (m)
a	(0.200, -0.100, 0.300)	(0.208, -0.094, 0.138)	0.016
b	(0.080, -0.180, 0.150)	(0.095, -0.167, 0.136)	0.024
c	(0.400, 0.050, 0.500)	(0.380, 0.054, 0.526)	0.033

Table 4-4: Calculated centre of pill location and error for 60º rotation, 4 transmitter layout

Table 4-4 displays the actual and calculated locations for the centre of the pill along with the errors for a 60º positive rotation. Errors at 60º are again similar to those observed for 0º rotation, with a 0.001 m increase in location 1 and a 0.003 m increase in location 3.

The results for a rotated pill show minimal difference to those for the non-rotated case, with the localisation errors for 45° pill rotation being within 0.010 m of the localisation errors for 0° pill rotation. The results suggest that the rotation of the pill does not have a significant impact on the localisation accuracy. While error is induced in the localisation accuracy due to the transmitter separation from a single point source rotation of the pill does not further increase this error.

The separation of transmitters from a single point has been demonstrated to introduce some error into the localisation, as the transmitter array no longer represents the centre of pill location and the signals received by different receivers have unique origin points. Through observing the range difference values between receivers it has been shown that for the distributed array these do not match those which are obtained for a single transmitter in the centre of the pill, which creates the error on the localisation result.

4.2.3 Summary of Simulation of a Multiple Transmitter Array

This section has investigated how the separation of transmitters from a point source on the pill to the periphery affects the localisation accuracy of the system. In [Chapter 3.0, section 3.2] it was demonstrated that a single transmitter could be localised with negligible error for ideal TDOA values when four receivers were utilised. The challenges associated with this project, as described in section 4.1 mean that a transmitter array is required which creates multiple signal origin points. Reported research within the field of TDOA considers only the single transmitter to multiple receivers scenario (Bakhoum, E.G. 2006), not that of multiple transmitters to multiple receivers. This section has therefore investigated the impact that using multiple transmitters has on localisation error.

For initial research a transmitter layout of 4 transmitters on the pill separated at 90° around the centre of the pill has been investigated with a corresponding receiver layout. With a pill diameter of 0.100 m the separation of transmitters from the centre of the pill is 0.050 m. Results have

demonstrated that due to the separation of the transmitters there is a localisation error induced when using the algorithm described in [Chapter 3.0, section 3.2]. With ideal TDOA and therefore range difference values it was shown in section 4.2.1 that the separation of transmitters induces a localisation error of 0.015 m on the true centre of pill location. For the 3 preliminary test locations it has been demonstrated that the maximum error is 0.030 m with an average error of 0.023 m. The result demonstrates that even with ideal TDOA values the separation of the transmitters on the pill means that the standard TDOA equations introduce error into the localisation result.

The target environment and pill design means that rotation of the pill in the vessel is anticipated. This means the individual coordinates of the transmitters will move while the centre of the pill coordinates remain stationary. Therefore another key area of research is how this rotation affects the localisation accuracy. Results in section 4.2.2 have considered rotation of the pill at 10°, 45° and 60° and suggest that rotation of the pill does not significantly affect the localisation error. For some rotation angles the errors reduces while for others there is a small increase however the changes are less than 0.001 m. While rotation does not significantly change the localisation any method implemented to reduce this error must be able to cope with pill rotation.

4.3 Localisation through Transmitter Offset Knowledge

4.3.1 Background

With a layout of multiple transmitters on the pill, which has been established as a requirement for adequate signal coverage within the vessel, simulations have demonstrated that the centre of the pill cannot be localised with negligible error, even under the conditions of ideal TDOA values. Through comparing the TDOA values for the case of a single transmitter against the values obtained for multiple transmitters on the pill it can be noted that due to the separation of the transmitters the TDOA values differ. Therefore using the same non-linear equations, however with different TDOA data, the solution returned will also differ.

In [Chapter 3.0, section 3.2.2] the TOF equation for a single transmitter to a receiver at coordinates (0, 0, 0) m was established,

$$T_A = \frac{1}{c}\left[\sqrt{(x)^2 + (y)^2 + (z)^2}\right] \quad \textbf{(3.5)}$$

Equation (3.5), defines the TOF from a single transmitter to the receiver mounted at location (0, 0, 0) m. This receiver location removes any receiver offset and that means the TOF is purely a function of the transmitter's location in the three coordinates *x, y* and *z.*

For a pill layout with multiple transmitters the distribution of the transmitters on the surface of the pill means that in equation (3.5) T_A represents the TOF from a transmitter which is offset from the centre of the pill to the receiver, it does not represent an accurate equation to solve for the centre

of the pill itself. Therefore, to solve for the centre of the pill the equation must be modified to include any offset of the transmitter from the centre of the pill in the *x, y* or *z* direction. The equation for the general case is specified in equation (4.1).

$$T_A = \frac{1}{c}\sqrt{(x - Offx)^2 + (y - Offy)^2 + (z - Offz)^2} \quad \textbf{(4.1)}$$

The speed of sound underwater is represented by *c* and *x, y, z* are the unknown coordinates of the centre of the pill. Off_X, Off_Y and Off_Z represent the offset of the transmitter from the centre of the pill in the *x, y* and *z* coordinate respectively.

Figure 4-6 has shown that for a pill centre of (0.200, -0.100, 0.300) m the transmitter closest to the receiver R_A (coordinates (0, 0, 0) m) for 0º rotation is T_1. T_1 is offset from the centre of the pill by 0.05 m, due to a pill diameter of 0.1 m. This offset means that the TOF which is observed from the transmitter T_1 to the receiver R_A is smaller than the TOF which would be observed if the signal originated from the centre of the pill. With knowledge of this offset the equations can be modified such that *x, y, z* represents the centre of the pill rather than the individual transmitter. As such the TOF equation, equation (3.5), can be amended for a signal from T_1 to R_A to become,

$$T_{1A} = \frac{1}{c}\sqrt{(x - 0.05)^2 + y^2 + z^2} \quad \textbf{(4.2)}$$

The speed of sound underwater is represented by *c* and *x, y, z* are the unknown coordinates of the centre of the pill. Through knowledge of the distribution of the transmitters around the pill and therefore their separation from the centre of the pill in the *x, y* and *z* coordinates, the required offsets for all of the transmitters can be calculated. This allows modifications to the TOF equations for all of the receivers, and subsequently the TDOA equations. The TOF equation to solve for the centre of the pill can therefore be defined for T_2 to R_B as,

$$T_{2B} = \frac{1}{c}\sqrt{[(x + 0.05) - x_B]^2 + (y - y_B)^2 + (z - z_B)^2} \quad \textbf{(4.3)}$$

The speed of sound is again represented by *c*, and *x, y, z* is the unknown location of the centre of the pill. The coordinates x_B, y_B, z_B refer to the coordinates of receiver R_B with respect to receiver R_A. Through knowledge of the TOF equations for receivers R_B and R_A the TDOA equation between these receivers can be modified. This is presented in equation (4.4).

$$\Delta_{BA} = \frac{1}{c}\left[\sqrt{[(x + 0.05) - x_B]^2 + (y - y_B)^2 + (z - z_B)^2} - \sqrt{(x - 0.05)^2 + y^2 + z^2}\right] \quad \textbf{(4.4)}$$

Equations (4.5) and (4.6) show the TDOA equations between arrivals at receivers R_C and R_A and R_D and R_A respectively. These equations assume that transmitter T_1 is the closest to receiver R_A; T_2 is the closest to R_B and so forth.

$$\Delta_{CA} = \frac{1}{c}\left[\sqrt{(x - x_C)^2 + [(y + 0.05) - y_C]^2 + (z - z_C)^2} - \sqrt{(x - 0.05)^2 + y^2 + z^2}\right] \quad \textbf{(4.5)}$$

$$\Delta_{DA} = \frac{1}{c}\left[\sqrt{(x - x_D)^2 + [(y - 0.05) - y_D]^2 + (z - z_D)^2} - \sqrt{(x - 0.05)^2 + y^2 + z^2}\right] \quad \textbf{(4.6)}$$

Expanding these non-linear equations allows a solution which represents the centre of the pill for 0º orientation to be calculated.

4.3.2 Localisation Error Results Using Offset Knowledge

Through the use of offset knowledge the TDOA equations now attempt to solve for the unknown centre of the pill rather than for individual transmitters. To allow a comparison with results from section 4.2 the same three test locations and pill rotation angles are simulated for a 4 transmitter pill utilising the modified TDOA equations.

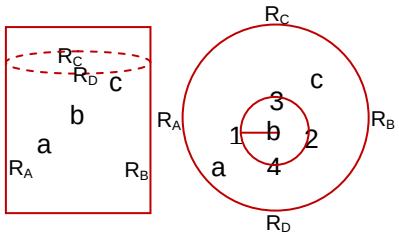

	Actual Location (m)	Calculated Location (m)	Error (m)
a	(0.200, -0.100, 0.300)	(0.200, -0.100, 0.300)	0.000
b	(0.080, -0.180, 0.150)	(0.047, -0.208, 0.140)	0.044
c	(0.400, 0.050, 0.500)	(0.400, 0.050, 0.500)	0.000

Table 4-5: Calculated location and error for 0º rotation using transmitter offset knowledge

Table 4-5 shows the actual and calculated location of the pill for 0º rotation. The results in locations (0.200, -0.100, 0.300) m and (0.400, 0.050, 0.500) m show the reduction in error as expected due to the modifications made to the TDOA equations. In these locations the error is negligible and the centre of the pill is accurately located. The modifications made to the equations mean that the TDOA values now represent the centre of the pill, and therefore with no errors on these values the centre of the pill can be located with negligible error.

In location (0.080, -0.180, 0.150) m however there is an error of 0.044 m. When compared to the results in this location with no offset knowledge, in section 4.2.1, the error has increased by almost 50%. This result demonstrates the limitations of using offset knowledge alone to attempt to localise the centre of the pill. For this pill location the signal arriving at R_A does not originate from T_1, the shortest path to the receiver is actually from T_3, which means that for this location the modified TDOA equation is incorrect.

For a centre of the pill location (0.080, -0.180, 0.150) m with 0º rotation the coordinates of transmitter T_1 are (0.030, -0.180, 0.150) m and the coordinates of T_3 are (0.080, -0.130, 0.150) m. This means that the range from T_1 to R_A is 0.236 m (3dp) and the range from T_3 to R_A is 0.214 m (3dp). The first signal therefore to reach receiver R_A originates from T_3 rather than the anticipated T_1. As stated, for the modified TDOA equations, it is assumed that R_A receives signal from T_1, R_B from T_2 and so forth. In this test location this is not the case, with the first signal to arrive at R_A originating from a transmitter not specified in the equations. As it is not possible to identify the origin of the signal as T_3 rather than T_1 through the TDOA values alone, the assumption that T_1 is the origin of the signal must be maintained. This results in an error on the calculated location, as the offset knowledge used is incorrect

If the TDOA equation is modified such that that the assumption is made that the first signal arriving at R_A originates from T_3 then the offset required from the centre of the pill changes. In this case, the offset required would be for the T_3 transmitter relative to the centre of the pill, rather than the T_1 transmitter. If modifications are made to the TDOA equations to account for the change in the origin of the signal, then the error on this test location, (0.080, -0.180, 0.150) m can be reduced to a negligible value. This modification would however then mean that the TDOA equations would not be accurate for locations 1 and 3 as the offsets for these locations would be incorrect.

The issue of specifying incorrect TDOA equations when using offset knowledge about the location of the transmitters on the pill is further compounded when the pill rotates. Rotation of the pill alters the offset values required to maintain the correct TOF and TDOA equations. Figure 4-7 illustrated the pill rotated at 45º. For this rotation the offset required for the TOF from transmitter T_1 to R_A alters and the equation must be modified as follows,

$$T_{1A} = \frac{1}{c}\sqrt{(x - 3.54)^2 + (y + 3.54)^2 + z^2} \qquad \textbf{(4.7)}$$

The speed of sound is represented by *c*, and *x, y, z* is the centre of the pill. As the distribution of the transmitters from the centre of the pill is known, then with knowledge of the pill's rotation angle calculating the new offsets that are required is a simple trigonometric problem. The issue however is that with the limited information obtained from TDOA using 4 receivers, it is not possible to resolve the pill rotation angle, and as such the equation offsets cannot be modified. This means that again the equations do not accurately represent the layout and orientation of the pill which will introduce an error on the localisation.

As it is not possible to resolve the rotation of the pill from TDOA values alone, then only one set of modified TDOA equations can be used. These are the equations established for 0º pill rotation. Therefore when the pill is rotated these equations will introduce some error into the localisation. To observe the affect this has on the localisation error and to compare with the results when no offset

knowledge is used the previous test locations and rotation angles of 10º, 45º and 60º are simulated. The offsets established in equations (4.4) to (4.6) are used for all of the tested locations.

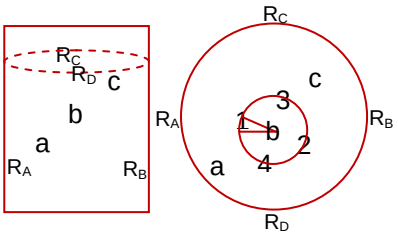

	Actual Location (m)	Calculated Location (m)	Error (m)
a	(0.200, -0.100, 0.300)	(0.120, -0.098, 0.300)	0.008
b	(0.080, -0.180, 0.150)	(0.046, -0.205, 0.146)	0.042
c	(0.400, 0.050, 0.500)	(0.403, 0.045, 0.501)	0.006

Table 4-6: Calculated location and error for 10º rotation using transmitter offset knowledge

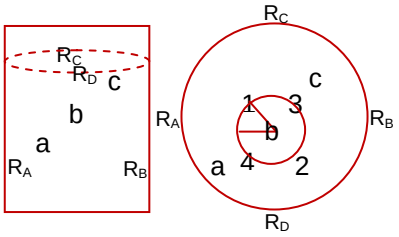

	Actual Location (m)	Calculated Location (m)	Error (m)
a	(0.200, -0.100, 0.300)	(0.196, -0.107, 0.296)	0.009
b	(0.080, -0.180, 0.150)	(0.046, -0.209, 0.139)	0.046
c	(0.400, 0.050, 0.500)	(0.416, 0.058, 0.519)	0.027

Table 4-7: Calculated location and error for 45º rotation using transmitter offset knowledge

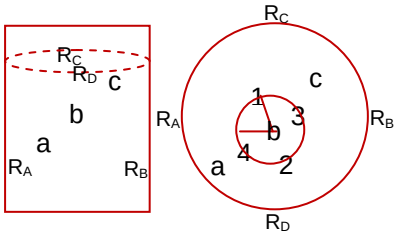

	Actual Location (m)	Calculated Location (m)	Error (m)
a	(0.200, -0.100, 0.300)	(0.203, -0.109, 0.297)	0.010
b	(0.080, -0.180, 0.150)	(0.046, -0.216, 0.131)	0.053
c	(0.400, 0.050, 0.500)	(0.405, 0.060, 0.508)	0.014

Table 4-8: Calculated location and error for 60º rotation using transmitter offset knowledge

Table 4-6 through to Table 4-8 displays the actual and calculated location of the pill along with the errors for the 4 transmitter layout for rotations of 10º, 45º and 60º respectively. The TDOA equations utilised to calculate these locations are those established for 0º rotation of the pill.

The negligible error which was previously obtained in locations 1 for 0º rotation is no longer observed as the pill has rotated. The error is approximately 0.010 m for all of the rotation angles. The errors in location 2 are again substantially higher than location 1 and 3 as the signals reaching the receivers originate from transmitters incorrectly specified in the equations.

From the selection of tested locations it can be shown that for locations 1 and 3 there is improvement in the localisation accuracy when offset knowledge is used, however for location 2 the use of offset knowledge causes the error on the localisation to increase in comparison to when offset knowledge is not used due to the incorrectly specified equation. It is therefore necessary to take a larger spread of results to observe how often this condition occurs, and what percentage of locations have improved results when using the offset knowledge method. To do this a wider range of potential pill locations were modelled, at 0.1 m intervals through the vessel stepped in *x* and *y*.

This gives 20 transmitter locations for a single z height. Rotation angles for the pill are considered from 0° through to 90° at intervals of 10°. The test locations are illustrated in Figure 4-8.

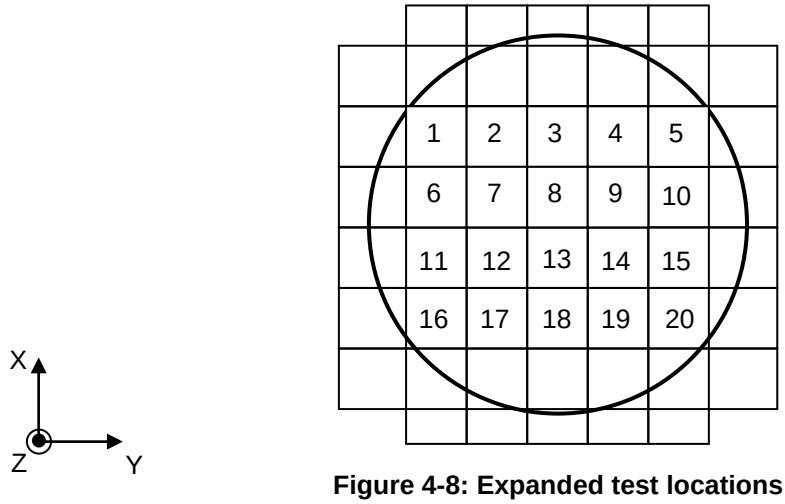

Figure 4-8: Expanded test locations

True position (m)			Error on true position without offset knowledge 0° rotation (m)	Error on true position with offset knowledge 0° rotation (m)
X	Y	Z		
0.100	-0.200	0.300	0.025	0.043
0.100	-0.100	0.300	0.029	0.000
0.100	0.000	0.300	0.023	0.000
0.100	0.100	0.300	0.029	0.000
0.100	0.200	0.300	0.025	0.043
0.200	-0.200	0.300	0.035	0.000
0.200	-0.100	0.300	0.015	0.000
0.200	0.000	0.300	0.008	0.000
0.200	0.100	0.300	0.015	0.000
0.200	0.200	0.300	0.035	0.000
0.300	-0.200	0.300	0.035	0.000
0.300	-0.100	0.300	0.015	0.000
0.300	0.000	0.300	0.008	0.000
0.300	0.100	0.300	0.015	0.000
0.300	0.200	0.300	0.035	0.000
0.400	-0.200	0.300	0.025	0.043
0.400	-0.100	0.300	0.029	0.000
0.400	0.000	0.300	0.023	0.000
0.400	0.100	0.300	0.029	0.000
0.400	0.200	0.300	0.025	0.043

Table 4-9: Comparison of localisation errors with and without offset knowledge 0° rotation

Table 4-9 shows a comparison of the localisation errors when the pill is located with and without offset knowledge for 0° rotation. The green box highlights the method with the smallest localisation error. It can be observed that for the 20 locations tested the error is improved in 16 locations using offset knowledge. For 0° rotation this result is anticipated as it can be observed that for the majority of pill locations the TDOA equation offsets used are correct. The average error without using offset knowledge is 0.024 m while the average error when offset knowledge is used is 0.009 m. The improvement in error is observed for 80% of the locations tested. To observe how rotation affects this result the same pill locations are tested with the orientation of the pill rotated.

True position (m)			10° rotation		20° rotation		30° rotation	
X	Y	Z	Error (m) without offset	Error (m) with offset	Error (m) without offset	Error (m) with offset	Error (m) without offset	Error (m) with offset
0.100	-0.200	0.300	0.026	0.044	0.027	0.046	0.025	0.044
0.100	-0.100	0.300	0.025	0.008	0.020	0.017	0.017	0.027
0.100	0.000	0.300	0.023	0.007	0.022	0.008	0.020	0.008
0.100	0.100	0.300	0.025	0.008	0.022	0.018	0.019	0.018
0.100	0.200	0.300	0.024	0.044	0.023	0.047	0.023	0.049
0.200	-0.200	0.300	0.033	0.010	0.029	0.012	0.025	0.016
0.200	-0.100	0.300	0.015	0.005	0.016	0.010	0.015	0.011
0.200	0.000	0.300	0.008	0.002	0.008	0.004	0.009	0.006
0.200	0.100	0.300	0.015	0.005	0.016	0.009	0.011	0.010
0.200	0.200	0.300	0.031	0.007	0.026	0.014	0.021	0.024
0.300	-0.200	0.300	0.031	0.007	0.026	0.014	0.021	0.024
0.300	-0.100	0.300	0.015	0.005	0.016	0.009	0.011	0.010
0.300	0.000	0.300	0.008	0.002	0.008	0.004	0.009	0.006
0.300	0.100	0.300	0.015	0.005	0.016	0.010	0.015	0.011
0.300	0.200	0.300	0.029	0.012	0.029	0.012	0.025	0.016
0.400	-0.200	0.300	0.024	0.044	0.023	0.047	0.023	0.049
0.400	-0.100	0.300	0.025	0.008	0.022	0.018	0.019	0.018
0.400	0.000	0.300	0.023	0.007	0.022	0.008	0.021	0.010
0.400	0.100	0.300	0.025	0.008	0.020	0.017	0.017	0.027
0.400	0.200	0.300	0.026	0.044	0.027	0.046	0.025	0.044

Table 4-10: Comparison of localisation errors with and without offset knowledge, pill rotation angles of 10°, 20° and 30°

Table 4-10 shows a comparison of the localisation errors when the pill is located with and without offset knowledge for 10°, 20° and 30° rotation. For pill rotations of 10° and 20° the offset knowledge method improves the result in 80 % of the locations tested. For 30° pill rotation the offset knowledge method provides improvement in 60% of the locations tested.

True position (m)			40° rotation		50° rotation		60° rotation	
X	Y	Z	Error (m) without offset	Error (m) with offset	Error (m) without offset	Error (m) with offset	Error (m) without offset	Error (m) with offset
0.100	-0.200	0.300	0.024	0.043	0.023	0.045	0.023	0.049
0.100	-0.100	0.300	0.016	0.023	0.017	0.019	0.019	0.018
0.100	0.000	0.300	0.019	0.012	0.019	0.012	0.020	0.008
0.100	0.100	0.300	0.017	0.019	0.016	0.023	0.017	0.027
0.100	0.200	0.300	0.023	0.045	0.024	0.043	0.025	0.044
0.200	-0.200	0.300	0.021	0.023	0.018	0.031	0.021	0.024
0.200	-0.100	0.300	0.010	0.008	0.007	0.011	0.011	0.010
0.200	0.000	0.300	0.008	0.004	0.008	0.004	0.009	0.006
0.200	0.100	0.300	0.007	0.011	0.010	0.008	0.015	0.011
0.200	0.200	0.300	0.018	0.031	0.021	0.023	0.025	0.016
0.300	-0.200	0.300	0.018	0.031	0.021	0.023	0.025	0.016
0.300	-0.100	0.300	0.007	0.011	0.010	0.008	0.015	0.011
0.300	0.000	0.300	0.008	0.004	0.008	0.004	0.009	0.006
0.300	0.100	0.300	0.010	0.008	0.007	0.011	0.011	0.010
0.300	0.200	0.300	0.021	0.023	0.018	0.031	0.021	0.024
0.400	-0.200	0.300	0.023	0.045	0.024	0.043	0.025	0.044
0.400	-0.100	0.300	0.017	0.019	0.016	0.023	0.017	0.027
0.400	0.000	0.300	0.020	0.014	0.020	0.014	0.021	0.010
0.400	0.100	0.300	0.016	0.023	0.017	0.019	0.019	0.018
0.400	0.200	0.300	0.024	0.043	0.023	0.045	0.023	0.049

Table 4-11: Comparison of localisation errors with and without offset knowledge, pill rotation angles of 40°, 50° and 60°

Table 4-11 shows a comparison of the localisation errors when the pill is located with and without offset knowledge for 40°, 50° and 60° rotation. It can be observed for 40° and 50° rotation of the pill the method without offset knowledge is superior. The TDOA equations using offset knowledge are still specified for 0° pill rotation as the rotation angle is unknown to the solver. However, for a pill rotation of 60° improvement is observed in 60% of the locations tested when offset knowledge is used.

True position (m)			70° rotation		80° rotation		90° rotation	
X	Y	Z	Error (m) without offset	Error (m) with offset	Error (m) without offset	Error (m) with offset	Error (m) without offset	Error (m) with offset
0.100	-0.200	0.300	0.023	0.047	0.024	0.044	0.025	0.043
0.100	-0.100	0.300	0.022	0.018	0.025	0.008	0.029	0.000
0.100	0.000	0.300	0.022	0.008	0.023	0.007	0.023	0.000
0.100	0.100	0.300	0.020	0.017	0.025	0.008	0.029	0.000
0.100	0.200	0.300	0.027	0.046	0.026	0.044	0.025	0.043
0.200	-0.200	0.300	0.026	0.014	0.031	0.007	0.035	0.000
0.200	-0.100	0.300	0.016	0.009	0.015	0.005	0.015	0.000
0.200	0.000	0.300	0.008	0.004	0.008	0.002	0.008	0.000
0.200	0.100	0.300	0.016	0.010	0.015	0.005	0.015	0.000
0.200	0.200	0.300	0.029	0.012	0.033	0.010	0.035	0.000
0.300	-0.200	0.300	0.029	0.012	0.029	0.012	0.035	0.000
0.300	-0.100	0.300	0.016	0.010	0.015	0.005	0.015	0.000
0.300	0.000	0.300	0.008	0.004	0.008	0.002	0.008	0.000
0.300	0.100	0.300	0.016	0.009	0.015	0.005	0.015	0.000
0.300	0.200	0.300	0.026	0.014	0.031	0.007	0.035	0.000
0.400	-0.200	0.300	0.027	0.046	0.026	0.044	0.025	0.043
0.400	-0.100	0.300	0.020	0.017	0.025	0.008	0.029	0.000
0.400	0.000	0.300	0.022	0.008	0.023	0.007	0.023	0.000
0.400	0.100	0.300	0.022	0.018	0.025	0.008	0.029	0.000
0.400	0.200	0.300	0.023	0.047	0.024	0.044	0.025	0.043

Table 4-12: Comparison of localisation errors with and without offset knowledge, pill rotation angles of 70°, 80° and 90°

Table 4-12 shows a comparison of the localisation errors when the pill is located with and without offset knowledge for 70°, 80° and 90° rotation. It can be observed that for all of these rotation angles the localisation method using offset knowledge proves superior, with 80% of the locations tested having a smaller localisation error when the method using offset knowledge is used.

For all of the locations and rotation angles tested it is observed that for 64 % of the locations tested there is an improvement in localisation accuracy when offset knowledge is used. The average error has also improved, from 0.020 m without offset knowledge to 0.018 m with offset knowledge. While this is only a small improvement in localisation accuracy this figure is heavily weighted by the locations in which the incorrect transmitter is specified in the equations. It can be observed that for certain locations when the pill is rotated 0° an error of 0.043 m is created due to the equation being specified with the wrong transmitter as discussed in section 4.3.2.

To remove this problem it is possible to code the transmitters such that they have unique identifiers, either through the use of small variations in frequency between transmitters or different transmission signals. If this is done then the origin point of each signal can be identified, and it is therefore possible to know that a received signal originated, for example, from transmitter T_3 rather than transmitter T_1. This allows the TDOA offsets utilised to be modified such that the offset for T_3 is specified in the TDOA equations.

If this unique transmitter identification is completed and the TDOA equations modified depending on the known origin of the signal then the offset localisation can be significantly improved. The percentage of improved localisation positions increases to 76 % and the average localisation error is reduced significantly to 0.011 m.

4.3.3 Accommodating Rotation of the Pill

In section 4.3.2 it has been demonstrated that for a pill rotation of 0° it is possible to localise the centre of the pill with negligible error using the transmitter offset method, provided that the origin of the transmitted signal can be determined and the equations updated accordingly. Results have demonstrated however that as the pill rotates, the offsets required in the TDOA equations change and the centre of the pill cannot be localised with negligible error.

Through TDOA alone it is not possible to determine the rotation angle of the pill, therefore modifications to the offset values required in the TDOA equations cannot be implemented. To eliminate the problems caused by rotation this thesis investigates two possible options. The first is to mount transmitters on the pill's surface such that they are not affected by rotation of the pill, and their coordinates do not alter in *x, y* or *z*. The second option is to code the signals transmitted from each transmitter uniquely, such that they can be identified at the receiver and provide additional information regarding the orientation of the pill. While a third option might be to use a compass to determine the orientation of the pill, it is anticipated that due to the nature of the metallic vessel this will not be possible and therefore this thesis investigates the more challenging case, when rotation of the pill is unknown.

Negating the Effects of Transmitter Rotation

To eliminate the requirement for knowledge of the pill's rotation relative to the receiver positions, one solution is to mount the transmitters on the pill in locations such that the rotation of the pill is negated in terms of movement of the transmitters in the *x, y* or *z* components.

This can be achieved by mounting the transmitters at the top and the bottom of the pill, along the central vertical axis. As presented in section 4.2.2 rotation around the *x* or *y* axes can be minimised through ballasting the pill at its base, this leaves only rotation around the *z* axis.

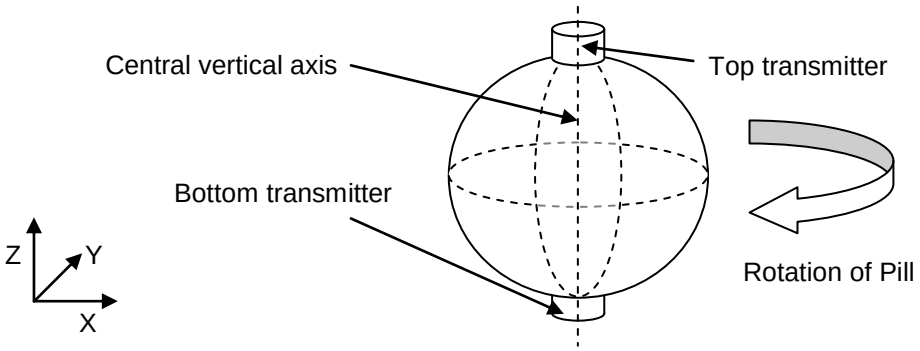

Figure 4-9: 2 transducer pill layout to negate rotation issues

Figure 4-9 displays the 2 transducer pill layout with transmitters mounted at the top and bottom of the pill along the *z*-axis. The transmitter mounting points eliminate the requirement for any offset in the *x* or *y* component, as the transmitters remain mounted directly above and below the centre of the pill, regardless of the rotation angle. The top transducer offset is 0.05 m above the centre of the pill; the bottom transducer is offset 0.05 m below the centre of the pill. With this knowledge the TDOA equations can be modified to accommodate the offsets and locate the centre of the pill. The TOF from the bottom transmitter to receiver R_A is therefore defined as,

$$T_A = \frac{1}{c}\sqrt{x^2 + y^2 + (z - 0.05)^2} \tag{4.8}$$

where *c* is the speed of sound and *x, y, z* the unknown location of the centre of the pill. For the other receivers the TOFs can be calculated, which gives the modified TDOA equations for the 2 transmitter layout shown in equations (4.9) through to (4.11),

$$\Delta_{BA} = \frac{1}{c}\left[\sqrt{(x - x_B)^2 + (y - y_B)^2 + [(z - 0.05) - z_B)]^2} - \sqrt{x^2 + y^2 + (z - 0.05)^2}\right] \tag{4.9}$$

$$\Delta_{CA} = \frac{1}{c}\left[\sqrt{(x - x_C)^2 + (y - y_C)^2 + [(z + 0.05) - z_C)]^2} - \sqrt{x^2 + y^2 + (z - 0.05)^2}\right] \tag{4.10}$$

$$\Delta_{DA} = \frac{1}{c}\left[\sqrt{(x - x_D)^2 + (y - y_D)^2 + [(z + 0.05) - z_D)]^2} - \sqrt{x^2 + y^2 + (z - 0.05)^2}\right] \tag{4.11}$$

where (x_B, y_B, z_B) refer to the coordinates of receiver R_B with respect to the coordinate origin at R_A, *c* is the speed of sound and *x, y, z* are the unknown coordinates of the centre of the pill. These equations remain correct provided that the pill's location remains in the area between the top and bottom receivers. If the pill moves above the top receivers, then all the signals reaching the receivers in the vessel originate from the bottom transmitter, and vice versa, if the pill moves below the bottom receivers. This condition however can be easily maintained by mounting the receivers at the top and bottom of the region of interest in the vessel.

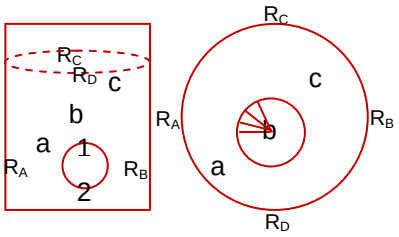

	Actual Location (m)	Calculated Location (m)	Error (m)
a	(0.200, -0.100, 0.300)	(0.200, -0.100, 0.300)	0.000
b	(0.080, -0.180, 0.150)	(0.080, -0.180, 0.150)	0.000
c	(0.400, 0.050, 0.500)	(0.400, 0.050, 0.500)	0.000

Table 4-13: Calculated location and error for 0º, 10°, 45° and 60° rotation with 2 transducer layout

Table 4-13 shows the actual and calculated location of the centre of the pill. For the three tested locations the error on localisation is negligible. This result is maintained for rotation angles of 0°, 10°, 45° and 60° pill rotation. Through altering the position of the transmitters on the pill, rotation of the pill does not change the offsets required and therefore for all rotation angles there is negligible localisation error. In comparison to the 4 transmitter pill layout for 0º rotation, it can be observed that the error in location 2 has been removed with this 2 transmitter pill layout.

While this result suggests that the 2 transmitter pill layout is a viable option to eliminate the localisation problems due to rotation of the pill, it does impose a strict transmitter layout on the pill. With a transmitter mounted to only the top and bottom of the pill it could be anticipated that the signal coverage available at the receivers will be poor, due to the beam width of an individual transmitter, as discussed in [Chapter 6.0]. It is therefore anticipated that this “above and below” transmitter layout will be unable to provide sufficient signal strength to all receivers for certain locations in the vessel. Therefore, while from a TDOA perspective this layout has merits, due to the limited beam coverage it is envisaged that it cannot be practically implemented.

Individual Transmitter Coding

To accurately locate the centre of the pill knowledge of the offset of transmitters from the centre of the pill is required. Through standard TDOA is it not possible to determine the pill’s orientation. This section introduces the method of individual transmitter coding to allow “double TDOA” which allows the rotation angle of the pill to be resolved.

Through the assignment of individual codes or frequencies to each transmitter, such that they have a unique identifier, then it is possible to derive more TDOA information which allows the orientation of the pill to be resolved. If each transmitter is assigned a unique identifier then it is possible for a single receiver to distinguish between the arrivals of signals from multiple transmitters. This allows the TDOA between the signals arrivals to be calculated, provided a receiver is able to obtain signal from more than one transmitter. This TDOA is the difference in arrival time, at a single receiver, of two signals which are transmitted from different transmitters, with different origin points. This is opposed to the previously stated TDOA which calculates the difference in arrival time of a signal at two receivers.

Through the use of unique identifiers for different transmitters, then the origin of a signal which arrives at any receiver can be identified, and the appropriate offset selected to alter the TDOA equations. This eliminates the problem identified for location 2 in section 4.3.2, whereby the equations are incorrectly specified. Through using the transmitter identifier code to modify the TDOA equations to accommodate the transmitter origin, the error can be removed, provided that the rotation of the pill is 0°. When the pill rotates this transmitter code on its own is insufficient to determine the pill's orientation. To do this the TDOA between signals from multiple transmitters to a single receiver must be utilised.

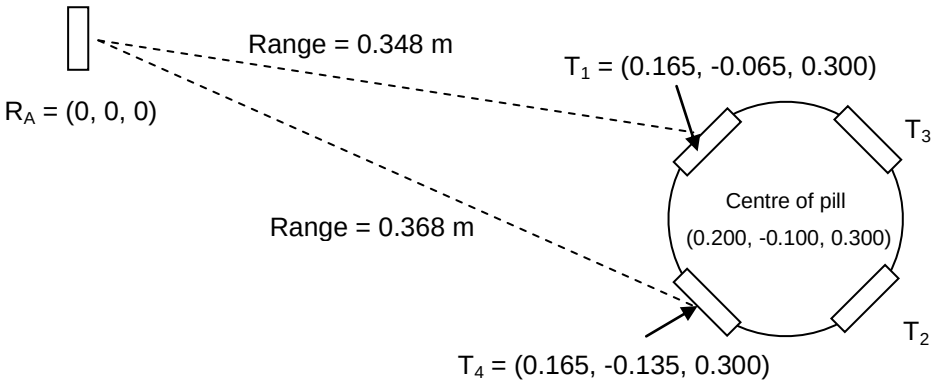

Figure 4-10: True position and orientation of pill

Figure 4-10 illustrates the case of 45º rotation for a pill centre of (0.200, -0.100, 0.300) m. The location calculated for this position using the solver in this thesis is (0.196, -0.107, 0.296) m. As the rotation of the pill is unknown, then the TDOA equations used by the solver are those specified for 0º rotation, and the calculated location therefore has an error of 0.009 m on the true location of the pill. From Figure 4-10 it can be calculated from the TOF that the range from transmitter T_1 to the receiver R_A is 0.348 m, while the range from transmitter T_4 to the receiver R_A is 0.368 m. This means that the range difference between these transmitters is 0.020 m for this pill position.

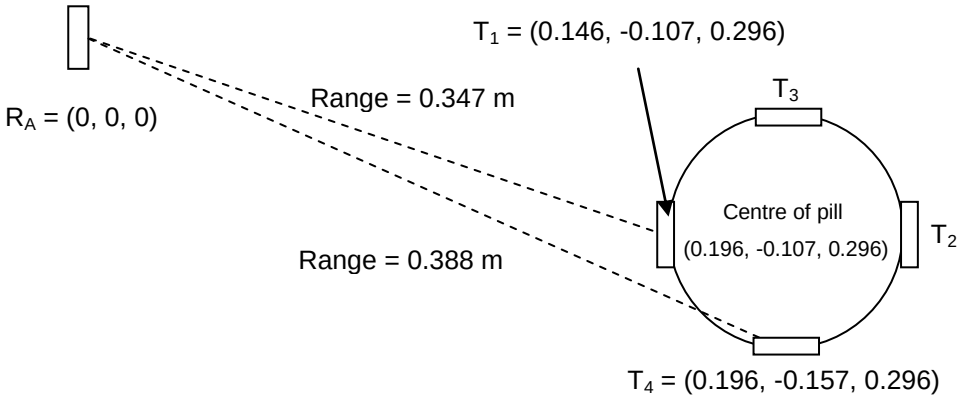

Figure 4-11: Fsolve calculated location, showing 0º rotation

Figure 4-11 illustrates the location of the pill calculated by the solver, (0.196, -0.107, 0.296) m. The solver uses a rotation angle of 0° as the actual rotation angle is unknown to the solver. Through

knowledge of the transmitter offsets (0.05 m from the centre of the pill) and assuming 0° rotation the solver is able to calculate, based on a centre of pill (0.196, -0.107, 0.296) m, that transmitter T_1 is located at (0.146, -0.107, 0.296) and transmitter T_4 is located at (0.196, -0.157, 0.296) m.

For each transmitter it is possible to calculate the range to receiver R_A. For transmitter T_1 this is 0.347 m and for transmitter T_4 this is 0.388 m. This gives a range difference between the signal arrivals of 0.041 m at receiver R_A.

The solver is then able to compare the range difference it has calculated (0.041 m) with that obtained from the actual experimental data (0.020 m as is observed in Figure 4-10). The solver is therefore able to determine that as the values do not match the 0° pill orientation it has assumed is incorrect.

Using this knowledge, and starting from its original calculated location of (0.196, -0.107, 0.296) m the solver can then alter the rotation angle of the pill in an iterative manner until the range difference calculated by the solver between the arrivals of signals T_1 and T_4 at the receiver R_A fits the experimental data. This can be observed in Table 4-14.

Rotation Angle (º)	**T_1 location**			**T_4 location**			**Range T_1**	**Range T_4**	**Range Difference**
	(x)	**(y)**	**(z)**	**(x)**	**(y)**	**(z)**			
0	0.146	-0.107	0.296	0.196	-0.157	0.296	0.347	0.388	0.041
10	0.147	-0.098	0.296	0.187	-0.156	0.296	0.345	0.384	0.039
20	0.149	-0.090	0.296	0.179	-0.154	0.296	0.343	0.379	0.035
30	0.153	-0.082	0.296	0.171	-0.150	0.296	0.343	0.373	0.030
40	0.158	-0.075	0.296	0.164	-0.145	0.296	0.344	0.368	0.025
50	0.164	-0.069	0.296	0.158	-0.139	0.296	0.345	0.363	0.018

Table 4-14: Pill rotation angle and corresponding TDOA values

Table 4-14 displays the locations of transmitter T_1 and T_4 for the centre of pill location (0.196, -0.107, 0.296) m with various pill rotation angles. The ranges to receiver R_A are also displayed along with the range difference between the arrivals of signals. From Figure 4-10 the range difference observed for the actual pill orientation is 0.020 m. From Table 4-14 it can be observed that this is calculated for a rotation angle between 40° and 50°. In this instance the closest rotation value which gives the desired 0.020 m range difference is 47°.

This information can then be used to modify the original TDOA equations such that they assume the pill is rotated 47º and the solver can then recalculate the centre of the pill. This allows a better approximation of the centre of the pill to be realised as the equations are closer to that which are required. This process can be repeated with the new calculated location iteratively until the error between the calculated and actual transmitter range difference is below an acceptable threshold. It

can however be observed that with a single iteration the rotation angle of 47º has been selected, which is only a 2º error in relation to the actual pill orientation of 45° in Figure 4-10.

Improving Localisation Accuracy through Alternative Methods

Another potential method to improve the localisation accuracy of the system is to use a pressure measurement to determine depth. In this way only the *x* and *y* coordinate of the pill need to be determined from TDOA information as the depth of the pill, *z,* can be inferred from the measured pressure. This allows a known value, *z* to be used in the TDOA equations to improve the solution.

The advantage of using this technique is that the measured pressure over a depth of 1 m can be recorded to a high accuracy, meaning that the depth can be estimated to within an accuracy of approximately 1 cm (Watson S.A and Green P.N. 2011) .This measurement however is only able to be referred to as a change in pressure and while the change in depth is known, the absolute depth is not known which means that the sensor would need to be calibrated every time it was placed into the vessel. This adds both time and complexity to the use of the sensor pills for monitoring and would limit their application when this calibration cannot be completed.

A final disadvantage of using a pressure measurement is that the pressure sensor must be mounted onboard the pill such that it is able to record depth changes as the pill moves. This information then needs to be relayed back to the external system and interpreted. This means there is a requirement to establish communication between the pill and the external hardware such that different values of pressure and therefore depth can be communicated. While communication is a long term goal for the pill, such that various sensor information can be relayed from the pill to an external monitoring station, this is beyond the scope of this thesis.

For this reason while pressure measurements are seen as a potential future measurement to improve the localisation accuracy, by informing TDOA or TOF localisation of the approximate *z* depth and therefore helping the equations to converge to a more accurate solution, this thesis considers the more difficult case where such measurements are not possible.

4.3.4 Summary of Localisation through Transmitter Offset Knowledge

In section 4.2 it has been demonstrated that the separation of transmitters on the pill causes a localisation error while using the standard TDOA equations. This section has investigated the cause of this localisation error and investigated methods to reduce this error.

In section 4.3.1 the background problem which causes the error is discussed. The separation of the transmitters means that the standard TDOA equations utilised now no longer represent the location to be solved for. To accommodate this, the method of offset knowledge is introduced which utilises knowledge of the separation of each transmitter from the centre of the pill so that the TDOA equations reference the centre of the pill rather than individual transmitter locations.

Section 4.3.2 investigates localisation of the pill utilising the offset knowledge method. The results for the same 3 test locations demonstrate that for two locations the localisation error has reduced to a negligible value however for the third location an error is still present. This error is caused because the transmitter offsets utilised in the equation are not correct for this pill location and the transmitters closest to the receivers are not those anticipated. This problem is further compounded due to the rotation of the pill. Due to a lack of information provided by standard TDOA the rotation of the pill cannot be resolved which again induces a localisation error.

Results demonstrating the localisation error are considered for the method of offset knowledge against standard TDOA equations. Twenty test locations across the vessel are tested for pill rotations of 0° through to 90°. While it can be observed that for certain test locations the error is smallest using standard TDOA equations across the cross section of test locations and pill rotations the localisation error is smallest in 64% when using offset knowledge and the error reduces from an average of 0.020 m to 0.018m.

If the transmitters are individually coded such that they have unique identifiers and therefore the arrival of a signal at a receiver can be associated with the correct transmitter then the percentage of improved locations increased to 76% and the localisation average error reduces to 0.011 m.

While it has been demonstrated that offset knowledge reduces localisation error because rotation of the pill cannot be determined there is always an error induced. In section 4.3.3 options to overcome the problem of rotation have been investigated. One possible option investigated is to negate the problem of rotation by careful placement of the transmitters on the pill. This method does however impose a strict limitation on the possible transmitter arrangements on the pill. With the limited beam coverage anticipated from a single transmitter then from a signal coverage perspective this layout cannot be utilised.

The second option investigated is through a combination of individual transmitter coding and utilising two TDOA techniques. As the distribution of transmitters relative to each other on the pill is fixed, then the difference in time of arrival for signals at a given receiver, allows information about the pill's orientation to be deciphered. This information can be used once the location of the pill is calculated expecting 0° rotation to determine the validity of the calculated location. If transmitter TDOAs do not fit then the rotation angle can be updated and the location of the pill recalculated.

Results have demonstrated that for a 45° pill rotation a single iteration of the transmitter TDOA allows a rotation angle of 47° to be determined allowing an updated pill location which has a smaller error. This method has the advantage of allowing a much wider range of possible transmitter layouts to be explored; it does however require a much greater computational processing power at the receiver. The orientation of the pill must be deciphered and then the equations modified in real time to allow the location of the pill to be accurately determined.

A further option that has been investigated to improve localisation accuracy is through the use of pressure measurements. The pressure measurement is only a relative measurement and not absolute which means calibration is required every time the pill is inserted into the vessel. Due to calibration requirements pressure measurements are not used within this thesis.

4.4 Optimising Receiver Layout

The development of a transmitter array creates the challenge to localise the centre of the pill from distributed transmitters. While this is important for localisation accuracy it represents only half of the localisation problem. The other key aspect which requires investigation is how the placement of receivers within the vessel affects the localisation accuracy of the system, particularly in the presence on non-perfect TDOA values due to noise. The original localisation system developed by Burnett-Thompson A. (2007) did not investigate the optimum receiver layout. This work was identified by external referees as a potential research interest and an area for future development.

In a noiseless environment each receiver layout is anticipated to perform to the same localisation accuracy, as the TDOA values are all ideal. For real world applications however, noise is anticipated on the TDOA values, creating errors which propagate through to the localisation. One of the key interests is therefore how different receiver layouts are able to cope with non-perfect TDOA values. In this instance the interest is in the size of the TDOA error which can be accommodated while still localising the transmitter, and the overall error on the TDOA localisation.

To evaluate the optimal receiver layout simulations are conducted applying errors to individual range values which then propagate through to the range difference values. Three receiver layouts are considered for exploration. The optimum receiver layout depends on two factors. Firstly the ability of the layout to cope with error on TDOA values such that they do not significantly impact the localisation accuracy. Secondly, that the receiver layout is able to adequately detect signal from the pill. If the receivers are located such that signal from the pill cannot be detected then there is no TDOA information available and the pill cannot be localised. It is therefore anticipated that the receiver layout will be a trade off between a layout which minimises the localisation error, while still being able to detect signal from the pill. The signal strength from the pill is modelled in [Chapter 6.0]. This chapter will investigate the optimum receiver layout from a minimisation of error standpoint

As a decision on the optimum layout for the transmitters is still to be determined, due to the work required on signal strength, which is presented in [Chapters 5.0 and 6.0] a single transmitter is considered for simulations.

4.4.1 Top Mounted Receiver Layout

One advantage of implementing a wireless pill in comparison to a technique such as tomography is the reduction in modifications required to the vessel. As stated in York T.A (2007) the use of tomography in a vessel usually involves a large amount of retrofitting of the vessel with electrodes. For the target environment of a mixing vessel there is also the possibility of an impeller, which must be avoided to ensure the mixing process is not compromised. As such one desirable option is to mount the receivers at the top of the vessel away from any impeller. This minimises intrusion into the vessel and makes the process of fitting the receivers both simple and inexpensive. In order to allow the 3D position of the transmitter to be obtained the receivers must not be mounted in a coplanar manner. However as the desire of any top mounted receiver layout is to keep the receivers away from the mixing area of the vessel the vertical displacement between receivers should be minimised. To achieve this, a top mounted receiver layout is considered with the separation between the top and bottom receivers limited to 0.05 m. This layout is shown in Figure 4-12.

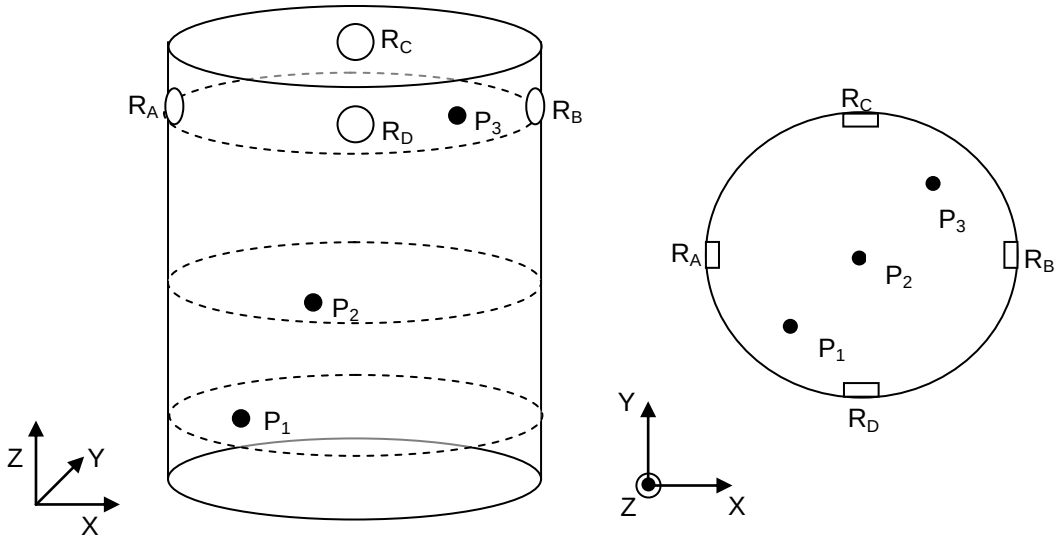

Figure 4-12: Top mounted receiver layout with three test locations

Figure 4-12 displays the position of the four receivers and also the transmitter test locations. The dimensions of the vessel for the simulations are 0.5 m by 1 m. The receiver coordinates in this instance are R_A = (0.000, 0.000, 0.950) m, R_B = (0.500, 0.000, 0.950) m, R_C = (0.250, 0.250, 1.000) m and R_D = (0.250, -0.250, 1.000) m.

For simulation three test transmitter locations in the vessel are selected. The three locations selected have coordinates, P_1 = (0.100, -0.050, 0.150) m, P_2 = (0.200, -0.130, 0.500) m and P_3 = (0.400, 0.070, 0.900) m. The three locations have been selected as a cross section of potential locations within the vessel with large variation in the *x, y* and *z* coordinate between transmitter locations. It is therefore anticipated that the TDOA values obtained at the receivers will vary significantly between transmitter locations allowing the receiver layout to be evaluated under a range of potential TDOA scenarios.

As established in [Chapter 3.0, section 3.2.1] the TDOA equations require a single receiver to be the coordinate origin of the system; in this set up the receiver labelled R_A is taken as the coordinate origin. The receiver R_A at position (0.000, 0.000, 0.950) m is therefore assigned the coordinates (0.000, 0.000, 0.000) m and the coordinates of the transmitters and the other receivers are identified with respect to this reference. For this receiver layout therefore the adjusted location of P_1 becomes (0.100, -0.050, -0.800) m from the actual location of (0.100, -0.050, 0.150) m.

To determine the resilience of the receiver layout in the presence of noise error is applied to individual range values to different receivers. From the experimental work conducted by Burnett-Thompson A. (2007) it was observed that the range between a single transmitter and receiver can be evaluated to within 1 cm accuracy of the actual range. The results in [Chapter 5.0] of this thesis concur that a maximum range error of approximately 1 cm is anticipated within the vessel. In most cases the error is significantly less than this. Range errors are possible at any of receivers; therefore the impact of range errors at each receiver is investigated in this thesis. The desire is to determine if the size of the localisation error is influenced by the receiver at which the range error is observed. To determine the resilience of the layouts to potential worst case scenario, a 5 cm error is also simulated.

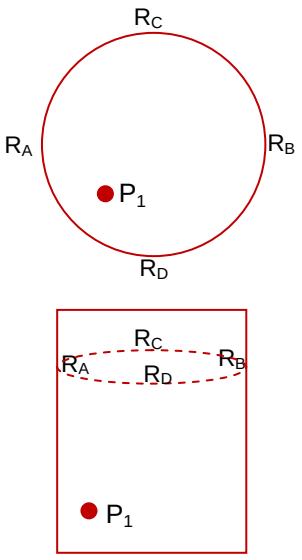

Applied Error (m)	Calculated Location			Overall Error (m)
	X (m)	Y (m)	Z (m)	
0.00	0.100	-0.050	-0.800	0.000
Range_R_A = 0.01	0.180	-0.027	-0.367	0.441
Range_R_B = 0.01	0.166	-0.026	-0.342	0.463
Range_R_C = 0.01	0.320	0.164	-0.256	0.625
Range_R_D = 0.01	0.360	0.256	-0.500	0.501
Range_R_A = 0.05	0.229	-0.016	-0.104	0.709
Range_R_B = 0.05	0.163	-0.027	-0.362	0.443
Range_R_C = 0.05	0.307	0.153	-0.126	0.734
Range_R_D = 0.05	0.067	-0.061	-0.982	0.185

Table 4-15: Error on calculated location P_1 with 0.01 m and 0.05 m range error applied

Table 4-15 shows the calculated location of the transmitter when error is applied to individual range values for position P_1. For the applied errors Range_R_A signifies that the error is applied to the range between the transmitter and receiver R_A. The diagram displays the location of the transmitter relative to the receivers in the vessel. With zero error applied the transmitter is located with negligible error. When an error of 0.01 m is applied to the range values the error on the localisation is substantial. The average localisation error is 0.510 m. The result demonstrates that for this transmitter location even a relatively small range error on an individual received value results in a large localisation error.

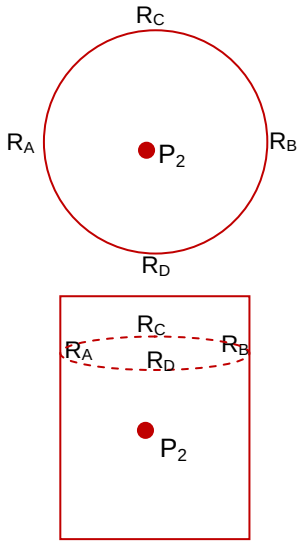

Applied Error (m)	Calculated Location			Overall Error (m)
	X (m)	Y (m)	Z (m)	
0.00	0.200	-0.130	-0.450	0.000
Range_R_A = 0.01	0.220	-0.101	-0.308	0.147
Range_R_B = 0.01	0.204	-0.100	-0.298	0.155
Range_R_C = 0.01	0.145	-0.288	-1.050	0.623
Range_R_D = 0.01	0.167	-0.192	-0.822	0.379
Range_R_A = 0.05	0.252	-0.066	-0.095	0.364
Range_R_B = 0.05	0.198	-0.064	-0.069	0.386
Range_R_C = 0.05	0.281	0.074	0.188	0.674
Range_R_D = 0.05	0.275	0.092	-0.006	0.503

Table 4-16: Error on calculated location P_2 with 0.01 m and 0.05 m range error applied

Table 4-16 shows the calculated location of the transmitter when error is applied for transmitter position P_2. Again the results show that for a small error on an individual range the overall localisation error is significant. The average localisation error for 0.01 m range error is 0.326 m. It can also be observed that where the range error is applied has a significant impact on the localisation result. For 0.01 m error applied to the range at receiver R_A the localisation error is 0.147 m. For the same applied error to receiver R_C this results in a localisation error of 0.623 m.

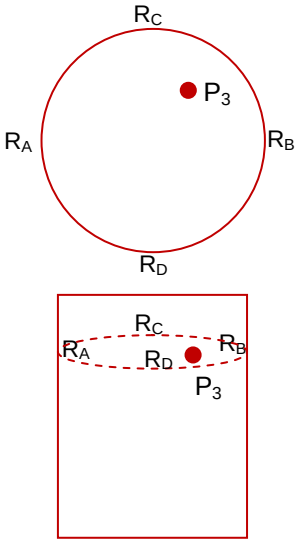

Applied Error (m)	Calculated Location			Overall Error (m)
	X (m)	Y (m)	Z (m)	
0.00	0.400	0.070	-0.050	0.000
Range_R_A = 0.01	0.401	0.067	0.000	0.050
Range_R_B = 0.01	0.391	0.068	-0.029	0.023
Range_R_C = 0.01	0.407	0.067	-0.087	0.038
Range_R_D = 0.01	0.420	0.086	-0.120	0.075
Range_R_A = 0.05	0.472	0.080	0.154	0.216
Range_R_B = 0.05	0.370	0.063	0.038	0.094
Range_R_C = 0.05	0.385	0.042	-0.117	0.074
Range_R_D = 0.05	0.388	0.096	-0.118	0.075

Table 4-17: Error on calculated location P_3 with 0.01 m and 0.05 m range error applied

Table 4-17 shows the calculated location with applied range errors for the location P_3. The average error for results in the location P_3 with 0.01 m range error is 0.047 m. When a larger error of 0.05 m is applied the average localisation error increases to 0.115 m.

For the three test locations the average localisation error is 0.29 m for 0.01 m ranging errors at the receivers. For ranging errors of 0.05 m the average localisation error increases to 0.37 m. The

results for this receiver layout show that it is very susceptible to noise on individual range values, with a relatively small 0.01 m range error being shown to have a significant impact on the localisation accuracy of the algorithm.

Results in location P_1 and P_2 have shown average error of 0.508 m and 0.326 m for 0.01 m applied range error. In both these locations the transmitter is positioned some distance away from the receivers, in the lower and middle sections of the vessel, see Figure 4-12.

The close proximity of the receivers in relation to each other in the vertical component suggests that from locations such as P_1 and P_2, where the transmitter to receiver range is large, the ranges from the transmitter to the different receivers are very similar. This is because in these locations the z component in the dominant value affecting the range. As the range from the transmitter to each receiver is similar then the range difference values will be very small. As such an applied error of 0.01 m is substantial on the range difference and alters the value by a large percentage, causing the solutions to the TDOA equations be to inaccurate when compared to the actual location of the transmitter.

The results with this receiver layout suggest that it is highly susceptible to noise and error on TDOA values. A 0.01 m error on a single range is realistic in the vessel with the timing equipment available for use in the project (Burnett-Thompson A. (2007)) and this receiver layout has shown that it is unable to accommodate this error. As such this receiver layout has been deemed unsuitable for use within the project.

4.4.2 Burnett-Thompson Receiver Layout

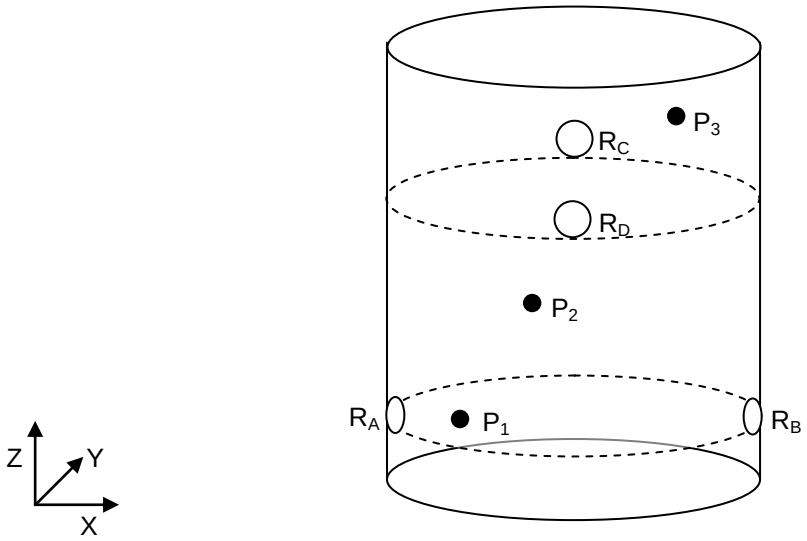

Figure 4-13: Burnett-Thompson receiver layout

Figure 4-13 shows the receiver layout considered by Burnett-Thompson A. (2007] this has coordinates R_A = (0.000, 0.000, 0.200) m, R_B = (0.500, 0.000, 0.200) m, R_C = (0.250, 0.250, 0.700)

m and R_D = (0.250, -0.250, 0.700) m. In this work a wired transmitter could be localised experimentally to within ±0.020 m of its true location. Due to the experimental validity of this layout using TOF localisation it was selected as an appropriate starting point to experiment with TDOA.

Receiver R_A at location (0.000, 0.000, 0.200) m is considered as the reference coordinate (0.000, 0.000, 0.000) m in this instance. The adjusted transmitter locations with respect to this reference receiver are therefore, P_1 = (0.100, -0.050, -0.050) m, P_2 = (0.200, -0.130, 0.300) m and location P_3 = (0.400, 0.070, 0.700) m.

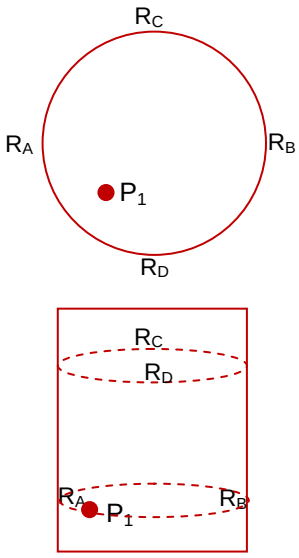

Applied Error (m)	Calculated Location			Overall Error (m)
	X (m)	Y (m)	Z (m)	
Range_R_A = 0.01	0.107	-0.049	-0.044	0.009
Range_R_B = 0.01	0.096	-0.049	-0.041	0.010
Range_R_C = 0.01	0.095	-0.064	-0.062	0.019
Range_R_D = 0.01	0.101	-0.038	-0.055	0.013
Range_R_A = 0.05	0.130	-0.047	-0.021	0.042
Range_R_B = 0.05	0.078	-0.048	-0.008	0.048
Range_R_C = 0.05	0.054	-0.132	-0.146	0.134
Range_R_D = 0.05	0.096	0.013	-0.087	0.074

Table 4-18: Localisation error on position P_1 with Burnett-Thompson receiver layout

Table 4-18 displays the location calculated by fsolve with applied range errors and the error on the true location for position P_1. It can be observed in this instance that the layout is able to cope with the errors applied and the localisation accuracy is excellent even with error applied. For 0.01 m applied error the average localisation error is 0.013 m. The spread of errors with this layout when compared to the top mounted receiver layout in section 4.4.1 is substantially reduced. It can also be observed that this layout is able to accommodate relatively large ranging errors. For 0.05 m applied range errors the average localisation error is still only 0.075 m.

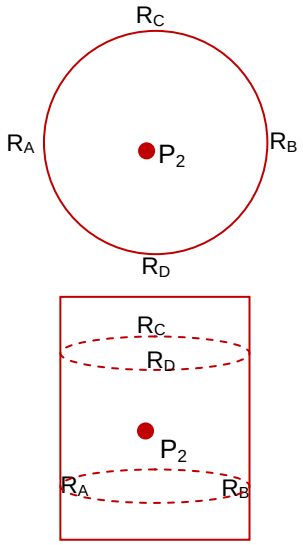

Applied Error (m)	Calculated Location			Overall Error (m)
	X (m)	Y (m)	Z (m)	
Range_R_A = 0.01	0.208	-0.129	0.303	0.009
Range_R_B = 0.01	0.191	-0.130	0.304	0.010
Range_R_C = 0.01	0.200	-0.139	0.296	0.010
Range_R_D = 0.01	0.201	-0.124	0.297	0.007
Range_R_A = 0.05	0.241	-0.124	0.317	0.045
Range_R_B = 0.05	0.154	-0.129	0.323	0.052
Range_R_C = 0.05	0.200	-0.176	0.277	0.052
Range_R_D = 0.05	0.203	-0.098	0.285	0.036

Table 4-19: Localisation error on position P_2 with Burnett-Thompson receiver layout

Table 4-19 shows the calculated transmitter location for 0.01 m and 0.05 m range errors for transmitter position P_2. The result again shows that a 0.01 m applied error on individual range has little impact on the overall localisation error. The average localisation error is 0.01 m. When the applied error is increased to 0.05 m the average localisation error increases but is still small at 0.046 m. For this transmitter location it can be observed that the average localisation error is less than the applied range errors demonstrating the resilience of the receiver layout to noise.

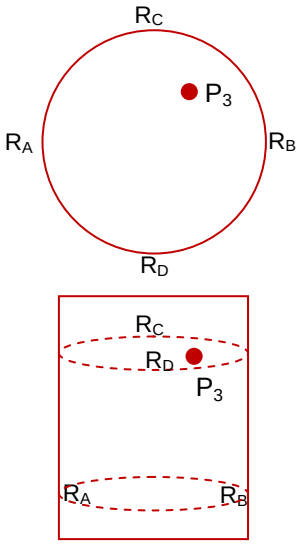

Applied Error (m)	Calculated Location			Overall Error (m)
	X (m)	Y (m)	Z (m)	
Range_R_A = 0.01	0.423	0.076	0.733	0.040
Range_R_B = 0.01	0.385	0.069	0.704	0.016
Range_R_C = 0.01	0.397	0.061	0.684	0.019
Range_R_D = 0.01	0.397	0.075	0.684	0.017
Range_R_A = 0.05	0.569	0.127	0.989	0.339
Range_R_B = 0.05	0.326	0.070	0.735	0.082
Range_R_C = 0.05	0.387	0.030	0.632	0.080
Range_R_D = 0.05	0.388	0.095	0.631	0.074

Table 4-20: Localisation error on position P_3 with Burnett-Thompson receiver layout

Table 4-20 shows the calculated transmitter location with applied errors for position P_3. For 0.01 m applied range error the average localisation error is 0.023 m. When the range error is increased to 0.05 m the average localisation error increases to 0.144 m.

The average error over all three test locations with this receiver layout when 0.01 m range error is applied is 0.0150 m. When 0.05 m range errors are applied the average localisation error increases to 0.089 m. The results suggest that this receiver layout is very resilient to noise on individual range values. For the anticipated range error of approximately 0.01 m the result on localisation accuracy is very small, with the algorithm calculating transmitter locations very close to the actual transmitter locations. The receiver layout has also demonstrated the ability to accommodate large ranging errors while still producing a reasonably accurate localisation result.

The separation of the receivers in the *z* component by 0.5 m means that there is a large difference in values for the range between the transmitter and different receivers; this results in large range differences. The applied error therefore on a single range is small when the range difference is calculated and the range difference is not significantly affected. With a large range difference value then the applied error becomes only a small percentage of the range difference.

The reduction in error with this receiver layout when compared to the top mounted receiver layout suggests that the ability of the receiver layout to minimise the localisation error, in the presence of noise, is dependent upon how large the applied error is as a percentage of the range differences between different receivers. With this suggestion the optimum receiver layout should be when the receivers are mounted at the extremities of the vessel, this maximises the difference in ranges and subsequent range difference values for the majority of transmitter locations.

4.4.3 Vessel Extremities Receiver Layout

To evaluate this hypothesis simulations are conducted with the receivers mounted at the maximum dimensions of the vessel. The positions are R_A = (0.000, 0.000, 0.000) m, R_B = (0.500, 0.000, 0.000) m, R_C = (0.250, 0.250, 1.000) m and R_D = (0.250, -0.250, 1.000) m. Receiver R_A is used as the reference coordinate. As R_A is already located at the reference coordinate then the positions of the transmitter do not require adjustment, therefore P_1 = (0.100, -0.050, 0.150) m, P_2 = (0.200, -0.130, 0.500) m and P_3 = (0.400, 0.070, 0.900) m.

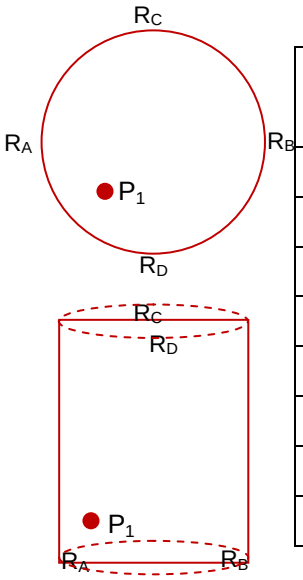

Applied Error (m)	Calculated Location			Overall Error (m)
	X (m)	Y (m)	Z (m)	
Range_R_A = 0.01	0.106	-0.050	0.153	0.007
Range_R_B = 0.01	0.092	-0.050	0.153	0.008
Range_R_C = 0.01	0.099	-0.068	0.145	0.019
Range_R_D = 0.01	0.102	-0.032	0.148	0.018
Range_R_A = 0.05	0.129	-0.049	0.167	0.034
Range_R_B = 0.05	0.058	-0.050	0.165	0.045
Range_R_C = 0.05	0.090	-0.147	0.114	0.104
Range_R_D = 0.05	0.106	0.041	0.134	0.092

Table 4-21: Localisation error on position P_1 with vessel extremities receiver layout

Table 4-21 shows the calculated location of the transmitter with the applied range errors for position P_1. For a 0.01 m applied range error the average localisation error is 0.013 m. When the applied error is increased to 0.05 m the average localisation error increases to 0.069 m. The result demonstrates that this receiver layout has shows excellent resilience to noise. It can be observed that again that for a 0.01 m applied range error the localisation result is very accurate in comparison to the actual transmitter layout. In comparison to the Burnett-Thompson receiver layout the average localisation error is the same for 0.01 m applied error but marginally better when 0.05 m error is applied. It can again be noted that the localisation error is larger when the range errors are applied to receivers R_C and R_D.

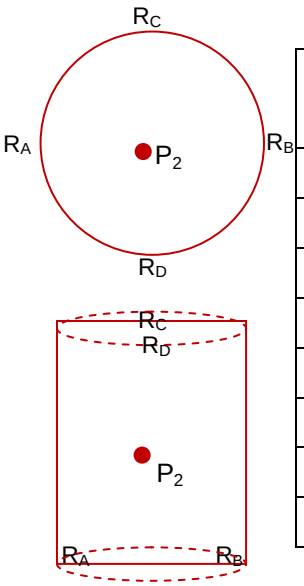

Applied Error (m)	Calculated Location			Overall Error (m)
	X (m)	Y (m)	Z (m)	
Range_R_A = 0.01	0.211	-0.129	0.503	0.012
Range_R_B = 0.01	0.188	-0.130	0.503	0.012
Range_R_C = 0.01	0.200	-0.143	0.497	0.013
Range_R_D = 0.01	0.200	-0.119	0.497	0.012
Range_R_A = 0.05	0.258	-0.066	0.530	0.091
Range_R_B = 0.05	0.139	-0.129	0.515	0.063
Range_R_C = 0.05	0.200	-0.197	0.484	0.069
Range_R_D = 0.05	0.202	-0.073	0.487	0.058

Table 4-22: Localisation error on position P_2 with vessel extremities receiver layout

Table 4-22 shows the calculated location of the transmitter with applied range error for position P_2. For 0.01 m applied error the average localisation error is 0.0122 m and for 0.05 m applied error 0.070 m. For this transmitter position it can be observed that the localisation errors are slightly

smaller when the Burnett-Thompson receiver layout is used. This receiver layout however still shows excellent resilience to noise on range values.

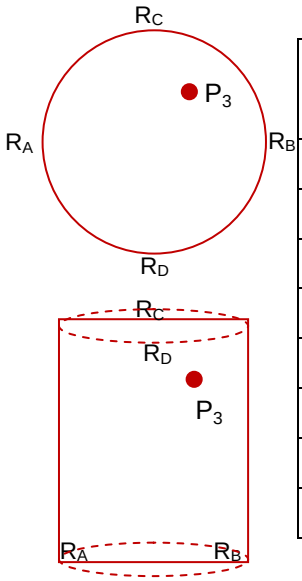

Applied Error (m)	Calculated Location			Overall Error (m)
	X (m)	Y (m)	Z (m)	
Range_R_A = 0.01	0.421	0.072	0.910	0.024
Range_R_B = 0.01	0.380	0.068	0.899	0.020
Range_R_C = 0.01	0.399	0.064	0.896	0.007
Range_R_D = 0.01	0.399	0.077	0.896	0.008
Range_R_A = 0.05	0.517	0.084	0.966	0.135
Range_R_B = 0.05	0.305	0.062	0.900	0.096
Range_R_C = 0.05	0.397	0.039	0.880	0.037
Range_R_D = 0.05	0.398	0.104	0.881	0.039

Table 4-23: Localisation error on position P_3 with vessel extremities receiver layout

Table 4-23 shows the calculated location of the transmitter for position P_3 with applied range errors. For 0.01 m applied range error the average localisation error is 0.015 m and for a 0.05 m applied range error the average localisation error is 0.077 m.

The average localisation error over the three positions simulated with this receiver layout is 0.013 m for applied range errors of 0.01 m and 0.072 m for applied range errors of 0.05 m. The result demonstrates that this receiver layout offers the best resilience to noise of those tested. While the average localisation error for 0.01 m applied error is close between the Burnett-Thompson and vessel extremities layout with 0.044 m against 0.040 m the standard deviation shows that the spread of error is better with the vessel extremities layout. For the vessel extremities layout the three average errors are 0.013 m, 0.012 m and 0.014 m giving a standard deviation of 0.001 m. For the Burnett-Thompson receiver layout the three average localisation errors are 0.013 m, 0.009 m and 0.023 m giving a standard deviation of 0.007 m.

This highlights that the localisation error is more uniformly distributed with the vessel extremities layout, this result means that regardless of the transmitter location in the vessel the localisation error should be consistent. While the Burnett-Thompson layout also shows good overall average error the error between different transmitter locations is more significant creating more uncertainty in the transmitter's true location depending on where it is located in the vessel. It can also be observed that when larger range error is applied the vessel extremities layout is better able to accommodate the error and maintain better localisation accuracy.

.

4.4.4 Summary of Optimising Receiver Layout

With ideal TDOA values the receiver layout is insignificant as a single transmitter can be localised with negligible error. Ideal values however are not anticipated in real world applications and therefore an interest is to observe which receiver layout is the most robust to realistic errors on range, and how this impacts the localisation accuracy.

In section 4.4.1 a top mounted receiver was investigated which makes implementation and retrofitting into a vessel a simple task. Receivers are mounted with a 5 cm vertical separation and at 90° in relation to each other. Results with range errors as little as 1 cm on individual ranges have demonstrated that the overall impact of the localisation error is large, with certain range errors meaning that a pill location cannot be determined. Results have shown that this receiver layout is not a viable option.

From the results in section 4.4.1 showing that a top receiver layout is not viable section 4.4.2 has tested a layout proven in Burnett-Thompson A. (2007) through experimental work. Results using the same ranging errors show that for the three test locations the overall average localisation error is 0.011 m. With a larger receiver separation the localisation error has been significantly reduced for the same ranging errors.

Based on this information, section 4.4.3 has investigated a strategy with the receivers at the vessel extremities. Results demonstrate that the average localisation error over the tested locations is again 0.011 m however the standard deviation for this layout is improved, with 0.0013 m in comparison to 0.0051 m for the Burnett-Thompson layout.

The simulations confirm that for the tested receiver locations the preferred layout for the receivers is to locate them at the extremities of the vessel. While the results from TDOA suggest mounting receivers at the extremities of the vessel, the final location selected will also depend on the ability of the transmitter array to provide adequate signal to the receivers.

4.5 Summary of TDOA Simulation

This chapter has investigated the influence that the distribution of transmitters on a pill has on the localisation accuracy of TDOA. Through knowledge of the transmitter locations on the pill methods have been introduced to reduce localisation error. This chapter has also investigated how the placement of receivers in the vessel affects the localisation accuracy of the system with noise on measurements.

One of the key aims of this thesis is to explore the accuracy of wireless localisation of the pill within the target environment. In section 4.1 the constraints arising due to having multiple transmitters on the housing are discussed. This requirement means that from a TDOA perspective there is not a single unique origin point for the signal but multiple transmitters to multiple receivers.

In section 4.2 the impact that this multiple transmitter array has on localisation accuracy is investigated. A four pill layout to four receivers was simulated with results demonstrating that with ideal TDOA values the separation of transmitters induces a localisation error. This section has also investigated how rotation of the pill affects accuracy, with results showing that rotation does not significantly further increase the localisation error.

In section 4.3 the method of offset knowledge has been investigated, allowing modifications of the TDOA equations to reduce error. It has been demonstrated that when offset knowledge is correctly applied the error can be reduced to negligible values however for certain pill locations within the vessel the closest transmitter to receiver pair changes which means that the modified equations are incorrect. This problem is further compounded when rotation of the pill is considered where the equations must be continually modified.

If offset knowledge alone is used then in 64% of the tested locations within the vessel there is a localisation error improvement for twenty test locations with pill rotations of 0° through to 90°. If the transmitters are uniquely coded such that the origin of a signal is known this increased to an improvement in 76% of locations.

This method however does not overcome the problem of rotation and the standard TDOA method is unable to identify rotation which means equations cannot be modified correctly. To overcome this, the use of TDOA between transmitter arrivals in conjunction with TDOA between receivers has been investigated. With this information it has been shown that for a calculated location it is possible to determine the rotation angle of the pill and recalculate the location of the pill, allowing an improvement in localisation accuracy.

In section 4.4 the influence that noise has on the localisation error is considered. Different receiver layouts are investigated to determine their resilience to noise on received signals. Simulations with different receiver layouts have demonstrated that when the receivers are mounted vertically close together a small ranging error significantly affects the localisation error, in certain cases creating locations which cannot be localised.

Through increasing the separation of the receivers it has been shown that the impact noise has on the localisation error is reduced. Results have demonstrated that the best resilience to noise is observed when receivers are located at the vessel extremities. In this instance ranging errors on the signals can be seen to create an average localisation error of 0.011 m. While this layout provides the best results for TDOA simulations the ability to receive the signal is also vital which is related to the transducer beam profile. This is discussed in [Chapter 5.0]. This information along with that known relating to the TDOA calculations will allow a viable transmitter and receiver layout to be proposed.

5.0 Vessel Characterisation and Transducer Testing

To localise the pill acoustic signals are to be transmitted from transducers mounted to the pill to receivers mounted within the vessel. This chapter investigates the beam profile of the selected transducers in water, considering the beam interaction between multiple transmitters and observing how reflections within the vessel impact the ranging accuracy of the detection methodology.

The challenges of developing a pill with uniform beam coverage are discussed in section 5.1. The localisation problems associated with the highly reflective vessel surface are explained and the advantage of using multiple transmitters on the pill is introduced.

Section 5.2 discusses the experimental set up for testing with a single transmitter, describing the detection methodology implemented and the advantages of this methodology for use within the project. Transmitter testing is undertaken for various locations within the vessel to explore the received signal strength and the impact of vessel reflections on the calculated range.

In section 5.3 the effect of mounting transmitters in close proximity to each other is investigated. Two transmitter angular separations are considered for implementation on the pill based on experimental results, 45° and 90°. The aim is to explore the beam interaction between transmitters and determine if their close proximity allows reflection issues within the vessel to be overcome.

The reflection characteristics of the vessel are explored in section 5.4. Based on observed experimental results simulations are conducted to model the reflection of the acoustic signals within the vessel to provide substantiation to experimental data.

5.1 Beam Coverage Challenges

The underwater medium creates a challenge for localisation, with typical transmission methods such as Radio Frequency (RF) unsuitable due to high frequency attenuation and short penetration depths, as discussed in [Chapter 2.0, section 2.2]. The limitations of RF transmission mean that acoustic signals have been suggested for implementation due to their excellent propagation characteristics through the underwater medium.

The challenge for this project is to develop a pill which is able to transmit sufficient signal strength in all directions, such that it can be localised from any position within the target environment. To achieve this, the most appropriate beam pattern for the pill to produce is an omnidirectional beam, such that signal propagates spherically and with uniform intensity.

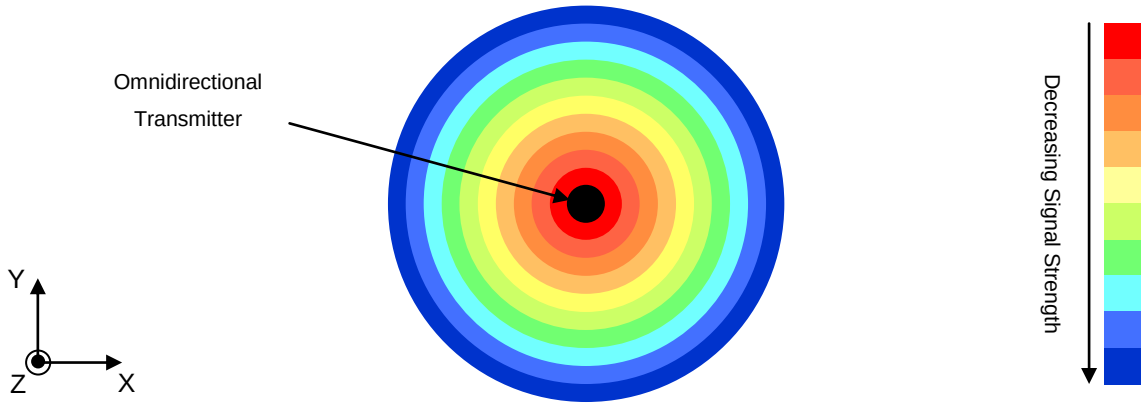

Figure 5-1: Omnidirectional beam pattern

Figure 5-1 displays a 2D slice of an omnidirectional beam pattern for a spherical omnidirectional transmitter. The signal strength emitted from the transmitter is of uniform intensity and the signal strength decreases as the distance from the transmitter increases. Expansion of this slice into a 3D object produces a sphere. The intensity of the signal decreases with distance from the transmitter due to attenuation associated with the transmission medium, which is in this case water. The uniform beam intensity means that the received signal strength is solely a function of the range between the transmitter and receiver and not a function of the transmission angle.

Due to the challenges with implementation established in [Chapter 4.0, section 4.1] the use of a single omnidirectional transmitter has already been eliminated as a suitable option for the pill. To approximate the beam pattern of an omnidirectional transmitter, the use of multiple transmitters mounted to the pill's surface was proposed. The challenges and details associated with this implementation are presented in more detail in this section.

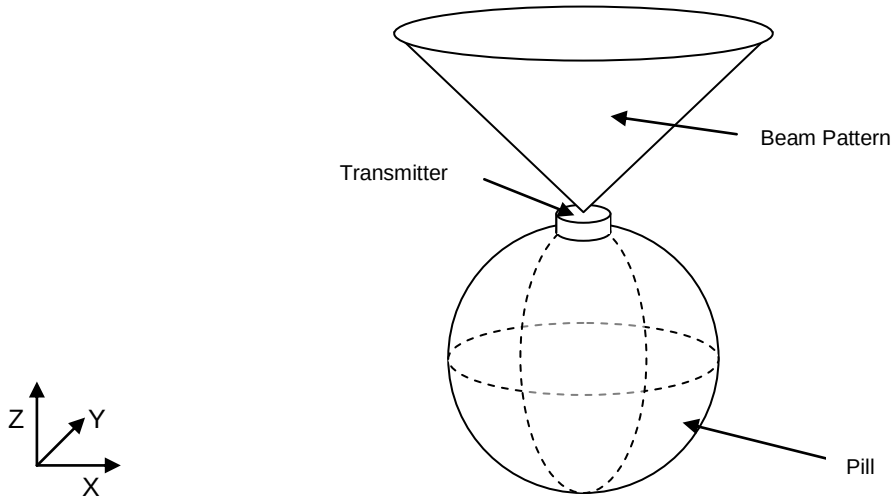

Figure 5-2: Beam pattern of pill with a single transmitter

Figure 5-2 illustrates the beam pattern from a single transmitter mounted to the surface of the pill, assuming a conical beam shape. The use of a single transmitter produces a narrow beam pattern with finite angular dispersion. When considering the overall beam pattern from the pill it is non-

uniform as the signal radiates in only a limited range of directions. This limited coverage means that once the pill moves or rotates, the line of sight (LOS) from the single transmitter to a receiver is lost and the pill can no longer be detected.

A further challenge due to the use of transmitters with non-uniform beam intensity emerges due to the high reflection coefficient of the target vessel. Typically the strength of the signal emitted from a transducer deteriorates with angle of transmission (Chupyra A.G. et al, 2006). With a reflection coefficient of 0.88 for the surface of the vessel the attenuation of any signal impacting it is minimal. The non-uniform transmission pattern of a single transmitter means that it is possible for a reflected signal to arrive at the receiver with larger amplitude than a direct path signal. This is illustrated in Figure 5-3.

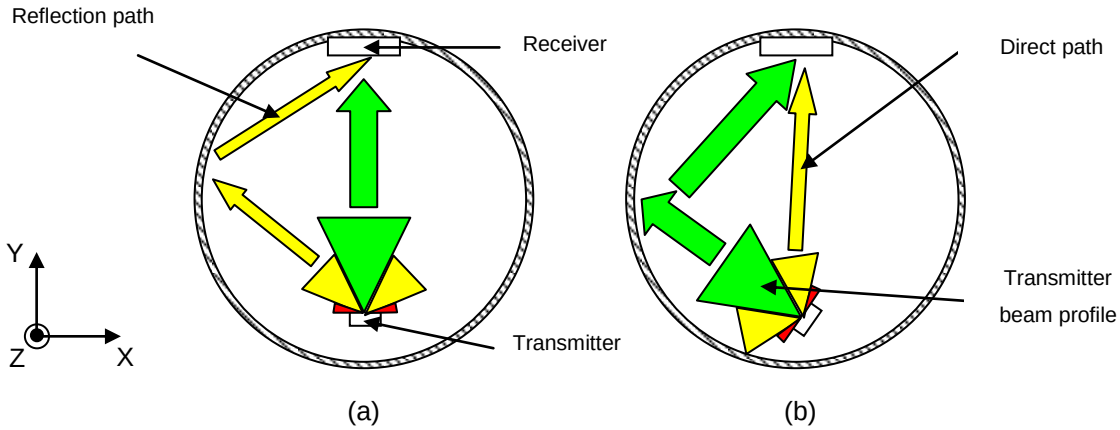

Figure 5-3: Reflective vessel problem due to non-uniform transmitter

Figure 5-3 illustrates the problem associated with a non-uniform transmitter in a highly reflective environment. The green region illustrates the strongest area of the transmitter beam pattern with the yellow and red regions illustrating areas of weaker beam strength. In Figure 5-3 (a) the transmitter faces the receiver such that the strongest signal is directly transmitted towards the receiver, with the reflection path signal emitted from a weaker part of the transmitter's beam.

In Figure 5-3 (b) with the transmitter rotated at an angle relative to the receiver, the strong region of the transmitter's beam faces the vessel wall, resulting in a strong reflection reaching the receiver as the high reflection coefficient of the vessel wall means it absorbs little signal. The direct path signal to the receiver is emitted from a weaker region of the transmitter in this instance. Therefore, it is possible for the reflection signal to arrive at the receiver with larger amplitude than the direct path.

This phenomenon is a challenge for localisation as it limits the available detection techniques for signal acquisition. With a non-uniform transmitter and highly-reflective vessel walls, it cannot be guaranteed that the received signal with peak amplitude will correspond to the direct path. Therefore, techniques which rely on the peak detection of signals cannot be utilised. These techniques are particularly useful for the project, as techniques such as cross correlation peak

detection allow the transmission of signals such as Binary Phase Shift Keying (BPSK) which are resilient to noise (Chandra P. et al, 2007). Resilience to noise is of particular interest for the intended target applications of this thesis, for example, environments with impellers, where simple thresholding techniques which rely on absolute signal level may suffer due to background noise. To facilitate the use of peak detection techniques, there is a requirement for the signal strength from the pill to be sufficiently uniform such that the direct path signal is always received with larger amplitude than reflections.

To overcome both the problems associated with lack of LOS and the detection of reflected signals with higher amplitude than direct path signals, the use of a multiple transmitter array has been proposed. Characteristically a signal transmitted from an angle of 0º (perpendicular to the transmitter's face) is the strongest signal. As the angle of transmission increases, the signal strength decreases (Chupyra A.G et al, 2006). Therefore, a specific transmitter only produces adequate signal strength over a small angular region. To maintain uniform signal strength over the entire pill, there is the requirement for transmitters to be mounted adjacent to each other. This idea is illustrated in Figure 5-4.

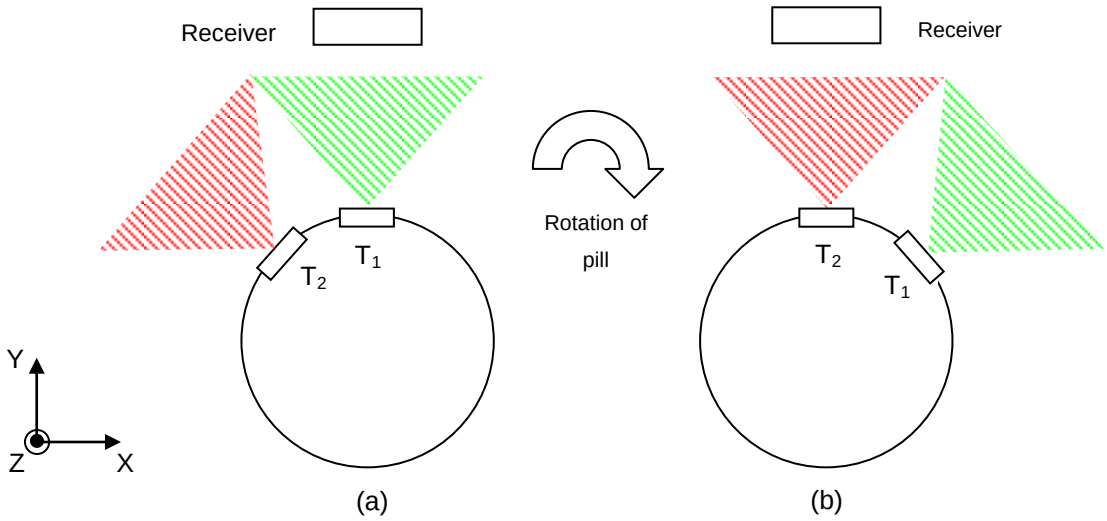

Figure 5-4: Uniform beam coverage through multiple transmitters

Figure 5-4 illustrates the idea of creating uniform signal coverage through the use of multiple transmitters. The region of uniform signal strength from transmitter T_1 is highlighted in green, while the region for T_2 is highlighted in red. In Figure 5-4 (a) the receiver is able to detect signal from T_1, this allows the range of the pill to be calculated. Figure 5-4 (b) shows the pill rotated. With this rotation any signal received from transmitter T_1 originates from an angle which is beyond the region of uniform signal level, meaning that the signal received by the receiver will be reduced. To alleviate this problem transmitter T_2 is positioned such that its region of uniform signal level is adjacent to that of T_1. Because the receiver now lies within the region of uniform signal level for T_2, the signal detected at the receiver remains uniform. With more transmitters placed on the surface of the pill this uniformity can be maintained for 360° pill rotation. In this way the signal origin effectively "switches" over from T_1 to T_2 which maintains a uniform signal level at the receiver.

The desired solution for this thesis is to create a completely uniform beam shape emanating from the pill through the use of multiple transducers, ensuring that for any pill rotation the signal strength obtained at a receiver is maintained. This beam uniformity should allow signal detection techniques which rely on peak detection to be implemented. Therefore, the challenge is to use multiple small and low cost transmitters, with relatively narrow beam width, to approximate the coverage provided by an omnidirectional transmitter.

The major challenge within this section of the project therefore includes identifying how the signal strength at the receiver varies for a single transmitter mounted to the surface of the pill, as the pill rotates. It is also crucial to observe how the use of multiple transmitters affects the received signal strength, and how the interaction of signals from the transmitters varies with angular separation. A final consideration is how the properties of the vessel affect the received signal strength in terms of reflections and multipath arrivals. It is important to determine if through the use of multiple transmitters, the signal produced from the pill becomes sufficiently uniform to implement peak detection techniques.

5.2 Single Transmitter Testing

The performance of the Senscomp 40KT08 transmitter selected in [Chapter 2.0, section 2.5] is specified for operation in air. Based on the intended operating environment there is a requirement to establish how the insertion of the device into water influences its performance. The primary concerns are to determine if the received signal strength obtained is sufficient over the ranges anticipated within the project, and how the insertion of the transmitter into water alters its beam profile.

A further desire is to observe the localisation accuracy when peak detection methodologies are used. This is to determine if the relatively flat profile of the transmitter can ensure that the peak received signal strength always corresponds to the direct path signal, even in a highly reflective environment. This information will enable a decision to be made as to whether peak amplitude detection techniques can be utilised, allowing noise resilient transmission signals such as BPSK to be implemented. Experimental work is conducted in the 250 litre target vessel described in [Chapter 3.0 section 3.1.4] to observe how the range of the peak received signal compares to the expected range of the transmitter.

5.2.1 Peak Signal Detection Methodology

One of the primary intended applications for the pill is in monitoring the environment in mixing vessels. With an impeller and motor, there is likely to be a significant amount of acoustic noise injected into the environment. Signal detection techniques which rely on amplitude thresholding are susceptible to noise, causing false triggers, if the noise is above the threshold level.

To alleviate this, there is the desire to transmit signals which have resilience to noise and use the technique of cross correlation at the receiver. Cross correlation is a standard method of estimating the degree to which two series are matched (Yan H. et al, 2010). The received and expected signals are compared for each term in the signal and the sum of the products is computed (Vyplavin, P. et al 2010). The received signal is then indexed one term along and the sum of products is again computed. When the expected and received signals are aligned such that the structure of the terms is similar, the sum of the products will be large. Therefore the peak of the correlation is when the two signals most closely align; this corresponds to the TOF of the signal and therefore the range between the transmitter and receiver (Hirata, S. et al, 2009). The amplitude of the cross-correlation function is proportional to the received signal strength. For continuous functions *f* and *g* the cross correlation is defined as,

$$(f \star g)(t) \stackrel{\text{def}}{=} \int_{-\infty}^{\infty} f^*(\tau) g(t+\tau) d\tau \qquad \textbf{(5.1)}$$

In equation (5.1) f^* denotes the complex conjugate of the function *f* (NagaJyothi A. et al, 2011). With a cross correlation detection technique, signals such as BPSK can be utilised with specific transmission codes, such that the signal is significantly different from the background noise. When the background noise is compared to the reference signal the correlation peak produced is small and hence noise is rejected even if the amplitude of the noise is large.

The reception of the transmitted BPSK signal correlates strongly with the reference signal and therefore a large peak is produced. As any reflections in the vessel are also BPSK signals, these will also correlate strongly and produce large peaks. Cross correlation relies on the peak detection of signals and therefore the largest correlation peak is selected and the range associated with the TOF of this peak calculated. Reflected signals must not arrive at the receiver with larger amplitude than a direct path signal otherwise the reflected signal will produce the largest correlation peak and would be incorrectly selected as the desired signal.

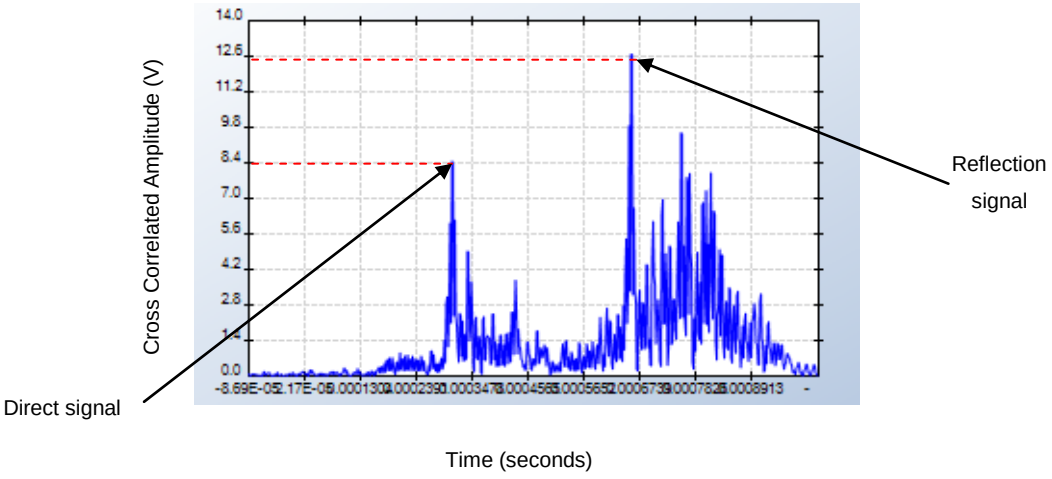

Figure 5-5: Typical cross correlated signal illustrating the reflection problems

Figure 5-5 illustrates the potential problem with using a cross correlation technique with a non-uniform transmitter. There are two distinct correlation peaks in the signal; the first is the direct path signal, while the second represents the arrival of a reflected signal at the receiver. In this instance, it can be observed that the reflection peak is significantly stronger than the peak corresponding to the direct path; therefore the peak detection method would incorrectly select the range which corresponds to the reflection signal. To alleviate this problem the signal strength from the pill must be uniform, such that the amplitude of the reflection signal at the receiver is never larger than that of the direct path.

5.2.2 Experimental Set-up

To determine the performance of the transmitter underwater and to observe how reflections affect the received signal strength, three test locations were selected for the transmitter in the 250 litre test vessel and these are illustrated in Figure 5-6. The first location selected is the central location, (X_1). The effect of reflections in this location is anticipated to be minimal due to the distance between the transmitter and the vessel walls. It is anticipated that for a wide range of transmitter rotation angles the peak received signal strength will correspond to the direct path signal; allowing a good approximation of the transmitter's beam profile underwater to be obtained.

The second location selected for the transmitter is (X_2) which is mounted close to the vessel wall. Due to the small separation between the transmitter and vessel wall it is anticipated this location will produce large amplitude reflections and as such could be envisaged to be one of the most challenging locations within the vessel to localise the pill.

The final location, (X_3), is selected due to the range between the transmitter and receiver. This location allows information relating to the attenuation of the signal as a function of range to be obtained and to determine if the transmitter can provide sufficient signal strength over the range of the test vessel. The location also suggests the possibility of receiving reflected signals from different walls of the vessel allowing investigations into the impact that multiple reflection signals have on the ranging accuracy of the system.

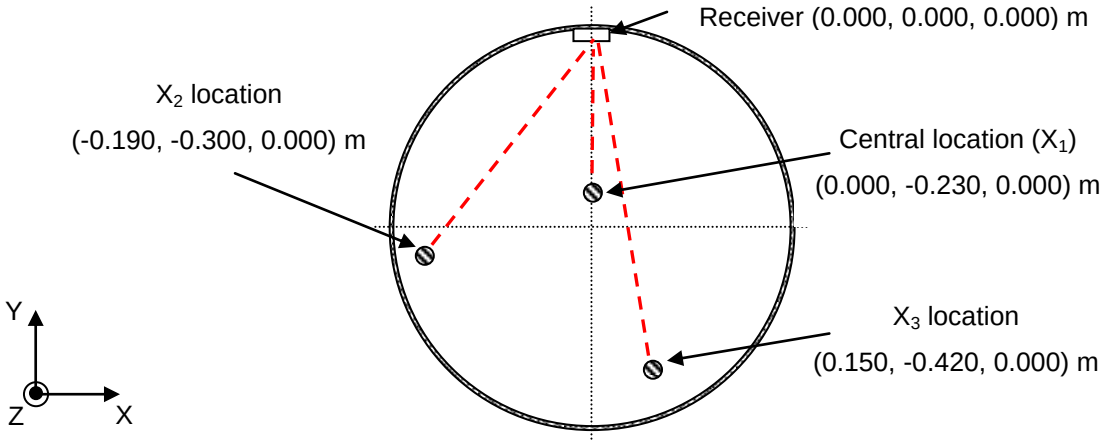

Figure 5-6: Vessel diagram with transducer test locations

In each test location the transmitter is aligned such that it is directly facing the receiver mounted to the wall. This is defined as the 0° angle (theta) and each rotation angle is referenced from this alignment. The red lines on Figure 5-6 illustrate the 0° angle for the three test locations and the arrows indicate the transducer orientation. The estimated error on the alignment angle is up to ± 5º for the X_1 location and ± 10º for locations X_2 and X_3. The smaller alignment error in location X_1 is because in this location the transmitter and receiver faces sit parallel and therefore it is easier to detect any misalignment.

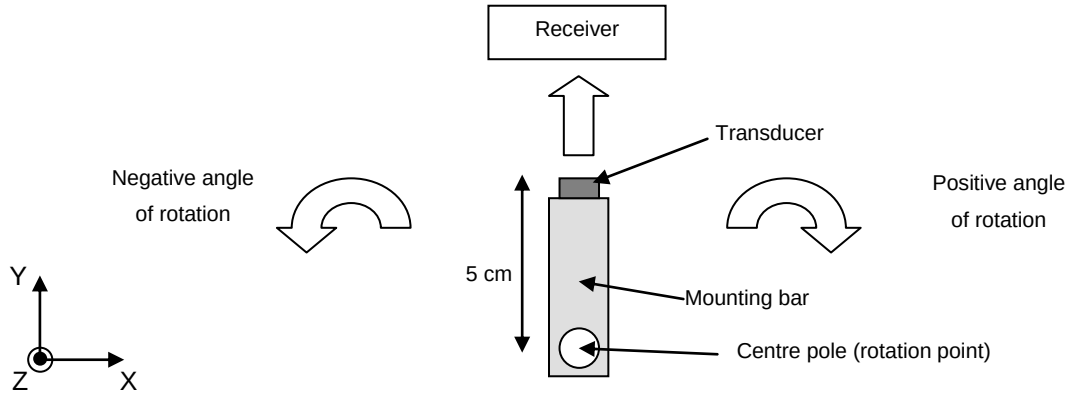

Figure 5-7: Single transmitter set-up, theta = 0°

Figure 5-7 illustrates the experimental set-up for a single transmitter. The receiver in this instance is one of the custom receivers from Burnett-Thompson A. (2007), which for use in this thesis will be referred to as the "5 cm receiver", while the transmitter is the Senscomp 40KT08.

For application onboard the pill the transmitter must be both small in size and low in power which has limited the selection to the Senscomp 40KT08, which is designed for use in air. In comparison the receiver does not have these limitations and the receiver utilised by Burnett-Thompson A. (2007) was specifically designed and constructed for underwater applications. For this reason it was anticipated that the results produced with the 5 cm receiver would be significantly better than using a Senscomp 40KT08 as a receiver.

As the 5 cm receiver is designed for underwater operation it was deemed that to maximise the results the transmission frequency used should be optimised for the receiver rather than the transmitter. The maximum sensitivity of the 5 cm receiver is 100 kHz (Burnett-Thompson A. 2007) in comparison to 40 kHz for the transmitter. It was therefore decided to utilise a 100 kHz transmission frequency. The shorter wavelength of the 100 kHz signal should also improve the potential localisation accuracy. With target localisation accuracy of 1 cm as discussed in [Chapter 2.0 section 2.5.2] a 100 kHz signal should produce improved localisation accuracy in comparison to a 40 kHz signal.

The 40KT08 transducer was attached to the localisation system used in Burnett-Thompson A. (2007) via coaxial cable. The transmitter was located on a mounting bar of length 5 cm which was the anticipated radius of the pill. A mounting arm was used to hold the transmitter in place and

provides the rotation point of the set-up as illustrated Figure 5-7. Rotation of the transmitter was conducted in intervals of 5º with an accuracy of ±1º. The transmitter and receiver were considered in line at 0º, with a positive angle representing rotation clockwise, and a negative angle rotation anticlockwise when viewed from above.

For experimentation, the driving voltage was fixed at 10 V peak to peak which was the anticipated driving voltage from a battery source mounted onboard the pill. From the work conducted by Burnett-Thompson A. (2007) the optimum results utilising BPSK were obtained using a 13 bit BPSK carrier signal selected due to its noise resilience in the target environment. Initial testing in the present utilised this signal with the carrier and modulation frequency both set at 100 kHz.

Detection of the signal is obtained via cross correlation, with the peak amplitude selected. The TOF which corresponds to the peak selected amplitude is recorded and this is used to calculate the range between the transmitter and receiver. From the experimental work conducted via Burnett-Thompson A. (2007) a transmission speed of 1380 ms^{-1} for sound underwater was observed to give the most accurate localisation results. The range between the transmitter and receiver is calculated using this transmission speed.

5.2.3 Single Transmitter Results

Central location (X1)

To observe how the received signal strength changes for a transmitter in the X_1 location, the amplitude of the peak cross correlated signal is recorded, along with the range corresponding to this peak amplitude.

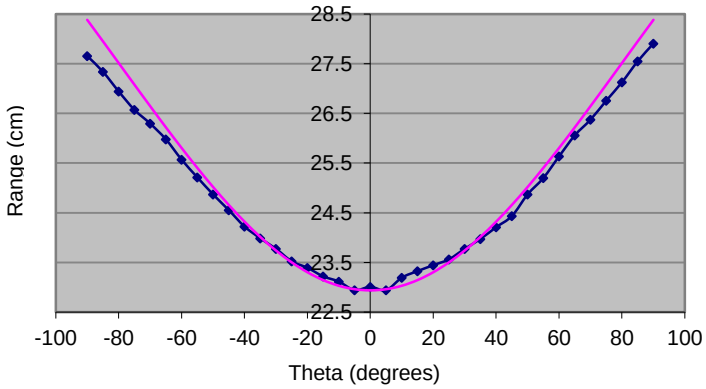

Figure 5-8: Range of peak amplitude signal vs. theta, X_1 location

Figure 5-8 illustrates how the range of the peak received signal alters as the transmitter is rotated using the mounting arrangement shown in Figure 5-7. The blue line shows the range calculated from the measured TOF values corresponding to the peak cross correlated amplitude. At 0° rotation the purple line shows the actual range between the transmitter and receiver, as the transmitter is rotated the purple line shows the expected increase in the actual range, calculated using trigonometry. It can be observed that the experimental values closely follow those expected, within approximately 0.5 cm for all angles of rotation.

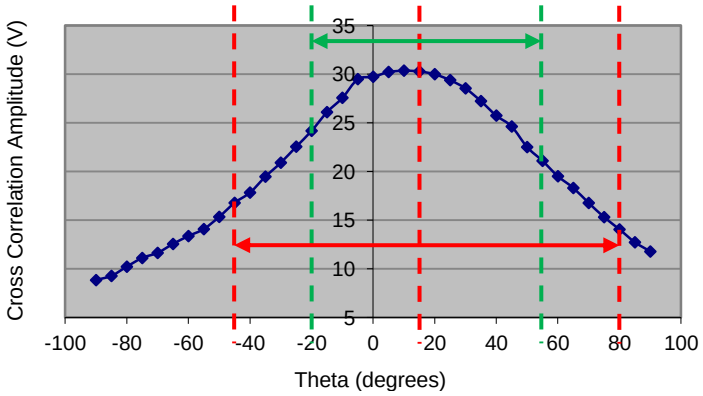

Figure 5-9: Peak cross correlated amplitude vs. theta, X_1 location

Figure 5-9 displays the received peak cross correlated amplitude of the signal as a function of rotation angle. The maximum cross correlated amplitude is not obtained when the transmitter is directly in line with the receiver, but at an angle of approximately 10° and has a cross correlation value of 30.4 V. The green arrow displays the region of transmitter rotation for which the amplitude detected at the receiver remains above 75 % of the 30.4 V maximum, this is approximately 75°. The red arrow illustrates the region where the amplitude value remains above 50% of the maximum amplitude which is approximately 125°.

The result suggests that to maintain a cross correlated amplitude at the receiver which is within 75% of the maximum amplitude; the transmitters on the pill would need to be spaced at 75° intervals. If 50% of the peak amplitude was to be maintained the transmitters on the pill could be spaced at intervals up to 125°. Within the experimental error (± 1%), 100% of the peak amplitude is only maintained for approximately 20° of transmitter rotation and therefore the transmitters on the pill would need to be spaced at 20° intervals to maintain uniform signal level at the receiver.

The received cross correlated peak amplitude observed shows a symmetrical profile however shifted by 10º. While a slight misalignment of the transmitter and receiver is possible, this does not explain the extent to which the maximum signal has been shifted. In the X_1 location the transmitter and receiver faces sit parallel to each other and as such any misalignment is easily noticeable, therefore the maximum misalignment is estimated at ±5º. The result suggests that either the transmitter peak amplitude is offset from 0º or that the receiver sensitivity is not a maximum at a reception angle of 0°.

The performance of the transmitter underwater seems comparable with that specified in the manufacturer's documentation [Chapter 2.0, section 2.5.3] with strong signal level maintained for a wide range of rotation angles. The result also illustrates that for a range of 23 cm between transmitter and receiver the received cross correlated amplitude appears strong in relation to noise, with a peak cross correlated amplitude of 30.4 V in comparison to background noise correlation of 3.5 V (not shown).

X_2 location

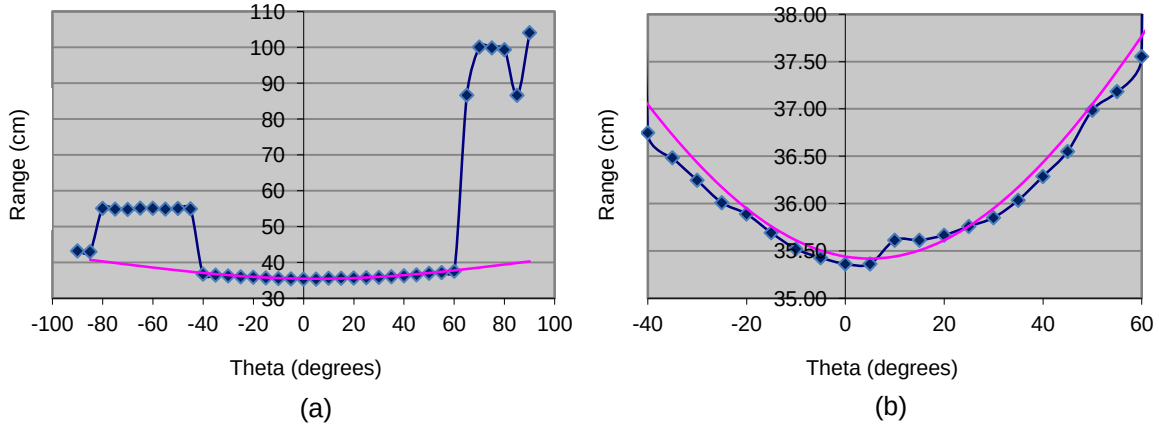

Figure 5-10: (a) Range of cross correlated peak amplitude signal vs. theta, X_2 location, (b) enlarged view of –40° to +60° region

Figure 5-10 (a) shows how the range of the peak cross correlated signal alters as the transmitter is rotated in the X_2 location. The blue line corresponds to the range as calculated from the received signal TOF, while the purple line shows the actual range. Figure 5-10 (b) shows a zoomed image of the region between –40° and +60°. Again the blue line represents the experimental results and the purple line the actual range, this however has been shifted by 10º to fit the recorded results and compensate for angular misalignment between the transmitter and receiver.

It can be observed that for angles between –40º and +60º the calculated range is in good agreement with the actual value. In this region, where the direct path is received as the strongest signal, the accuracy of the calculated and theoretical range has an error of less than 0.5 cm. The small kink observed at approximately 10° suggests that while the range agreement between experimental and anticipated values is good, as the transmitter is rotated if the transmission point on the transmitter face or reception point at the receiver changes this causes a shift in the range observed.

Beyond these bounds however the calculated range changes substantially. The sudden alteration in range observed within the results suggests that outside of the –40º to +60º region the peak received signal no longer corresponds to the direct path but relates to reflections from the vessel wall.

The range results in Figure 5-10 illustrate that the peak cross correlated amplitude cannot be guaranteed to correspond to the direct path signal for a single 40KT08 transmitter. When the transmitter is rotated beyond the region of –40º to +60º the peak amplitude signal corresponds to a reflection path and not the direct path. To overcome this problem the use of multiple transmitters is discussed in section 5.3 of this chapter.

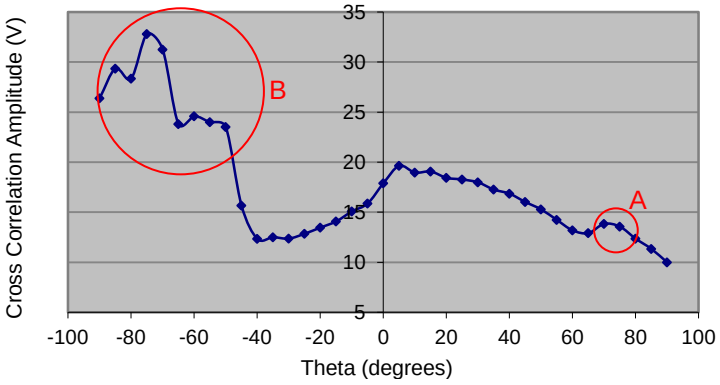

Figure 5-11: Cross correlated peak amplitude vs. theta, X_2 location

Figure 5-11 displays the amplitude of the peak cross correlated received signal for location X_2. In comparison to the results in the X_1 location the 0º cross correlated amplitude is reduced by approximately 30 % from 30.4 V down to 20 V. One reason for this is the increase in range between the transmitter and receiver, from 23 cm to 37 cm. A second reason relates to the receiver sensitivity. In the X_2 location the angle at which the signal impacts the receiver has altered in comparison to the X_1 location, therefore it is possible that the receiver's sensitivity at this reception angle is reduced. Work on identifying the transmitter and receiver beam profile is conducted in [Chapter 6.0] in order to optimise the transmitter layout on the pill.

The profile of the peak cross correlated signal between –40º and 60º in Figure 5-11 for the X_2 location resembles that observed in the X_1 location, Figure 5-9. Outside of these bounds the amplitude varies from those previously seen. The bump observed at 70º (A) can be attributed to a reflection signal, which is verified by the range calculations seen in Figure 5-10.

Of particular interest however is how the cross correlated amplitude between –45° and –90° alters (B). In Figure 5-10 it can be observed that for rotation angles between –45° to –90° the range corresponds to a reflection path signal rather than the direct path signal. Therefore the cross correlated amplitude of the signal in Figure 5-11 between these angles represents the strength of the reflection signals.

While the profile of the transmitter has been observed to be relatively flat, for a rotation of –50º in Figure 5-9 it can be observed that there is a reduction in amplitude of approximately 50 % in comparison to the signal emitted for 0° rotation. In the X_2 location when the transmitter is rotated –50° the signal emitted directly from the face of the transmitter (0°) is directed at the left hand vessel wall. With the high reflection coefficient of the vessel surface the attenuation of the signal impacting the wall is minimal, which allows reflections to arrive at the receiver with higher amplitude than the direct path.

The unexpected result observed is that the cross correlated peak of the reflected signal for a rotation of –50º (23.5 V) on Figure 5-11 is larger than that observed for the direct path signal with

0º alignment, (19.6 V). Assuming a perfect reflection coefficient of 1 for the vessel surface, any reflected signal should at most be detected with amplitude equal to that observed for 0º alignment, as this represents the maximum amplitude the transmitter can produce.

There are two possible explanations for this unexpected increase in signal amplitude. The first relates to the sensitivity of the receiver as a function of reception angle. For location X_2 the angle of incidence at the receiver for the direct path (α) is approximately 40º to the normal as shown in Figure 5-12. With -50º rotation the expected reflection path for any signal is from the left vessel wall, which corresponds to the ranges observed in Figure 5-10. Any reflection therefore impinging on the receiver would have an angle of incidence (β) greater than 40º as shown in Figure 5-12. If the receiver sensitivity is such that for large angles of incidence it is more sensitive, then for a signal of equal strength impacting the receiver at an angle α and an angle β the receiver would produce a stronger response for the signal impacting at angle β. Therefore while the signals impacting the receiver are of equal amplitude the output signals from the receiver are different. This could make it appear the reflection is received with larger amplitude at the receiver.

From observing the receiver profile however, which is detailed in [Chapter 6.0, section 6.3.2], it can be observed that the receiver sensitivity is not increased with angle of incidence and therefore receiver sensitivity does not account for the increase in amplitude. The second option which could explain the increase in amplitude is beam focussing.

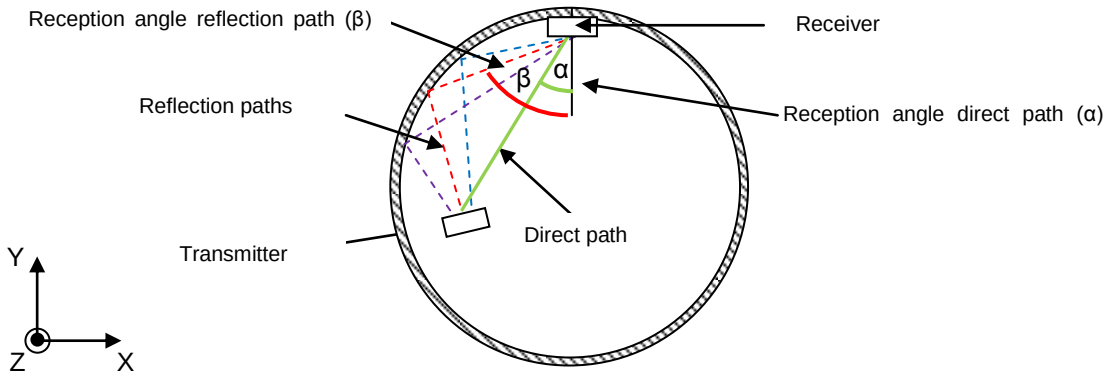

Figure 5-12: Potential beam focussing due to curved vessel surface

Figure 5-12 illustrates the potential beam focussing in the vessel due to the curved vessel surface. The curved surface of the vessel means that signals that are reflected from different parts of the wall may be focussed onto a single point at the receiver. The diagram illustrates the potential path of 3 signals from the transmitter and the reflection of these signals from the vessel wall. If the TOFs and therefore the ranges of these signals are equal, within the measurement error, it is possible that the receiver is unable to differentiate between the arrivals of these signals, creating the false impression of only a single signal with increased amplitude. To consider this further section 5.4 discusses a ray tracing model which models the path of signals and reflections in the vessel.

X_3 location

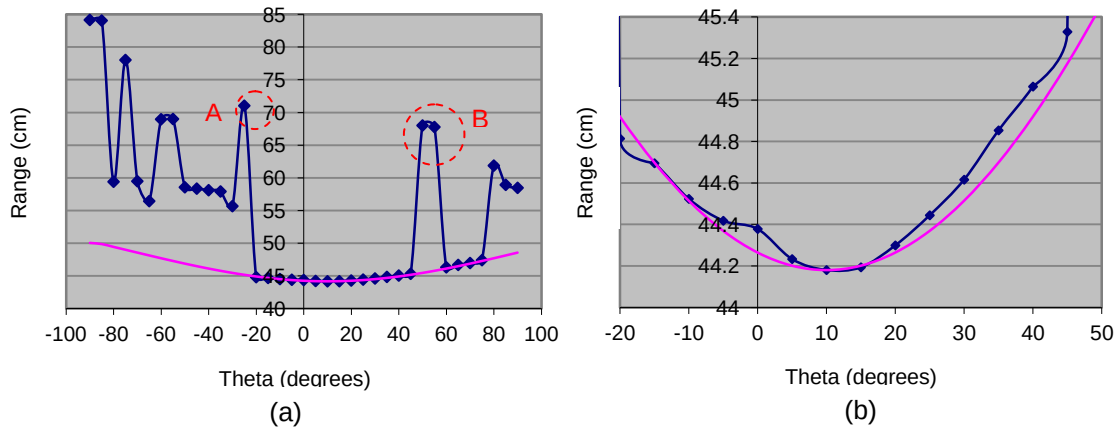

Figure 5-13: (a) Range of cross correlated peak amplitude signal vs. theta, X_3 location, (b) enlarged view of –20° to +40° region

Figure 5-13 (a) shows the range associated with the peak cross correlated amplitude signal received for transmitter location X_3, while Figure 5-13 (b) shows an enlarged view of the -20º to 40º region. The blue line in both instances shows the experimentally calculated range while the purple line shows the actual increase in range, again the actual range has been shifted to account for angular misalignment. The red circles labelled A and B, highlight the first rotation angles at which the range no longer corresponds to that anticipated, and relates to a reflection rather than a direct path. Again it can be observed that in the region where the peak received signal corresponds to the direct path the actual and calculated range show very good correspondence.

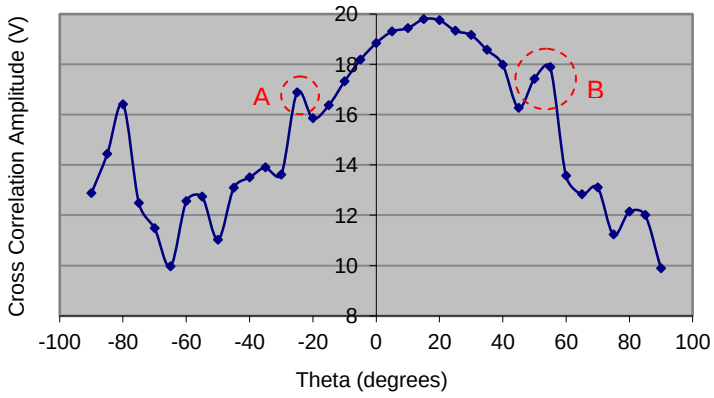

Figure 5-14: Cross correlated peak amplitude vs. theta, X_3 location

Figure 5-14 shows the peak cross correlated amplitude received as the transmitter is rotated in location X_3. The envelope of the amplitude pattern resembles that previously observed in location X_1 in Figure 5-9. The maximum signal is observed at 15°, which suggests angular misalignment in the experiment consistent with the range data observed in Figure 5-13 (b). In Figure 5-14 small spikes in amplitude can be seen highlighted, for instance, by the red circles A and B on the graph. Through examining the range corresponding to these spikes in Figure 5-13 (a), the result shows that these are the rotation angles at which the peak cross correlated amplitude no longer corresponds to a direct path signal.

5.2.4 Summary of Single Transmitter Testing

This section has investigated how the operation of the Senscomp 40KT08 in water influences the performance of the transducer. This section has also investigated how reflections in the vessel impact the peak received signal strength, and examines whether peak detection methodologies are suitable for use within the vessel.

In section 5.2.1 peak signal detection methodologies are discussed, with the technique of BPSK signal transmission illustrated. The advantage of such techniques is that the coded signal is resilient to background noise, for example from impellers which could make it beneficial for implementation. Large amplitude reflections in the vessel however have the ability to cause localisation errors if the received signal strength is larger than the direct path signal. Research has therefore been undertaken to investigate if the vessel can accommodate peak detection methodologies.

The experimental set-up for testing is illustrated in section 5.2.2. Three locations within the vessel were considered. X_1 was located in the centre of the vessel, where reflections were anticipated to be minimal and where the profile of the transmitter could be identified. X_2 was located close to the vessel wall where reflections were anticipated to be a significant factor at the receiver. Finally X_3 was located such that there was a large distance between the transmitter and receiver; this reduces the direct path amplitude and also presents the possibility of reflections from multiple vessel walls.

Results in the X_1 location, section 5.2.3 provide a good approximation of the transmitter beam profile. Peak received signal is observed for a 10º transmitter rotation; however the profile is symmetrical and has good signal strength over a wide angular region. 75% of peak amplitude is maintained for a transmitter rotation of 75° and 50% of peak amplitude observed for 125° transmitter rotation. In the X_1 location the accuracy between theoretical and actual range of the signal is excellent, within 0.5 cm when calculating the range from the peak amplitude signal, with no errors observed due to reflections.

Results in the X_2 location demonstrate the issues in the vessel when using peak detection. It can be demonstrated that for certain transmitter rotation angles the peak signal at the receiver does not correspond to the direct path but to reflections, which leads to significant ranging errors. Another point observed in the X_2 location is that the received signal strength for certain rotation angles is above the 0° direct path signal. This result suggests that some form of beam focussing is present in the vessel; this is significant as even for a pill with uniform coverage it cannot be guaranteed the peak received signal corresponds to the direct path due to this beam focussing. To determine if this is the cause of the observed results section 5.4 investigates the possibility of beam focussing in the vessel.

In the X_3 location results again demonstrate reflection signals with amplitude larger than the direct path signal causing ranging errors. The results in this section demonstrate that even for a transmitter with a relatively uniform transmitter profile reflections still cause significant localisation problems.

5.3 Multiple Transmitter Testing

5.3.1 Background

Due to the directionality of a single transducer and the extremely high reflective properties of the metallic vessel, it has been demonstrated in Figure 5-11 that it is possible for reflected signals to arrive at a receiver with larger cross correlated amplitude than the direct path signal. While the profile of the present transmitter tested is relatively flat between -5° and +25°, it is reduced to approximately 30% of the maximum for -90° rotation as shown in Figure 5-9. Therefore, in location X_2 when the transmitter is rotated to face the vessel wall it is possible to detect reflection signals with greater amplitude than the direct path.

To maintain a more uniform signal level at the receiver the use of multiple transmitters on the pill's surface is suggested. It is anticipated that by placing multiple transducers on the pill's surface improved uniformity of the beam strength can be realised. By ensuring that the amplitude of the direct path signal is larger than reflections peak detection strategies can be used in the vessel.

One of the main concerns in creating a pill with multiple transmitters is how the transmitters interfere with each other when placed in close proximity. To facilitate in the understanding of beam interaction, and to allow for a comparison between previous tests undertaken, the same three transmitter test locations were selected, X_1, X_2 and X_3 as shown in Figure 5-6. The angular separation between transmitters for testing is informed by the beam profile observed in location X_1, Figure 5-9. The spacing should be consistent in order to provide a uniform beam pattern. To maintain received cross correlated amplitude within 50 % of the maximum value Figure 5-9 suggests that an angular separation between transmitters no greater than 125º is required. From this information an angular separation of 90º was selected. While a transmitter separation of 120º would also allow even distribution of transmitters on the pill with fewer transducers it was rejected as a potential solution due to the small margin between it and the absolute maximum separation of 125º.

Acknowledging that 50 % of the maximum cross correlated amplitude may be insufficient to guarantee that the strongest received signal relates to the direct path, a layout utilising the signal within 75 % of the maximum amplitude was also tested. With 75 % of maximum amplitude observed over a 75º region a transmitter separation of 45º was selected, again allowing a 3D pill with equal transmitter spacing to be realised.

5.3.2 90º Transmitter Separation Beam Interaction

Set-up

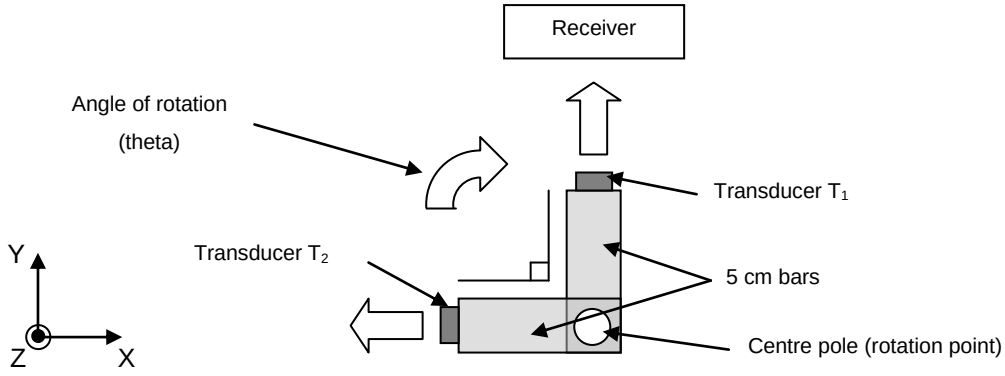

Figure 5-15: 90º transducer separation layout

Figure 5-15 displays the arrangement for testing with multiple transmitters. Both transmitters are mounted onto 5 cm bars which are attached to the mounting pole within the vessel. The transducers are mounted such that the separation between them is 90° ±1º. Transmission of the signals is maintained as BPSK with a transmission frequency of 100 kHz, both carrier and modulation. The amplitude of the transmitted signal is 10 V peak to peak.

To observe and document the beam interaction of the transmitters as a function of rotation, the transducer set-up is rotated in intervals of 5º ±1°. The transducers are aligned such that T_1 faces directly at the receiver for rotation of 0º and T_2 aligns with the receiver for 90º rotation. This alignment is again subject to a possible misalignment of ±5º in location X_1 and ±10º in locations X_2 and X_3.

X_1 Location

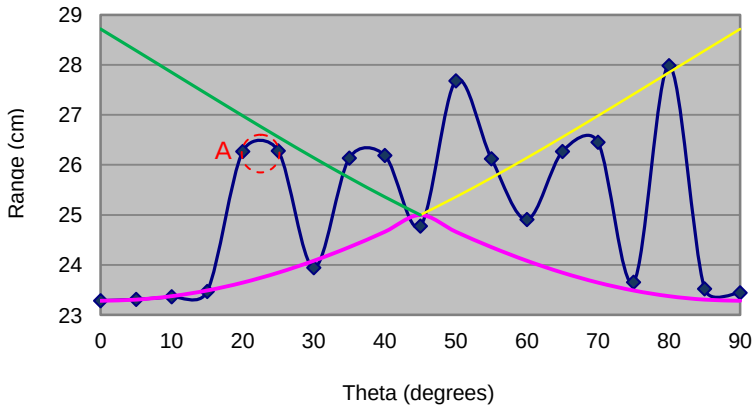

Figure 5-16: Range of peak amplitude signal vs. theta, 90º transmitter separation, X_1 location

Figure 5-16 shows how the range of the peak received signal alters as the 90º transmitter separation set-up is rotated in location X_1. The dark blue line displays the calculated range from experimental TOF data. The yellow line illustrates how the range of transmitter T_1 increases as calculated by trigonometry, the green line illustrates the range of T_2 calculated by trigonometry. The

purple line represents how the range should alter if the transmitter which is closest to the receiver is always detected with peak amplitude.

Until the 45º rotation point is reached T_1 is the closest transducer to the receiver. At 45º rotation T_1 and T_2 are an equal distance from the receiver; this is the expected maximum range for this set-up. For rotation angles above 45° the range between T_1 and the receiver increases however the range between the receiver and T_2 decreases and as such the range calculated should decrease.

It can be observed that for rotations between 0° and 15° the experimental range closely follows that anticipated from T_1. However, at 20° rotation, identified by location “A”, there is an increase in range and an error of approximately 2.5 cm between the calculated and expected range. The 2.5 cm range error does not suggest a reflection from the vessel wall. It can be observed that the range calculated from TOF data is within 1 cm of the expected range for transmitter T_2. The result suggests that for 20° rotation the peak received signal corresponds to a reception from T_2 rather than T_1. The results for rotation at 20º and 25º both follow the expected range for transmitter T_2 rather than T_1.

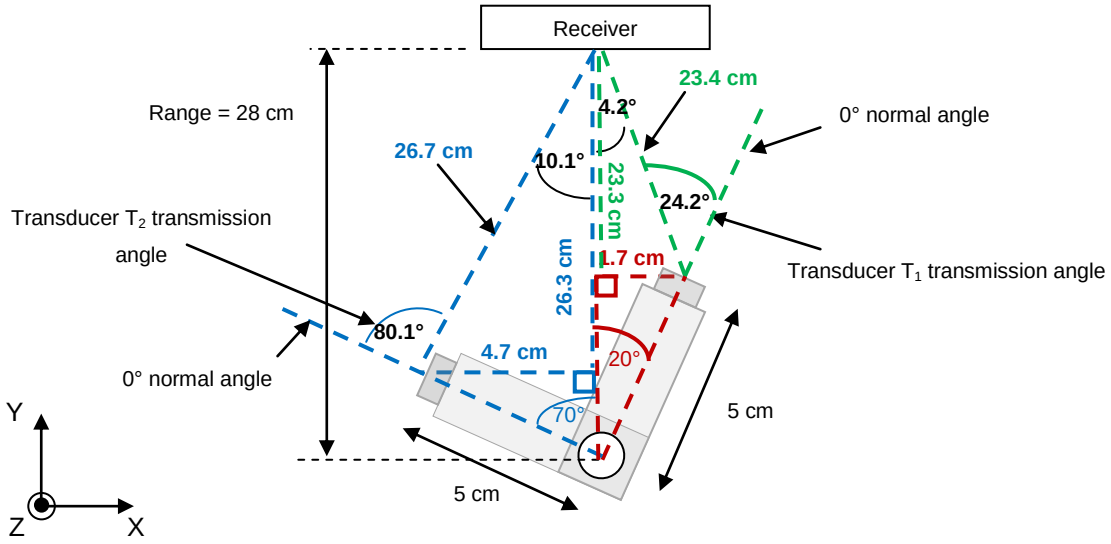

Figure 5-17: Transmitter set-up 20° rotation

Figure 5-17 illustrates the situation with the transmitter set-up rotated 20°. The direct signal emitted from T_2 departs the transmitter at an angle of 80º, while the direct signal from T_1 departs at an angle of only -24º. Transmission and reception angles to the right of the 0° normal are considered positive and transmission and reception angles to the left of the 0° normal are considered negative. From the beam pattern observed in Figure 5-9 T_1 should produce the stronger signal.

While variation between transmitters in relation to the beam strength they produce is anticipated, this would not account for the difference in the received signal strength observed. The result suggests that the receiver beam profile is non-uniform and that the signal from T_2 is detected at a more sensitive angle of the receiver; hence the output of the receiver is larger than for the signal

from T_1 which impacts the receiver at a shallower angle. This variation in receiver profile is confirmed by results in [Chapter 6.0, section 6.3.2].

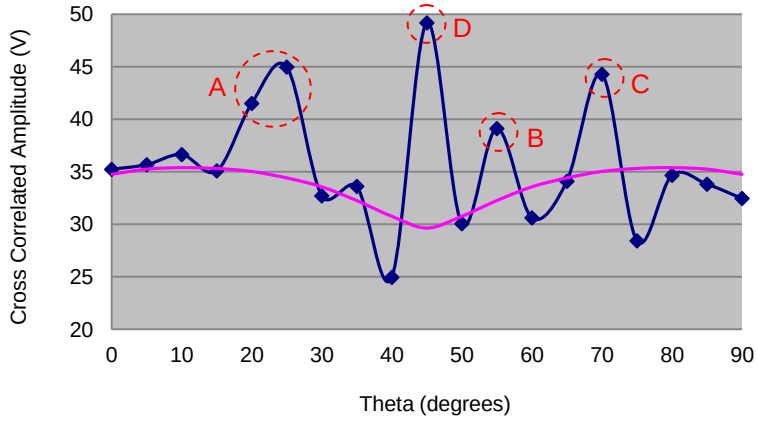

Figure 5-18: Peak cross correlated amplitude vs. theta, 90º transmitter separation, X_1 location

Figure 5-18 displays the peak cross correlated amplitude for location X_1 in blue, while the purple line displays the anticipated amplitude using knowledge of the beam pattern for a single transmitter observed in Figure 5-9, the amplitude of which has been shifted to align with the result at 0º.

For 0^0 to 15º rotation it can be observed that the peak amplitude detected closely aligns with the anticipated amplitude, this region corresponds to detection of the signal from T_1 as confirmed in Figure 5-16. For region A on Figure 5-18 the amplitude is substantially higher than anticipated, which from the range profile in Figure 5-16 can be observed to correspond to the detection of signal from T_2 rather than T_1. The same is true for the amplitude spikes observed at locations B and C, which in this case originate from T_1 rather than the expected transmitter T_2.

There is also a large amplitude increase observed at location D which is approximately 45º rotation of the transmitter set-up. From Figure 5-16 it can be observed that the range of the peak signal for 45° rotation closely fits with that anticipated and is therefore not a reflection. The amplitude at location D in Figure 5-18 is larger than when either transmitter is directly lined up with the receiver, at rotation angles of 0º and 90º respectively.

The rotation angle of this increased signal suggests a similar problem to that observed due to beam focussing. For rotation of the set-up to 45º the ranges between T_1 and the receiver and T_2 and the receiver are equal, which suggests that the increase in amplitude is caused by the beam interaction between these transmitters. Both signals from T_1 and T_2 arrive at the receiver with almost identical TOF values and therefore identical ranges. There are two potential options for this increase in amplitude. The first is that the receiver is unable to distinguish between these arrivals and therefore the result appears as a single detection but with larger amplitude. The second options relates to constructive interference between the transmitters. As the transmitters are an equal distance to the receivers and are excited at the same time then it is possible that the signals

from both transmitters constructively interfere, increasing the signal strength detected at the receiver.

To determine if the amplitude observed at location D is caused by the interaction of signals from two different transmitters, the first correlation peak above noise was also observed for the results in location X_1. This is manually selected and represents the amplitude and the corresponding range of the first signal to arrive at the receiver which is above the noise level.

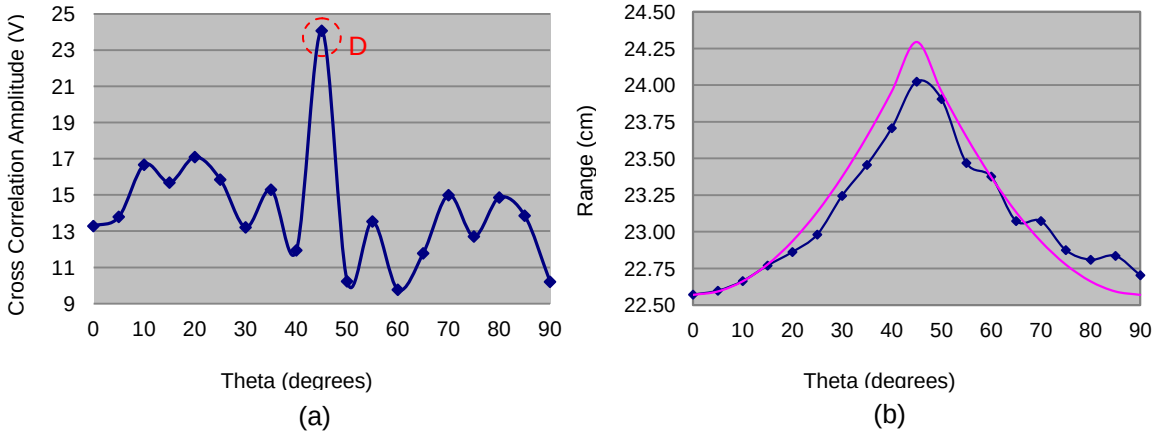

Figure 5-19: (a) Direct signal amplitude vs. theta, 90º transmitter separation, X_1 location, (b) Direct signal range vs. theta

Figure 5-19 (a) shows the cross-correlated amplitude of the direct path signal. Figure 5-19 (b) shows the range of the direct signal. The blue line is the range calculated from experimental data while the purple line shows the actual range.

At location D there is a substantial deviation in the received amplitude and a large amplitude increase is observed. The amplitude increase in this instance is only observed at location D in Figure 5-19 which suggests that some form of beam interaction or beam focussing is causing the cross correlated amplitude of the received signal to increase.

The experimental range data, Figure 5-19 (b) closely follows the actual data, within 0.25 cm for all rotation angles tested. This result again illustrates that provided the direct path can be determined the relationship between experimental and actual range is excellent. This result also provides evidence to suggest that the signals selected in Figure 5-19 (a) are the first arrival of the signal at the receiver as there are no large deviations in the range results.

X_2 Location

Figure 5-20 (a) shows the range of the peak cross correlated received signal. The purple line represents the actual range while the blue line corresponds to the calculated range from TOF data. Within the region of 0º to 35º the range suggests a typical error of 20 cm when compared to the actual position of the transmitter. This result is comparable to previous results observed with a

single transmitter, Figure 5-10 which showed a multipath reflection was received as the strongest signal in this region. The experimental data suggests a range of 55 cm for 0° rotation. Due to the location of the transducers this rules out the possibility of the received signal being a direct path from T_2 as the range is too large. Instead the range of the signal suggests it must be reflected off the vessel wall.

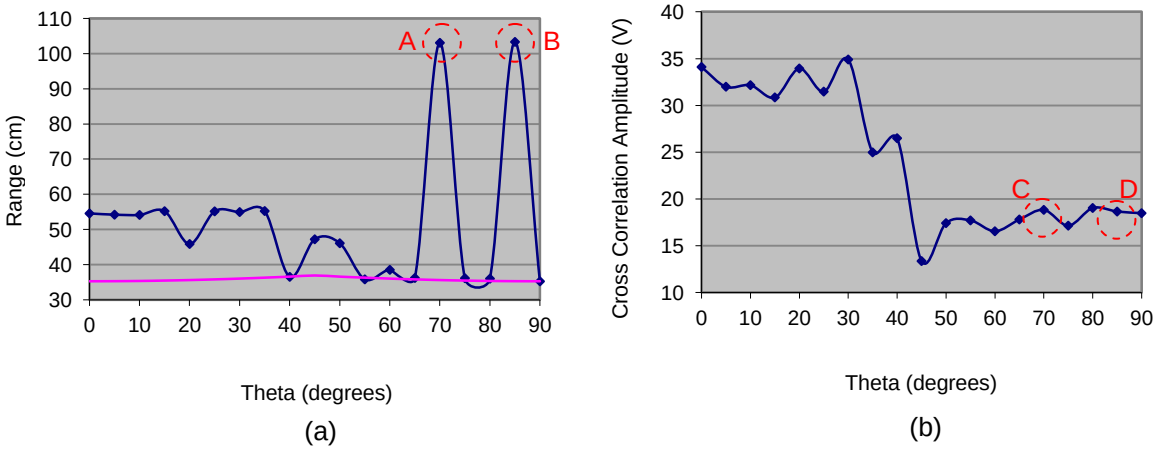

Figure 5-20: (a) Range of peak amplitude signal vs. theta, 90º transmitter separation, X_2 location, (b) Cross correlated peak amplitude

For this two transmitter set-up even though for 0° rotation T_1 directly faces the receiver the 90° separation of the transmitters means that T_2 is facing into the vessel wall. The results in section 5.2.3 suggested that the curved surface of the vessel wall causes beam focussing and as such the signal originating from T_2 is focused off the wall and arrives at the receiver as a reflection with larger amplitude than the direct path signal from T_1.

Figure 5-20 (a) also shows some long range reflections indicated by “A” and “B”. Again these have been observed in previous tests with a single transducer, see Figure 5-10. In this case while T_2 has rotated such that it is facing the receiver, T_1 is now facing the opposite vessel wall. In this instance the signal is reflecting off the wall and arriving at the receiver as the strongest signal.

Figure 5-20 (b) shows the cross correlated amplitude of the peak received signal. The received signal strength for 0º rotation (when T_1 faces the receiver) is substantially higher than that for 90º rotation (when T_2 faces the receiver). The range of the received signal for 0º rotation has been shown to correspond to a reflection, Figure 5-20 (a). The cross correlated amplitude for the region 0º to 40º can be observed to be substantially higher than for the region 45° to 90º.

While reflections are stronger than the direct path for locations A and B, Figure 5-20 (a) the corresponding cross correlated amplitude for these signals in Figure 5-20 (b), locations C and D, does not show a significant increase, suggesting that while the reflection signal has larger amplitude than the direct path it is not due to beam focussing. This suggests that the use of a transmitter separation of 90º on the pill is still insufficient to guarantee that the peak signal received

corresponds to the direct path signal. In the X_2 location a substantial proportion of the peak cross correlated amplitude signals correspond to reflections from the vessel surface and not the direct path.

X_3 Location

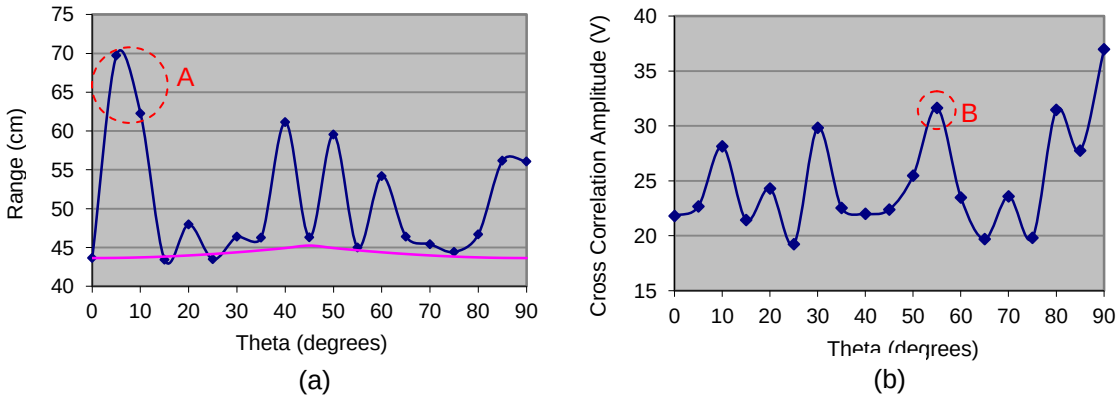

Figure 5-21: (a) Range of peak received signal vs. theta, X_3 location (b) Cross correlated amplitude vs. theta

Figure 5-21 (a) shows the range of the cross correlated peak signal as a function of angular rotation. The blue represents the calculated range from TOF data while the purple line represents the actual range. It can be observed that there are a significant number of angles for which the peak received signal is that of a reflection and not the direct path. Again the separation of transmitters at 90º is insufficient to guarantee that the peak cross correlated signal corresponds to the direct path.

In this case the use of a second transmitter causes many of the reflections. While for rotation angles of 5º and 10º transmitter T_1 faces almost directly at the receiver the results highlighted at "A" show that the peak amplitude signal corresponds to a reflection. This result was not observed in the X_3 location for a single transmitter, Figure 5-13. For the results in Figure 5-21 (a) the use of a second transmitter T_2 which faces the vessel wall causes additional reflection signals, some of which are of larger amplitude than the direct path signal from T_1.

Figure 5-21 (b) shows the variation in the peak cross correlated amplitude as a function of angular rotation. Due to the difference between reflection and direct path signals the amplitudes vary widely. In this instance there is no obvious peak in the signal at 45º, the strongest peak which is close to 45º is at location B which could suggest an angular misalignment between the transmitter and receiver.

5.3.3 45º Transmitter Separation Beam Interaction

Set-up

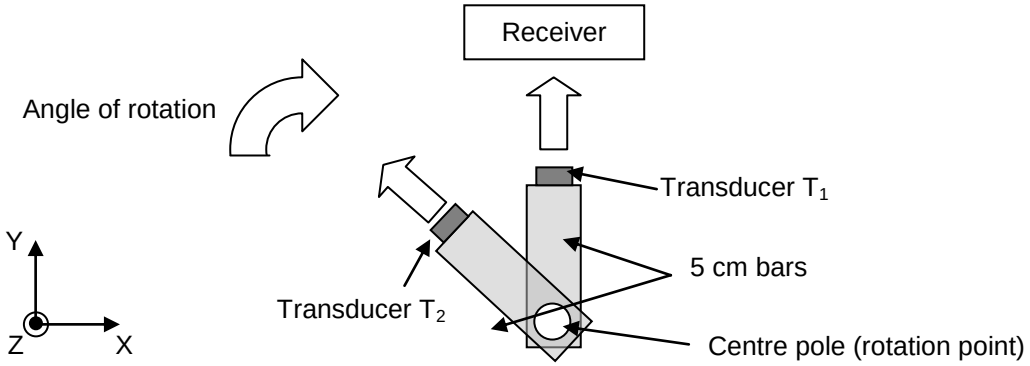

Figure 5-22: 45º transducer separation layout

Figure 5-22 illustrates the experimental set-up for testing two transmitters with 45º separation. The transducers were mounted such that the angular separation between them is 45° ± 1°. The transmission method for the signals was maintained as BPSK with frequency of 100 kHz for both the carrier and modulation. The transducers were driven with a 10 V peak to peak signal.

Rotation of the set-up was again completed in intervals of 5° with accuracy of ± 1°. The range and amplitude of the peak cross correlated signal was recorded for each angle. 0° alignment is achieved when T_1 faces the receiver, the unit is then rotated 45° clockwise.

X_1 Location

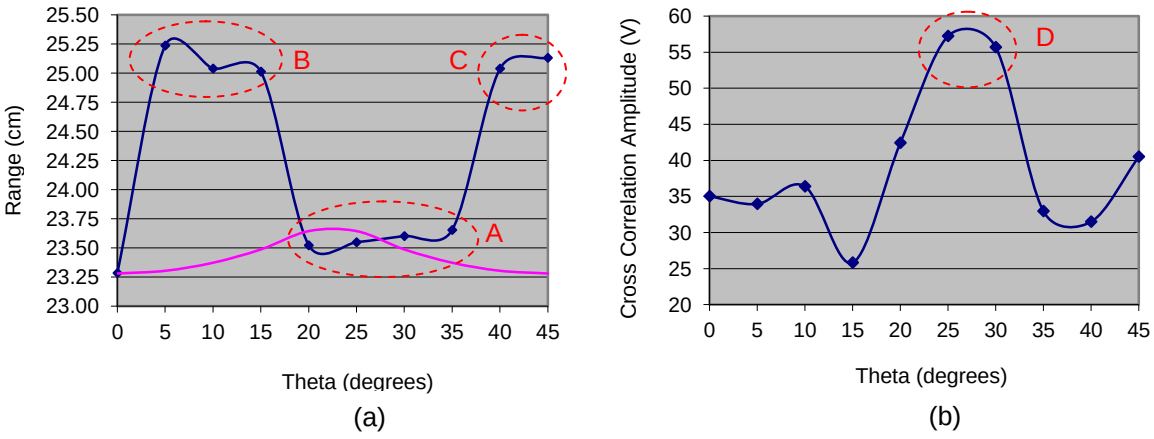

Figure 5-23: (a) Range of peak received signal vs. theta, (b) Cross correlated amplitude of peak signal vs. theta, X_1 location

Figure 5-23 (a) shows the range of the cross correlated peak received signal as a function of rotation. The blue line is the range determined through experimental data while the purple line represents the actual range. In location A the experimental and actual range shows good correspondence. While there is potentially some divergence at 35° is should be noted that the accuracy is still within 0.25 cm.

The variation between the experimental and anticipated range in location B is approximately 2 cm. This suggests that rather than being reflections from the vessel wall these ranges correspond to direct path signals which originate from transmitter T_2 rather than T_1. In location C the result suggests these are direct signals from T_1 rather than the anticipated T_2. This result is comparable to that observed from the testing completed with 90º transmitter separation, Figure 5-16.

The small transmitter separation of 45° means the transmitters are located physically close together. Therefore even when the peak cross correlated amplitude corresponds to the direct path signal from the transmitter which is furthest away from the receiver, the results are still accurate to within 2 cm of the actual range.

Figure 5-23 (b) displays the cross correlated amplitude of the peak received signal as a function of rotation. The profile is much smoother than that observed for 90º transducer separation. The offset of the maximum value, situated at location D, suggests a small angular misalignment between the transmitter and receiver as the peak is expected at half the transmitter separation, 22.5°.

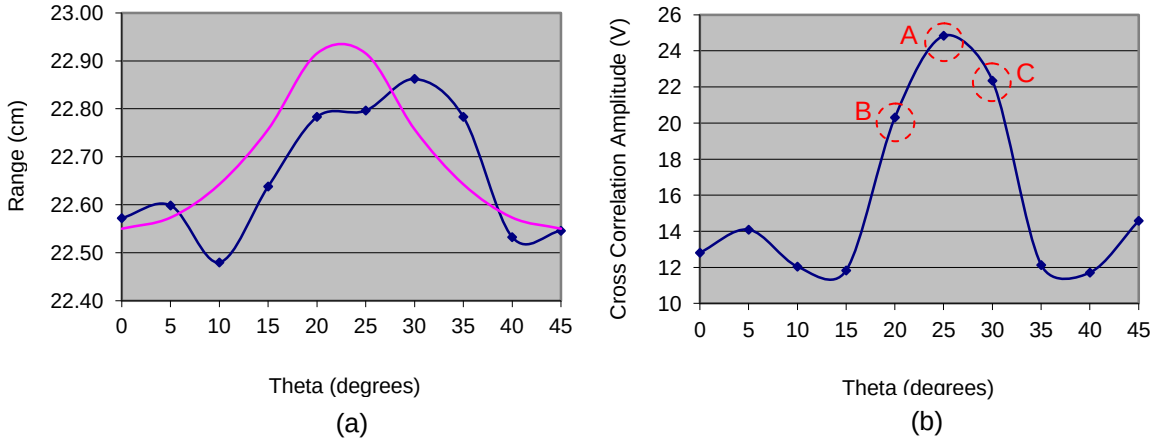

Figure 5-24: (a) Direct signal range vs. theta, (b) Direct signal amplitude vs. theta, 45º transmitter separation, X_1 location

Figure 5-24 (a) displays the direct path range as a function of angular rotation; this is again manually selected as the first signal above the noise level. The blue line represents the range calculated from experimental data while the purple line illustrates the actual range profile. Noting the vertical axis which covers only a range of 0.6 cm, the result again illustrates the close comparison which can be observed between the actual and experimental range if the selected peak corresponds to the direct path signal. The maximum error between the expected and experimental range in this instance is less than 0.2 cm.

Figure 5-24 (b) displays the amplitude of the cross correlated direct signal. The location of the maximum amplitude, location A, suggests a minor misalignment of transmitter and receiver,

approximately 2.5°. This compares favourably with the range results in Figure 5-24 (a) which also appear marginally misaligned when compared to the anticipated range.

It can be noticed in Figure 5-24 (b) that the maximum cross correlated amplitude is observed at location A. In addition the amplitude of the signals at location B and C are also significantly above that observed for 0° or 45° rotation, when T_1 and T_2 are inline with the receiver respectively. This result was not observed for the 90° transmitter separation in Figure 5-19 (a). The physical separation between the transmitters for the 45° set-up is small. It is therefore possible that for the rotation angles associated with locations B and C, while the range from T_1 to the receiver and T_2 to the receiver will not be equal the range difference could be too small to be distinguished by the receiver. This could again be interpreted as the reception of a single signal with increased amplitude. The implication of this result is that for close proximity transmitters on the pill the variation in received signal strength as the pill is rotated may be difficult to predict.

X_2 Location

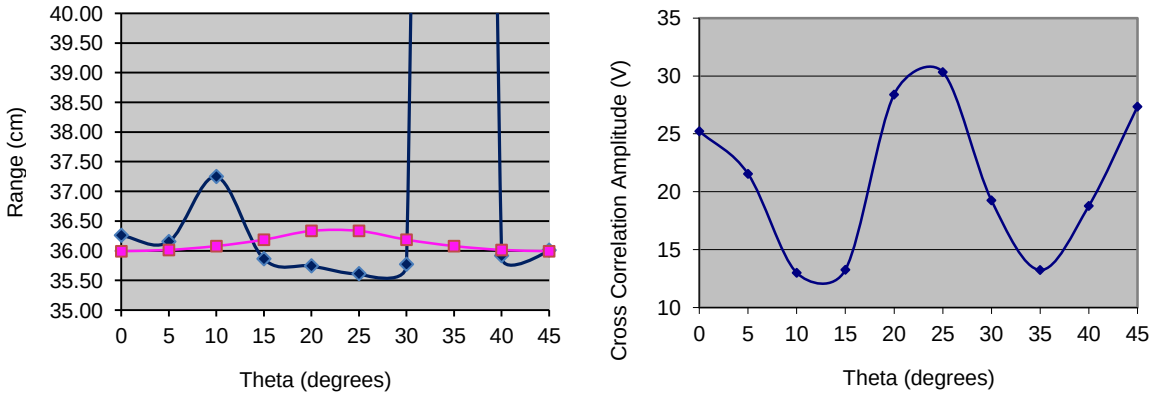

(a) (b)

Figure 5-25: (a) Range of peak received signal vs. theta (b) Cross-correlated amplitude of peak signal vs. theta, X_2 location

Figure 5-25 (a) displays the range of the peak cross correlated signal. The blue line signifies the experimentally calculated range while the purple line displays the actual range. For the tested rotation angles the experimental and actual range show good correspondence. The result for a rotation angle of 10° suggests the reception of signal from T_2 rather than T_1 as observed in Figure 5-23 (a). At a rotation angle of 35° it can be observed the result corresponds to a large range reflection, 106 cm. This is highlighted in more detail in Figure 5-26 (a).

Figure 5-25 (b) shows the peak cross correlated amplitude of the signal. It can be observed that the amplitude received decreases from 0° and 45° respectively where T_1 and T_2 face the receiver. The maximum amplitude is observed at 22.5°, half the transmitter separation of 45°.

In Figure 5-25 (a) for 0º rotation the experimental and anticipated range show close correspondence. This is true even though T_2 is aligned 45º to the left and facing the vessel wall. While in this instance it appears that the previous problem observed in the X_2 location for a transmitter separation of 90° as shown in Figure 5-20 (a) has been overcome, with no beam focussing from the vessel wall, this is purely related to the angle of transmitter T_2. To create a full pill with transmitters separated at 45° there would be transmitters spaced at angles of 0°, 45°, 90°, 135° and so forth. Therefore the cross correlated peak amplitude related to a 90° transmitter separation would still be observed. This is not observed in this result as only two transmitters are tested; the third transmitter (90° from T_1) which would cause the reflection problem is not tested. For a 90° transmitter separation, Figure 5-20 (b) shows that for 0° rotation the reflection path has a cross correlated amplitude of 34.1 V. This is significantly above the direct path at 0° in Figure 5-25 (b) which is 25 V. Therefore it is suggested that the peak detected signal would again correspond to a reflection path due to beam focussing.

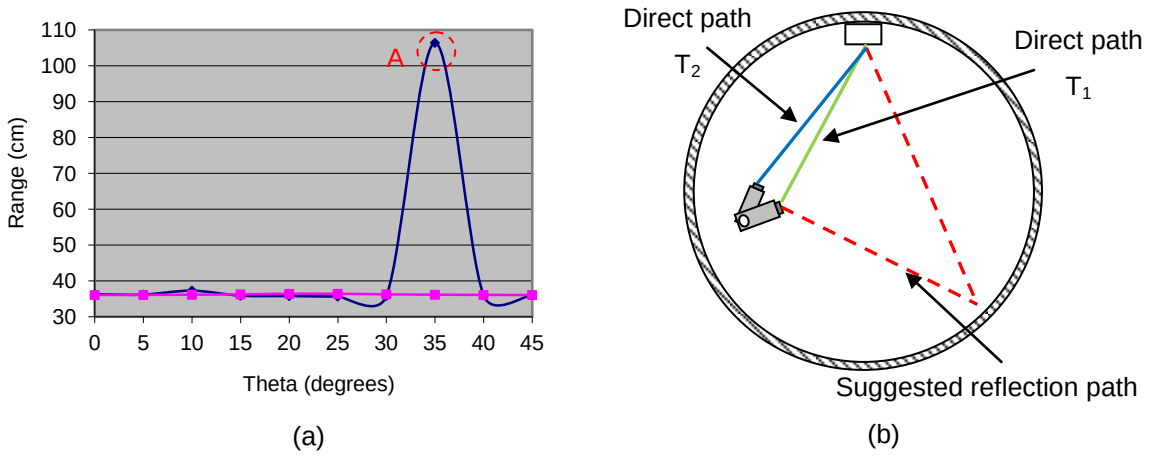

Figure 5-26: (a) Range of peak received signal vs. theta (b) Transmitter location in vessel for 35° rotation in X_2 location

Figure 5-26 (a) displays the range of the peak cross correlated signal as seen in Figure 5-25 (a) however scaled to fit the large range reflection. The blue line signifies the experimentally calculated range while the purple line displays the actual range. It can be observed that at location A, a large range reflection is observed which equates to a range of 106 cm.

Figure 5-26 (b) illustrates the transmitter set-up in the X_2 location and with the set-up rotated 35°. Based on the observed reflection range of 106 cm the red line suggests the possible reflection path. For a vessel diameter of 60 cm the reflection must cross the vessel almost twice before it hits the receiver. Even though transmitter T_2 is only misaligned with the receiver by 10° when the set-up is rotated 35° the peak cross correlated signal still corresponds to this long range reflection.

X_3 Location

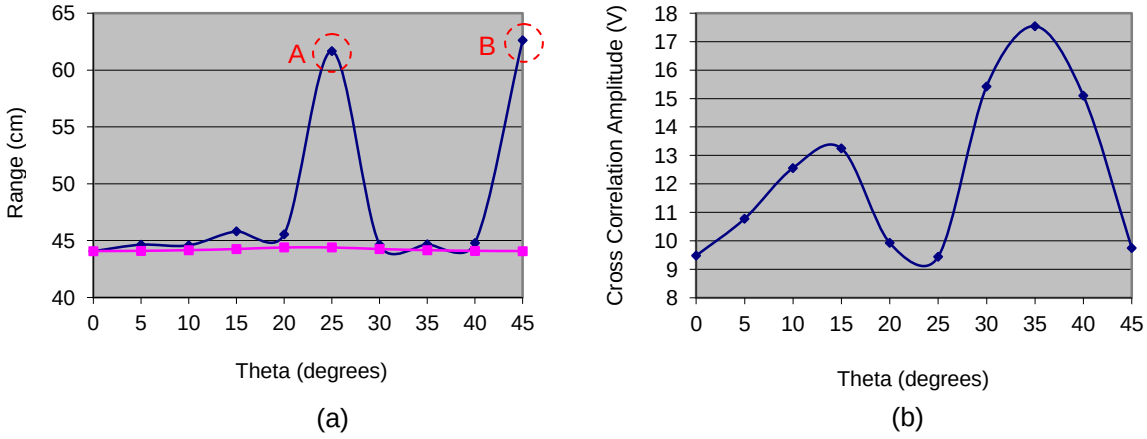

Figure 5-27: (a) Range of peak received signal vs. theta, (b) Cross-correlated amplitude of peak signal vs. theta, X_3 location

Figure 5-27 (a) displays the range of the cross-correlated peak signal. The blue line represents the range calculated from experimental TOF values while the purple line represents the actual range. Large range reflections can be observed in locations A and B where again the strongest path is from a reflection in the vessel.

Figure 5-27 (b) displays the cross correlated amplitude of the peak signal. The maximum cross correlated amplitude at observed at approximately 35º. This is in comparison to a maximum observed cross correlated amplitude at 25° in both Figure 5-23 (b) (X_1 location) and Figure 5-25 (a) (X_2 location). This result would suggest a misalignment of the transmitter and receivers of approximately 10º for the X_3 location as the maximum value should be observed at half the 45° transmitter separation. As previously suggested with the equipment available to achieve alignment this is a realistic error.

5.3.4 Summary of Multiple Transducer Testing

In section 5.2 it was observed that when a single transmitter is rotated it is possible for reflections to arrive at the receiver with larger amplitude than the direct path signal leading to range errors. This section has investigated if through the use of multiple transmitters on the pill this problem can be overcome. This section has also investigated the beam interaction between two transmitters mounted in close proximity.

In section 5.2 it has been observed that the received cross correlated amplitude for a single transmitter remains within 75 % of the maximum value for 75° rotation of the transmitter and within 50% of the maximum for 125° of rotation. From this information in section 5.3.1 two pill layouts have been considered with angular separation of the transmitters on the pill at 90° and 45°.

In section 5.3.2 the transmitter separation of 90° is tested. Results in the X_1 location have demonstrated that unlike when a single transmitter is used the use of two transmitters creates ranging errors. It has been observed that the peak signal detected at the receiver does not always correspond to the transducer closest to the receiver. This result has been suggested due to variation between individual transmitters and also the receiver sensitivity at different reception angles. Results investigating beam interaction have also demonstrated that for a rotation of 45° there is a strong increase in the received signal strength, suggesting beam interaction between the two transmitters. This creates a further problem for maintaining uniform received signal strength.

In the X_2 location, results demonstrate that ranging errors due to reflections in the vessel have not been overcome through the use of multiple transmitters. In this instance, the issues with reflected signals arriving with larger amplitude than the direct path signals have again been observed. The same results are observed in the X_3 location, with peak received signals corresponding to reflections rather than direct path for certain rotations. The results suggest that for 90º transmitter separation it is not possible to implement peak detection techniques within the vessel.

In section 5.3.3 a 45° transmitter layout was considered. By locating the transmitters closer together the received amplitude should remain higher, with a reduction of 25% from the maximum received value. Results in the X_1 location again demonstrate that the peak received signal does not always correspond to the transducer closest to the receiver again causing ranging errors. If the direct path amplitude is however considered, it can be shown that the accuracy of the system is very good, accurate to approximately 0.2 cm of true range. In the X_2 and X_3 locations results demonstrate that even with a small angular transmitter separation the peak detected signal can correspond to reflections, with large ranging errors observed for both the X_2 and X_3 locations.

The results for both the 90° and 45° transmitter layouts suggest that techniques which rely on peak cross correlated amplitude detection will not be effective within the vessel. For both transmitter layouts it has been observed that the peak cross correlated amplitude does not always correspond to the direct path signal. If the first arrival of the signal above noise however is considered then results have shown that the ranging accuracy is very good. For this reason the technique which will be used to detect the acoustic signals is thresholding above noise.

5.4 Ray Tracing Model

For certain transmitter locations, results in section 5.2.3 have shown that it is possible for reflected signals to be detected at the receiver with higher cross correlated amplitude than direct path signals. Results have also suggested that with a single transmitter in the X_2 location it is possible to receive a reflected signal at -45° rotation which has larger amplitude than the direct path signal at 0° rotation. From the results testing a single transmitter, shown in Figure 5-9, it has been shown that the maximum amplitude from the transmitter is produced close to 0°, therefore, in the X_2

location even assuming the reflection coefficient of the vessel is 1 and no signal is absorbed, the reflection signal should at most be received with the same amplitude as the 0° direct path.

To explain this result the possibility of beam focussing has been suggested due to the curved surface of the vessel. It is suggested that if the difference in TOF of multiple signals which impact the receiver is small, then the receiver may be unable to resolve the difference in arrivals, which creates the impression of only a single signal arrival with larger amplitude.

To determine the feasibility of this suggestion a ray tracing model was constructed in MATLAB to model the transmitter and vessel and determine if it is possible, in certain transmitter locations, for multiple signals to arrive at the receiver with, essentially, the same TOF value and therefore range.

5.4.1 Ray Tracing Model Outline

A MATLAB model has been constructed to model a single transmitter in the vessel, allowing the location of the transmitter and its rotation angle to be varied. The signal emitted from the transmitter is considered to travel in straight lines. Beams leaving the transmitter are modelled at discrete 1° intervals and are modelled over an angular range of ± 90º from the normal to the surface. The angle at which the signal leaves the transmitters face is referred to as the propagation angle. The transmitter is considered as a point source. Reflections within the vessel are considered under the constraints that the angle of incidence is equal to the angle of reflection at the vessel surface.

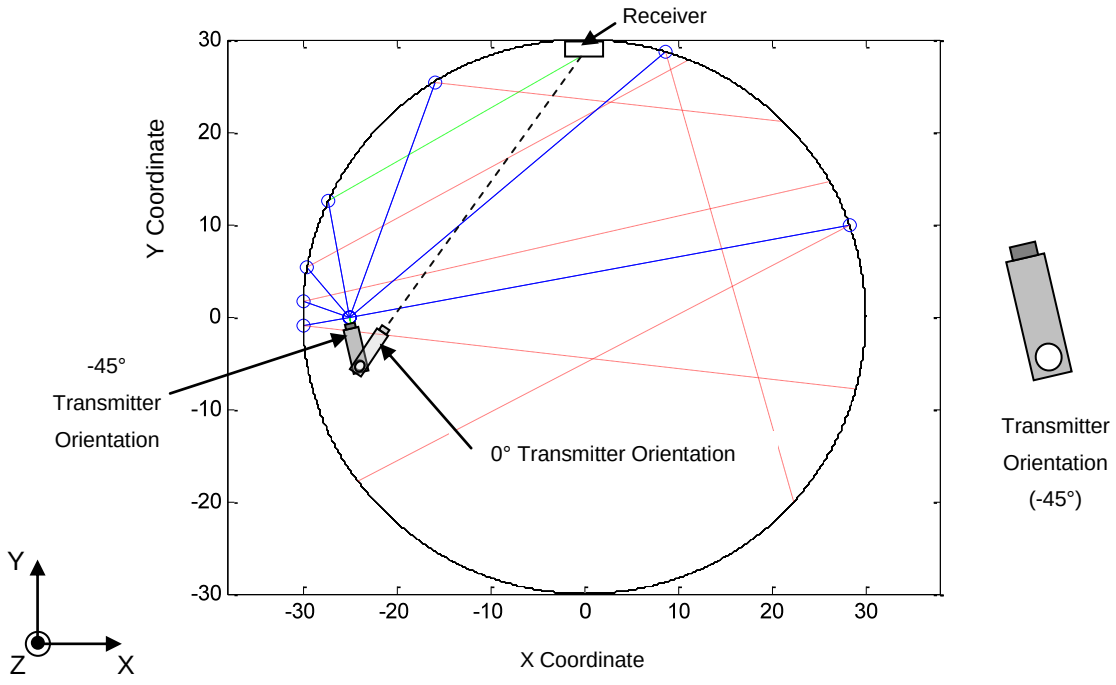

Figure 5-28: Simulated X_2 location transmitter response, -45º transmitter rotation, 30° steps

Figure 5-28 displays the simulated response of the transmitter in the X_2 location for -45° rotation. To aid visual clarity the 0° transmitter orientation is also shown. In this instance the transmission

beams have been modelled at 30° intervals to illustrate how the model works. The blue lines represent discrete beams from the transmitter while the blue circles highlight the intersection of the transmission beam with the vessel surface. The red dotted lines illustrate the reflected path of the signal. To aid visual display any reflected signals which subsequently impact the receiver are highlighted in green. The orientation of the transmitter is displayed alongside the figure.

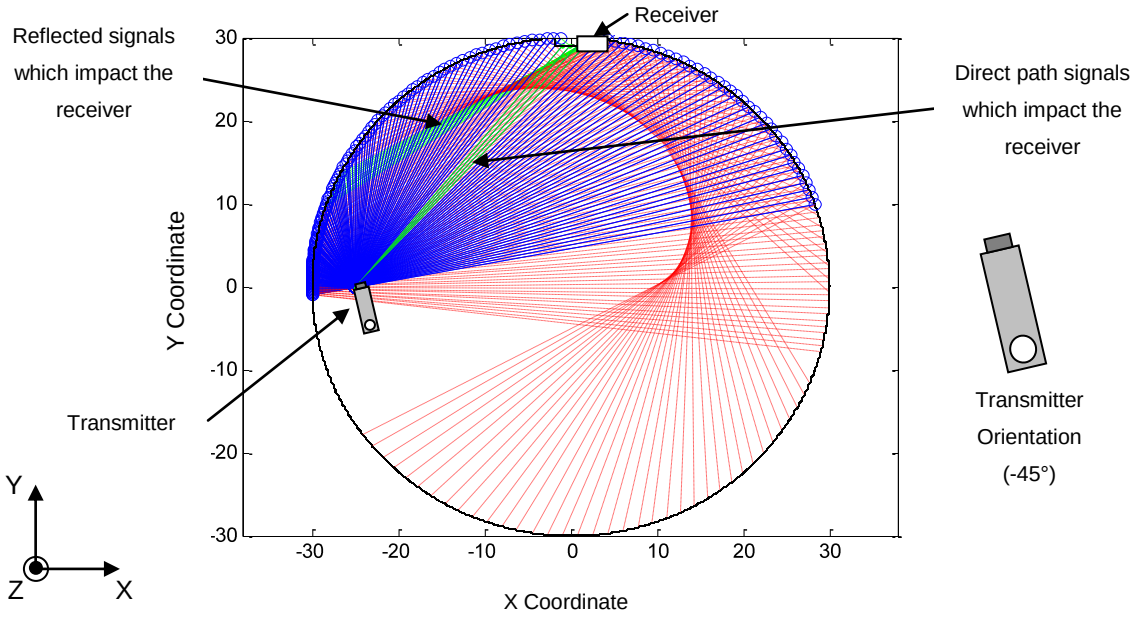

Figure 5-29: Simulated X_2 location transmitter response, -45º transmitter rotation

Figure 5-29 displays the simulated response of the transmitter in the X_2 location when rotated to -45°. The beam separation from the transmitter face in this instance is considered at 1º intervals from –90° to 90º. The blue lines represent signals from the transmitter face, while the red lines represent reflections which miss the receiver. The green lines represent signals which originate from the transmitter and reach the receiver either directly or as reflected signals.

For the rotation angle of -45º in the X_2 location there is a range of direct path signals which impact the receiver, as highlighted on Figure 5-29. It is also possible to observe a group of reflection signals which are reflected off the left hand side vessel wall and which also impact the receiver. These are shown in more detail in Figure 5-30.

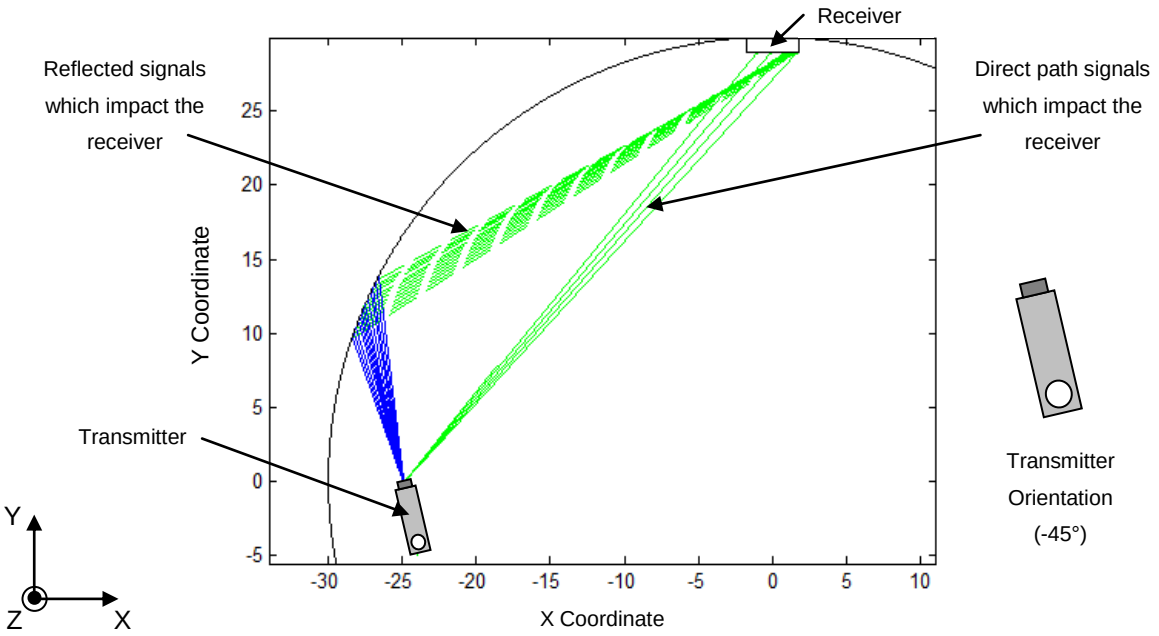

Figure 5-30: Direct path and reflection signals which impact the receiver

Figure 5-30 displays only the signals which impact the receiver either directly or as reflections as previously observed in Figure 5-29. The blue lines are beams from the transmitter face which hit the vessel wall while the green lines show signal paths which impact the receiver either directly or as reflection. The reflected signals also appear to be focused onto a small area of the receiver. To determine if these signals could produce the observed increase in amplitude the range of the reflections must be considered.

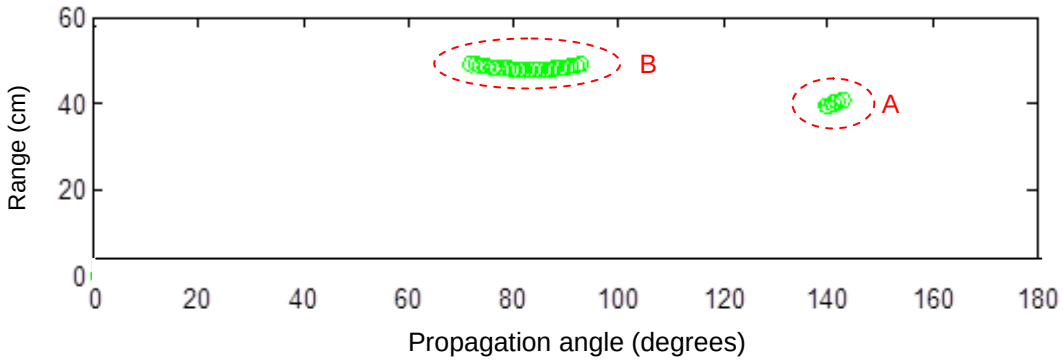

Figure 5-31: Range of impacts on receiver vs. propagation angle

Figure 5-31 illustrates the range of the signals which impact the receiver for different propagation angles from the transmitter's face. There are two groups of signals, signals which impact the receiver directly or those which impact the receiver after a single reflection. The direct path signals, highlighted as group A, have a range of approximately 40 cm. The reflection path signals highlighted as group B have range of approximately 50 cm.

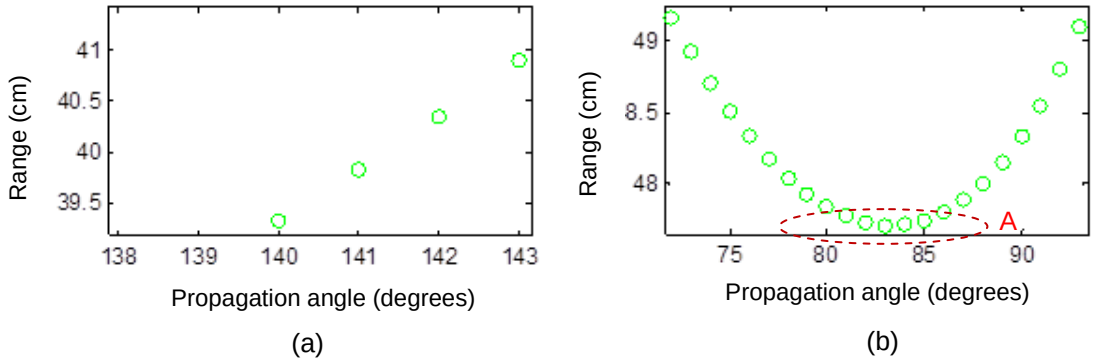

Figure 5-32: (a) Range of direct signals, (b) Range of reflected signals

Figure 5-32 (a) shows the range of the direct path signals from the transmitter, while Figure 5-32 (b) illustrates the range of the reflected signals. While multiple direct path signals impinge on the receiver these have a variation in range between 39.3 cm and 40.9 cm in Figure 5-32 (a). From examination of the ranges in Figure 5-32 (a) it can be observed that the smallest variation between any two impacts is approximately 0.5 cm. It has been observed in section 5.2.3, Figure 5-8 that as a single transmitter was rotated in 5° intervals the observed range alteration was as small as 0.1 cm, which the receiver was able to accurately detect. As such it could be anticipated that the receiver is able to differentiate between the arrival of signals 0.5 cm apart.

The ranges of the reflected signals vary between 47.7 cm and 49.2 cm. It can however be noted that for the group of signals highlighted in location A, the ranges are almost identical. In location A the smallest range difference between signal arrivals is less than 0.01 cm, as such it could be anticipated that the receiver would be unable to distinguish between the arrival of these signals and it is therefore possible these signals are the cause of the large amplitude reflection signals observed.

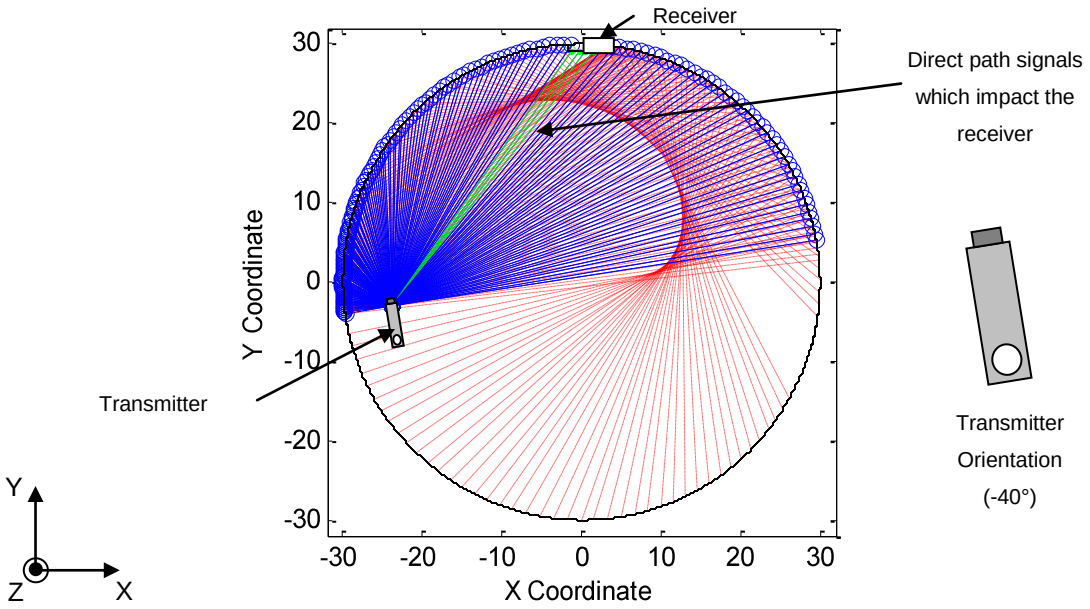

Figure 5-33: Simulated X_2 location transmitter response, -40º transmitter rotation

Figure 5-33 shows the simulated X_2 location for a transmitter rotation of –40º. The group of direct path signals which impact the receiver is still present for this rotation angle. The reflected signals however, which were seen to impact the receiver from the left hand vessel wall in Figure 5-29 and Figure 5-30 are no longer present. For the transmitter rotation angle of –40° the model suggests that there are no signals which after a single reflection impact the receiver and no beam focussing takes place. This corresponds well with the experimental data shown in Figure 5-10 (a), which showed that for –40° rotation of the transmitter the range of the peak amplitude signal corresponded to the direct path. It was not until a rotation angle of –45° that the range suggested a reflected rather than a direct path signal.

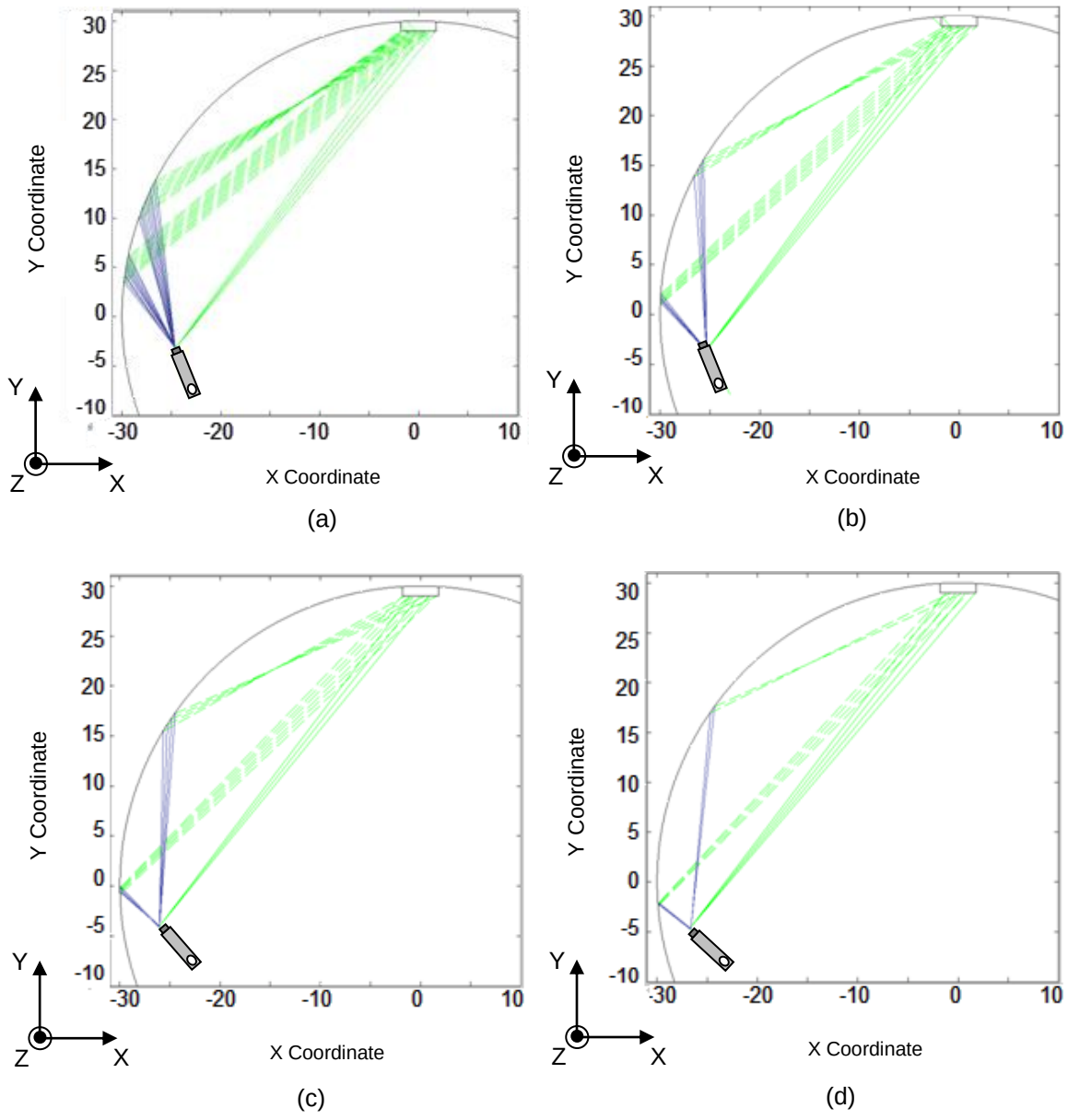

Figure 5-34: Simulated X_2 location transmitter response, transmitter rotation angles

(a) -50º (b) -60º (c) -70º (d) -80º

Figure 5-34 shows the simulated X_2 location transmitter response for rotation angles of (a) -50°, (b) -60°, (c) -70° and (d) -80°. It can be observed that for each of these rotation angles there are multipath reflections observed from the vessel wall as was observed from experimental data shown in Figure 5-10 (a). This result suggests that the beam focussing observed in the vessel is highly dependent upon both the transmitter location and rotation angle. For most locations in the vessel the focussing from the vessel wall will direct the reflections to a location which is not a receiver position. The result however does suggest that the curved nature of the vessel can yield reflected signals with higher amplitude than might otherwise be expected. This creates problems of uniform signal coverage even for the "perfect" omnidirectional transmitter profile.

5.4.2 Summary of Ray Tracing Model

Experimental results observed in section 5.2.3 have demonstrated the reception of reflection signals with cross correlated amplitude above that expected from the transmitter. The results suggest beam focussing from the vessel wall, causing an increase in received signal strength. This section has undertaken simulations of the signals to investigate this possibility.

Simulations of the X_2 location show that for a -45° transmitter rotation reflections from the vessel wall impact the receiver as observed in experiments. The range of these reflections is approximately 50 cm in comparison to the direct signal path of approximately 40 cm. More significantly however is that due to the curved vessel surface the difference in range of these reflections is very small, less than 0.01 cm. It is possible that the receiver is unable to distinguish between these arrivals, resulting in the production of a single received signal with increased amplitude, which would correspond to that observed experimentally.

The model has also demonstrated how this reflection problem is highly localised, which fits with experimental results. For a rotation of -40° it can be observed that there is no single impact reflection path which impacts the receiver, which again fits with experimental results.

The result suggests that due to the curved construction of the vessel wall the ability to provide uniform signal coverage in the vessel cannot be achieved, even if an omnidirectional transmitter was to be used. The curved vessel surface appears to focus beams in the vessel and as such reflections are still able to impinge on the receiver with larger amplitude than the direct path.

5.5 Summary of Vessel Characterisation and Transducer Testing

This chapter has investigated how the Senscomp 40KT08 transducer performs underwater along with investigating reflections within the vessel to determine if peak signal detection methodologies can be utilised. The interaction of multiple transmitters in close proximity has been investigated and modelling has been undertaken investigating the range of reflections in the vessel to provide supporting evidence for experimental results.

In section 5.1 the challenges associated with the pill are described with the desire to use multiple transmitters to achieve signal coverage introduced. This section has highlighted the problems associated with reflections in the vessel due to non-uniform transmitters and suggested methods to overcome these problems through the use of multiple transmitters. This chapter investigates if this technique is sufficient to allow the use of peak detection techniques for signal detection.

In section 5.2 experiments have been conducted with a single transmitter to identify both the transmission properties of the transducer underwater and also the impact of reflections within the vessel. This section is summarised in section 5.2.4. Results have demonstrated that in the centre of the vessel the peak received cross correlated signal corresponds to the direct path, allowing accurate ranging. When the transmitter is located close to the vessel wall however it can be observed that reflections arrive at the receiver with larger amplitude than the direct path, leading to incorrect range calculations and ranging errors using peak detection methodologies. Another result observed is the emergence of beam focussing due to the curved vessel surface, which creates reflections at the receiver with amplitude above that expected from the transmitter.

In section 5.3 experiments has been conducted with multiple transmitters to observe beam interaction and to attempt to overcome reflection issues. From the experimental results in section 5.2 two transmitter layouts were tested 45° and 90° separation. Results have demonstrated that due to the variation between individual transmitters and the impact that the receiver reception angle has on the signal accurate ranging using peak detection is not possible. Large range reflections can still be observed with amplitude stronger than direct path signals. This result has suggested that the use of peak detection methodologies for signal detection is not effective in this target environment.

In section 5.4 simulations were conducted to determine the impact that beam focussing has in the vessel in accordance with experimental results. Simulations have demonstrated that for certain transmitter locations the curved nature of the vessel surface focuses reflections onto the receiver. These reflected signals arrive with minimal range difference, approximately 0.01 cm. This suggests that multiple signal impacts cannot be determined and instead a single impact with increased amplitude is observed.

To allow detection of the localisation signal accurately techniques which detect the first arrival of the signal rather than the peak value must be used. For this application the technique of thresholding is envisaged. To ensure thresholding techniques perform well in the vessel it must be guaranteed that for any pill location or orientation the received signal strength is above the threshold value. Therefore there is the requirement to create a pill transmitter array which is able to produce uniform signal coverage such that the received signal is always above the threshold level. [Chapter 6.0] will investigate the transmitter and receiver beam profiles to predict the signal levels for various transmitter layouts on the pill.

6.0 Pill Transmitter Array

The original desire for the pill, to produce uniform signal coverage regardless of its orientation or location within the vessel has been updated based on the experimental research conducted in [Chapter 5.0, section 5.3]. Based on the updated requirements for the pill this chapter discusses the work undertaken to investigate potential transmitter layouts on the pill in an effort to maximise the received signal strength at any receiver. Experimental profiling is undertaken of the transmitter, receiver, and attenuation of the acoustic signal as function of range to allow a model to be constructed to calculate the anticipated received signal strength. This model is then expanded to allow various transmitter and receiver layouts within the vessel to be tested.

In section 6.1 the motivation behind the design of a transmitter array on the pill is reiterated along with the modifications made to this requirement based on the research conducted within [Chapter 5.0, section 5.3]. In section 6.2 the experimental test set-up is detailed along with a more detailed explanation of the detection method for the acoustic localisation signals.

Section 6.3 undertakes experimental profiling to evaluate the possible receiver options for use within the project. A comparison is made between the reception profiles and attenuation of the signal as a function of range for the two available transducers and a selection made for implementation. This section also highlights the alteration in the received signal strength as the underwater medium is altered in the vessel.

In section 6.4 experiments are undertaken to determine the transmission profile of the transducer in the underwater medium. From this profile along with those determined in section 6.3 it is possible to create a model to calculate the anticipated signal amplitude at any receiver. This model is then used to investigate multiple transmitter and receiver layouts within the vessel, and the received signal strength at each receiver to be calculated. This section investigates how the number and placement of transmitters affects the received signal strength, before discussing how through varying the mounting angles of both transmitters on the pill, and receivers in the vessel, the received signal strength can be improved.

6.1 Background

The initial aim of the project was to develop a pill which produced a uniform omnidirectional beam pattern. Based on this beam pattern the peak received signal detected at any receiver, for a single pill in the vessel, corresponds to the direct path signal and not a reflection. By guaranteeing the direct path signal is the peak received signal then detection strategies which utilise peak detection could be implemented, allowing noise tolerant transmission signals to be used.

From the research conducted in [Chapter 5.0, section 5.2] investigating the reflection characteristics of the vessel, it has been observed that peak detection strategies are not effective

for use within this project. Results in [Chapter 5.0, section 5.2] have suggested that due to the curved nature of the vessel, beam focussing from the vessel wall allows reflections to arrive at the receiver with larger amplitude than the direct path signal.

This observation has suggested that signal detection methodologies which utilise peak detection for signal acquisition will be ineffective in the vessel. To detect the arrival of signals at the receivers the use of thresholding is anticipated. As previously established in [Chapter 2.0, section 2.5], thresholding relies on the reception of a signal at the receiver whose amplitude is above that of the threshold value. To ensure the detection of the acoustic signal from the pill, it must be guaranteed that the signal received from the pill regardless of its location within the vessel exceeds the threshold value. This threshold may need to be set high for future applications as the amplitude of background noise could be potentially large from, for instance, motors or mixing impellers.

Therefore, while there is no longer the requirement for the pill to produce uniform signal strength in all directions, it is essential that the signal from the pill which reaches the receivers remains above that of the threshold level. This chapter therefore models the anticipated signal strength at the receivers for various pill layouts to allow the selection of a transmitter layout on the pill which maximises the received signal strength. This chapter investigates the profiles of the transmitter, receiver and attenuation of the underwater medium to allow modelling of the received signal strength for different transmitter layouts on the pill, considering potential “worst case” pill locations within the vessel.

6.2 Experimental Set-up

To determine the signal strength which is output from the receiver for any possible transmitter location in the vessel, the signal amplitude observed during testing as described in [Chapter 5.0, section 5.2] must be deconstructed into its constituent parts. The detected signal strength at the receiver depends on three factors: the strength of the signal from the transmitter as a function of transmission angle, the sensitivity of the receiver as a function of reception angle, and the attenuation of the signal as a function of range due to the transmission medium.

As established in section 6.1 the TOF corresponding to the received signal is to be selected via amplitude thresholding techniques. Therefore the experimental profiling of the transmitter and receiver is to be undertaken with the anticipated final transmission signal. From work conducted in Burnett-Thompson A. (2007) it was determined that a short pulsed sine wave provided the best localisation results in a similar target environment. The use of a short pulsed sine wave allows the TOF and subsequent range of the signal to be detected and allows multiple transmissions per second, enabling a fast update of the position of the pill for future localisation.

While the Senscomp 40KT08 has been selected as the transmitter to be mounted on the pill, due to the requirement for small size, there is no corresponding limitation for the receiver. Results in

[Chapter 5.0, section 5.2] were obtained using the 5 cm receiver at 100 kHz. While the cross correlated received amplitude showed reasonable signal level it was apparent that the receiver profile might not be uniform. This section therefore investigates the reception profile of both the 5 cm receiver and the Senscomp 40KT08 to observe which is the most suitable for use within the project. All the experiments are conducted in the underwater medium.

6.2.1 Experimental Test Rig

To allow an accurate representation of the transmitter and receiver profiles to be determined, along with allowing repeatable and controllable measurements, an *x-y* plotter mounted to the vessel was used to control the position of the transmitter. The plotter consisted of two independent axes which were driven by two separate toothed belts and motors. Figure 6-1 shows a diagram of the plotter.

The plotter was controlled via software on the host PC which allowed independent movement in either the *x* or *y* direction. As the plotter moved the host PC recorded and tracked the movement and updated the expected coordinate position of the transmitter. Experimental testing has demonstrated that for each axis the error between the actual and expected position is a maximum of 5 mm. Experiments were conducted in the 250 litre test vessel described in [Chapter 3.0, section 3.1.4].

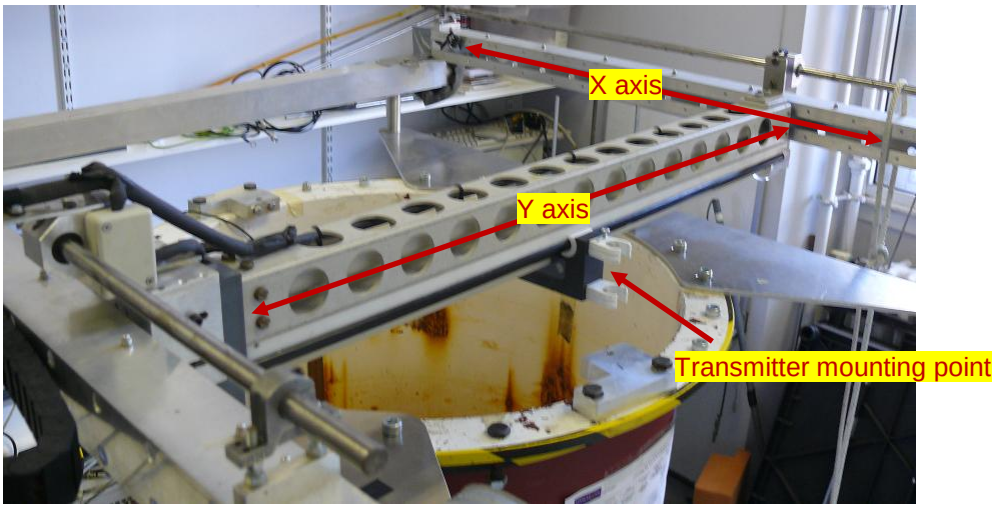

Figure 6-1: *X-Y* plotter attached to vessel

6.2.2 Signal Detection

From the work conducted in [Chapter 5.0, section 5.2] it has been suggested that the use of peak detection signal methodologies were not effective for implementation within the vessel due to large amplitude reflections. To allow localisation of the pill signals were to be detected at the receiver using amplitude thresholding. At the receiver the signal amplitude was compared with a threshold level. When the received signal amplitude exceeds the threshold level then the TOF corresponding to the point at which the signal exceeded the threshold was selected. This allows the range of the

signal to be calculated. This method overcomes the issue of large amplitude reflections as, for a single pill; the direct path signal will always arrive at the receiver first. If the amplitude of the signal was above the threshold level it was selected.

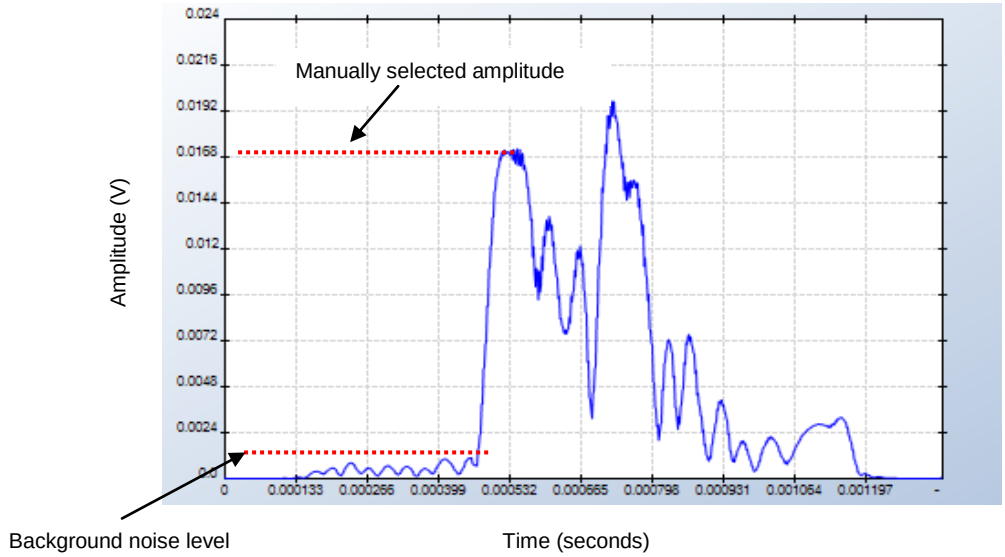

Figure 6-2: Typical signal arrival after filtering and envelope detection

Figure 6-2 shows a typical received signal after filtering and envelope detection. The acoustic signal from the transmitter is the vessel which impacts the receiver is amplified at the receiver card before being transmitted to the data acquisition card (DAQ). Onboard the host PC the signal is processed by custom software developed in Burnett-Thompson A. (2007) and the raw signal is band-pass filtered to remove noise and envelope detection is undertaken to increase the signal strength. It can be observed that the background noise level in the vessel is approximately 1 mV. To determine the strength of the direct path signal the maximum amplitude of the first peak to arrive at the receiver above the background noise level is manually selected. This manually selected amplitude is illustrated in Figure 6-2.

6.3 Receiver Selection

This section details the experimental research undertaken to determine the attenuation of the signal as a function of range and the receiver profiles for the two available receiver options. From this research a selection is made on the most appropriate transducer for use as the receiver within this project.

6.3.1 Attenuation as a Function of Range, 5 cm Receiver

To develop a model which calculates the output from a receiver for any transmitter location within the vessel the impact that the transmission medium has upon the signal must be determined. The attenuation of the signal is profiled as a function of range between the transmitter and receiver. Figure 6-7 displays the experimental set-up to determine the attenuation of the signal.

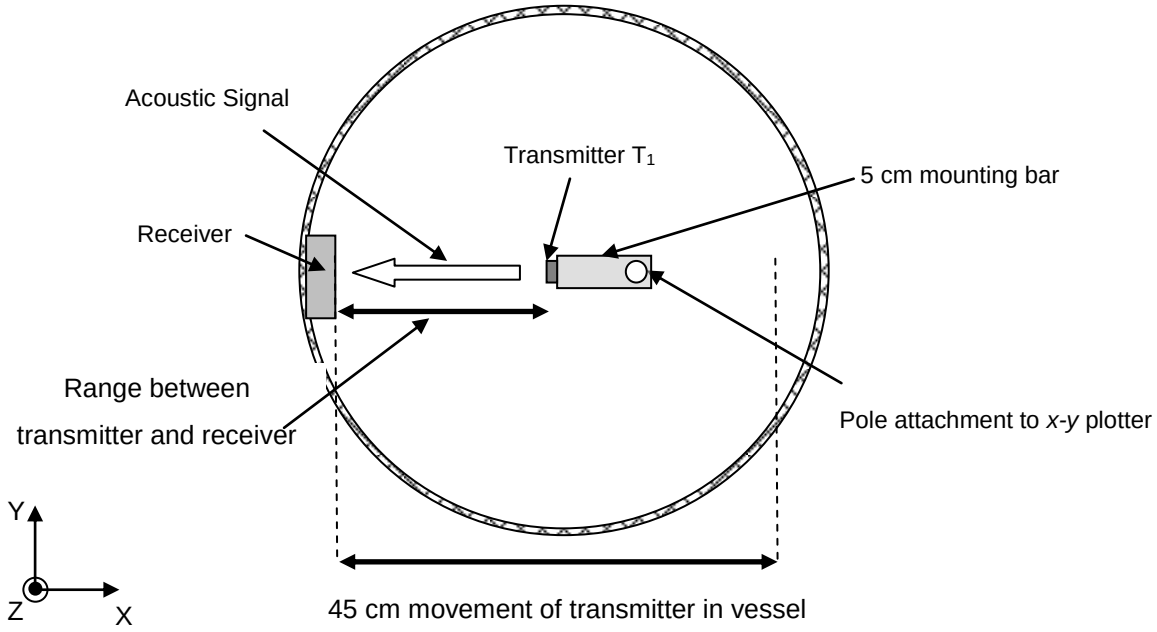

Figure 6-3: Experimental set-up for profiling the attenuation as a function of range

The transmitter utilised for the first test is the Senscomp 40KT08, labelled T_1 in Figure 6-3, while the receiver utilised is the 5 cm receiver described in [Chapter 5.0, section 5.2]. The experiments profile the received signal strength for transmission through the underwater medium. The transmitter is located as shown in Figure 6-3 and moved though a range between 0 cm and 45 cm (which is the limit of movement within the vessel due to the plotter attachment). The range between transmitter and receiver is increased in intervals of 2.5 cm ± 0.5 cm using the *x-y* plotter. The location of the transmitter helps to minimise the potential impact of reflections, however as the signal is manually selected as the first signal above noise reflections do not impact the signal strength calculated. A 10 cycle sine wave is used as the transmission signal with a transmission frequency of 100 kHz as used in [Chapter 5.0, section 5.2].

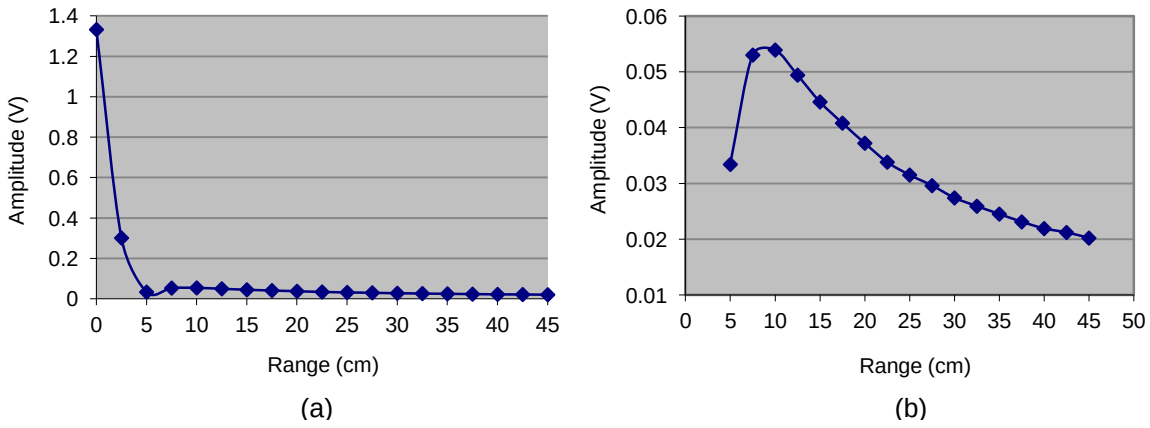

Figure 6-4 (a): Amplitude at receiver vs. range, T_1, (b): Region from 5 cm to 45 cm

Figure 6-4 (a) displays the received amplitude at the external system as a function of range between the transmitter and receiver. Figure 6-4 (b) shows a zoomed image of the amplitude of the signal for the ranges 5 cm to 45 cm. From Figure 6-4 (a) it can be observed that the amplitude when the transmitter and receiver are in direct contact is approximately 1.3 V. For the range 0 cm to 5 cm the amplitude of the received signal decreases sharply. At a range of 5 cm the amplitude is 0.032 V. Figure 6-4 (b) illustrates that in the region from 5 cm to 10 cm the amplitude of the received signal actually increases, from 0.032 V to 0.054 V. From 10 cm to 45 cm the amplitude of the received signal decreases to a minimum of 0.02 V at 45 cm. While this amplitude is low it is still considerably larger than the background noise level in the vessel for a typical measurement is approximately 0.001 V.

The result suggests two regions for reception of the signal which relate to operation in the near and far field regions (Chupyra A.G. et al, 2006). The ultrasonic signal originates from a number of points along the transducer's face which means that the signal strength is influenced by constructive and destructive interference (Chupyra A.G et al, 2006). This leads to fluctuations in the signal intensity near to the transmitter and is known as the near field. The location of the end of the near field region, known as the natural focus can be calculated using equation (4.1).

$$N = \frac{d^2 f}{4v} \qquad \textbf{(6.1)}$$

where d is the diameter of the transducer, f is the frequency of operation and v is the velocity of sound in the medium[36]. If it is considered that at a receiver the near field effect is also present and that for short range signals the impact of the signal at multiple points on the receiver increases the signal strength then for a transmission frequency of 100 kHz, using a receiver diameter of 50 mm and a propagation velocity of 1480 ms^{-1} the natural focus is calculated to be 45 mm which corresponds well with experimental data. Beyond the natural focus the amplitude reduces smoothly (Chupyra A.G, et al 2006). This is known as the far field region. The influence of the near field region is an important consideration as the amplitude variation in this region is significant and difficult to predict. This could prove a challenge for techniques which use thresholding as the received signal can vary significantly for small changes in range.

[36] http://www.ndt-ed.org/GeneralResources/Formula/UTFormula/near_field/near.htm

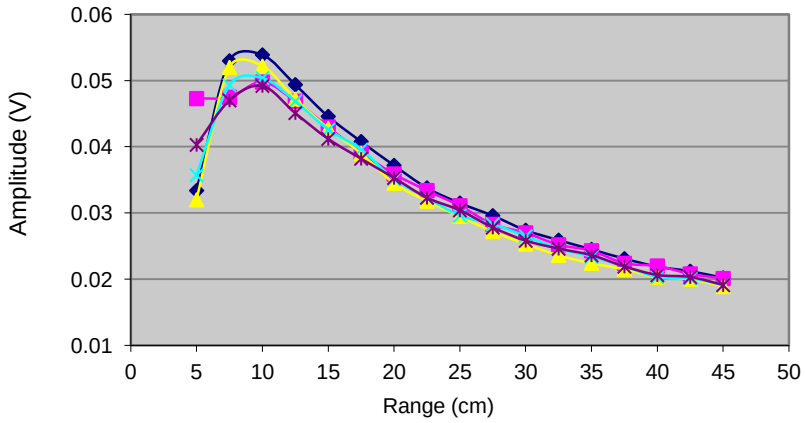

Figure 6-5: Repeatability of attenuation of signal in vessel, Senscomp 40K08 T_1

Figure 6-5 displays the repeatability of the results observed in Figure 6-4. The graph displays 5 repeats of the experiment utilising the same set-up. It can be observed that at a range of 5 cm there is significant variation in the received signal strength. At this point as it is anticipated the transmitter is operating in the near field region then any small variation in range could produce large changes in amplitude. For the range between 10 cm and 45 cm the results show excellent repeatability. The best standard deviation result is observed at a range of 32.5 cm and is 0.0009 V while the worst standard deviation result is observed in the near field region at a range of 5 cm and is 0.006 V. To observe the natural variation between transmitters of the same type and construction the experiment is repeated with a second Senscomp 40KT08 transmitter.

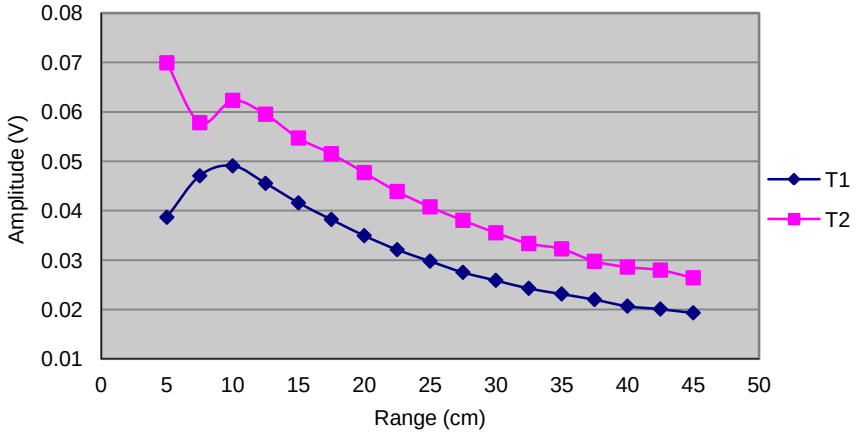

Figure 6-6: Comparability of received signal in vessel, T_1 against T_2

Figure 6-6 compares the signal strength received by two Senscomp 40KT08 transmitters labelled T_1 and T_2. The result displays the mean value for each transmitter at each point from 5 experimental repeats. For a range less than 10 cm there is some variation in the amplitude profiles which would be anticipated due to the operation of the transmitters in the near field region.

The received amplitude for a range of 10 cm is 0.062 V for T_2 in comparison to 0.049 V for T_1. From a range of 10 cm to 45 cm it can be observed that the two attenuation profiles are similar. While T_2 can be observed to produce a stronger signal the profile of the attenuation curve is similar

to that of T_1. At a range of 10 cm the amplitude from T_2 is 0.062 V. At 45 cm the amplitude is 42% of the 10 cm value at 0.026 V. The amplitude from transmitter T_1 at 10 cm is 0.049 V. At 45 cm the amplitude is 41% of the 10 cm value at 0.02 V. The worst standard deviation result for T_2 over 5 tests is observed for a range of 5 cm and has a value of 0.007 V while the best result is observed at a range of 37.5 cm and is 0.001 V. Both of these are comparable to those previously calculated for T_1.

6.3.2 Receiver Profile, 5 cm receiver

To allow the received signal strength for any transmitter location in the vessel to be predicted, the sensitivity of the receiver as a function of reception angle must be investigated. To ensure that the received signal strength corresponds to only the receiver sensitivity the profile of the transmitter and the attenuation of the signal must be decoupled from the received signal strength.

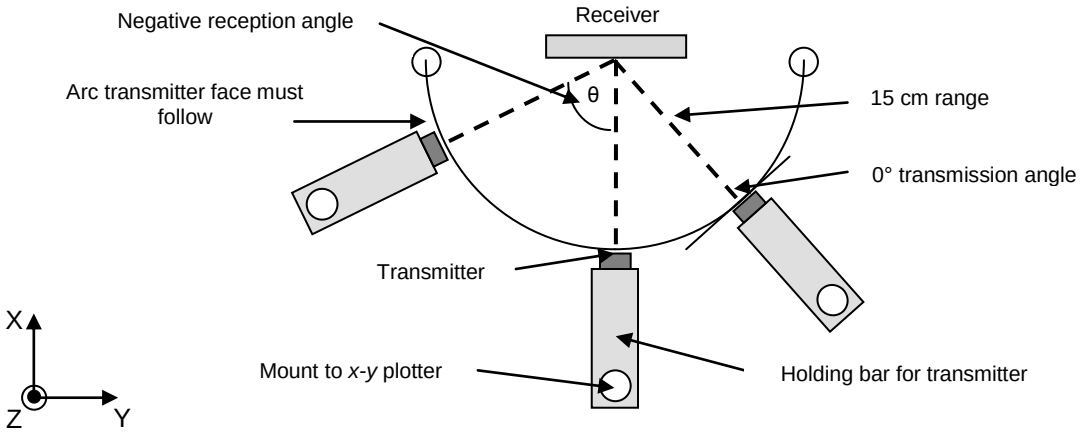

Figure 6-7: Experimental set-up to determine the profile of the receiver

Figure 6-7 displays the experimental set-up for determining the horizontal sensitivity profile of the receiver. This was the response of the receiver as the horizontal incidence angle was varied for a fixed vertical reception angle. The transmitter used was the Senscomp 40KT08 while the receiver was the 5 cm receiver. The transmission frequency was 100 kHz and the transmission signal was a 10 cycle sine wave. 100 kHz was used as the 5 cm receiver is designed for use underwater and is designed for 100 kHz operation. It was anticipated that as the receiver is designed for underwater use the maximum received strength would be obtained by operating it at its optimum frequency rather than at the transmitter's optimum frequency as explained in section 5.2.2 To decouple the transmitter profile from the received signal strength the transmitter was rotated such that while the reception angle at the receiver changes the transmission angle remains at 0°. To decouple the attenuation of the signal due to the underwater medium the range between the transmitter and receiver was maintained at a fixed value as the transmitter was rotated. The range was maintained at 15 cm which was in the far field region of the transmitter; Figure 6-4 (a) so that the incident signal strength was consistent between results. The transmitter position was altered such that the receiver sensitivity was profiled at 5º intervals ± 1°. Positive reception angles were considered when the transmitter was positioned to the right of the receiver as viewed in Figure 6-7.

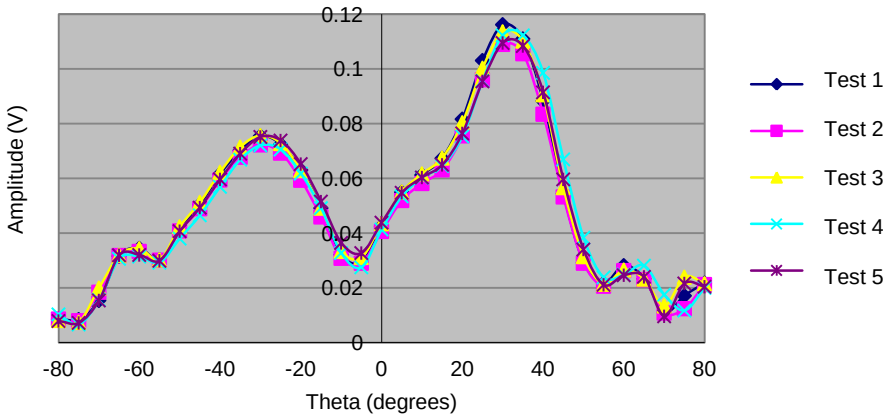

Figure 6-8: Receiver sensitivity profile when using transmitter T_1

Figure 6-8 displays the manually selected received signal amplitude against the reception angle at the receiver. The transmitter is this instance is T_1. The result displays 5 separate runs of the experiment to confirm the validity of the profile and to determine its repeatability. The largest standard deviation between the results is observed for a reception angle of 40° and has a value of 0.006 V while the smallest standard deviation is obtained for a reception angle of -65° and has a value of 0.0006 V.

The result suggests that the voltage produced by the receiver is highly dependent upon the reception angle at which the signal arrives. The peak receiver sensitivity is located at a reception angle of approximately 35°. While the result suggests that the sensitivity of the receiver is not equal for positive and negative reception angles the receiver does show some symmetry in terms of its response. The peak positive sensitivity reception angle appears at approximately 35° and the peak negative sensitivity reception angle appears at approximately -30°.

The asymmetry in output amplitude for positive and negative reception angles could be explained by the construction of the receivers. The ceramic crystals within the receivers are encased in a hard epoxy resin. If the thickness of the epoxy between the impacting acoustic signal and the internal ceramic crystal is not uniform across the receiver then it is possible the epoxy absorbs more signal on one side of the receiver. This would result in a smaller amplitude signal impacting the ceramic crystal inside meaning the output of the crystal would be smaller. This could account for the variation in the output of the receiver for positive and negative reception angles.

The receiver profile observed in Figure 6-8 helps to clarify some of the results observed in [Chapter 5.0, section 5.2.3] in relation to the received peak cross correlated amplitude in the X_2 location. The sensitivity profile of the receiver obtained in Figure 6-8 provides supporting evidence for the notion of beam focussing within the vessel, as the receiver sensitivity profile would not account for the increase in amplitude of reflections observed in location X_2 in [Chapter 5.0, section 5.2.3]. This idea is illustrated in Figure 6-9.

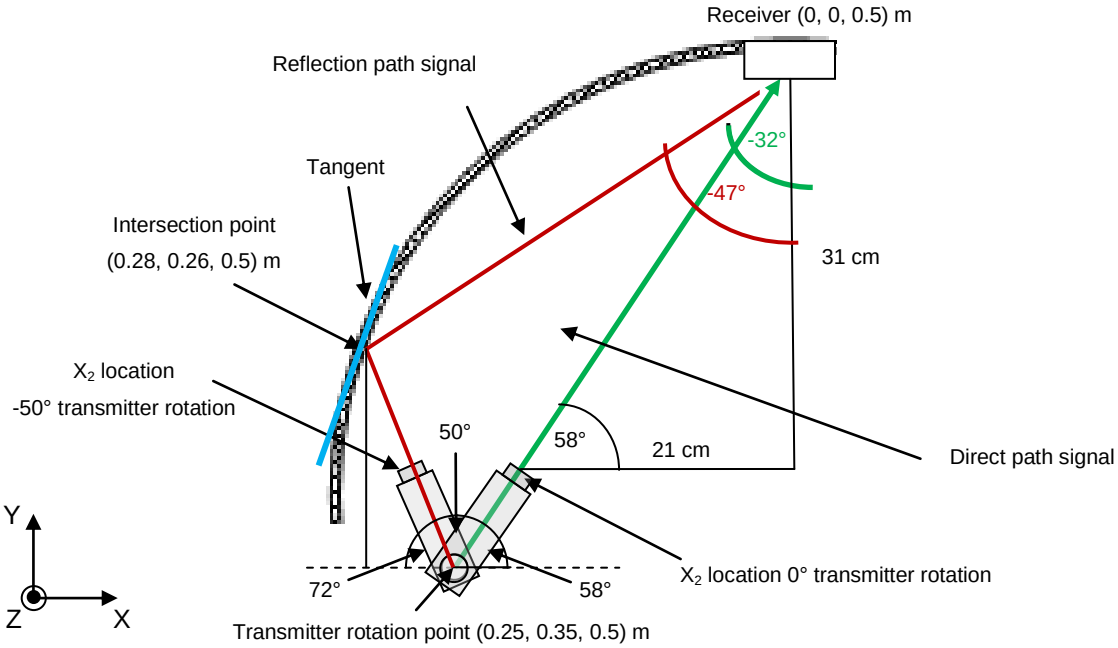

Figure 6-9: Reflection signals observed in X_2 location [Chapter 5.0, section 5.2.3]

Figure 6-9 displays the set-up as tested in [Chapter 5.0, section 5.2.3] for the X_2 location with a single transmitter rotated at 0° and -50°. The rotation angle of -50° is the first point at which the amplitude of the peak cross correlated received signal was above that of the 0° alignment direct path amplitude.

The direct path signal (green line) from the transmitter at 0° rotation impinges the receiver at a reception angle of approximately -32°. From the range of the reflections observed in [Chapter 5.0, section 5.2.3] for -50° rotation, (approximately 55 cm) and through modelling the expected reflection path, it has been suggested that reflections are from the left vessel wall as illustrated by the red line in Figure 6-9. It can be observed that the reception angle at the receiver for the reflected signals when the transmitter is rotated to -50° is approximately -47°. This reception angle is calculated using the model in [Chapter 5.0, section 5.2.3].

The receiver profile in Figure 6-8 demonstrates that from a reception angle of approximately -30° through to -55° the receiver sensitivity decreases. Therefore, as the reception angle of the reflected signal for -50° transmitter rotation is -47° the receiver should be less sensitive to this signal than the direct path signal for 0° transmitter rotation which impacts at a reception angle of -32°. This suggests that the increased cross correlated amplitude of the reflection signals observed in location X_2 is not related to the receiver sensitivity profile, which suggests that beam focussing could be the cause of the increased amplitude.

The horizontal receiver sensitivity profiles shows that the output of the receiver is highly dependent upon the reception angle of the signal. It is therefore anticipated that the sensitivity of the receiver as a function of vertical impact angle will also vary. Work has therefore been undertaken to determine the horizontal receiver sensitivity as the vertical impact angle is altered.

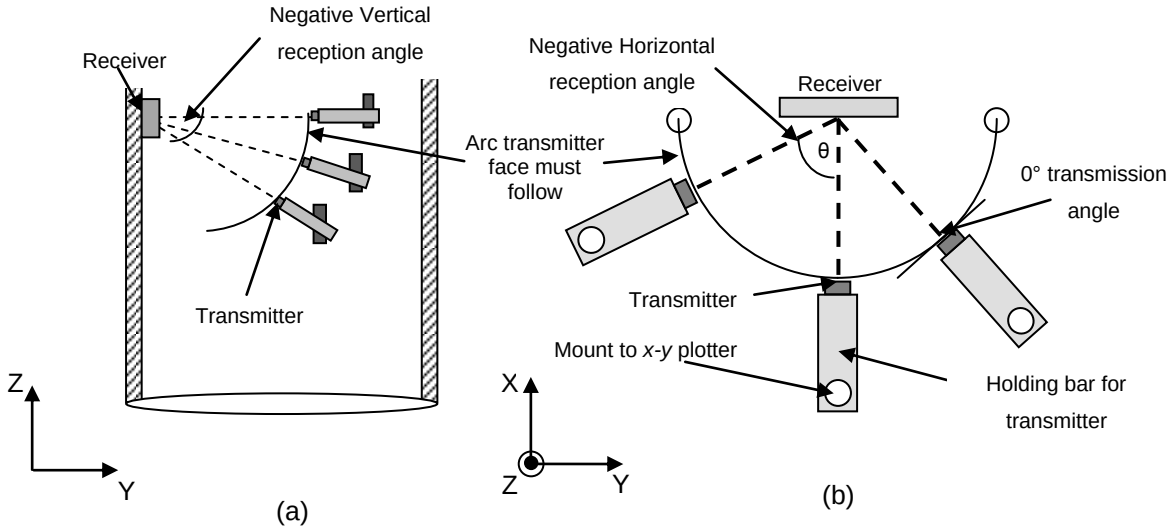

Figure 6-10 (a): Movement of transmitter to alter vertical reception angle (b) rotation of transmitter to alter horizontal reception angle

Figure 6-10 displays the experimental set-up for determining the horizontal receiver sensitivity as the vertical reception angle is altered. In Figure 6-10 (a) the transmitter is moved vertically such that the vertical reception angle at the receiver is altered. The range is maintained at 15 cm and the transmitter is rotated such that the vertical transmission angle is maintained at 0°. For each vertical reception angle the transmitter is then rotated as shown in Figure 6-10 (b) such that the horizontal reception angle at the receiver is altered. The range remains fixed and the horizontal transmission angle remains at 0°. The horizontal receiver sensitivity is obtained at 5° intervals ± 1° and the vertical reception angle is changed in intervals of 10° ± 5°. Positive horizontal reception angles are considered when the transmitter is located to the right of the receiver; positive vertical reception angles are considered when the transmitter is located above the receiver.

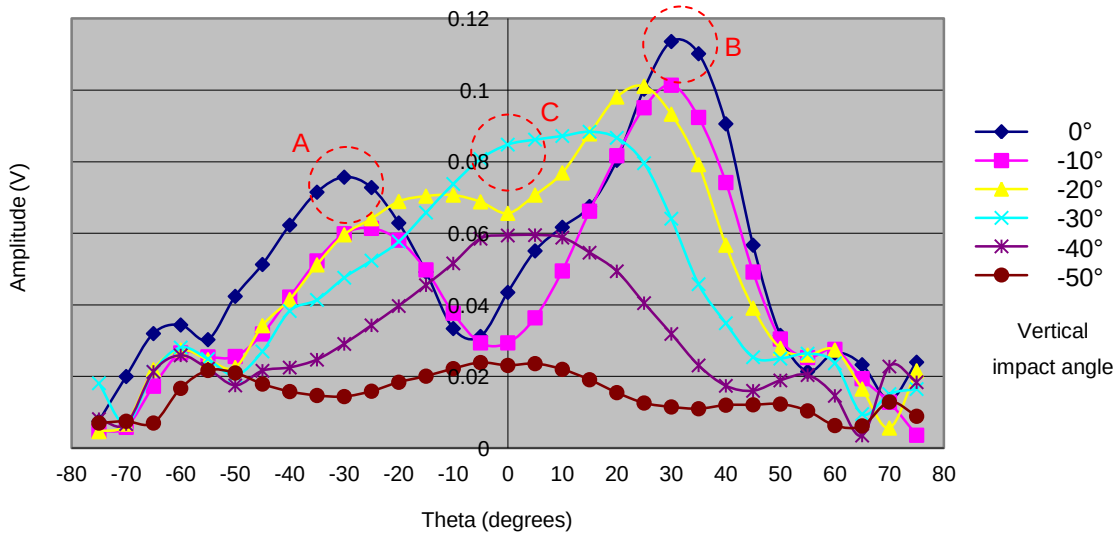

Figure 6-11: Horizontal receiver profile with respect to negative vertical reception angle

Figure 6-11 displays the horizontal receiver sensitivity with respect to negative vertical reception angle. To aide visual clarity only vertical reception angles between 0° and -50° are displayed. It can

be observed that the horizontal receiver sensitivity changes significantly as the vertical reception angle is varied.

It was anticipated that the horizontal receiver sensitivity profile would remain largely consistent for different vertical reception angles. The horizontal sensitivity profile was expected to maintain the same shape but be shifted in amplitude in relation to the vertical sensitivity of the receiver. From the results in Figure 6-11 this is not the case.

The result for 0° vertical reception angle shows peaks located at approximately ± 30°, locations A and B. As the vertical reception angle is altered from 0° through to -50° it can be observed that the peaks situated at ± 30° for 0° vertical reception, locations A and B, begin to decrease in amplitude but their position alters such that they shift towards a horizontal angle of 0°. For a -30° vertical angle (turquoise line) the two peaks have shifted such that they combine to produce a single central peak, location C. For -40° and -50° the amplitude of this central peak can be observed to reduce.

Experimental results detailing the sensitivity of the receiver have illustrated that the profile of the receiver is non-uniform. While it was anticipated that the peak receiver sensitivity would be obtained for a 0° horizontal reception angle, this has been shown not to be the case. The peak horizontal receiver sensitivity is obtained at ± 30° respectively for a 0° vertical reception angle.

The significant result observed during profiling of the receiver is that the horizontal sensitivity of the receiver is not consistent for varying vertical reception angles. Experimental results indicate that the receiver profile varies significantly depending on the vertical reception angle at the receiver. The result suggests that the sensitivity of the receiver as a function of the horizontal and vertical reception angle is a complex problem. While changes in the thickness of the epoxy resin could account for some of the variation in receiver profile the result suggests that the ceramic crystal inside the receiver has a complex response which is difficult to predict. This provides a significant challenge for modelling the received signal strength for a given transmitter location but provides further evidence to support thresholding rather than peak detection for ranging.

6.3.3 Attenuation as a Function of Range, Senscomp 40KT08 Receiver

To allow a comparison between the available transducers the Senscomp 40KT08 is also profiled as a receiver to allow the attenuation of the signal as a function of range to be obtained. As the Senscomp 40KT08 transducer has a nominal operating frequency of 40 kHz the transmission signal utilised is a 40 kHz 10 cycle sine wave. The transmitter and receiver are both Senscomp 40KT08 units. The experimental set-up is maintained as that in [section 6.3.1] to allow a comparison between results.

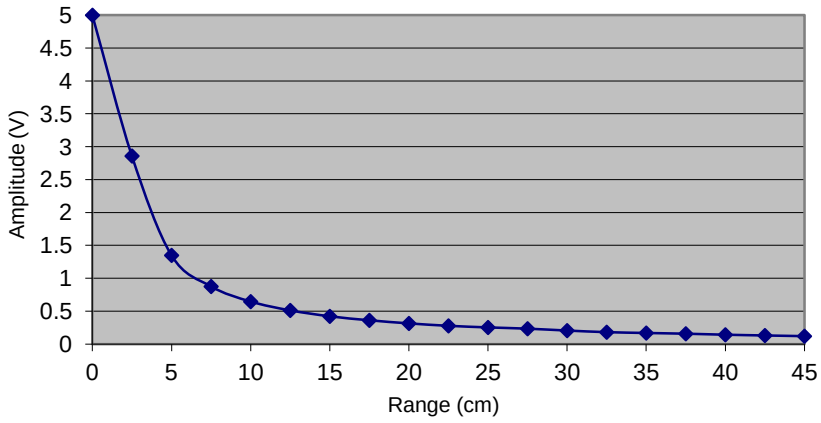

Figure 6-12: Attenuation profile as a function of range 40 kHz

Figure 6-12 displays the received signal strength as a function of range for the Senscomp 40KT08 receiver. When the transmitter and receiver are in direct contact the received amplitude is 5 V, the amplitude is reduced as the range is increased. At 45 cm the received signal strength is 0.12 V. It can be observed that in comparison to the results for the 5 cm receiver the attenuation profile shows a continuous smooth reduction in amplitude from 0 cm to 45 cm, with no increase due to the change between the near and far field region.

With the smaller diameter receiver, of only 20 mm, it can be calculated that the end of the near field region should be observed at a range of only 7 mm. Therefore within the experimental resolution of the range measurements at 2.5 cm intervals the change between the near and far field region is not observed. The near field effect is therefore only observed over a very short range with this transducer which means the attenuation profile is smoother over a larger range. In addition the range over which there is anticipated variation in the received amplitude between measurements is substantially reduced, from approximately 50 mm with the 5 cm receiver to 7 mm with the Senscomp receiver. The matching of the Senscomp 40KT08 as a transmitter/receiver pair also means the operating frequency is optimised for both units. The received amplitude at 45 cm of 0.12 V is significantly increased in comparison to the 5 cm receiver, which is 0.02 V for 45 cm as seen in Figure 6-4.

6.3.4 Receiver Profile, Senscomp 40KT08 Receiver

Experimental results in section 6.3.2 have shown that the receiver profile of the 5 cm receiver is highly dependent upon both the horizontal and vertical reception angle. To allow a comparison between results the same testing set-up is utilised as in Figure 6-10 (a) and (b) with the Senscomp 40KT08 utilised as the receiver. The transmission frequency is 40 kHz.

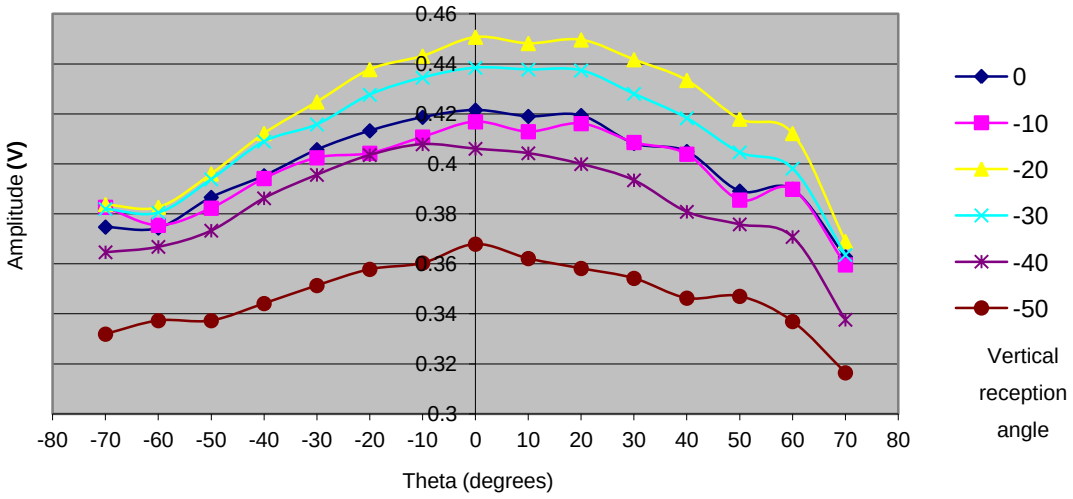

Figure 6-13: Senscomp profile as receiver at 40 kHz

Figure 6-13 shows the horizontal reception profile of the Senscomp device when used as a receiver for operation at 40 kHz for varying vertical reception angle. Again to aid visual clarity only the results between 0° and -50° are illustrated. It can be observed that for a vertical reception angle of 0° (dark blue line) the horizontal reception profile for ±30° is within 5% of the 0° horizontal value. The profile of the receiver seems comparable with that anticipated from the data sheet, [Chapter 2.0, section 2.5.3] with maximum signal observed at 0° and then a roll off in sensitivity from that point (Chupyra A.G et al, 2006).

The results show that, unlike the results with the 5 cm receiver shown in Figure 6-11, the shape of the horizontal receiver profile is consistent as the vertical reception angle is altered. The relatively flat response of the receiver means that regardless of the horizontal reception angle the strength output from the receiver remains similar.

6.3.5 Influence of Water Quality on Received Signal

While the results in Figure 6-8 have demonstrated that the receiver profile remains consistent between repeat tests, it was observed during testing that changing the water in the vessel has a significant impact on the receiver profile. This result is important as it suggests that during a mixing process, where the medium could alter due to the injection of fresh materials, the signal strength received from a pill location could change. To determine the effect that water composition has on the receiver sensitivity, tests were completed profiling the receiver sensitivity after changing the water in the vessel. The experimental set-up utilised the 5 cm receiver.

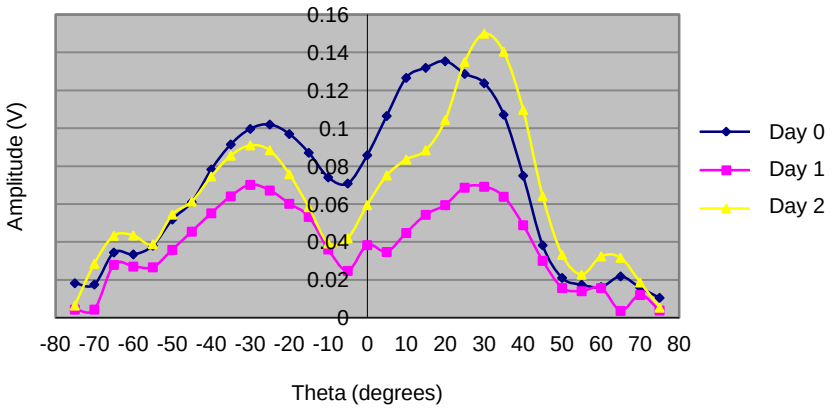

Figure 6-14: Received signal strength varying over days from vessel water change

Figure 6-14 displays the profile of the receiver as observed over a number of days from changing the water in the vessel. On day 0 the water in the vessel is removed and replaced with water from a mains source. Once the tank has been filled the receiver profile is measured. The measurement is repeated on day 1 and then on day 2.

The results show that the profile of the receiver on day 2 closely matches that previously observed in Figure 6-8 which suggests that after changing the water in the vessel it takes 2 days before the conditions within the vessel return to the long term trend. After directly changing the water, (day 0) it can be observed that the peak sensitivity of the receiver has shifted from 35° (day 2, long term trend) to 20° (day 0). The amplitude of the peak has also reduced in comparison to the long term trend, down from 0.150 V to 0.135 V.

The results obtained on day 1 show a significant reduction in amplitude in comparison to day 0. The peak amplitude is obtained for a negative reception angle and is 0.07 V. The positive reception peak and the negative reception peak have very similar amplitude for the testing on day 1. It can also be observed that the peak angle for both negative and positive receptions has increased in comparison to day 0, with the positive peak shifting to 30° from 20° on day 0.

The main alteration in water composition which is suggested for this change is the level of dissolved oxygen in the water. As the water is allowed to sit in the vessel it can be observed that bubbles induced into the tank during the filling process begin to rise to the surface and dissipate. The concentration of dissolved oxygen in the vessel changes as the water is left, which means that the results for freshly changed water and water which has been left in the vessel for a few days differ.

After allowing the water to sit in the vessel for one day, a large quantity of bubbles was observed on the surfaces of both the transmitter and receiver. After removing these bubbles it could be observed that the amplitude output by the receiver increased for a short duration of time (approximately 30 minutes) until the bubbles started to reform on both the transmitter and receiver

faces. This result suggests that the low amplitude received on day 1 is due to the bubble formation which absorbs the signal, reducing the output amplitude of the receiver.

This result is important for potential applications where the transmission medium may change either during mixing or whereby the contents of the vessel are purged between mixing processes. The change in attenuation suggests that areas of the vessel which could be anticipated to provide adequate acoustic signal level at the receivers may change during the process or due to the insertion of fresh material into the medium. This could present localisation challenges due to low amplitude signal detection at the receivers. To maintain consistent results further experimentation within this project ensures that the medium has returned to its “steady state” response before experiments are conducted. This result however further emphasises the requirement to develop a transmitter array which maximises signal strength at the receivers. While the formation of bubbles is difficult to prevent, if the received signal strength is maximised this provides some tolerance, or “performance reserve”, to accommodate the signal absorption due to bubble formation and still provide sufficient amplitude signal at the receivers for detection.

6.3.6 Summary of Experimental Profiling

This section has investigated two potential receiver options for localisation within the vessel. From experimental profiles the Senscomp transducer has been selected as the most appropriate for this project. The reception and attenuation profiles of the transducer have been investigated. This data allows the construction of a model which is able to investigate the impact of different pill transmitter layouts on the received signal strength.

The attenuation of the acoustic signal due to the underwater medium is investigated in section 6.3.1 for the 5 cm receiver used previously in Burnett-Thompson A. (2007). Experiments have been conducted to observe how increasing the range between the transmitter and receiver alters the received signal strength. Results demonstrate that there are two distinct regions for reception, the near and far field. In the near field it can be seen that the amplitude drops quickly before increasing. In the far field region the reduction is much smoother. Results have also demonstrated that the repeatability of measurements is very good. The near and far field regions are important for modelling to accurately determine the received signal from the pill.

In section 6.3.2 experimental testing is undertaken to determine the profile of the 5 cm receiver. Results have demonstrated that the received signal strength shows large variations for only small changes in horizontal reception angle. In addition results have demonstrated that the profile of the receiver is sensitive to the vertical reception angle. While designed for underwater operation, the results have shown that the unit is not suitable for this project.

Section 6.3.3 has investigated the attenuation of the signal when both the transmitter and receiver are Senscomp 40KT08 transducers. The results show that unlike in section 6.3.1 the variation

between the near and far field regions of the transducer are not so evident with a smooth reduction in amplitude from a range of 0 cm through to 45 cm. The small diameter of the transducer means that the near field region is much smaller, approximately 7 mm.

Section 6.3.4 has investigated the receiver profile of the Senscomp 40KT08 receiver at its nominal operating frequency of 40 kHz. In contrast to the results observed in section 6.3.2 the results testing the Senscomp unit demonstrate that the profile of the receiver shows excellent characteristics for implementation, with a large region of flat sensitivity between approximately ±30° and reduction in sensitivity beyond this region. The sensitivity profile is also consistent as the vertical reception angle is altered, with the profile shape remaining however with a shift in amplitude. The overall received amplitude is also significantly higher in comparison to the 5 cm receiver. For this reason the Senscomp 40KT08 unit has been selected as the receiver unit.

In section 6.3.5 the influence that water composition has on the received signal strength is documented. Through testing it was observed that the reception profiles were influenced by the water composition in the vessel. During routine vessel cleaning and refilling it was observed that bubbles formed on both the transmitter and receiver. The change in the level of dissolved oxygen in the vessel due to the insertion of fresh water has a large influence on the received signals. This result is significant for operation in process vessels were materials may be purged between processes or ingredients added during mixing. Both of these operations may cause alterations in the received signal level and the ability to detect the pill. To accommodate this there is the desire to implement a transmitter layout on the pill which maximises the received signal strength at any receiver providing a “performance reserve” such that even with reduction in received signal amplitude at a receiver due to bubble formation, the received signal strength is still sufficient to be detected.

6.4 Transmitter Array Modelling

To maximise the received signal amplitude there is a desire to investigate different transmitter layouts on the pill, observing how the received signal strength alters as the location of the pill in the vessel changes. From this information it is possible to realise a transmitter layout which ensures maximum received signal strength for the largest number of pill locations within the vessel.

6.4.1 Transmitter Profile at 40 kHz

From the experimental research conducted in section 6.3.4 it has been shown that using the Senscomp 40KT08 as the receiver option provides a flatter reception profile and increased amplitude in comparison to the 5 cm receiver. The Senscomp 40KT08 transducer is therefore to be used as both the transmitter and receiver at an operating frequency of 40 kHz. To allow a model to be constructed to determine the received signal strength at a receiver the Senscomp 40KT08 transmission profile must be obtained. To determine the transmitter profile the influence of receiver sensitivity and attenuation due to range must be decoupled from the received signal strength.

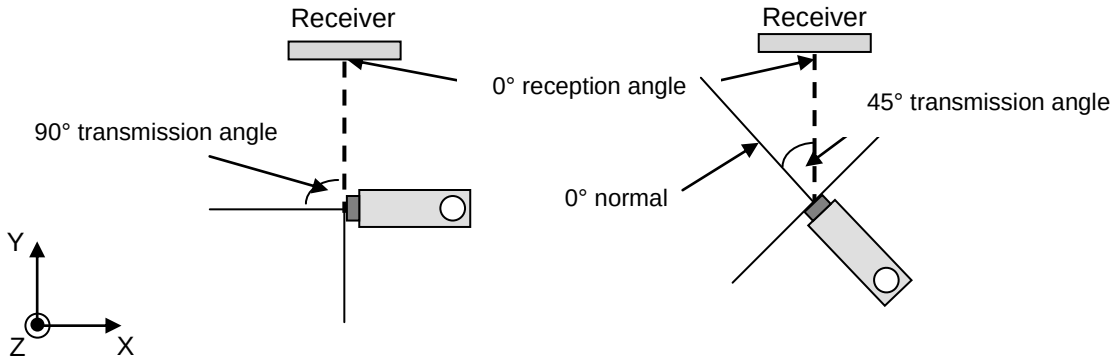

Figure 6-15: Experimental set up to determine the profile of the transmitter

Figure 6-15 displays the experimental set-up for determining the profile of the transmitter. The transmitter and receiver are both Senscomp 40KT08 transducers. The transmission signal is a 40 kHz 10 cycle pulsed sine wave. The transmitter is attached to the *x-y* plotter and its position altered such that the range between the transmitter and receiver is maintained at 15 cm. Rotation of the transmitter is completed such that while the transmission angle is altered, the angle at which the signal is received is maintained at 0°. The transmitter is profiled for rotations of 5° ±1°. Positive transmission angles are considered to leave the transmitter to the right of the 0° normal.

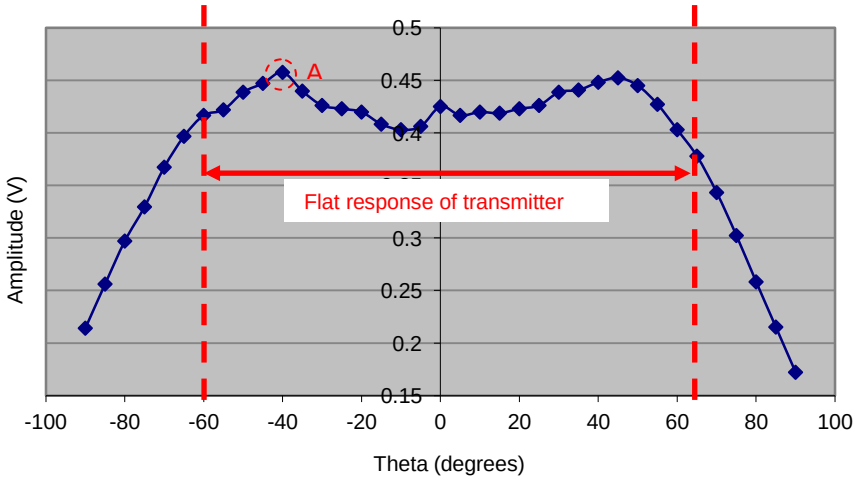

Figure 6-16: Horizontal transmitter profile for 0° vertical transmission angle

Figure 6-16 displays the experimentally obtained horizontal transmission profile for a 0° vertical transmission angle. It can be observed that the profile of the transmitter closely resembles the manufacturer's data sheet[37], [Chapter 2.0, section 2.5.3] with regards to roll off and the flat region. In comparison to the reception profile for the Senscomp 40KT08 Figure 6-13, it can be observed that the amplitude of the transmission signal remains flat for a larger angular rotation. For rotation between –60° and 60° the transmission amplitude remains within a 5 % tolerance of the 0° amplitude except for a single point at location A, which has amplitude 108 % of that observed for 0°.

[37] http://www.senscomp.com/specs/40KT08%20%20spec.pdf

Beyond the limits of ± 60° the amplitude from the transmitter decreases as the horizontal transmission angle increases. At –90° the amplitude is approximately 0.21 V which is 50% of the amplitude for a 0° transmission angle. For 90° the amplitude is 0.17 V which is 40 % of the amplitude for a 0° transmission angle.

To observe how the transmission profile alters as the vertical transmission angle is altered experiments are conducted moving the transmitter such that while the vertical reception angle remains at 0° the vertical transmission angle is altered.

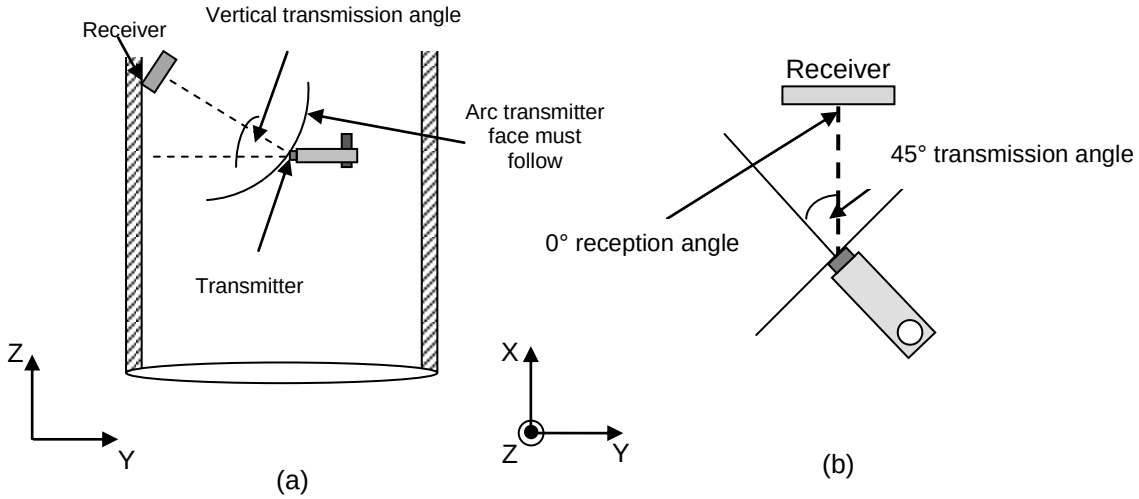

Figure 6-17 (a): Movement of transmitter to alter vertical transmission angle (b) rotation of transmitter to alter horizontal transmission angle

Figure 6-17 displays the experimental set-up for determining the horizontal transmission profile as the vertical transmission angle is altered. In Figure 6-17 (a) the transmitter is moved vertically such that the vertical transmission angle is altered. The range is maintained at 15 cm and the receiver is rotated such that the vertical reception angle is maintained at 0°. For each vertical transmission angle the transmitter is then rotated as shown in Figure 6-17 (b) such that the horizontal transmission angle is altered. The range remains fixed and the horizontal reception angle remains at 0°. The horizontal transmission profile is obtained at 5° intervals ± 1° and the vertical transmission angle is changed in intervals of 10° ± 5°. Positive vertical transmission angles are considered when the transmitter is below the receiver, positive horizontal transmission angles are considered when the transmission signal leaves to the right of the 0° normal.

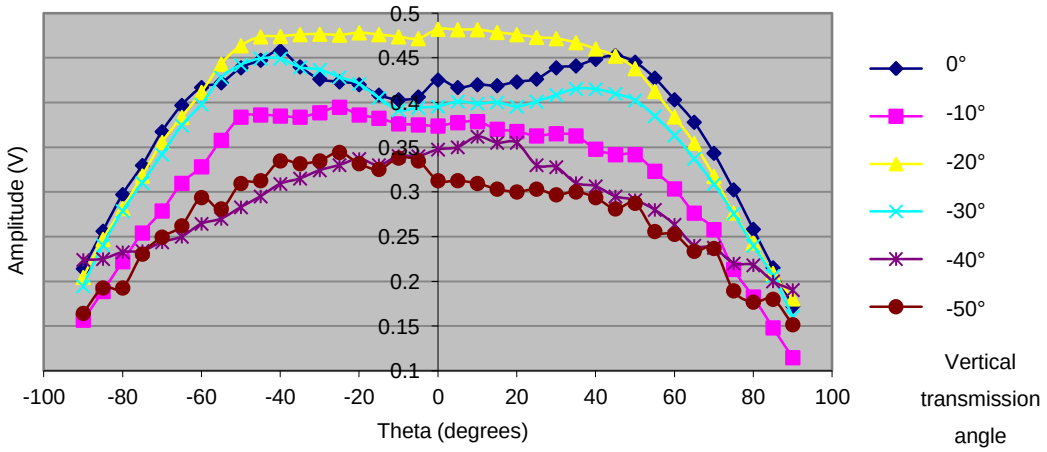

Figure 6-18: Horizontal transmission profile for varying vertical transmission angle

Figure 6-18 shows how the horizontal transmitter profile varies with vertical transmission angle. Vertical transmission angles between only 0° and -50° have been shown to aide visual clarity. It can be observed that as with the receiver profile for the Senscomp transducer, Figure 6-13, the horizontal transmission profile maintains a similar shape as the vertical transmission angle is varied. In comparison to the receiver profile the horizontal transmission profile shows more variation as the vertical transmission angle is altered however strong amplitude is again centred around a horizontal angle of 0° with decreasing amplitude as the horizontal transmission angle is increased. The result also shows the same increase in signal level for a vertical transmission angle of -20° as was observed for the receiver in Figure 6-13.

6.4.2 Profile Approximation

The data obtained for the transmitter profile, receiver sensitivity and attenuation of the signal as a function of range are discrete samples of data. For the transmitter and receiver, the data is discrete at 5° horizontal rotation intervals and 10° vertical intervals. For the attenuation of the signal as a function of range the data is discrete at intervals of 2.5 cm.

To allow the model to determine the received signal strength when either the rotation angle or the range lies in-between these discrete data points there is a requirement to approximate the profiles using equations. The discrete data are approximated in Excel using polynomial and exponential equations where appropriate. Due to the complex nature of some profiles, in certain instances the profile is split into sections and approximated through the use of multiple equations. This minimises the error between the approximation and experimental result.

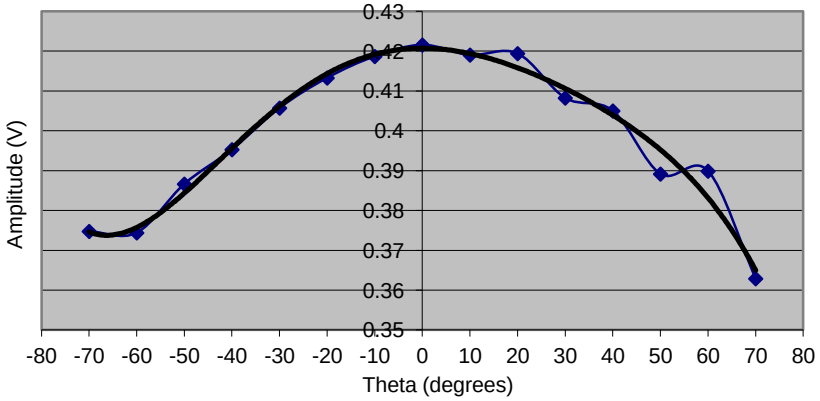

Figure 6-19: Receiver approximation using polynomial equation

Figure 6-19 shows the horizontal receiver profile for a 0° vertical reception angle. The blue line represents the experimental data while the black line shows how the polynomial equation used to approximate the profile fits the data. The equation which represents this fit line is shown in (6.2).

$$y = -2e^{-11}x^5 + 8e^{-10}x^4 + e^{-7}x^3 - e^{-5}x^2 + -3e^{-7}x + 0.4207 \quad \textbf{(6.2)}$$

where x is the transmission angle in degrees and y is the amplitude at the receiver. It can be observed that this polynomial equation closely fits the experimental data, with a maximum error of 0.010 V between any point on the experimental trend line and the experimental data. Based on the 0° transmission value of 0.421 V, 0.01 V represents an error of 2.4%. Using this equation it is possible for the model to predict the received amplitude at points in between discrete data values for a vertical reception angle of 0°. For each of the data profiles obtained an equation is used to approximate the experimental data.

6.4.3 Single Transmitter Model Methodology

To determine the received signal strength for any given transmitter location within the vessel there is a requirement to determine the influence of the strength of the transmitted signal as a function of transmission angle, the sensitivity of the receiver as a function of reception angle and the attenuation of the signal as a function of range. Through combining these three profiles it is possible to calculate the anticipated received signal strength.

The model allows the user to define a 3D receiver position along with the vertical mounting angle of the receiver against the vessel wall. The user can then define both the transmitter vertical and horizontal rotation angles. The model then sequentially moves the transmitter location within the vessel in increments of 5 cm in the x and y component for a user specified z component and calculates the anticipated signal strength at the receiver for each of the transmitter locations.

Through knowledge of both the transmitter and receiver coordinates in 3D the model is able to use trigonometry to calculate the range between the transmitter and receiver. It is also possible from this information to calculate the vertical and horizontal reception angle for the signal impacting the receiver along with the horizontal and vertical transmission angle from the transmitter.

The receiver vertical reception angle is then adjusted to account for the mounting angle of the receiver on the vessel wall. Through knowledge of the vertical transmitter mounting angle (user specified parameter) the vertical transmission angle can also be adjusted.

The model firstly calculates the anticipated received signal strength solely as a function of range. It does not consider the horizontal or vertical transmission or reception angles. The anticipated received signal strength is calculated using an approximation of the attenuation as a function of range profile observed in Figure 6-12. The discrete profile in Figure 6-12 is approximated into a continuous function using a power equation which fits the data, an example of how the continuous function is generated from discrete data is shown in Figure 6-19. Using the known range value the equation returns the anticipated received signal strength due to the attenuation of the acoustic signal solely as a function of the range between the transmitter and receiver, this is known as ‘amplitude A’.

The ‘amplitude A’ value must then be modified to account for the horizontal and vertical reception angles. The ‘amplitude A’ value is first scaled to account for the vertical reception angle at the receiver. The received signal, for a 0° horizontal reception angle, has been demonstrated to alter with vertical reception angle as shown in Figure 6-13. The vertical receiver sensitivity is approximated using a polynomial equation from the discrete data in Figure 6-13. For a 0° vertical reception angle (0° horizontal reception angle) the received amplitude in Figure 6-13 is 0.42 V, however if the vertical reception angle is -20° then the received signal amplitude for the same 0° horizontal reception angle is 0.45 V. Therefore the model uses knowledge of the vertical reception angle to scale the ‘amplitude A’ value to account for the vertical receiver sensitivity. For this example with a vertical reception angle of -20° the ‘amplitude A’ value would be scaled by (0.45/0.42)*100% = 107%. The received signal strength now accounts for both the attenuation of the signal as a function of range and the vertical sensitivity of the receiver. The same process is undertaken for the transmitter vertical sensitivity profile using data from Figure 6-18 to create the polynomial equation. This produces a received signal strength which considers the attenuation of the signal as a function of range and both the vertical transmitter sensitivity and vertical receiver sensitivity, referred to as ‘amplitude B’.

The final adjustment to the calculated received signal strength is to account for the horizontal sensitivity of the transmitter and receiver. Based on the transmitter and receiver coordinates the horizontal transmission and reception angles can be calculated. From Figure 6-13 it can be observed that the horizontal sensitivity of the receiver changes as the vertical reception angle is altered. Each horizontal receiver sensitivity profile is approximated using a polynomial equation as

illustrated in Figure 6-19. The model first selects the correct horizontal receiver profile to use based on the vertical reception angle. The horizontal reception profile is then used to scale 'amplitude B' based on the horizontal reception angle. If we consider the same vertical reception angle of -20° then the profile used from Figure 6-13 is the yellow line. If the horizontal reception angle based on the transmitter's position within the vessel was 40° then it can be observed that looking at Figure 6-13 this value is 0.43 V in comparison to 0.45 V for a 0° horizontal reception angle. Therefore 'amplitude B' would be scaled by (0.43/0.45)*100% = 96%. Again the same process can be done for the horizontal transmission angle based on the transmission sensitivity profiles observed in Figure 6-18.

The calculated received amplitude from the model now accounts for the attenuation of the signal as a function of range through the underwater medium, considers the change in received signal strength due the horizontal and vertical receiver sensitivity and also considers the impact that the horizontal and vertical transmission sensitivity of the transmitter have on the received signal strength. The equations used to calculate the received signal strength are all approximated from the profile of the transducer obtained through experiments. Therefore if either the transmitter or receiver is changed the profile for the changed transducer can be obtained and the model updated.

6.4.4 Transmitter Layout Testing

To investigate the received signal strength from the pill the location of the receivers must first be selected. From work conducted in [Chapter 5.0, section 5.2] it has been observed that the localisation error when using TDOA is minimised for the vessel extremities layout. For the 250 litre vessel this is a vertical separation of 1 m and a horizontal separation of 0.6 m. Two receivers are mounted at the top of the vessel (upper receiver) with two at the bottom (lower receiver) offset by 90° as shown in Figure 6-21.

From the work completed in [Chapter 4.0, section 4.2] on modelling transmitter layouts from a TDOA perspective, initially a pill layout with 4 transmitters around the centre of the pill was considered with transmitter separation of 90°. Based on the experimental results observed in [Chapter 5.0, section 5.3] with 45° and 90° transmitter separations and the horizontal transmission profile in Figure 6-16 it can be observed that with 90° transmitter separation on the pill good signal coverage levels can be maintained as the pill is rotated. For this reason this section initially considers 90° transmitter separation for transmitter layouts on the pill. An illustration of the initial 4 transmitter layout modelled is presented in Figure 6-20.

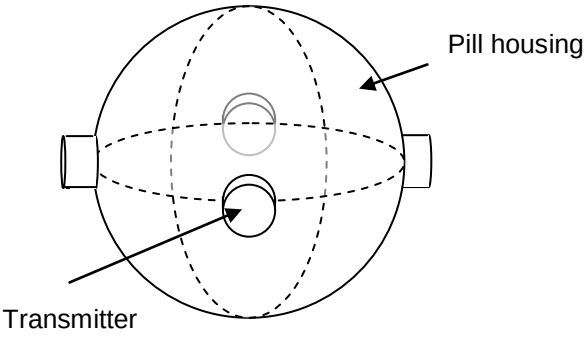

Figure 6-20: Pill layout with 4 transmitters

The use of multiple transmitters on the pill is intended to maintain signal coverage throughout the vessel as the location of the pill alters. To determine the performance of the transmitter layout the pill is modelled in what is anticipated to be the "worst case" location in relation to the received signal strength. From the work completed in sections 6.3.4 and 6.4.1 it has been shown that as the vertical transmission and reception angles are increased the received signal strength decreases. Therefore for the lower receivers it is anticipated that the worst location for the pill to be situated is at the top of the vessel and for the upper receivers the worst location for the pill is at the bottom of the vessel. As the received signal at the upper receivers when the pill is at the bottom of the vessel will be the same as the result at the lower receivers when the pill is at the top of the vessel only one situation is modelled. The received signal strength is modelled for when the pill is at the top of the vessel. The signal strength modelled is the strength of the first arrival (direct path) and does not consider reflections. This is illustrated in Figure 6-21. As the pill is modelled in the "worst case" scenario location for a receiver at the top and bottom of the vessel the transmitter layout on the pill is model using the single transmitter model detailed in section 6.4.3. Based on the transmitter layout the location of each transmitter is calculated and the single transmitter model used to calculate the signal at each receiver.

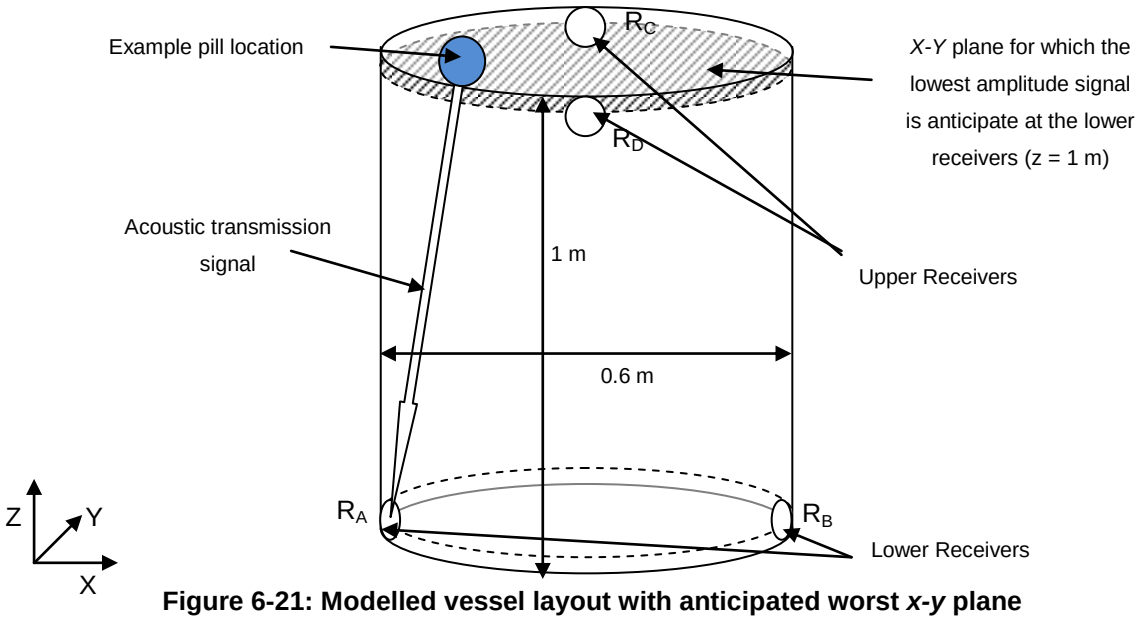

Figure 6-21: Modelled vessel layout with anticipated worst *x-y* plane

Figure 6-21 shows the location of receivers within the vessel and illustrates the *x-y* plane which it is anticipated will result in the lowest signal strength at the lower receivers. For pill locations on this plane the range between the lower receivers and pill is maximised and also the transmission and reception angles are maximised. This should result in the lowest received signal strength.

The *z* co-ordinate of the pill is referenced from the bottom of the vessel, *z* = 0 m, with the top of the vessel being a plane at *z* = 1 m. For a given *z* co-ordinate the pill is modelled at 5 cm intervals in the *x* and *y* coordinates. For each plane the received signal strength is displayed for one upper and one lower receiver.

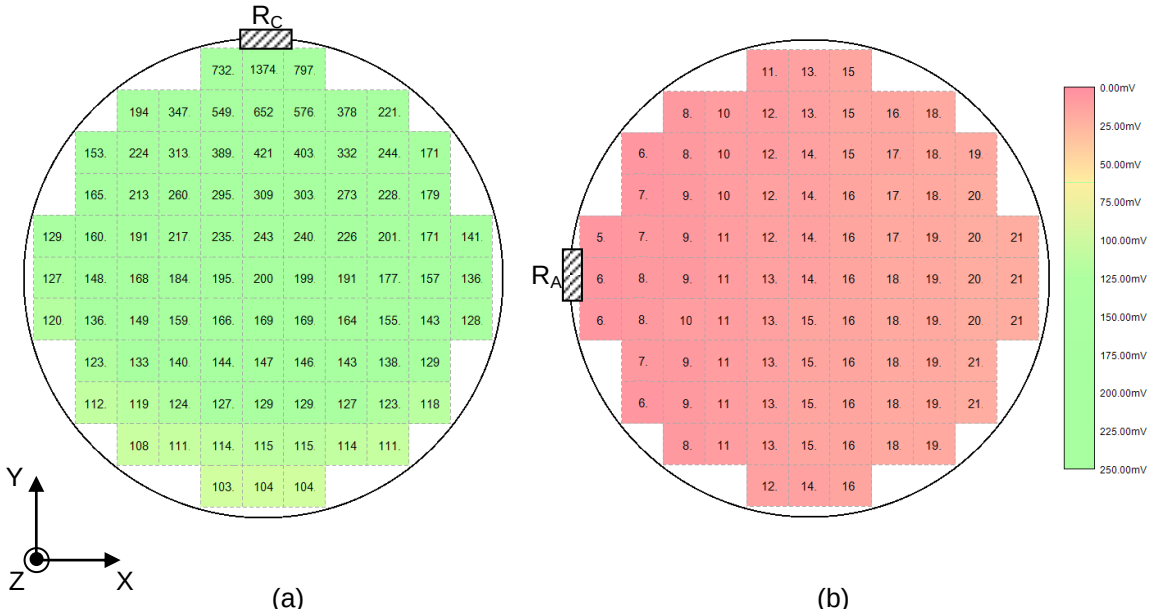

Figure 6-22: (a) Predicted signal strength at upper receiver, R_C, 4 transmitter pill (b) Predicted signal strength at lower receiver, R_A, 4 transmitter pill

Figure 6-22 (a) shows the anticipated received signal strength in millivolts at the upper receiver R_C when the centre of the pill is located on the *z* = 1 m plane. The value in each square represents the anticipated signal at the receiver if the pill were located in that square. Figure 6-22 (b) shows the anticipated received signal strength in millivolts at the lower receiver R_A when the pill is located on the *z* = 1 m plane. The received signal strength is determined from the transmitter which is closest to the receiver, as this will be the shortest TOF and therefore the first signal to arrive at the receiver. The figures are colour coded to illustrate locations from which good signal strength can be anticipated and also those which have low received signal strength.

In Figure 6-22 (a) it can be observed that for all of the simulated pill locations on the *z* = 1 m plane the received signal at R_C is large. The average value across the results is 223 mV with a minimum received signal of 103 mV. As the upper receivers are on the same z plane as the transmitters then the vertical transmission angle from the pill and the vertical reception angle are both 0°. From tests of the Senscomp 40KT08 profile the transducer produces good signal strength at these angles.

In Figure 6-22 (b) it can be observed that for certain pill locations the received signal at R_A is very weak. The average received signal across the vessel for this plane is 14 mV with a minimum signal of 5 mV. Due to the location of the pill the transmission angle of the signal and reception angle of the signal at the receivers are both high. As the Senscomp 40KT08 transducer transmission profile and reception sensitivity roll off with increasing amplitude the received signal strength decreases. The signal strength is observed to increase as the pill is moved further from the receiver R_A in the *x* direction as this reduces the vertical transmission and reception angle between the pill and receiver.

As the receivers are located at two different heights within the vessel to allow the location of the pill to be calculated through TDOA or TOF measurements, when the pill is located at the top of the vessel, the lower receivers have poor signal strength. Similarly, when the pill is located at the bottom of the vessel, the upper receivers will have poor signal strength.

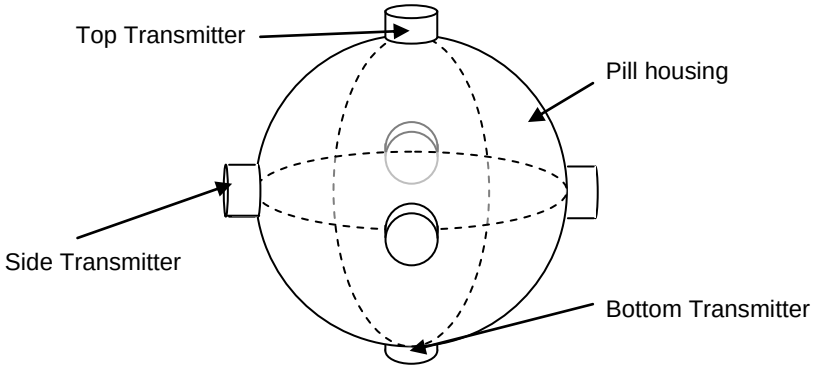

Figure 6-23: Pill layout with 6 transmitters

Figure 6-23 illustrates a pill layout with 6 transmitters to increase the signal strength at receivers. Through mounting a transmitter to the bottom of the pill then the transmission angle at which the signal is emitted from the pill can be reduced. With this layout the signal at the lower receivers should be increased as the signal leaving the pill is transmitted from a smaller transmission angle. The results for modelling this transmitter layout are observed in Figure 6-24.

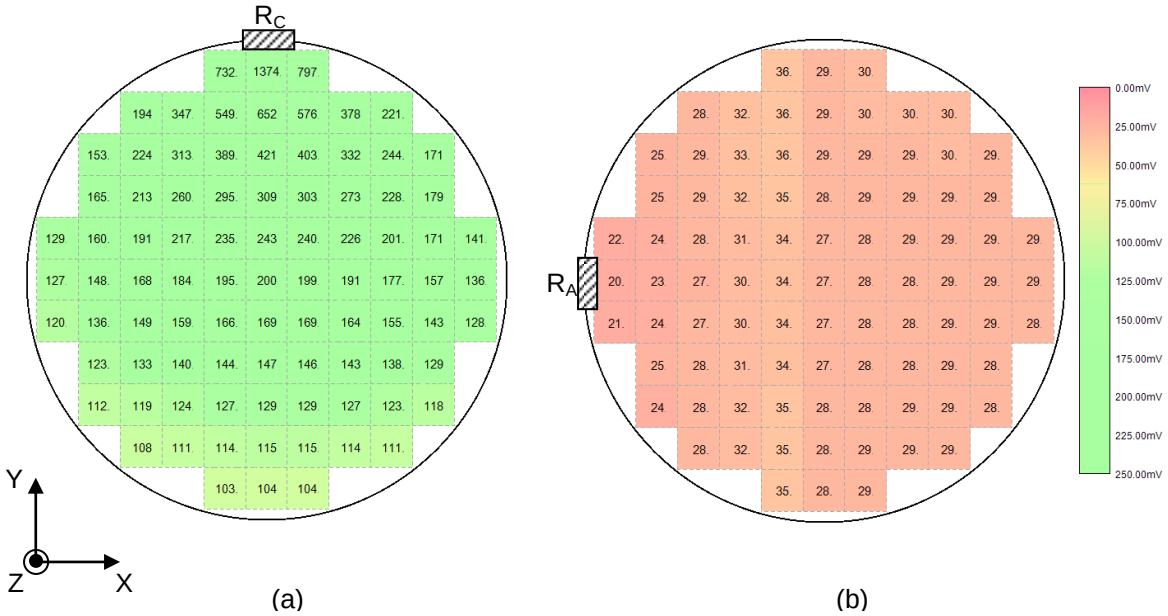

Figure 6-24: (a) Predicted signal strength at upper receiver, R_C, 6 transmitter pill (b) Predicted signal strength at lower receiver, R_A, 6 transmitter pill

Figure 6-24 (a) shows the predicted signal strength at the upper receiver using a 6 transmitter layout on the pill. The pill is located on the plane z = 1 m. Figure 6-24 (b) shows the predicted signal strength at the lower receiver using a 6 transmitter layout on the pill. The pill is located on the plane z = 1 m.

It can be observed in Figure 6-24 (a) that the inclusion of transmitters on the top and bottom of the pill has not altered the received signal at the upper receiver R_C. Due to the pill's location the signal reaching the receiver is still transmitted from the side transmitter and the top or bottom transmitter do not influence the received signal strength. The average across the plane is still 223 mV with a minimum signal of 103 mV.

In Figure 6-24 (b) it can be observed that that the inclusion of the bottom transmitter has made some improvements to the received signal strength at the lower receiver R_A. The average received signal strength for the lower receiver across the tested pill locations is now 29 mV and the minimum received signal is now 20 mV. While the signal strength has improved for all of the tested locations the largest improvement is for locations close to the receiver in the x direction. In these locations the use of a bottom transmitter means that while the reception angle is still large at the receiver the transmission angle is significantly reduced.

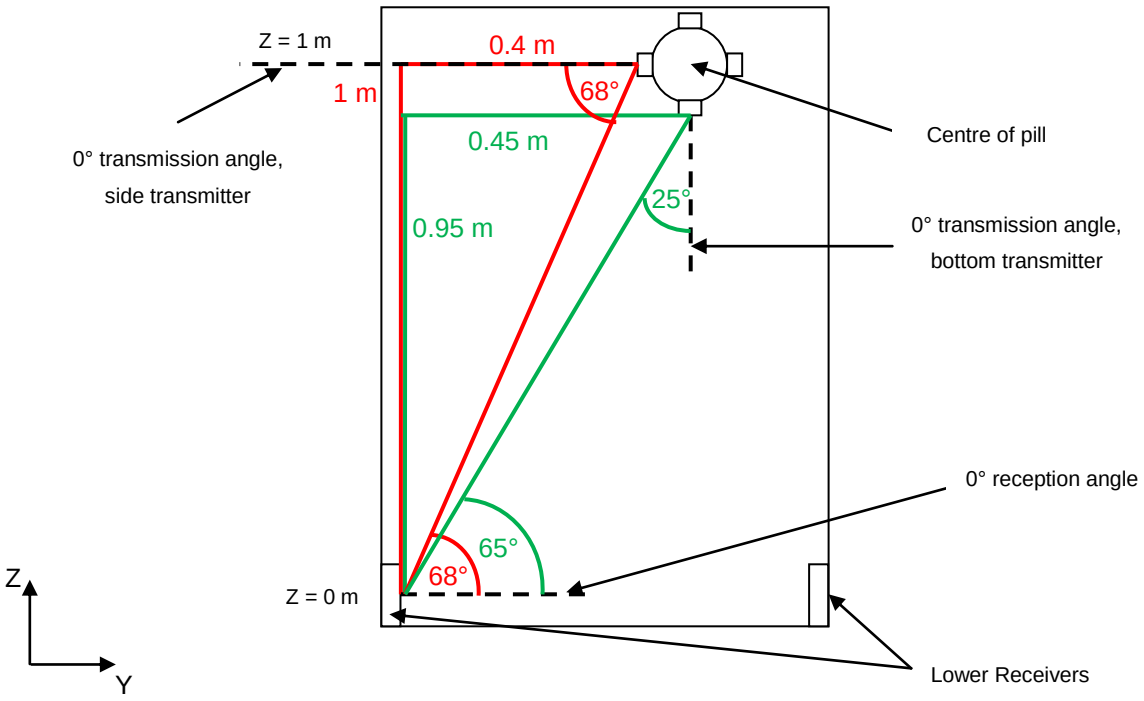

Figure 6-25: Improvement in received amplitude due to bottom mounted transmitter

Figure 6-25 illustrates the improvement in reception and transmission angle for an example pill location due to the addition of a transmitter mounted to the bottom of the pill for a 0.1 m diameter pill. For a centre of pill location which is 1 m above the lower receiver and 0.45 m from the receiver in the *y* coordinate it can be observed that from the side mounted transmitter the transmission and reception angles are both 68°.

By mounting a transmitter to the bottom of the pill the orientation of the transmitter means that the transmission angle is 25°. Therefore, the signal transmitted from the pill is stronger. The diameter of the pill means the bottom transmitter is also 0.05 m further away from the receiver than the side mounted transmitted in the *y* coordinate, which provides a small improvement to the receiver reception angle from 68° to 65°.

Through mounting transmitters to the top and bottom of the pill the transmission angle from the pill has been improved which has increased the signal strength from the pill and therefore increased the received signal strength at the lower receivers. To further improve the signal strength at the receiver the reception angle needs to be altered. Significant improvements in the reception angle for this *z* plane cannot be achieved by adjusting the transmitter locations on the pill.

One option to improve the reception angle at the receivers is to reduce the vertical separation between the upper and lower receivers. When the pill is then located at the top or the bottom of the vessel the reception angle the signal impacts the receiver at will be reduced. This idea is illustrated in Figure 6-26.

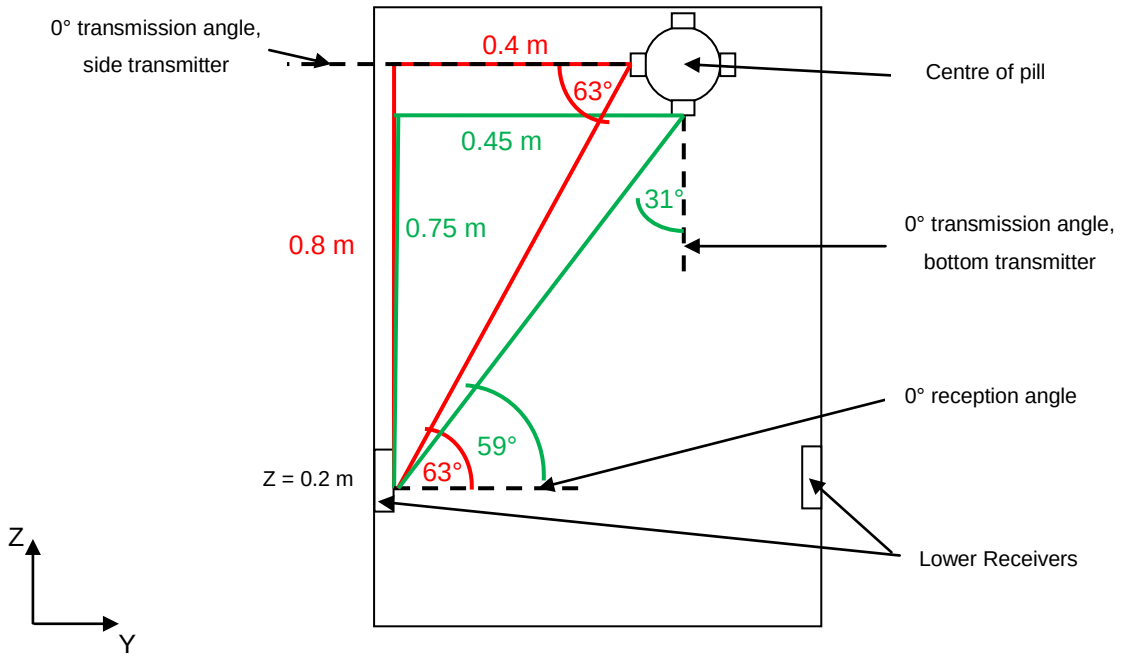

Figure 6-26: Reduction in receiver vertical impact angle by reducing receiver separation

Figure 6-26 illustrates the situation where the lower receivers are moved to *z* = 0.2 m and the upper receivers moved to 0.8 m, which is the layout utilised in Burnett-Thompson A. (2007). For a centre of pill location which is *z* = 1 m and 0.45 m from the receiver in the *y* coordinate it can be observed that from the side mounted transmitter the vertical transmission and vertical reception angles are now 63° in comparison to 68° for the receiver locations in Figure 6-25. For the bottom mounted transmitter the transmission angle has become 31° from 25° and the reception angle has improved from 65° to 59°.

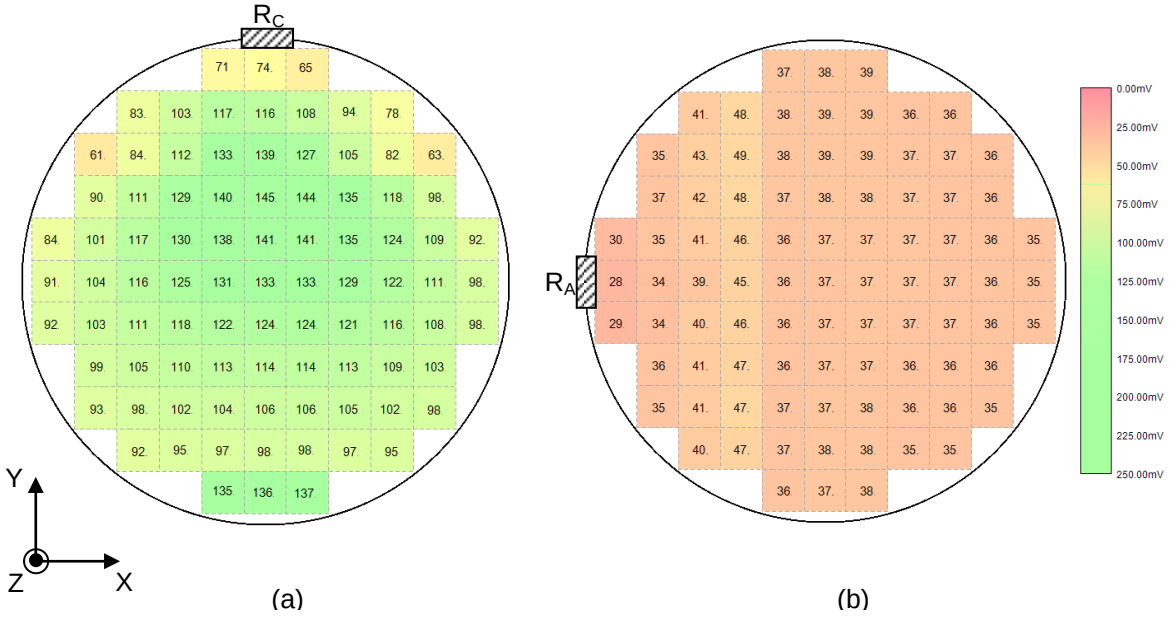

(a) (b)

Figure 6-27: (a) Predicted signal strength at upper receiver, z = 0.8m R_C, 6 transmitter pill (b) Predicted signal strength at lower receiver, z = 0.2 m R_A, 6 transmitter pill

Figure 6-27 (a) shows the predicted signal strength at the upper receiver using a 6 transmitter layout on the pill. The pill is located on the *z* plane *z* = 1 m. Figure 6-27 (b) shows the predicted signal strength at the lower receiver using a 6 transmitter layout on the pill. The pill is located on the *z* plane *z* = 1 m.

It can be observed in Figure 6-27 (a) that moving the upper receiver location has significantly reduced the received signal strength observed. The average received signal strength at the upper receiver is now 109 mV with a minimum value of 61 mV. By mounting the upper receiver at *z* = 0.8 m there is now a vertical transmission and vertical reception angle between the transmitter and receiver which has reduced the signal strength. The received signal is still however above 100 mV for the majority of locations.

In Figure 6-27 (b) it can be observed that moving the lower receiver to *z* = 0.2 m has improved the received signal detected when the pill is at the top of the vessel. The average received amplitude at receiver R_A is now 38 mV with a minimum signal of 28 mV. Moving the lower receiver to *z* = 0.2 m means that the range between the pill and receiver, and the vertical reception angle at the receiver are both reduced which helps to improve the received signal strength.

The largest reduction in vertical reception angle can be achieved by mounting both the upper and lower receivers in the vessel at *z* = 0.5 m. With this mounting location when the pill is at the top or bottom of the vessel the vertical separation between the pill and the receivers is only 0.5 m which reduces the range and the reception angle. However, through the work undertaken in [Chapter 4.0, section 4.4] it has been observed that with a small separation in *z* component between the upper and lower receivers there is a large impact on the localisation error using TDOA. Therefore, to mount the receivers at *z* = 0.5 m would have a significant effect on the localisation accuracy and is not an effective solution for this work.

As the vertical reception angle at the receivers is a crucial factor limiting the received signal strength, to produce an efficient transmitter layout for the pill the transmitter layout must be considered in conjunction with the receiver layout, such that it minimises both the vertical transmission and reception angles. One potential option to improve the vertical reception angle is to alter the mounting angle of the receivers. From the Senscomp reception profile, Figure 6-13, it is observed that the received amplitude is reduced as the vertical reception angle increases. Therefore, to increase the received amplitude the receivers need to be mounted to reduce this vertical reception angle.

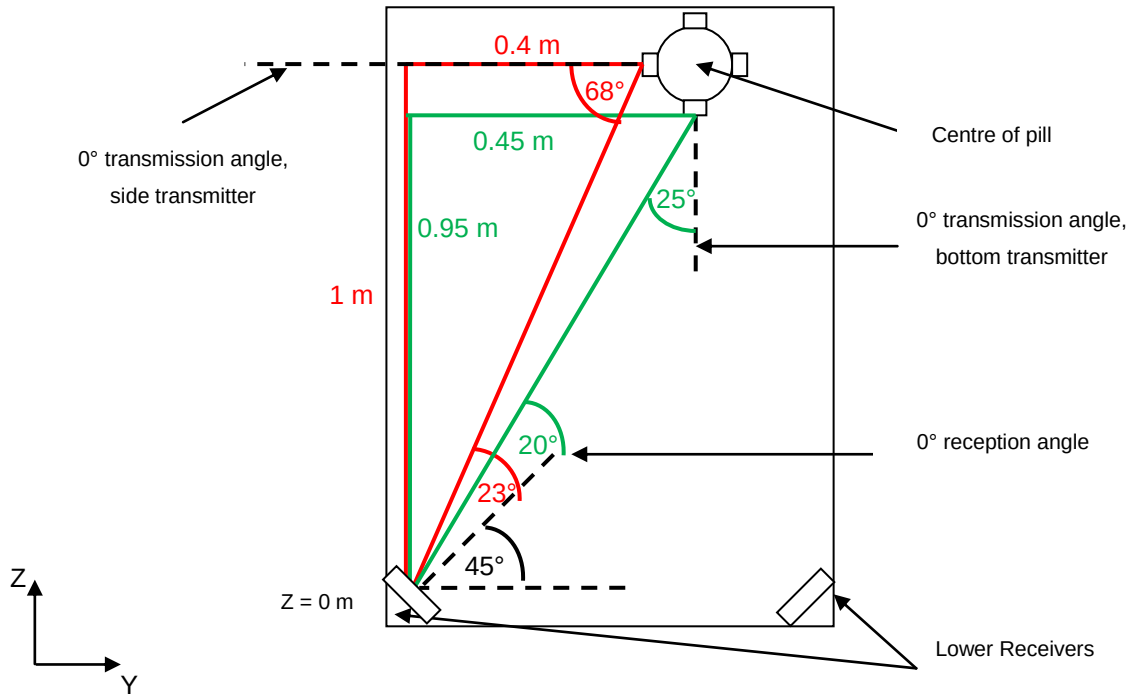

Figure 6-28: Rotation of receiver to improve reception angle

Figure 6-28 displays a method to improve the vertical reception angle at the receivers to increase the received signal strength. By rotating the receivers 45° it is possible to reduce the vertical reception angle. In comparison to the results in Figure 6-25 the vertical reception angle for the signal originating at the side transmitter has been improved from 68° to 23° and the vertical reception angle from the bottom transmitter has been improved from 65° to 20°.

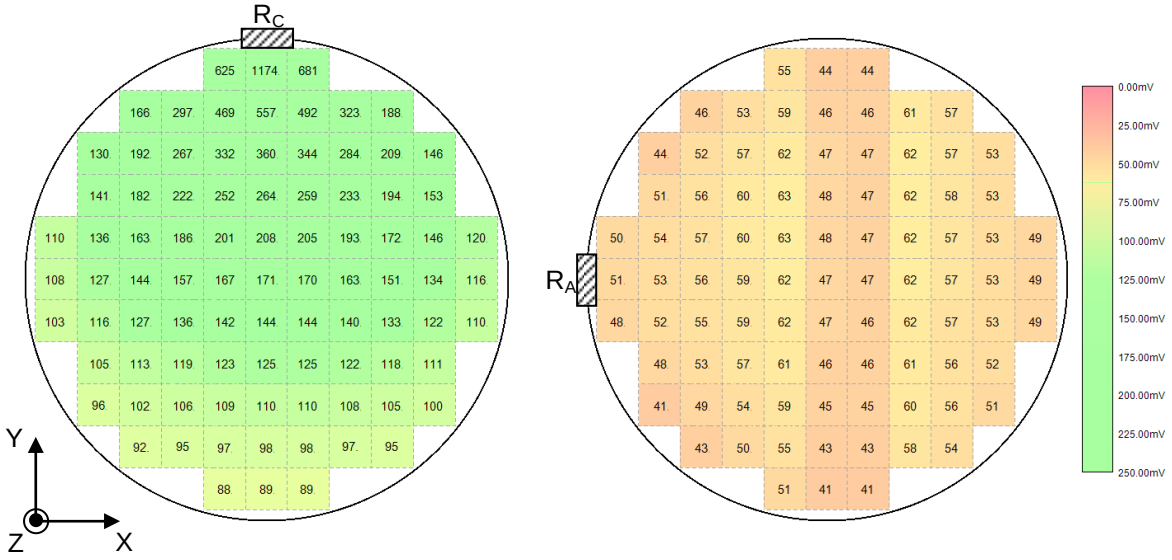

(a) (b)

Figure 6-29: (a) Predicted signal strength at upper receiver, R_C, 6 transmitter pill, 45° receiver (b) Predicted signal strength at lower receiver, R_A, 6 transmitter pill, 45° receiver

Figure 6-29 (a) shows the received signal strength at the upper receiver R_C (0.300, 0.300, 1.000) m while Figure 6-29 (b) shows the received signal strength at the lower R_A (0.000, 0.000, 0.000) m. At

the upper receiver the average received signal is 190 mV with a minimum value of 88 mV, this compares to an average of 223 mV and a minimum of 103 mV when the upper receiver was not rotated, Figure 6-24 (a). While the vertical reception angle at the upper receiver has been increased from 0° to 45° due to the receiver rotation the relatively flat profile of the receiver, Figure 6-13 means that the reduction in received amplitude is minimal and good signal strength can still be observed for all the tested pill locations.

At the lower receiver, Figure 6-29 (b) shows that the average received signal is 53 mV with a minimum value of 41 mV, this is in comparison to an average of 29 mV and a minimum value of 20 mV when the receiver is not rotated, Figure 6-24 (b). Through rotating the receiver results suggest that the received signal strength at the lower receiver can be increased. For the anticipated “worst case” pill locations this increase in amplitude is important for detecting the signal above background noise levels.

As one of the target applications for this project is a generic mixing vessel it is desired that any transmitter/receiver layout should be selected such that it provides consistent coverage throughout the vessel and does not produce bias to one section of the vessel. For this reason a vertical receiver angle of 45° is suitable as it ensures that the maximum vertical reception angle from the pill is 45° regardless of its location in the vessel, provided the receivers are mounted at the vessel extremities. If a rotation angle of greater than 45° was used then while the vertical reception angle for a pill located at the side of the vessel would be small when the pill was located at the top or bottom of the vessel the reception angle would again be large.

One limitation of rotating the receivers is that they must be located at the extremities of the area in which the pill is to be localised. If for example the pill was moved below the lower receivers, then due to the receiver’s rotation angle it would detect minimal signal as again the reception angle would be large, Figure 6-28. This restriction of receiver location is acceptable as from the work conducted in [Chapter 4.0, section 4.4] it has been observed that for TDOA localisation a receiver layout at the extremities of the vessel reduces the localisation error in the presence of noise.

While the rotation of the receivers means that within the vessel the maximum vertical reception angle is 45°, depending on which transmitter the signal originates from the vertical transmission angle can vary significantly. It can be seen in Figure 6-28 that for the lower receiver the side transmitter has a transmission angle of 68° while the bottom transmitter has a transmission angle of only 25°. Depending on which transmitter is closer to the receiver and therefore has the shortest TOF the signal strength impacting the receiver could change significantly.

To reduce this variation in transmission angle one option available is to rotate the transmitters on the pill such that they match the receivers. If the transmitters are rotated to 45° then the maximum vertical transmission angle from the pill is 45° regardless of its location within the vessel. This is illustrated in Figure 6-30.

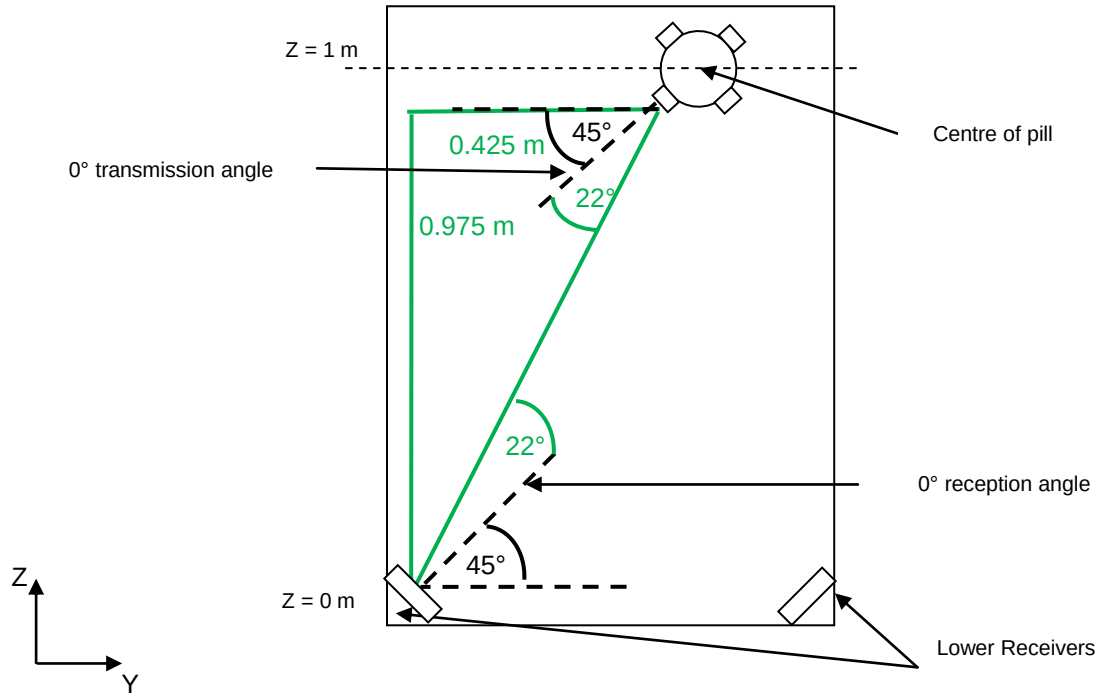

Figure 6-30: Rotation of transmitter to improve transmission angle

Figure 6-30 shows the vertical rotation of the transmitters on the pill to 45°. Through rotating the transmitters the transmission angle from the pill to the receiver has been reduced to 22° while the reception angle at the receiver is also 22°. This rotation of transmitters means that even when the pill is against a vessel wall the maximum transmission angle is 45°. The rotation of the transmitters does however mean that the number of transmitters on the pill must be increased to maintain signal coverage as the pill rotates. With a horizontal spacing of transmitters on the pill of 90°, to maintain this horizontal separation 8 transmitters are required.

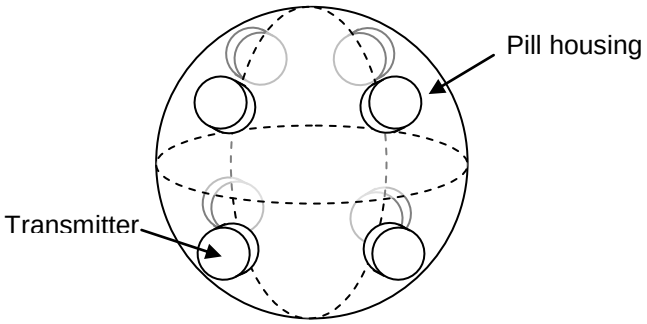

Figure 6-31: Pill layout with 8 transmitters

Figure 6-31 illustrates the pill layout with 8 transmitters, with the transmitters rotated at 45°. Through the use of 8 transmitters signal coverage at the upper and lower receivers can be maintained while the pill rotates. The maximum horizontal transmission angle is maintained at 45° with this transmitter layout.

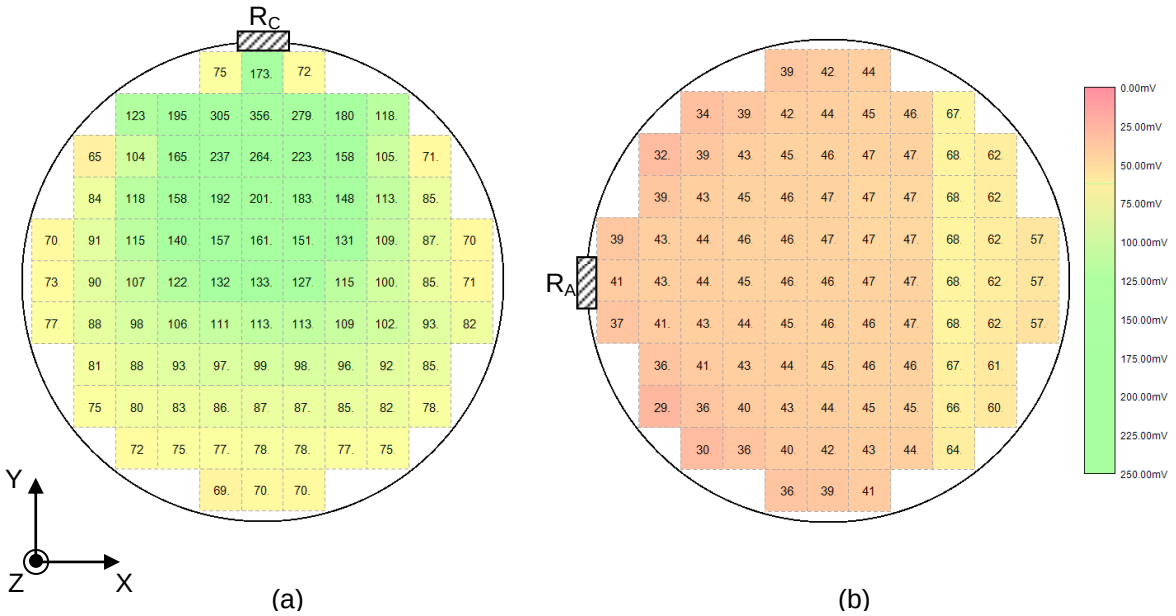

Figure 6-32: (a) Predicted signal strength at upper receiver, R_C, 8 transmitter pill (b) Predicted signal strength at lower receiver, R_A, 8 transmitter pill

Figure 6-32 (a) displays the received signal strength at the upper receiver, R_C while Figure 6-32 (b) shows the anticipated received signal strength for the lower receiver, R_A using a pill with 8 transmitters. At the upper receiver the average received signal strength is 117 mV with a minimum value of 65 mV observed. At the lower receiver the average received signal strength is 47 mV with a minimum of 29 mV. The result shows that through rotation of the transmitters the average and minimum received signal strength at both the upper and lower receiver has become worse in comparison to a 6 transmitter pill layout with only the receivers rotated, Figure 6-29 (a) and (b).

At the upper receiver the reception angle and transmission angle are both 45° for the 8 transmitter pill layout whereas for the 6 transmitter pill the reception angle is 45° but the transmission angle is 0° from the side transmitter which means the received signal strength is larger. At the lower receiver the 8 transmitter pill shows increased signal strength on the right hand side of the vessel, Figure 6-32 (b) as at this point the reception and transmission angles are small. In comparison the 6 transmitter layout, Figure 6-29 (b) shows a reasonably even distribution of received signal strength; on the left hand side of the vessel the bottom mounted transmitter means the transmission angle is small while on the right hand side of the vessel the reception angle is small which increases signal strength.

While the 6 transmitter pill layout with rotated receivers has demonstrated the largest average received amplitude at the lower receivers for the anticipated “worst case” pill location the transmitter arrangement does create a challenge for localisation. The offset of the side and bottom transmitter in relation to each other means that the first signal detected at any receiver is highly dependent upon the location of the pill in the vessel. For certain pill locations the side transmitter will be closest to the receiver while for other locations the bottom transmitter will be closest to the receiver. This means that the transmitter offsets required will change solely due to movement of the

pill within the vessel, not just rotation of the pill. As the origin of the signal is unknown then it is envisaged that this change in transmitter origin will produce localisation errors.

In comparison, for the 8 transmitter pill layout signal detected at the lower receivers will always originate from the lower transmitters and signal detected at the upper receivers will always originate form the upper transmitters. The required offset in z component is therefore known which should allow better localisation accuracy. For this reason while the 6 transmitter layout has been shown to produce the largest received amplitude for a pill in the “worst case” location the selection of transmitter layout on the pill is a compromise between received signal strength and overall localisation accuracy. For this reason the 8 transmitter pill layout and receivers rotated at 45° has been selected for implementation.

6.4.5 Summary of Transmitter Array Modelling

This section has investigated the influence that different transmitter layouts on the pill have on the signal strength detected at the receivers. This has been undertaken to allow a comparison between different transmitter layouts on the pill to be made and select a suitable option for testing the localisation accuracy of the system. Based on the experimental data obtained in section 6.3 a model has been constructed to calculate the received signal strength anticipated at the receiver for a given pill location within the vessel. This is important to allow the design of a transmitter layout which maximises signal strength at the receiver to negate against potential false triggers due to noise.

In section 6.4.1 the transmission profile for the Senscomp 40KT08 is investigated. The results observed show that the transmission and reception profile of the transducers to be largely similar, with a flat region centred on 0° and then with roll off from approximately ± 60°. From a transmission perspective the flat amplitude region appears larger than when the unit is used as a receiver.

Section 6.4.2 describes how continuous profiles have been created from the discrete data obtained for the receiver, transmitter and attenuation functions. Polynomial equations are used to create continuous functions which approximate the shape of the profiles and allow the model to calculate the anticipated values between the discrete data points observed in experimentation. It has been demonstrated that the polynomial equations used fit the experimental data within 0.01 V of actual values.

In section 6.4.3 the single transmitter model methodology is presented. This section details how the amplitude at the receiver is calculated as a function of range, transmission angle and reception angle. From an accurate model for a single transmitter it is possible to simulate different transmitter pill layouts and investigate the received amplitude at different receivers.

In section 6.4.4 work is undertaken simulating different transmitter layouts on the pill to determine the anticipated received signal strength at the receivers. Due to the large number of potential locations for the pill in the vessel, the worst case pill locations have been considered to determine the lowest anticipated received amplitude.

Based on the TDOA simulation work undertaken in [Chapter 4.0, section 4.2] initial simulations were undertaken with 4 transmitters on the pill at 90° separation. For a pill at the top of the vessel it can be observed that the lowest received signal strength is at the lower receivers and is approximately 5 mV. For this layout both the transmission and reception angle of the acoustic signal is large, where the sensitivity of the transducer is reduced resulting in a weak detected signal.

Through the addition of transmitters on the top and bottom of the pill improvements have been made to the received signal strength. Results demonstrate that with the additional transmitters the transmission angle has been significantly reduced, increasing the transmitted signal level. While the vertical offset of the additional transducers has also improved the reception angle, the large range between the transmitter and receiver means that the overall improvement on received signal strength is minimal.

Results have demonstrated that the limiting factor to improve the received signal strength is the reception angle of the signal, which cannot be influenced significantly by the transmitter layout on the pill. To reduce the reception angle consideration has been given to moving the receiver locations. While moving the receivers has again demonstrated marginal improvement in the received signal strength the movement of the receivers is limited based on the research in [Chapter 4.0, section 4.4]. With minimal vertical separation between the receivers small ranging errors cause significant TDOA localisation errors. Therefore the improvement in received signal level which is possible through only moving the receivers is limited.

Through modelling it has been demonstrated that the received signal strength can be maximised if the receivers are rotated to 45° and a 6 transmitter pill layout is used. While this layout shows the largest received signal strength the transmitter layout means that the origin of a signal can switch between the side and bottom transducer depending on the location of the pill in the vessel which may cause localisation errors. Therefore, a transmitter layout with 8 transmitters on the pill rotated at 45° has been selected for implementation. While the received signal strength is not as large as that observed for a 6 transmitter pill layout the origin of the signal is known (excluding pill rotation) which means that as a compromise between received signal strength and localisation accuracy it presents a suitable option for the project.

6.5 Summary of Pill Transmitter Array

To accurately localise the pill within the target vessel it is essential that the pill is able to transmit adequate signal which can be detected at the receivers for pill locations throughout the vessel. This chapter has investigated the reception profiles for different transducer options and from this constructed a model to allow various transmitter layouts on the pill to be simulated, observing the anticipated received signal strength.

Through the research conducted in [Chapter 5.0, section 5.2] and the problems associated with reflections the technique to detect the acoustic localisation signal has been altered. Based on this alteration section 6.1 defines how the requirements for the transmitter array on the pill have changed and the updated criteria which the transmitter array must now meet.

In section 6.2 the methodology for experimental research is presented. This section details the experimental set up including the test rig and positioning equipment for the pill, along with defining in more detail how the acoustic thresholding technique is implemented and how this overcomes reflection problems.

In section 6.3 experimental research has been conducted investigating the reception profiles of the two available transducer options. Results have demonstrated that due to the increased received amplitude and more consistent profile in relation to both horizontal and vertical reception angle, the Senscomp 40KT08 transducer is the preferred option for implementation.

Results have also demonstrated that while the repeatability of results is excellent between repeat tests, changes in the composition of the water have a significant impact on both the reception and attenuation profiles. For vessels where the liquid is flushed between processes this could be an important consideration.

In section 6.4 a model has been constructed to allow the modelling of anticipated signal strength at the receivers for different transmitter pill layouts. Through simulations it has been observed that the limiting factor in increasing the received signal strength in the vessel relates to the reception angle at the receiver. By implementing a transmitter/receiver layout with transducers rotated at 45° this offers the best compromise between received amplitude and localisation accuracy and is the preferred option for use within this thesis. Based on the simulations a transmitter pill layout with 8 transducers has been selected. In [Chapter 7.0] experimental results are conducted with this pill investing the localisation accuracy of both TDOA and TOF localisation techniques.

7.0 Pill Localisation

This chapter describes experiments to determine the localisation accuracy of the system for the 8 transmitter pill in the target environment. Two alternative localisation strategies are investigated; synchronisation between the pill and external hardware to allow TOF measurements to be obtained and localisation through TDOA measurements. The chapter discusses the experimental tests undertaken and compares the localisation accuracy of both techniques within the vessel.

In section 7.1 the experimental set-up for both localisation strategies is discussed. The architecture of the system is introduced along with the hardware and software implementation for both techniques. The modifications required to implement TDOA localisation are discussed and preliminary results are shown confirming the accuracy of TDOA measurements.

Section 7.2 introduces the localisation results utilising TOF measurements. Pill locations are considered across the vessel with tests undertaken on 3 separate *x-y* planes. Experiments considered the influence of pill rotation on the localisation error and results discuss the localisation error determined for each of the pill locations tested.

In section 7.3 localisation using TDOA measurements is considered. Test locations are maintained as those in section 7.2 and a comparison between the localisation accuracy of TDOA and TOF techniques is presented for a pill with distributed transmitters.

Finally section 7.4 investigates localisation using TDOA measurements but with the use off offset knowledge in the TDOA equations. Again test locations were the same as those in 7.4 and a comparison is presented between the localisation accuracy of TDOA with and without the use of offset knowledge.

7.1 System Implementation

7.1.1 System Architecture

The original system, inherited from Burnett-Thompson A. (2007), allows the localisation of a single transmitter in an underwater confined space using TOF localisation techniques. The system consists of a transmission card, which is used to generate the required waveform and a receiver card which is used to filter and amplify the signal received from the receivers. On board the host PC a 20 million samples per second (MSPS) Adept Scientic data acquisition card (DAQ) is used to acquire the received data. The system is controlled from custom software described in Burnett-Thompson A. (2007) which allows selection of the waveforms to be generated, and computes the location of the unknown transmitter. The architecture of the system is shown in Figure 7-1.

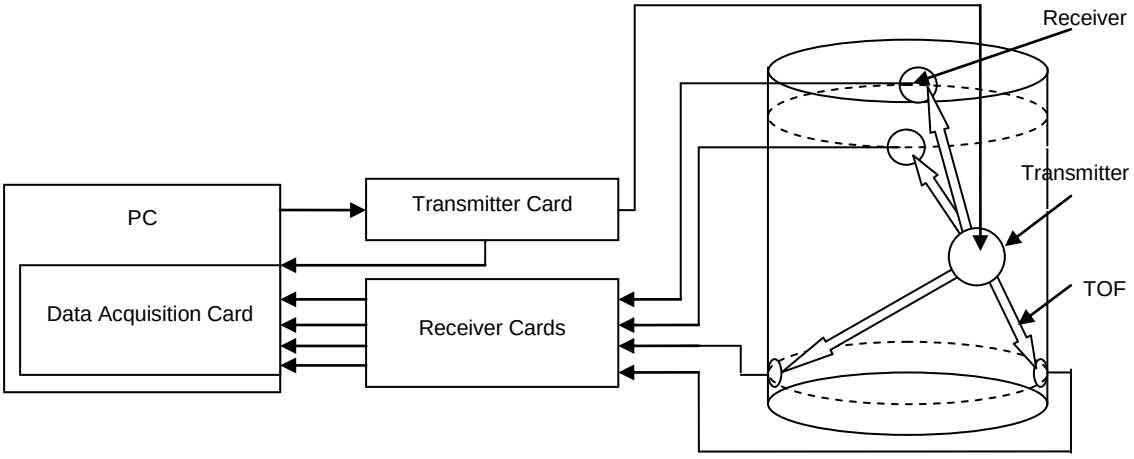

Figure 7-1: Localisation system architecture

The sequence of operation for the system is as follows. The transmission waveform is selected on the PC and this information is sent to the transmitter card. The transmitter card produces the desired waveform and instructs the DAQ card to begin timing. The transmitted waveform is then sent from the transmitter to the receivers whereby it is relayed to the receiver card. The receiver card filters and amplifies the signal from each channel and the 4 channels are fed to the DAQ card which records the signal waveform.

Software onboard the PC is used to process the information from the DAQ card allowing the range of the signal from each receiver to be calculated. The software then employs a least mean square algorithm to calculate the location of the pill.

7.1.2 TOF Implementation for Pill Localisation

To localise the pill from TOF measurements trilateration is used. At a single receiver one TOF value represents a sphere of uncertainty where it is possible the transmitter is located. This was illustrated in [Chapter 3.0, section 3.2]. To locate an unknown transmitter in 3D the intersection of 4 spheres is required. Therefore, there is the requirement for 4 receivers. Due to noise on the signals the 4 spheres representing the TOFs will not have a single point of intersection but a region of uncertainty where the pill could be located. The TOF localisation algorithm utilised in this thesis uses an iterative implementation of the least mean squared error, as utilised in Burnett-Thompson A. (2007)

This thesis is concerned with localisation in confined spaces of pills with dimensions that, inevitably, obscure the signal between individual transducers and receivers on the vessel wall. Future wireless implementation will be informed by the results but, for the present experiments, TOF localisation relies on wired signal generation and triggering of the DAQ. The pill consists of 8 transmitters which are driven from the external transmitter card and synchronisation is completed via triggering of the DAQ from the external transmitter card.

7.1.3 TDOA Implementation for Pill Localisation

The second localisation technique experimented with utilises TDOA. Unlike TOF which employs trilateration to locate an unknown transmitters TDOA utilises multilateration which does not require the synchronisation of the transmitter and receiver.

TDOA utilises knowledge of the difference in the time of arrival of a transmitted signal at multiple receivers. With these TDOA values it is possible to solve the non-linear equations as seen in [Chapter 3.0, section 3.2.1] which allows the location of the pill to be determined.

The system architecture for the TDOA experimental set-up is similar to that observed in Figure 7-1, however the transmitter and DAQ card are no longer synchronised such that the time of transmission is not known. This creates a challenge for detection of the acoustic signal. For the TOF implementation the DAQ card is triggered when the signal is transmitted from the pill. As the maximum potential range within the vessel is known, then the data buffer used onboard the DAQ can be configured such that it is large enough to store data corresponding to this maximum range.

However, for the TDOA implementation as there is no synchronisation the point in time at which the signal is transmitted from the pill is unknown. Therefore ideally, the data buffer must be an infinite length, as it is possible that the received signal could appear at any time. There is also the issue of triggering the DAQ card to start signal acquisition. Unlike for the TOF implementation, where the DAQ card is triggered via the transmitter card, for the TDOA implementation there is no external signal to trigger the DAQ card acquisition.

To overcome these problems a circular buffer and acoustic threshold are used onboard the DAQ. The use of a circular buffer means that the oldest data in the buffer is overwritten. An acoustic threshold is used on the DAQ to trigger data storage. When an acoustic localisation signal is received at the receiver which is above the threshold level the DAQ stores the received signal waveform in the buffer. The DAQ card has 4 input channels which allow information from each receiver to be stored. Upon the detection of an acoustic signal on the first channel the DAQ card begins to store data on that channel and also the other 3 channels. As the storage of data is synchronised between receiver channels then the difference in the time of arrival of the signals can be calculated.

Using an appropriate acoustic threshold for the target environment the software onboard the PC is able to scan through the data buffer for each received signal. At the index in the buffer that the received signal amplitude is above the threshold the index value is stored. Through knowledge of the sampling frequency of the DAQ card, and the difference in the index between receive buffers it is possible to calculate the TDOA between the receptions of signals at the receivers.

The DAQ card inherited from the original system (Burnett-Thompson A. 2007) can only be triggered from one receive channel. Depending on the pill location within the vessel any of the 4 receivers could be the first receiver to detect an acoustic localisation signal. If, for example, the DAQ card is triggered by an acoustic threshold on receiver R_1, but the pill is closer to R_2 then at the point in time which the localisation signal reaches receiver R_1 and the DAQ card begins to store data the information from the reception of signal at receiver R_2 will have been lost.

To overcome this problem the DAQ card implements a *pretriggering* methodology. With the *pretrigger* function the DAQ card uses a circular buffer to store information from before the triggering signal was detected. This principal is illustrated in Figure 7-2.

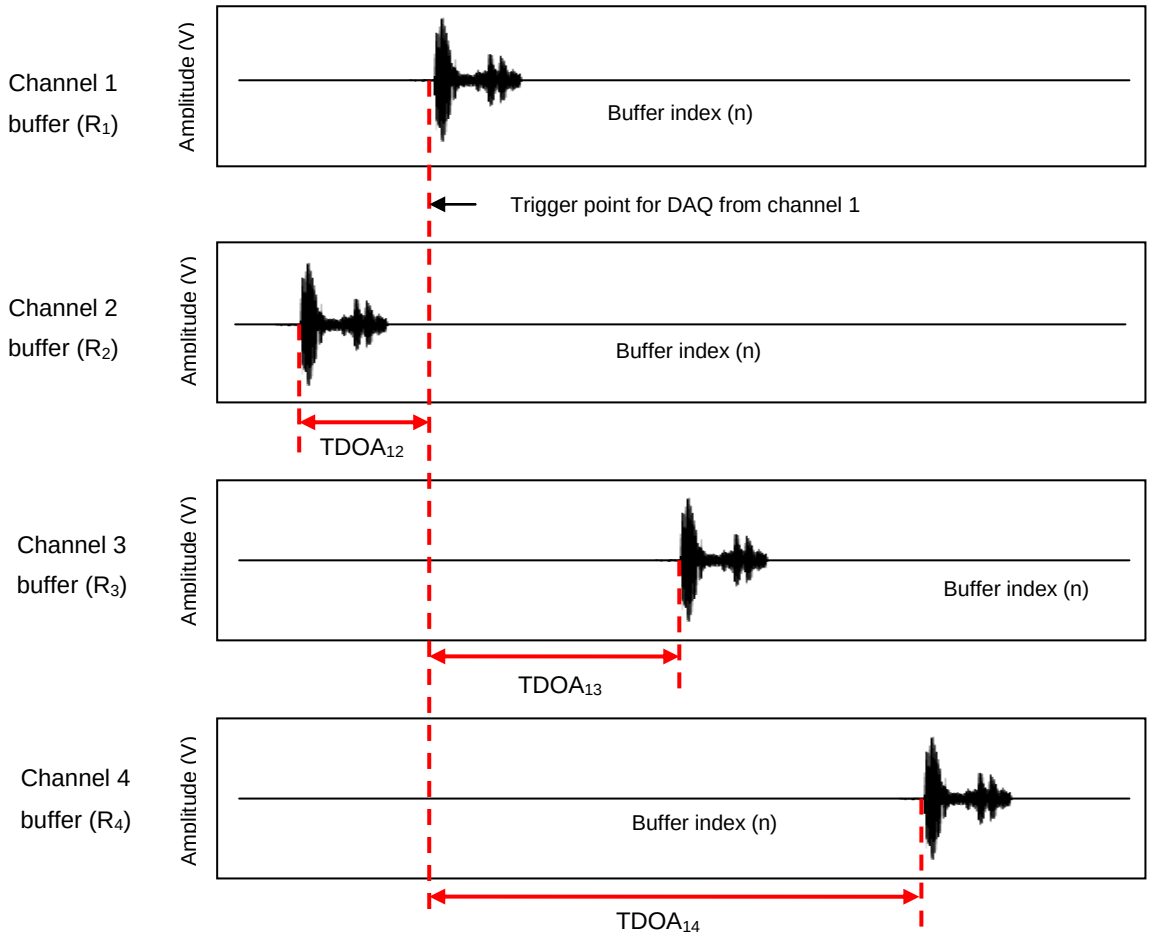

Figure 7-2: *Pretrigger* function of DAQ card

Figure 7-2 displays the reception of acoustic signals at all 4 receive channels at varying times. Data acquisition is triggered on the DAQ via the reception of an acoustic signal above the required threshold at receiver R_1. With the use of *pretriggering* and the circular buffer on the DAQ information before the trigger point of the DAQ is stored, this allows the TDOA between the receivers to be calculated. The receive buffers must be sized such that there is sufficient space both before and after the trigger point to store all of the data from the receivers. It can be observed that after the trigger point signal is received at R_3 and R_4. The system therefore needs to store data for a timeframe of 1.33 ms based on a maximum vessel range of 1 m and the requirement to be

able to store data for 1 m both before and after the trigger point, this is sufficient to allow the acoustic localisation signal to reach these receivers and be detected. The trigger point at receiver R_1 is considered the 0 index.

To determine the functionality of the TDOA implementation two receivers are initially considered. Senscomp 40KT08 transducers are used as the transmitter and receiver. The transmission signal is a pulsed sine wave of 10 cycles with a frequency of 40 kHz. The transmitter is located in the centre of the 250 litre test vessel using the *x-y* plotter, described in [Chapter 6.0, section 6.2.1] such that the transmitter is equidistant to each receiver. The DAQ card is triggered above a threshold level of 0.1 V which has been suggested from the work modelling the anticipated signal strength in [Chapter 6.0, section 6.4.4]. The sampling frequency for the DAQ is set at 400 kHz.

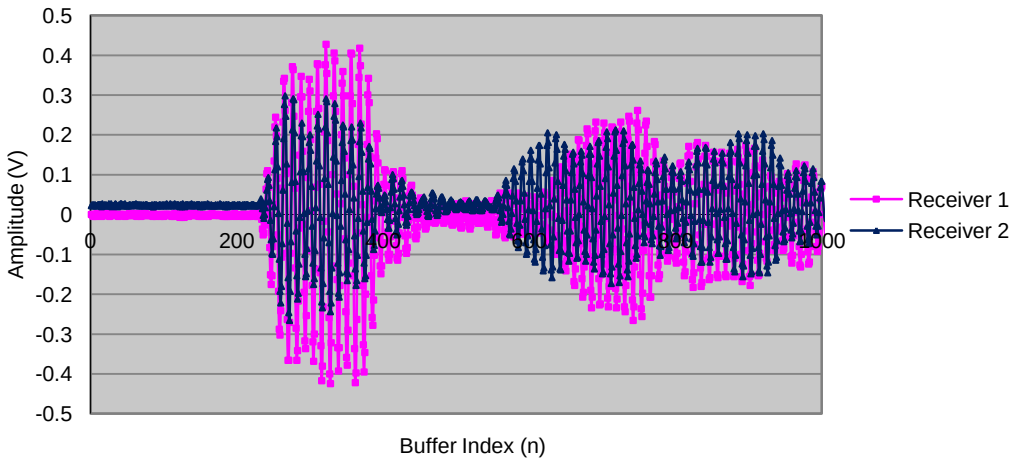

Figure 7-3: Reception of acoustic signal at 2 receivers, range difference 0 cm

Figure 7-3 shows the reception of the transmission signal at both receivers. Due to the equidistant nature of the receivers from the transmitter the result demonstrates that the signals are received with an index difference of 1 in the respective receive buffers which based on a sampling frequency of 400 kHz equates to a 2.5 µs time difference. This is highlighted in more detail in Figure 7-4.

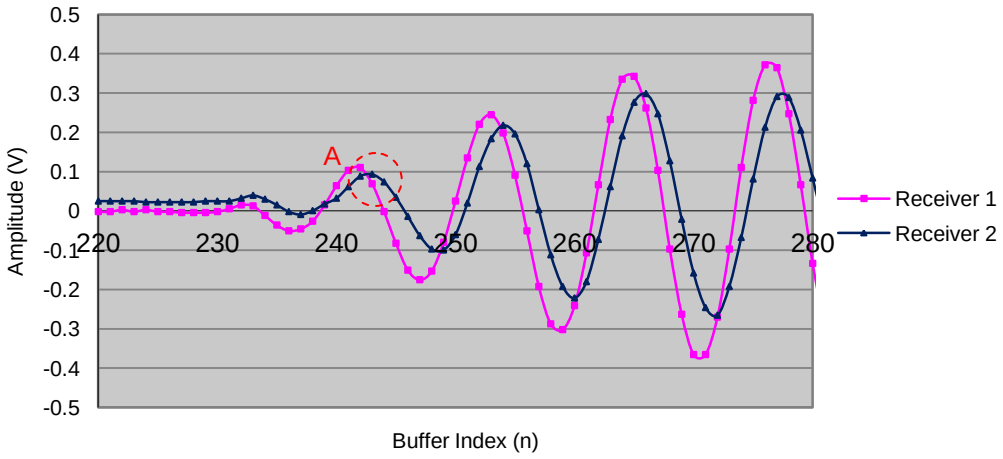

Figure 7-4: Zoomed plot of received signals at R_1 and R_2

Figure 7-4 shows a zoomed plot of the received signals at R_1 and R_2. It can be observed that the peak of the first arrival above noise for R_1 is located at "A". It has an index reference point of 242 in the buffer. The peak of the first signal above noise at R_2 also indicated by "A" is detected with an index reference of 243. Therefore, the TDOA between the arrival of the signals at the respective receivers is negligible, as would be anticipated when the transmitter is equidistant to both receivers.

To determine that a TDOA value can be accurately determined by the system the transmitter is positioned such that it is closer to R_1 than to R_2. In this instance the transmitter is positioned such that the range difference between the receivers should be 11 cm ± 0.5 cm. For this set up the transmission signal will impact receiver R_1 before receiver R_2. Therefore the DAQ card will trigger on R_1 and the signal will impact R_2 some time after this trigger. The system therefore needs to continue to store information in the buffer to allow this reception to be detected.

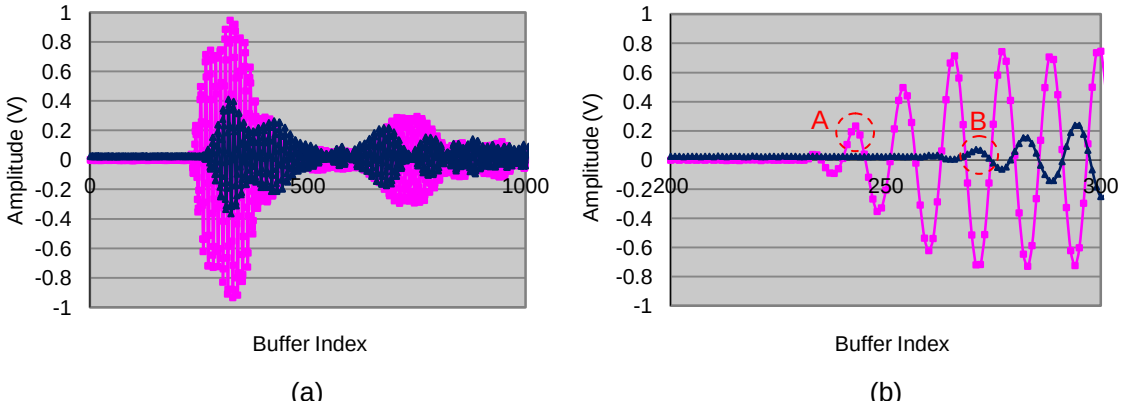

Figure 7-5: (a) TDOA value for reception at R_1 before R_2 (b) Zoomed plot of reception indexes

Figure 7-5 (a) shows the received waveforms at receivers 1 and 2 after filtering. The pink waveform is that received at receiver R_1 while the blue line is that received at R_2. Figure 7-5 (b) shows a zoomed plot focusing on the first peak above background noise. The transmission signal is detected first at R_1. The index point of the signal at the first peak above background noise is 243, "A". The signal arriving at R_2 is received at a later time and therefore the index point of the first peak above noise is 271, "B". As the receive buffers are synchronised in relation to each other then the shift in the arrival of these signals relates to the TDOA. The difference in indexes is 28 which, with a time segment of 2.5 µs for a single index, gives a TDOA of 70 µs. Using a speed of sound in water of 1480 ms^{-1} it can be determined that this equates to a range difference of 10.4 cm. This is a 0.6 cm error on the true range difference of 11 cm.

To demonstrate the operation of the pretrigger buffer the set up is modified such that the transmitter is positioned closer to R_2 than to R_1. The transmitter is positioned such that the observed range difference should be 9 cm ± 0.5 cm. In this case the signal should be detected at

R_2 first which equates to a range offset of -9 cm. In this instance the signal arrives at R_2 before the DAQ is triggered by the reception of a signal at R_1.

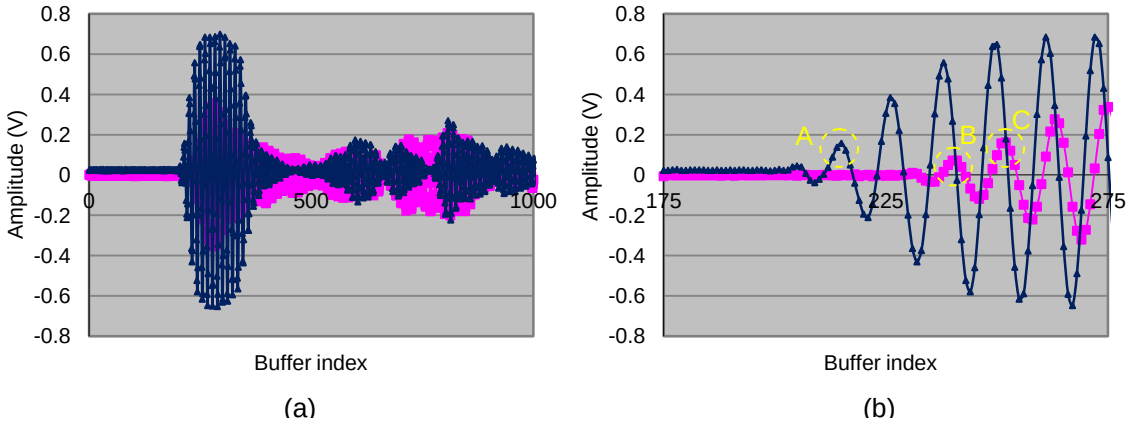

Figure 7-6: (a) TDOA value for reception at R_2 before R_1 (b) Zoomed plot of reception indexes

Figure 7-6 (a) shows the received waveforms at receivers 1 and 2 after filtering. The pink waveform is that received at receiver R_1 while the blue line is that received at R_2. Figure 7-6 (b) shows a zoomed plot of the index point at which the first signal reception is observed above background noise. Results demonstrate that in this instance the signal arrives at R_2 before R_1 showing the correct operation of the *pretrigger* functionality of the DAQ card and the correct retention of data before an event to trigger the system.

In Figure 7-6 (b) the transmission signal is detected first at R_2. The index point of the signal at the first peak above noise is 215, “A”. The signal at R_1 is received at a later time and therefore the index point at the peak of this signal is 240, “B”. As the receive buffers are synchronised to each other then the shift in the arrival of these signals relates to the TDOA. As the index point for receiver R_1 is considered to be the 0 index then any signal detected before this point is considered to have been detected at a negative index. The index shift is -25 which equates to a TDOA of -62.5 µs, equating to a range difference of -9.25 cm. This is a 0.25 cm error on the actual range difference of -9 cm which is within the error in positioning of the transducers.

From Figure 7-6 (b) it can be observed that the strength of the first peak above background noise can vary between the signals at receiver R_1 and R_2. If a 0.1 V threshold is used to select the index based on the results in Figure 7-6 (b) then while the first peak “A” is selected as the peak is above 0.1 V the peak at “B” would not be selected as the amplitude falls just below the 0.1 V threshold. Instead the peak selected for R_2 would be location C, which is index 251. This would mean the range difference is -13.3 cm, which is a 4.3 cm error on the actual range difference. To overcome this problem envelope detection is used such that the amplitude of each peak does not cause such a large change in the index point of the signals. Envelope detection rectifies the negative portion of the signal and then smoothes the signal such that the envelope of the signal amplitude is observed. This is shown in Figure 7-7.

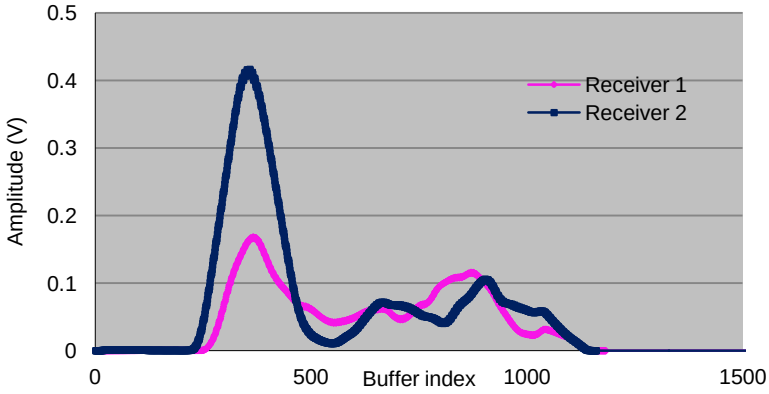

Figure 7-7: Operation of pretrigger buffer

Figure 7-7 shows the same received signal in Figure 7-6 (a) after envelope detection. Through the use of envelope detection the individual waveform peaks have been smoothed into a continuous amplitude function and the negative portion of the signal rectified. Therefore the large index shift between peaks of differing amplitudes as was observed in Figure 7-6 (b) between locations B and C has been removed. This allows a more reliable TDOA calculation.

7.1.4 Summary of System Implementation

This section has described the architecture of the localisation system together with the issues relating to implementation for both TOF and TDOA localisation. While the inherited system from Burnett-Thompson A. (2007) was configured for TOF localisation modifications have been made to implement TDOA localisation. Experimental results are illustrated to show the correct functionality of the TDOA implementation.

In section 7.1.1 the system architecture is described, with the functional operation of the localisation system detailed and an overview of the hardware presented. In section 7.1.2 the implementation of the TOF localisation is discussed, with the current status of the pill for TOF localisation detailed.

The practical implementation of TDOA is described in section 7.1.3. The limitations of the existing hardware are detailed and the modifications to the system to implement TDOA are explained. Preliminary results are presented demonstrating the correct operation of the system and the accurate detection of TDOA signals between two receivers. Results suggest that for a single TDOA the range difference can be obtained accurate to within approximately 1 cm of the actual range difference. These results provide a basis to implement 3D localisation using TDOA.

7.2 Localisation Utilising TOF Measurements

7.2.1 Test Configuration

To test the localisation accuracy of the system tests are conducted in the 250 litre vessel for localisation utilising both TOF and TDOA measurements. Testing within the vessel is considered

over only a section of the vessel to ensure that the received signal strength is adequate to allow detection of the pill. From the work in [Chapter 6.0, section 6.4] simulations have suggested that the dominant factor regarding received signal strength is the range between transmitter and receiver. Therefore, based on this information a section of the vessel is tested to ensure signal detection. Initial results consider localisation with vertical receiver separation of 0.4 m, approximately half the vessel area. To allow the location of the pill to be accurately tracked the *x-y* plotter is utilised to move the pill throughout the vessel. The pill is moved in 5 cm intervals ± 0.5 cm in the *x* and *y* direction for a given *z* value. For each location the true *x, y, z* position of the centre of the pill is recorded along with the calculated location. The transmitter array on the pill is driven using a 40 kHz pulsed sine wave of 10 cycles with a driving voltage of 10 V pk – pk. The full experimental set up can be observed in Figure 7-8. Based on the simulations in [Chapter 6.0, section 6.4] a detection threshold of 50 mV is set. As the received signal amplitude crosses this threshold the TOF corresponding to the signal is calculated.

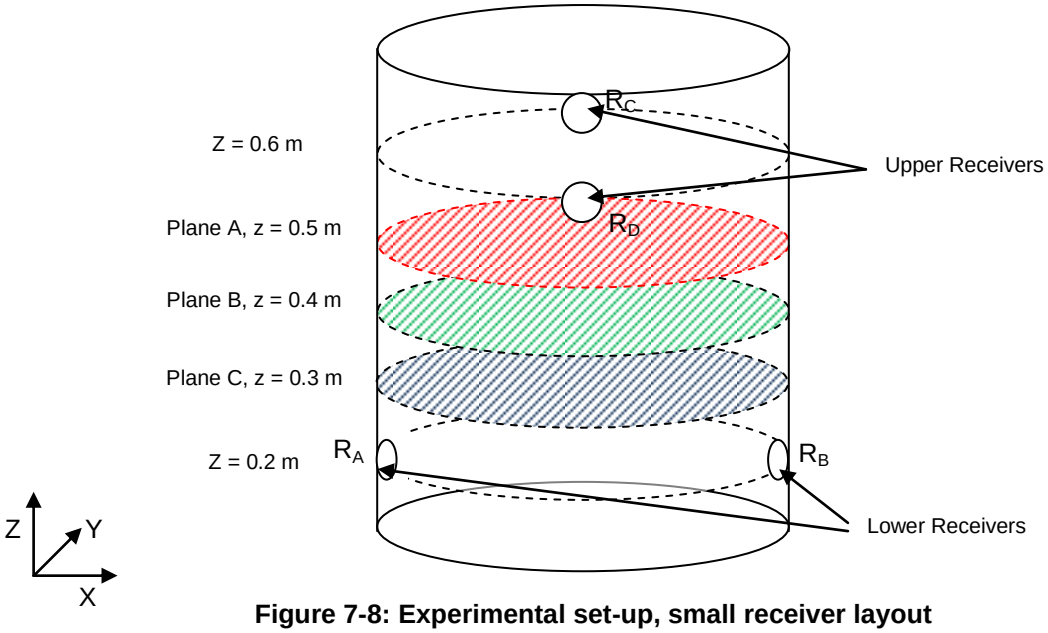

Figure 7-8: Experimental set-up, small receiver layout

Figure 7-8 illustrates the initial receiver layout tested within the vessel. The receivers are mounted at heights of z =0.6 m and z = 0.2 m respectively. The coordinate locations of the receivers are R_A = (0, 0, 0) m, R_B = (0.5, 0, 0) m, R_C = (0.25, 0.25, 0.4) m, R_D = (0.25, -0.25, 0.4) m. For the section of the vessel tested these receiver locations represent the extremities of the test area which based on simulations in [Chapter 4.0, section 4.4] have been suggested to improve the localisation accuracy for TDOA localisation. The pill is tested over 3 horizontal planes within the vessel, plane A, B and C as highlighted in Figure 7-8. The pill is aligned such that the centre of the pill is within the plane.

7.2.2 TOF Localisation Accuracy Plane A

For each location within the vessel the results show the overall error in *x, y, z* between the actual centre of pill position and that calculated by the system from the TOF values obtained. Localisation using TOF synchronisation uses a least mean square algorithm to minimise the localisation error.

For each plane 3 sets of test results are taken and the average of these is displayed. The results show both the error on location and the standard deviation between repeat measurements. Due to the movement of the plotter and the size of the pill certain locations within the vessel are inaccessible. These are around the edge of the vessel and are shown as blank squares on the results. The location of receiver R_A is highlighted to clarify the orientation of the results. Each location is coloured to aide in the visual display of locations which show good accuracy between the calculated and true location of the pill and those which show poor accuracy.

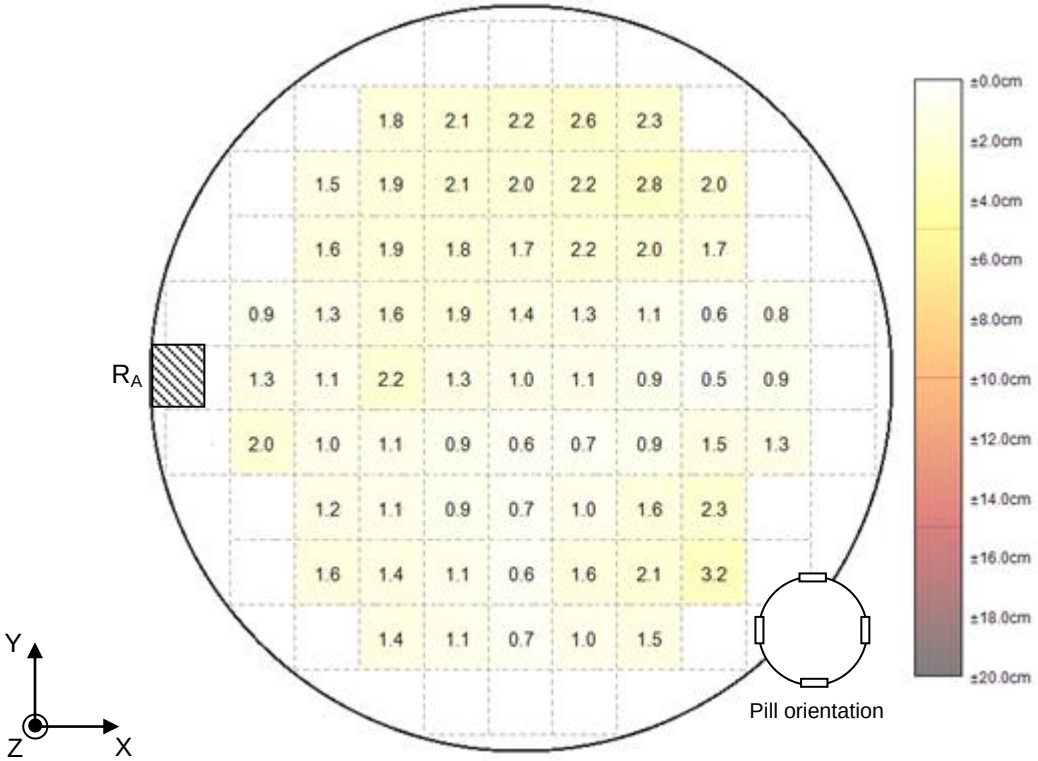

Figure 7-9: Localisation error, plane A, 0° pill rotation

Figure 7-9 displays the localisation error on plane A using TOF localisation. Each location is the centre of the pill. At each location the average positional error is calculated on the actual position of the centre of the pill. The result is for 0° pill rotation. The orientation of the pill is shown in Figure 7-9. It can be observed that the localisation accuracy for results on plane A show that pill location calculated through TOF information is in good agreement with the actual position of the pill. The average localisation error on this plane is 1.5 cm with the largest error being 3.2 cm and the smallest error 0.6 cm.

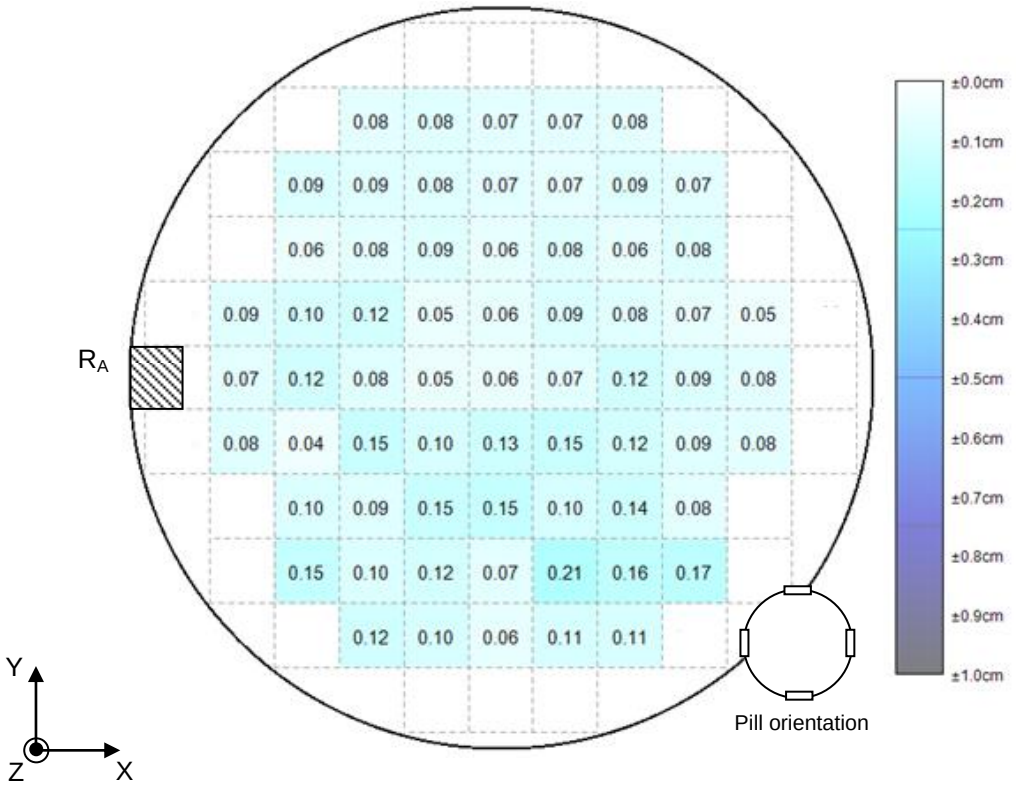

Figure 7-10: Standard deviation, plane A, 0° pill rotation

Figure 7-10 displays the standard deviation for each pill location over the three sets of repeat measurements for plane A. The smallest standard deviation is 0.04 cm while the largest standard deviation is 0.21 cm. It can be observed that for 63% of the tested pill locations the result falls within 2 standard deviations. The result suggests that on this plane the deviation between repeat measurements is very small.

To observe how rotation of the pill affects the localisation accuracy using TOF the condition with the pill rotated is also considered. The same centre of pill test locations throughout the vessel are maintained however the pill is rotated 45° ± 5° around the *z* axis such that the transmitters are in different *x-y* positions relative to the receivers.

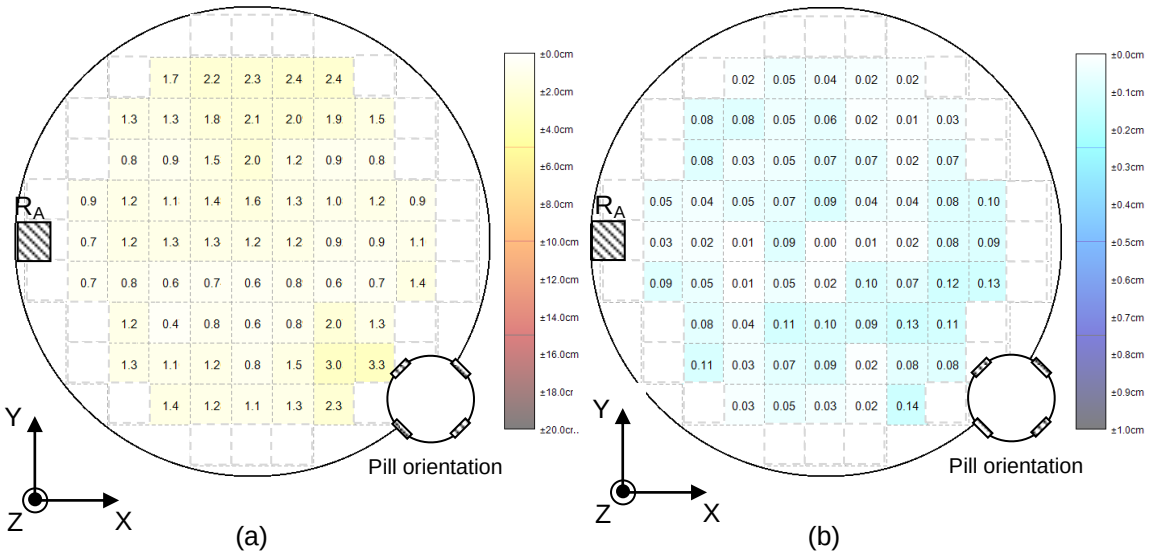

Figure 7-11: Plane A, 45° pill rotation (a) Localisation error (b) Standard deviation

Figure 7-11 (a) shows the average localisation error for each centre of pill location in the vessel when the pill is rotated at 45°, the orientation of the pill is illustrated. The results illustrate the average localisation error from three repeat tests. Figure 7-11 (b) shows the standard deviation results for each pill location over the three repeat tests.

The average localisation error within the vessel for this plane and pill rotation is 1.3 cm, with a maximum error of 3.3 cm and a minimum error of 0.5 cm between the actual and calculated pill location. The highest standard deviation in Figure 7-11 (b) is 0.14 cm with the smallest standard deviation being 0.00 cm between repeat tests.

The results suggest that for a pill rotation 45° the centre of the pill can be localised with excellent accuracy. The average accuracy is comparable to that observed when the pill is rotated at 0° and shows a small reduction in average error, from 1.5 cm to 1.3 cm. The standard deviation results also suggest that the repeatability of measurements is excellent. This suggests that with TOF localisation rotation of the pill can be accommodated and does not have a significant impact on the localisation accuracy.

7.2.3 TOF Localisation Accuracy Plane B

This section details the localisation accuracy of the TOF localisation technique for a pill located on plane B in the vessel. Plane B is situated 10 cm below plane A which increases both the transmission and reception angle for the acoustic signal at the receiver. The location of the pill is again altered in intervals of 5 cm in the *x* and *y* coordinates.

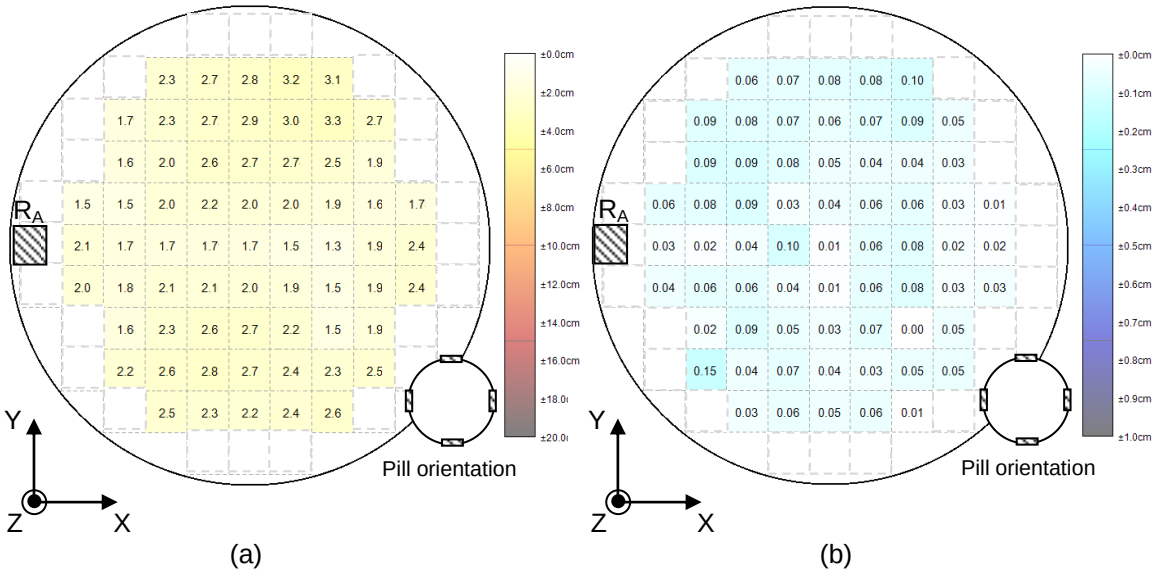

Figure 7-12: Plane B, 0° pill rotation (a) Localisation error (b) Standard deviation

Figure 7-12 (a) shows the average localisation error between the actual centre of pill location and that calculated through TOF localisation. Figure 7-12 (b) shows the standard deviation for each location in the vessel tested. The average error and standard deviation are obtained from three experimental tests and the pill orientation is 0°.

It can be observed in Figure 7-12 (a) that the average localisation error for plane B for 0° pill orientation is 2.2 cm. The maximum error on a single position is 3.3 cm with a minimum localisation error of 1.38 cm. In comparison to plane A the average localisation error for plane B has increased by approximately 0.7 cm.

From Figure 7-12 (b) it can be observed that the maximum standard deviation for the results is 0.15 cm with a minimum of 0.01 cm. The result suggests that while there has been an increase in the localisation error for TOF localisation on plane B the calculated location of the pill is consistent between repeat tests.

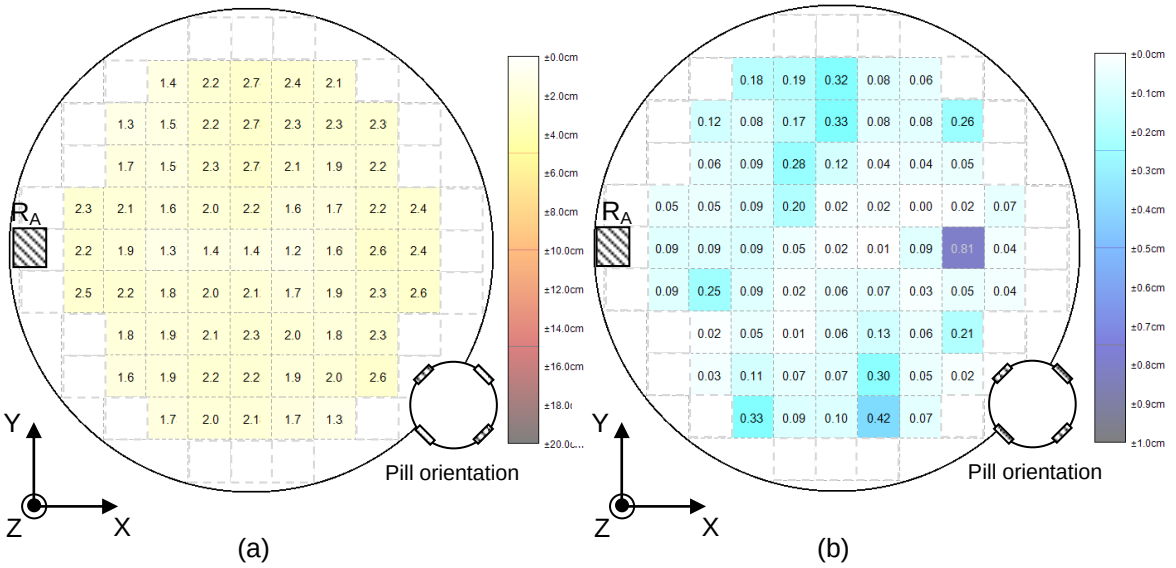

Figure 7-13: Plane B, 45° pill rotation (a) Localisation error (b) Standard deviation

Figure 7-13 (a) shows the average localisation error between the actual centre of pill location and that calculated through TOF localisation when the pill is rotated 45°. Figure 7-13 (b) shows the standard deviation for each location in the vessel tested. The average error and standard deviation are obtained from three experimental repeats.

The maximum localisation error for plane B and a pill rotation of 45° is 2.7 cm, with a minimum error of 1.2 cm. The average localisation error across the plane is 2.0 cm. The result shows comparable accuracy to the results on this plane for a pill orientation of 0°. Again the results suggest that when the pill is rotated the average localisation accuracy is marginally better.

The standard deviation results in Figure 7-13 (b) show more variation for this test plane and pill orientation. The largest standard deviation between repeat tests is 0.81 cm while the smallest standard deviation is 0.01 cm. While there is more variation for certain pill locations between repeat tests the highest standard deviation is only 0.81 cm and this is only observed for a single location within the test plane. The majority of results still show excellent repeatability between measurements.

7.2.4 TOF Localisation Accuracy Plane C

The localisation accuracy of the system for a pill located on plane C is tested. The locations of the pill in the *x* and *y* coordinates are maintained as for planes A and B and the pill is again tested for orientations of 0° and 45°.

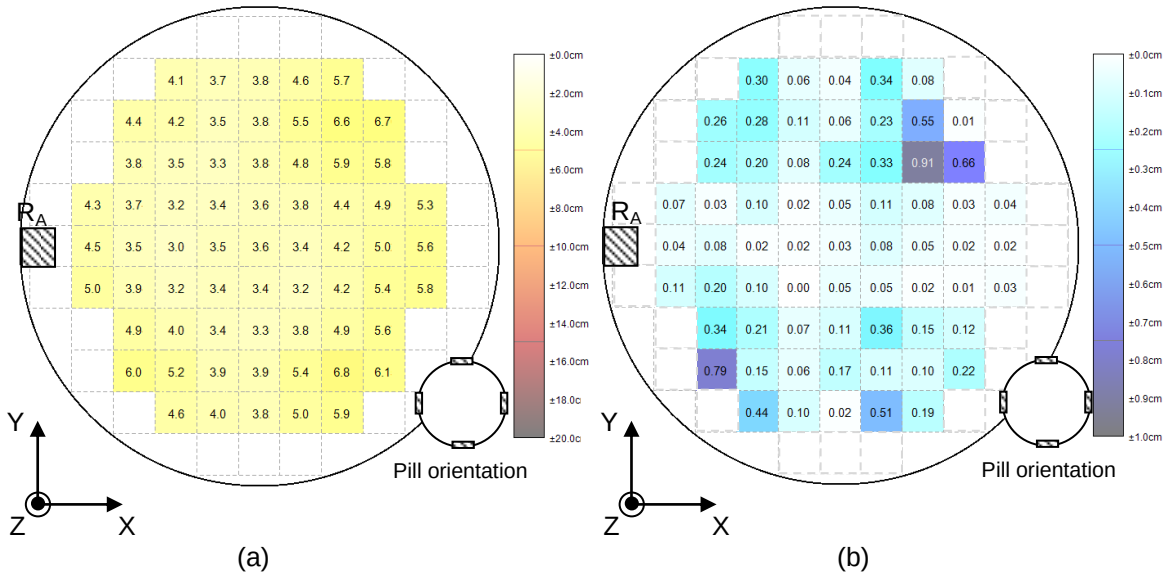

Figure 7-14: Plane C, 0° pill rotation (a) Localisation error (b) Standard deviation

Figure 7-14 (a) shows the average localisation accuracy for each centre of pill location on plane C over three test experiments for a pill rotation of 0°. Figure 7-14 (b) shows the standard deviation for each of these test locations between repeat measurements.

It can be observed from Figure 7-14 (a) that the average localisation error across all of the tested locations in the vessel is higher for this depth than those previously tested. In this instance the maximum error is 6.8 cm with a minimum error of 3.0 cm. The average error across all of the tested locations is considerably higher than previously observed on plane A or B at 4.4 cm.

In Figure 7-14 (b) the result illustrates that there is more variation in the standard deviation at each test location in the vessel. The maximum standard deviation is observed as 0.91 cm with a minimum variation of 0.02 cm still possible. It can be observed that the locations which seem to show more variation are situated around the edge of the vessel and seem to largely coincide with the pill locations where the largest localisation error is observed.

The localisation result suggests that for this plane within the vessel the TOF signals calculated at the receivers show more variation between repeat measurements and also show more inaccuracy in comparison to the TOFs anticipated for the pill location. If the TOF values calculated do not show good agreement with those anticipated from trigonometric consideration then the location calculated for the pill will be inaccurate.

This result suggests that the received signal shows more variation which could be due to the received signal strength being close to the threshold set for detection. If the received signal strength is below the amplitude threshold for reception then the signal will not be selected and the TOF incorrectly calculated.

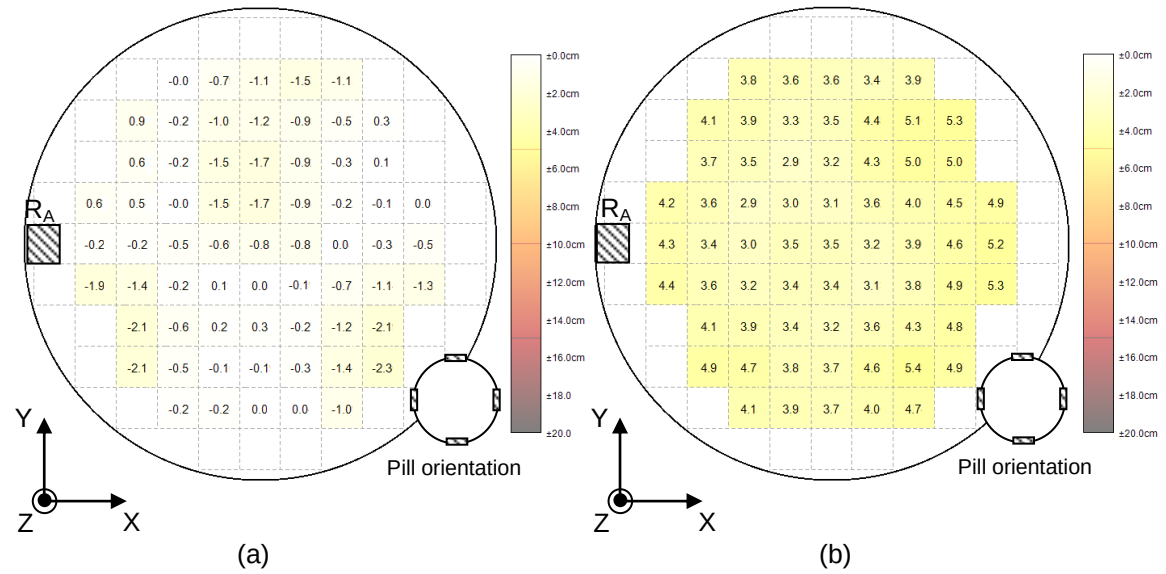

Figure 7-15: Plane C, 0° pill rotation (a) Error in x component (b) Error in z component

Figure 7-15 shows a comparison of the error components for plane C with 0° pill rotation. Figure 7-15 (a) shows the error which is observed in the *x* component between the actual and calculated *x* position of the centre of the pill while Figure 7-15 (b) shows the error between the actual and calculated *z* position of the pill.

It can be observed that for plane C the dominant factor in the location error is the *z* component. While the error in the *x* component remains relatively low at this depth, with a maximum error of 2.3 cm and average error of 0.6 cm the error observed in the *z* component is significantly higher. The maximum error due to the *z* component is 5.4 cm with an average error of 4.0 cm. The result illustrates that the overall error is dominated due to the error in the *z* component.

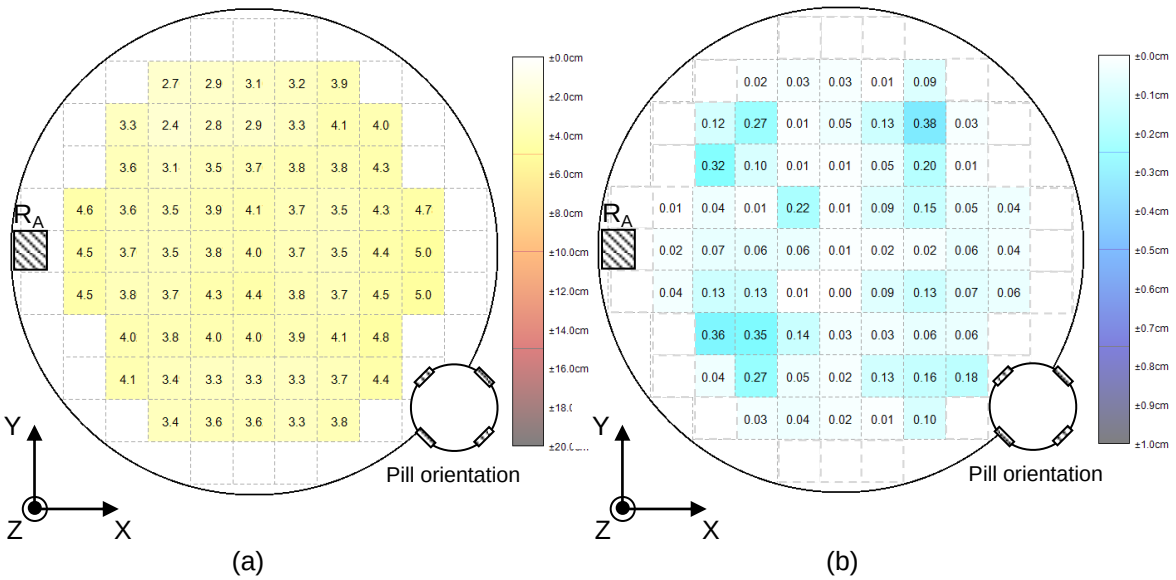

Figure 7-16: Plane C, 45° pill rotation (a) Localisation error (b) Standard deviation

Figure 7-16 (a) illustrates the error in localisation on plane C when the pill is rotated 45°. These results are the average error for each position from three experimental tests. Figure 7-16 (b) illustrates the standard deviation between results at each pill location.

The average positional error is 4.2 cm with a maximum error observed of 6.2 cm and a minimum error of 2.7 cm. The standard deviation of the results illustrates that that maximum standard deviation for a single pill location is 0.38 cm.

The results again illustrate that while the average error has increased as the depth of the pill in the vessel has increased the repeatability of the results remains good. With a worst case standard deviation of only 0.38 cm observed through multiple tests. The result suggests that as with testing undertaken on plane A and plane B the average localisation accuracy is marginally better when the pill is rotated at 45° in the vessel.

7.2.5 Summary of Localisation Utilising TOF Measurements

This section has investigated localisation of the pill using TOF measurements. Results are presented showing the localisation error between the actual pill location and the calculated location. The section has investigated how rotation of the pill affects the localisation accuracy of the system and also the repeatability of localisation errors.

Section 7.2.1 describes the vessel test configuration. The experimental set up is detailed describing the positioning test equipment to position the pill within the vessel and the location of receivers. Three test planes are investigated with sixty five pill locations on each plane.

The results for the localisation accuracy of the system for the pill located on plane A are detailed in section 7.2.2. Results demonstrate that the localisation accuracy for this plane is very good, with an average localisation error of 1.5 cm for 0° pill rotation. The repeatability of these localisation results is also excellent with millimetre repeatability observed. When the pill is rotated 45° results show that the average localisation error reduces to 1.3 cm with millimetre variation between repeat tests.

In section 7.2.3 the localisation errors for the pill located on plane B are detailed. Results again demonstrate good localisation accuracy, with average error of 2.3 cm and 2.8 cm for 0° and 45° pill rotation respectively. While the results demonstrate that for certain pill locations there is more variability between repeat measurements overall the repeatability is excellent with variation between tests less than 0.5 cm.

Section 7.2.4 describes the results for localisation on plane C in the vessel. The results on this plane show an increase in average error to 4.5 cm for 0° pill rotation. Through investigations of the dominant component in this error it can be observed that this relates to the z component. The average error in x is 1.2 cm while the average error in z is 4.0 cm.

Overall the results demonstrate that the system is able to accurately locate the pill in 3D using TOF measurements. For the three tested planes the results show excellent correlation between the actual and calculated pill location within the vessel.

7.3 Localisation utilising TDOA Measurements

This section investigates the localisation accuracy of the system when TDOA measurements are considered. To allow a comparison to be made between the localisation accuracy using TOF and TDOA measurements the test locations and test methodologies are maintained as those in section 7.2.1

7.3.1 TDOA Localisation Accuracy, Plane A

To calculate the location of the pill and thus the error on each location the MATLAB program established in [Chapter 3.0, section 3.2.2] is used. TDOA values from the hardware are obtained as the pill is moved through the vessel and the MATLAB program used to calculate the expected pill position. These results are then compared with the actual pill location and the error is calculated. The TDOA algorithm implemented does not use transmitter offset knowledge and assumes the pill is a single transmitter point source.

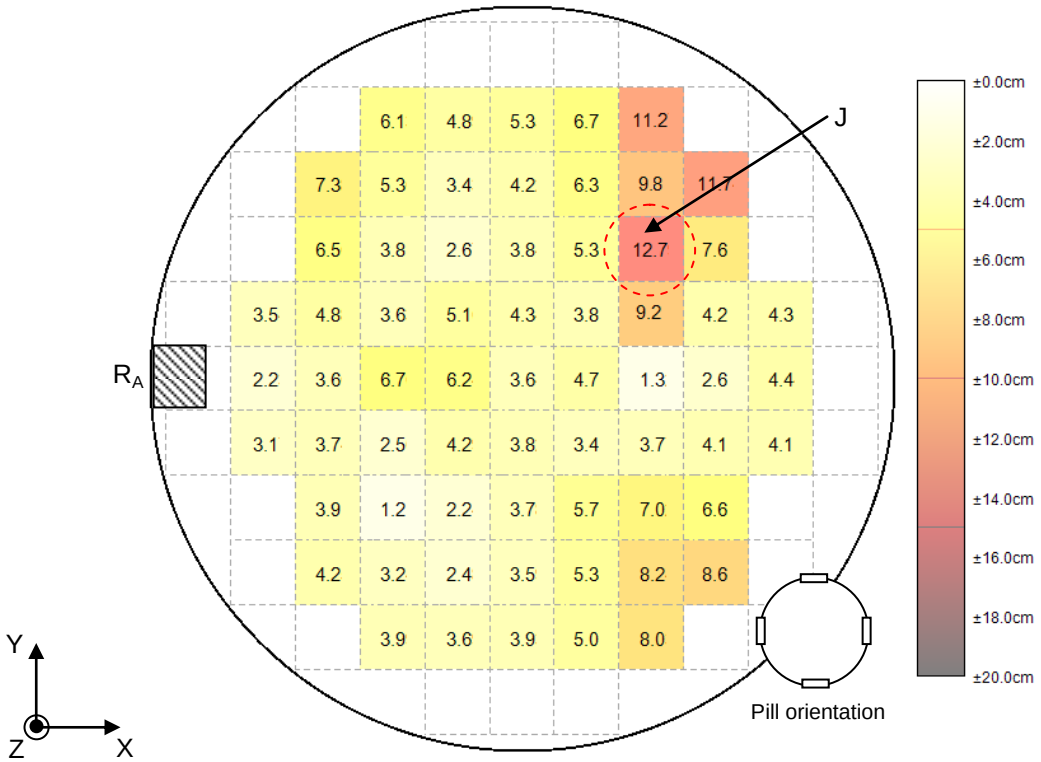

Figure 7-17: Localisation error using TDOA, plane A, 0° pill rotation

Figure 7-17 displays the localisation accuracy throughout the vessel using TDOA localisation for plane A and 0° pill orientation. The overall localisation error is presented for each test location

within the vessel, where the value shown is the localisation error for the pill situated in that location. The results represent the average error for each location from three repeat measurements.

It can be observed that, in general, the localisation accuracy within the vessel is reasonable however; in comparison to TOF measurements the localisation error is larger. The largest error can be observed to be 12.7 cm with the smallest error of 1.2 cm. The average error is 5.0 cm but there are some locations which display poor results. For instance, the largest error is 12.7 cm for this set of results, highlighted as “J” in Figure 7-17.

Experiment	Range Difference$_{BA}$ (cm)	Range Difference$_{CA}$ (cm)	Range Difference$_{DA}$ (cm)
1	22.12	31.00	15.11
2	21.83	30.71	14.43
3	21.46	30.34	14.80

Table 7-1: Range difference values for largest error location

Table 7-1 shows the range difference values obtained for location J over the 3 experimental tests. Range difference$_{BA}$ represents the range difference between the arrival of the received signal at receivers R_B and R_A. It can be observed that the repeatability of the results between experimental tests is excellent, with less than 1 cm variation between tests for each of the range difference values calculated.

The localisation error in “J” is observed because the range difference values obtained through experiments show large error in comparison to the theoretical values expected for this pill location. For the location highlighted A the anticipated range difference results based on trigonometry are R_{BA} = 16.26 cm, R_{CA} = 24.20 cm and R_{DA} = 13.58 cm respectively. Therefore, while the experimental results show good repeatability between tests the measured values show large variation. The error in range difference for R_{BA} is approximately 5 cm from that anticipated and for R_{DA} approximately 6 cm. Therefore the pill location calculated from these TDOA values is inaccurate compared to the actual pill location.

It can be observed that the results for pill locations situated near to location J in Figure 7-17 also show larger ranging errors that observed in other pill locations within the vessel. One possible reason for this is if the signal strength received for these pill locations is close to the threshold value for calculating the TDOA values. If this is the case it is possible that the received signal is just below the threshold level and therefore the TDOA values and subsequent RDOA show error in relation to that anticipated through trigonometry.

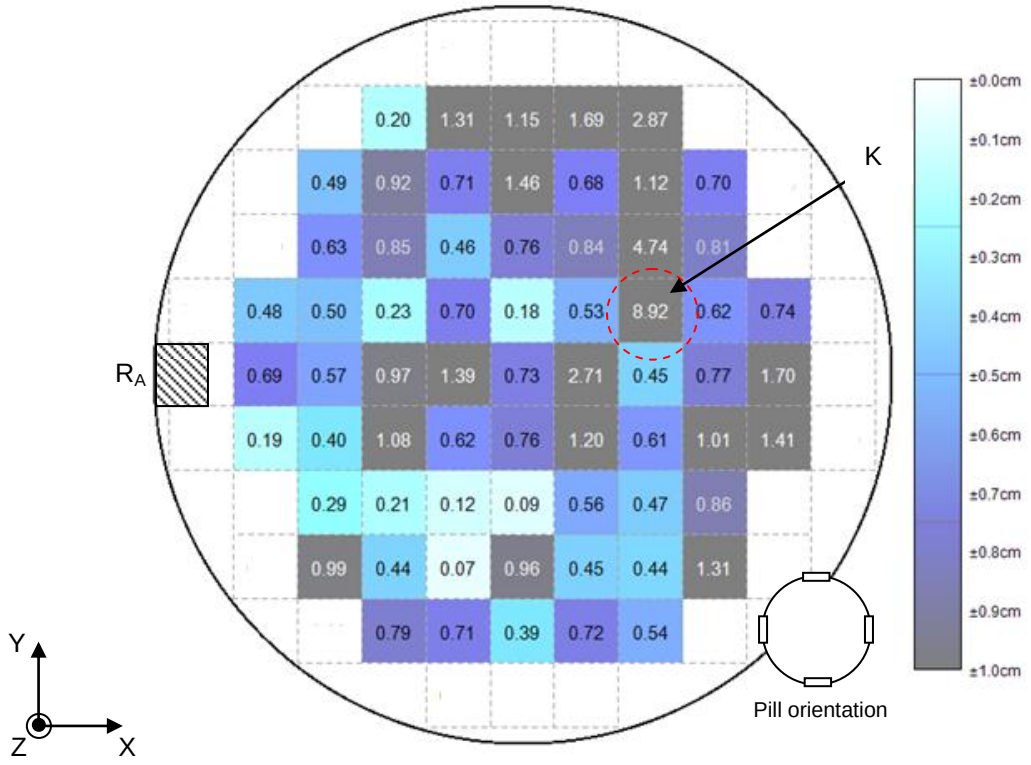

Figure 7-18: Standard deviation using TDOA, plane A, 0° pill rotation

Figure 7-18 displays the standard deviation of each location over the three sets of results. It can be observed that the best case standard deviation is 0.07 cm while the worst case standard deviation is 8.92 cm. The average standard deviation is 0.97 cm. In comparison to the results observed for TOF localisation the results obtained using TDOA show more variation between repeat experimental tests. From examining the TDOA data obtained during experimentation it can be observed that there are some large variations between repeats of the same experiment which causes the solver to tend to different solutions, resulting in large standard deviation between the results. The largest standard deviation is 8.92 cm for this set of results, highlighted as “K” in Figure 7-18.

Experiment	Range Difference $_{BA}$ (cm)	Range Difference $_{CA}$ (cm)	Range Difference $_{DA}$ (cm)
1	-28.82	-4.52	-18.69
2	-14.06	9.25	-3.70
3	-11.84	12.95	-1.11

Table 7-2: Range difference values for largest error location

Table 7-2 shows the range difference values obtained for location K over the 3 experimental tests. Range difference $_{BA}$ represents the range difference between receivers R_B and R_A. It can be observed that there are significant differences between the experimental values obtained for the same location. Between experiments 1, 2 and 3 there are large differences between results. Therefore, the calculated pill location for these will be different and a large standard deviation

observed. One possible reason for this is if the signal level detected by the receivers is marginal in relation to the threshold level. If the received signal level is marginal in relation to the threshold value then it is possible that a small change in pill location between repeat tests causes the received amplitude to be above the threshold for one test and below if for a repeat experiment. Therefore there will be a large variation in the TDOA and subsequent RDOA values between the repeat tests as has been observed in Table 7-2.

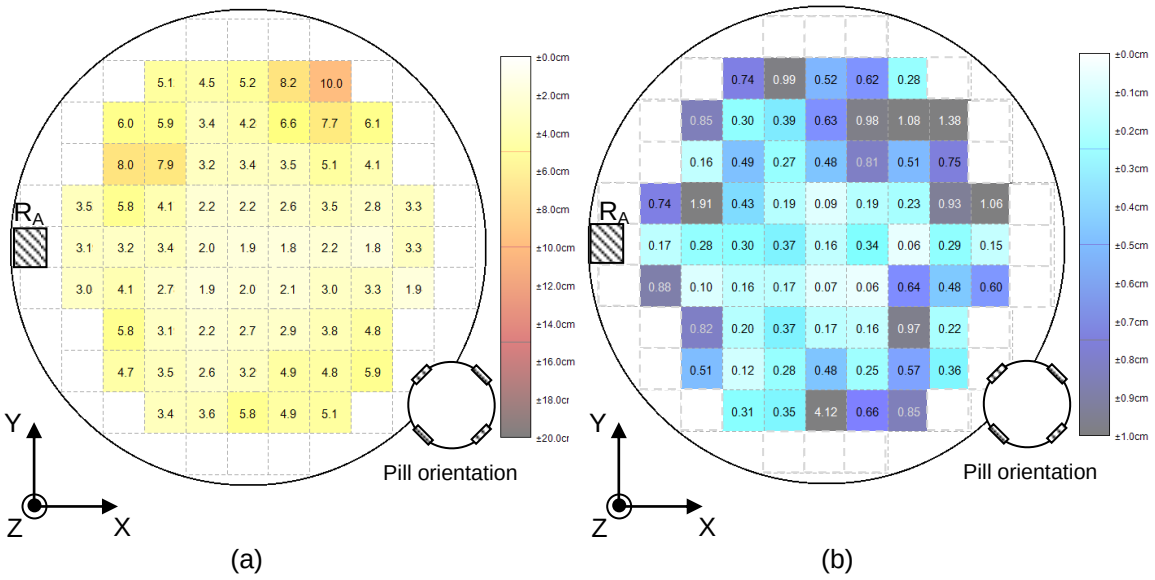

Figure 7-19: TDOA, Plane A, 45° pill rotation (a) Localisation error (b) Standard deviation

Figure 7-19 (a) shows the average localisation error for each centre of pill location in the vessel when the pill is rotated at 45°. These results are for an average of three tests. Figure 7-19 (b) shows the standard deviation of the results for each pill location.

Figure 7-19 (a) shows the average localisation error within the vessel is 4.1 cm with a maximum error of 10.8 cm and a minimum error of 1.8 cm on the actual centre of the pill. In comparison to the results for 0° pill rotation, Figure 7-17, the average localisation error has improved when the pill is rotated, as was observed for TOF localisation. The large error observed at location J, Figure 7-17, has been reduced which suggests the TDOA values obtained for this location now more closely approximate those anticipated.

The largest standard deviation observed in Figure 7-19 (b) is 4.11 cm with the lowest standard deviation being 0.06 cm. The average standard deviation is 0.54 cm. These results again show significant improvement to those observed for 0° pill rotation in Figure 7-18. The large standard deviation error observed in location “K”, Figure 7-18 has been reduced from 8.92 cm to 0.23 cm suggesting that for this pill rotation angle the signal detected is much stronger at the receivers and therefore the localisation result does not change significantly between repeat tests.

7.3.2 TDOA Localisation Accuracy, Plane B

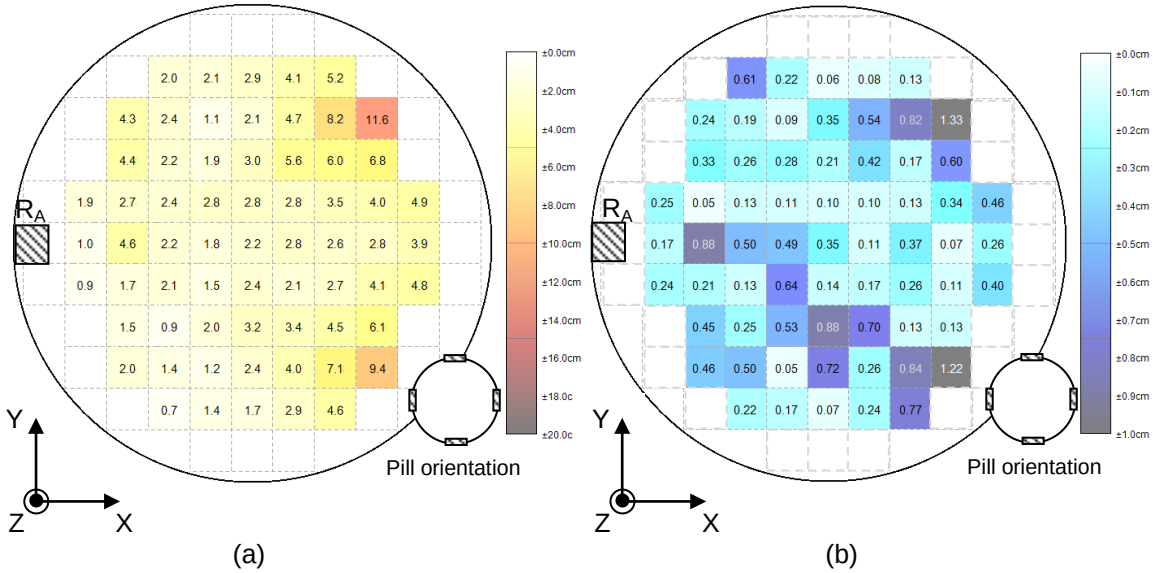

Figure 7-20: TDOA, Plane B, 0° pill rotation (a) Localisation error (b) Standard deviation

Figure 7-20 (a) shows the average localisation error between the actual centre of pill location and that calculated through TDOA localisation for plane B. Figure 7-20 (b) shows the standard deviation for each location in the vessel tested. The average error and standard deviation are obtained from three experimental tests.

It can be observed in Figure 7-20 (a) that the average error for this plane in the vessel is 3.3 cm in comparison to 2.2 cm for TOF. The maximum error on a single position is 11.6 cm with a minimum localisation error of 0.8 cm. The results show that in comparison to plane A the average localisation error has decreased by approximately 1.7 cm.

From Figure 7-20 (b) it can be observed that the maximum standard deviation for the results is 1.33 cm with a minimum of 0.05 cm. The average value is 0.35 cm. This result shows that as the average localisation error has decreased when the pill has been lowered in the vessel the repeatability of the results has also improved, with a much lower standard deviation observed between repeated tests than for plane A.

For this plane the pill is lower in the vessel which means that as the transmitter and receivers are rotated at 45° both the transmission and reception angle of the signal is shallower where the transmission and reception sensitivity of the transducer is stronger, as observed in [Chapter 6.0, section 6.3.4]. Therefore for this plane the received signal strength at the receivers should be higher producing a more accurate localisation result.

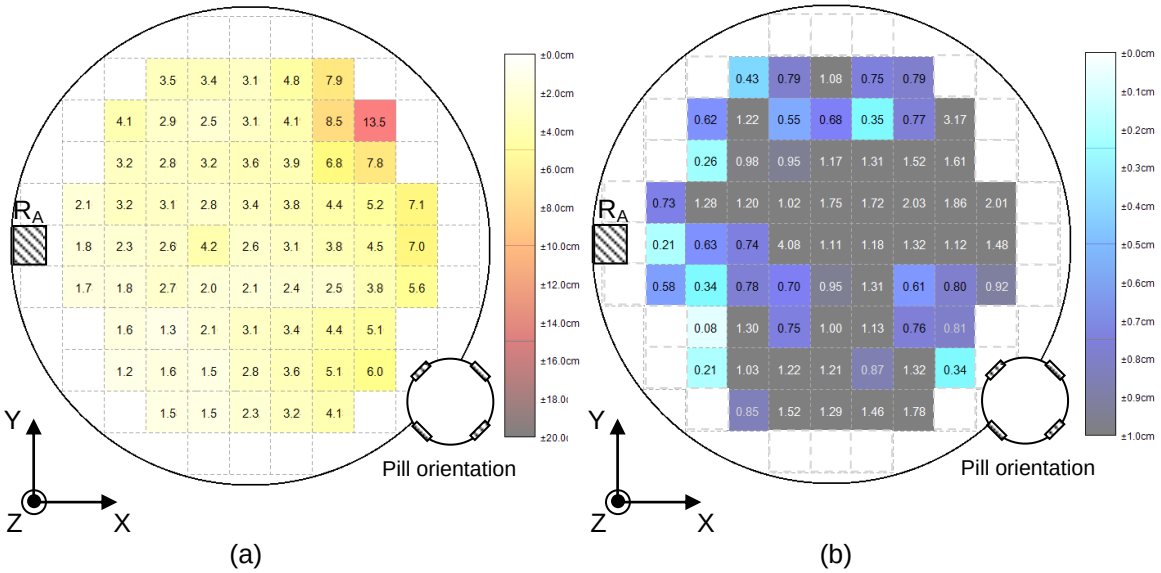

Figure 7-21: TDOA, Plane B, 45° pill rotation (a) Localisation error (b) Standard deviation

Figure 7-21 (a) shows the average localisation error between the actual centre of pill location and that calculated through TDOA localisation when the pill is rotated 45°. Figure 7-21 (b) shows the standard deviation for each location in the vessel tested. The average error and standard deviation are obtained from three experimental tests.

Figure 7-21 (a) illustrates that the maximum localisation for this plane and pill rotation is 13.6 cm with a minimum error of 1.3 cm. It can be observed that the average localisation error throughout this plane is 3.7 cm. The result shows comparable accuracy to the results at this depth when the pill orientation is 0°. In this instance the accuracy is marginally worse when the pill is rotated at 45°.

For the standard deviation, Figure 7-21 (b), it can be observed that as the pill has rotated the variation in error has increased between experimental results, with an average standard deviation of 1.08 cm. The largest standard deviation in the vessel is 4.08 cm with the lowest standard deviation observed at 0.08 cm.

7.3.3 TDOA Localisation Accuracy, Plane C

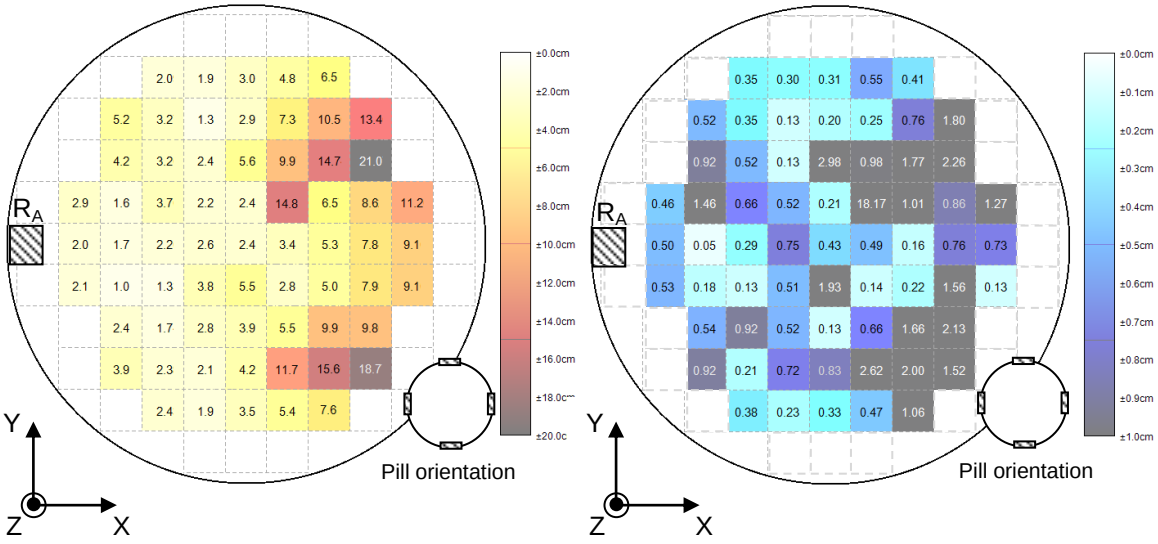

Figure 7-22: TDOA, Plane C, 0° pill rotation (a) Localisation error (b) Standard deviation

Figure 7-22 (a) shows the average localisation accuracy for each centre of pill location on plane C over three repeat experiments. Figure 7-22 (b) shows the standard deviation for each of the test locations.

It can be observed from Figure 7-22 (a) that the average localisation error across all of the tested locations in the vessel is higher for this depth than those previously tested. In this instance the maximum error is 21.1 cm with a minimum error of 1.3 cm. The average error across all of the tested locations is 5.7 cm.

In Figure 7-22 (b) the result illustrates that there is variation in the standard deviation at each test location in the vessel. This depth again shows that the calculated location of the centre of the pill and therefore the calculated error has more variation between experimental tests. The maximum standard deviation is observed as 18.17 cm with a minimum variation of 0.05 cm still possible. It can be observed that the locations which seem to show more variation are situated around the edge of the vessel. The average standard deviation is 1.03 cm.

The result again shows that the large errors are observed in the top right corner of the vessel, as was observed in Figure 7-17. The large errors being again localised to this region suggest that the received signal strength is close to the reception threshold causing ranging errors and resulting in localisation errors.

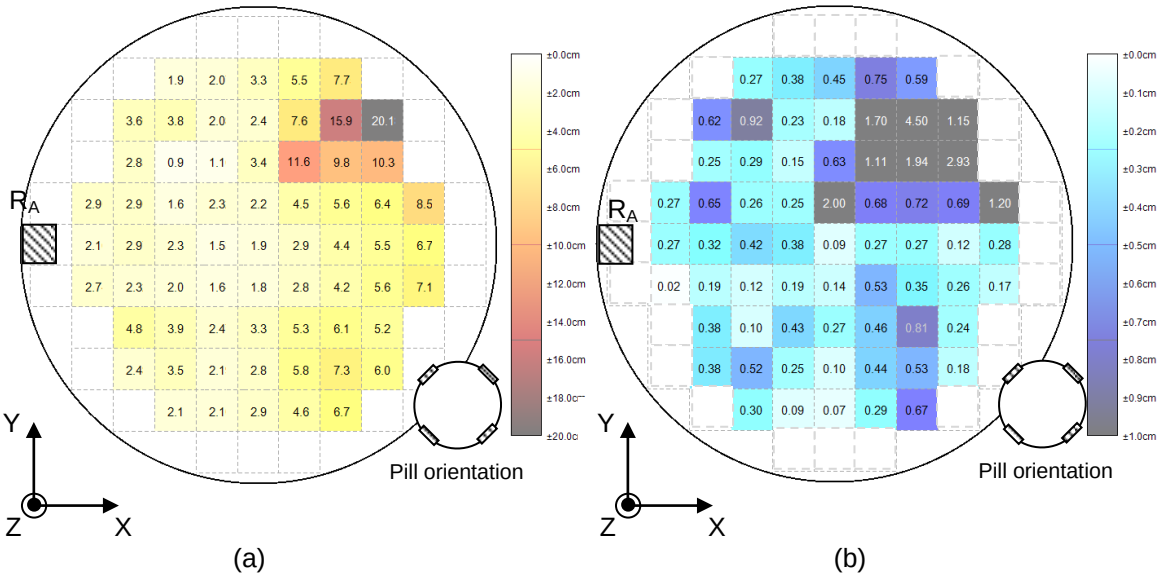

Figure 7-23: TDOA, Plane C, 45° pill rotation (a) Localisation error (b) Standard deviation

Figure 7-23 illustrates the error in localisation for the pill locations in the vessel when the pill is rotated 45°. These results are the average error for each position from three experimental tests; Figure 7-23 (b) illustrates the standard deviation for each location.

The average positional error for this plane is 4.5 cm in comparison to 4.3 cm using TOF. The maximum error observed of 20.2 cm and a minimum error of 1.0 cm. The standard deviation of the results illustrates that that maximum standard deviation for a single pill location is 4.50 cm with a minimum value of 0.09 cm. The average standard deviation is 0.56 cm.

7.3.4 Summary of Localisation Utilising TDOA Measurements

This section has investigated localisation of the pill using TDOA measurements. TDOA has the advantage of not requiring synchronisation between the transmitter and receiver. This section utilises the same test locations as that of section 7.2 to allow a comparison to be made between the location accuracy when TOF and TDOA measurements are used.

In section 7.3.1 the localisation accuracy of the system for a pill on plane A is investigated. The average location error across this plane for 0° pill rotation is 5.0 cm; with a worst case error of 12.8 cm. Through investigations of the pill location with the largest localisation error results have demonstrated that while the measurements between repeat tests show good repeatability the values have a large error in relation to what trigonometric calculations suggest. As the areas with large localisation are grouped close together it is suggested that in these areas the signal received from the transmitter array is not above the required threshold level which results in ranging and subsequently localisation errors.

The average standard deviation for the tested plane is 0.97 cm which demonstrates considerably more variation between repeat tests than was observed for TOF results. Investigating the worst case location has demonstrated that between tests there are large changes in the measurements observed for the same pill location. As TDOA is a technique which employs the difference measurement between signals then the variation of each signal is combined which could explain some of the large variations in observed measurements.

In section 7.3.2 the localisation accuracy is observed for the pill located on plane B. The results show improved localisation accuracy in comparison to plane A with average error of 3.3 cm. Again it can be observed there are a few locations where the localisation error is significantly higher. The repeatability of results has also improved in comparison to plane A however there is still more variation than observed for TOF results. By lowering the pill in the vessel the reception and transmission angles have both improved, increasing the signal strength at the receiver reducing incorrect TDOA results.

The localisation results for the pill located on plane C are detailed in section 7.3.3.The results demonstrate that the localisation accuracy for this plane has an average value of 5.7 cm with again large variations between repeated measurements. Based on the three tested planes it can be observed that the pill locations with higher localisation error are clustered in the top right corner of the vessel which suggests that potentially in this location the signal provided by the pill is insufficient to maintain good localisation accuracy.

7.4 Localisation Utilising TDOA Measurements with Offset Knowledge

This section investigates the localisation accuracy of the system when TDOA measurements using offset knowledge are considered. To allow a comparison to be made between the localisation accuracy using standard TDOA measurements the test locations are maintained as those in section 7.2.1. Through knowledge of the transmitter layout on the pill it is possible to update the TDOA equations to account for the separation of transmitters from the centre of the pill. In [Chapter 4.0, section 4.3] simulations suggested that through offset knowledge it was possible to reduce the localisation error using TDOA localisation for results in a noiseless environment. This section investigates the localisation accuracy of TDOA when offset knowledge of the transmitters is known.

7.4.1 Localisation Accuracy Plane A

To calculate the location of the pill and thus the error on each location the MATLAB program established in [Chapter 3.0, section 3.2.2] is used with offset knowledge of the separation of transmitters from the centre of the pill. As the transmitters are not uniquely coded and it is not possible to determine the rotation angle of the pill then offset knowledge used for a 0° pill orientation is maintained throughout the tests.

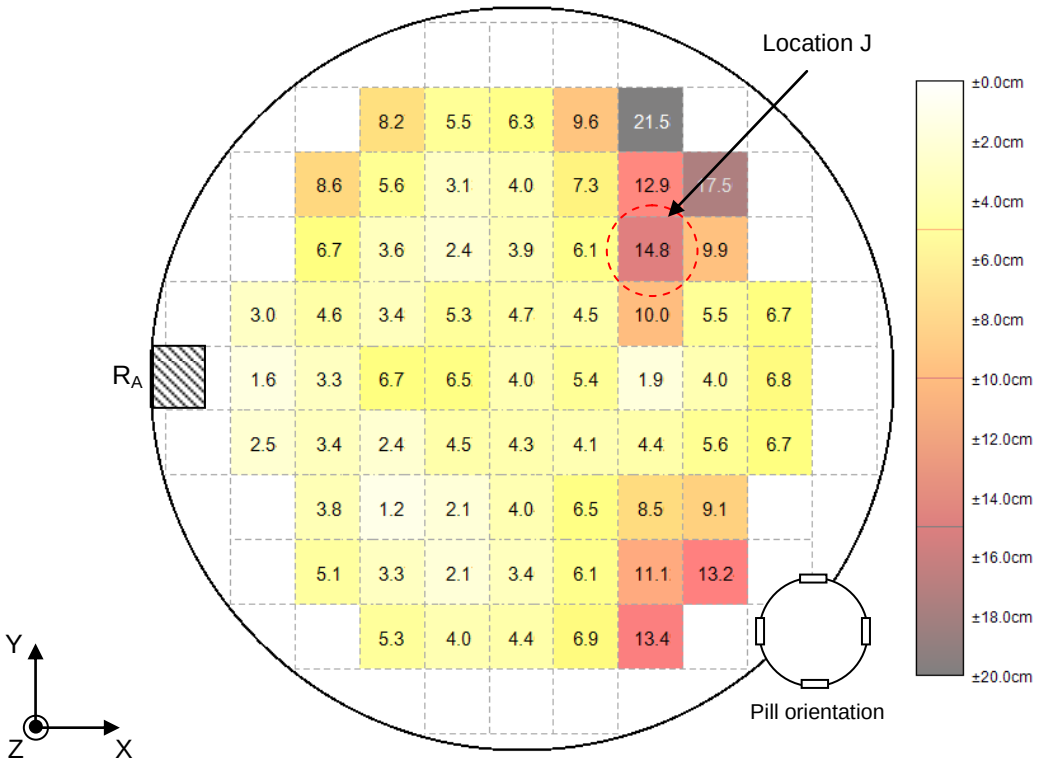

Figure 7-24: Localisation error using TDOA offset knowledge; plane A, 0° pill rotation

Figure 7-24 displays the localisation accuracy throughout the vessel using TDOA localisation with offset knowledge for plane A and 0° pill orientation. The overall localisation error is presented for each test location within the vessel, where the value presented is the localisation error for the pill situated in that location. The results represent the average error for each location from three repeat measurements.

It can be observed that in comparison to standard TDOA the localisation accuracy within the vessel has decreased. The largest error can be observed to be 21.6 cm with the smallest error 1.2 cm. The average error through the results is 6.1 cm in comparison to 5.0 cm when standard TDOA techniques are used.

While in some locations within the vessel it can be observed that compared to the standard TDOA localisation results, Figure 7-17, the error has been reduced, for the areas where the localisation error is large the use of offset knowledge has considerably increased the localisation error. Location “J” highlighted in Figure 7-24 has a localisation error of 14.8 cm, for the same location as observed in Figure 7-17, using standard TDOA the localisation error is 12.8 cm. Based on the results in section 7.2.2 it has been demonstrated that in this location the TDOA values are inaccurate when compared to those anticipated for the location of the pill. The result suggests that when the TDOA values obtained are inaccurate in comparison to those anticipated; the use of offset knowledge further increases the localisation error.

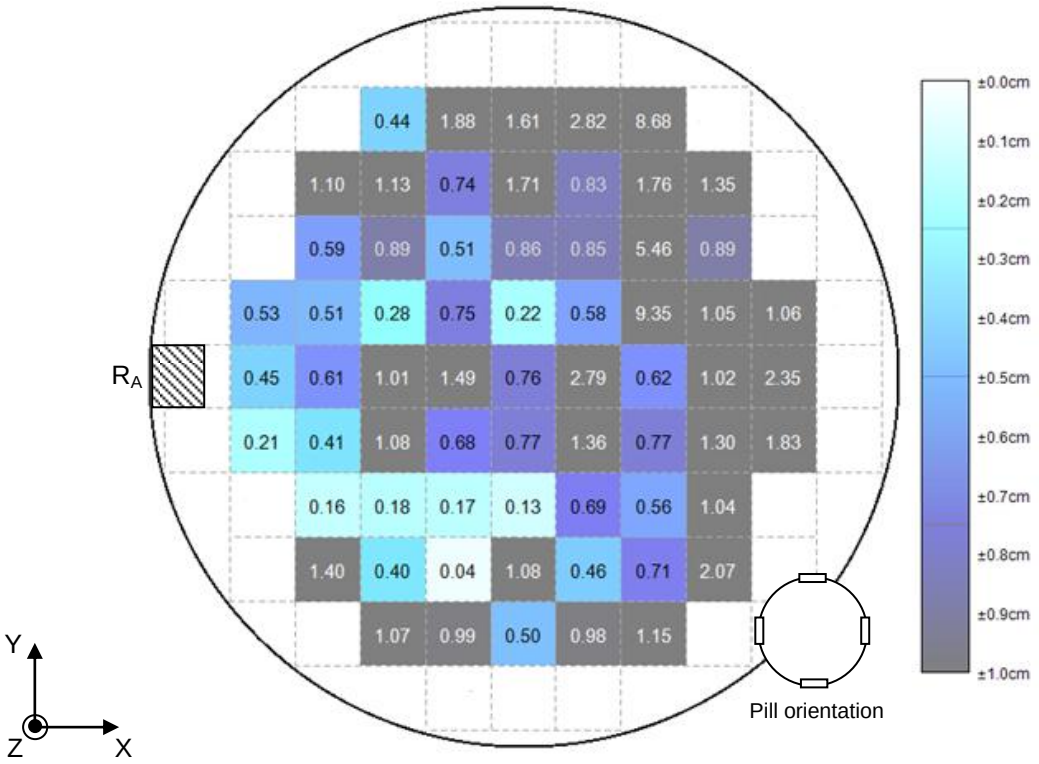

Figure 7-25: Standard deviation using TDOA offset knowledge; plane A, 0° pill rotation

Figure 7-25 shows the standard deviation between 3 repeat tests for TDOA localisation using offset knowledge. The maximum standard deviation is 9.35 cm, with a minimum of 0.04 cm and an average for this plane and rotation angle of 1.26 cm. In addition to showing an increased localisation error it can also be observed that for the results also show more variation using the TDOA offset method than in comparison to standard TDOA.

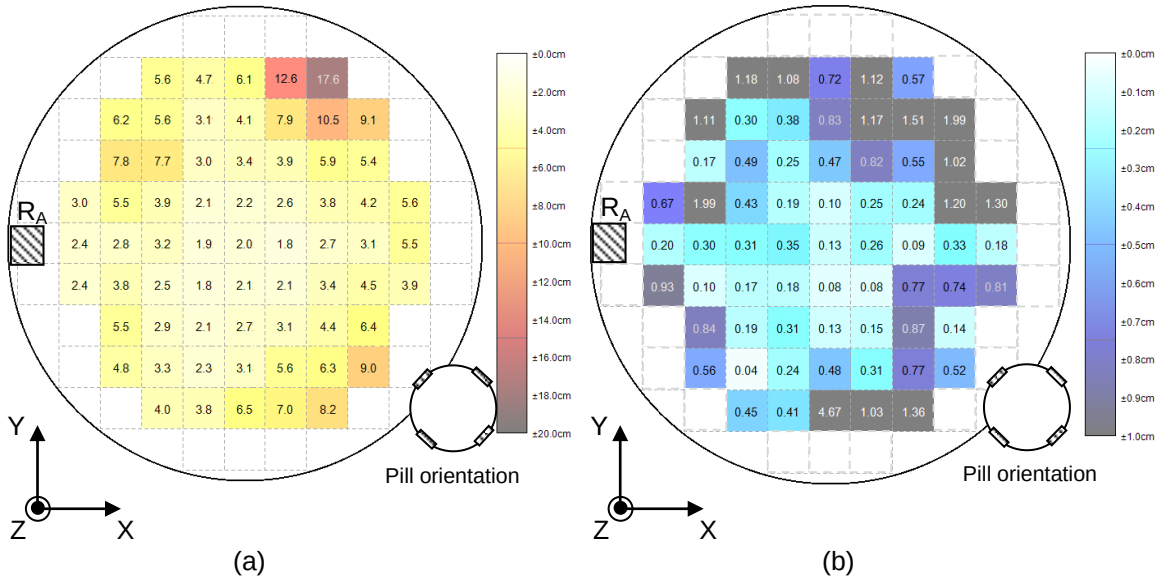

Figure 7-26: TDOA using offset knowledge, Plane A, 45° pill rotation (a) Localisation error

(b) Standard deviation

Figure 7-26 (a) shows the average localisation error for TDOA using offset knowledge on plane A with 45° pill rotation while Figure 7-26 (b) shows the standard deviation between results for three repeat tests. The average localisation error is 4.7 cm with a worst case error of 17.7 cm. The average standard deviation is 0.64 cm with a worst case result of 4.67 cm. The result again suggests that where the localisation error is high with standard TDOA, offset knowledge does not improve the localisation accuracy.

7.4.2 Localisation Accuracy Plane B

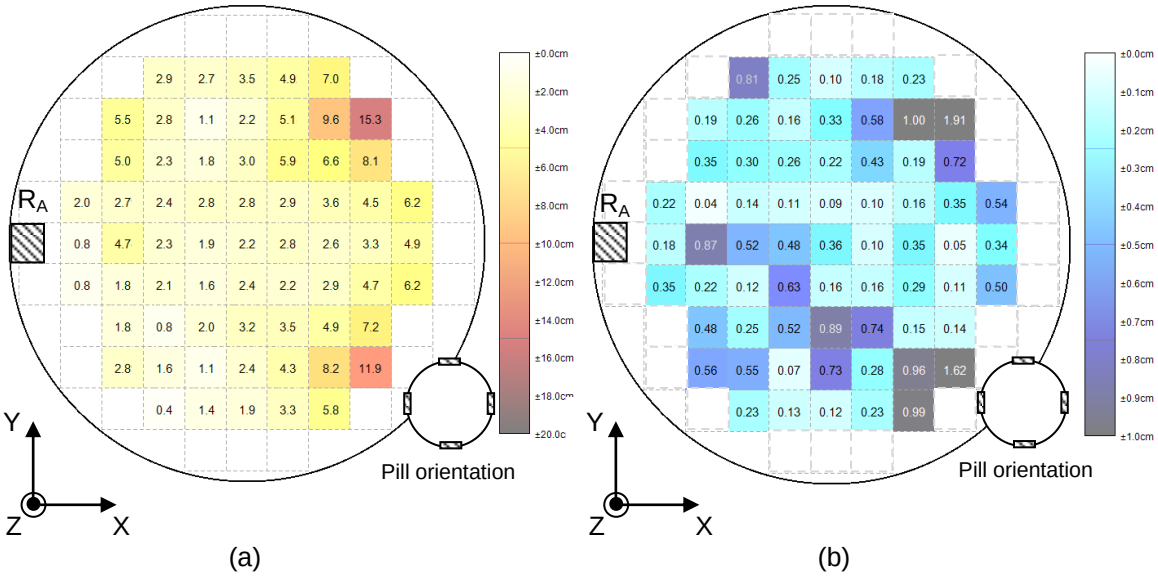

Figure 7-27: TDOA using offset knowledge, Plane B, 0° pill rotation (a) Localisation error (b) Standard deviation

Figure 7-27 (a) shows the average localisation error using TDOA offset knowledge from three repeat tests while Figure 7-27 (b) shows the standard deviation between results. This is for tests undertaken on plane B with 0° pill rotation. The average localisation error is 3.8 cm with a maximum error of 15.4 cm. The average standard deviation is 0.40 cm with a maximum of 1.91 cm. The result shows that some excellent localisation results are possible, with errors of less than 1 cm for certain locations however again some large errors are observed. The results again show slightly worse performance than those observed using standard TDOA.

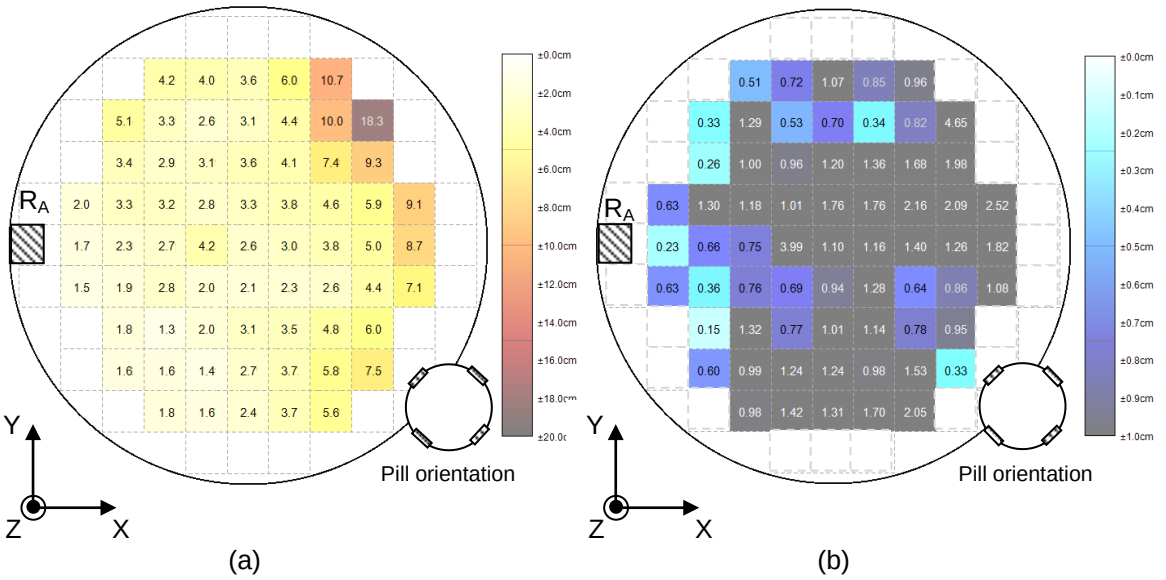

Figure 7-28: TDOA using offset knowledge, Plane B, 45° pill rotation (a) Localisation error (b) Standard deviation

Figure 7-28 (a) shows the average localisation accuracy using TDOA with offset knowledge on plane B for 45° pill rotation while Figure 7-28 (b) shows the standard deviation from three repeat measurements. The average localisation accuracy is 4.2 cm with a worst case error of 18.4 cm and the average standard deviation is 1.16 cm with a worst case error of 4.64 cm.

7.4.3 Localisation Accuracy Plane C

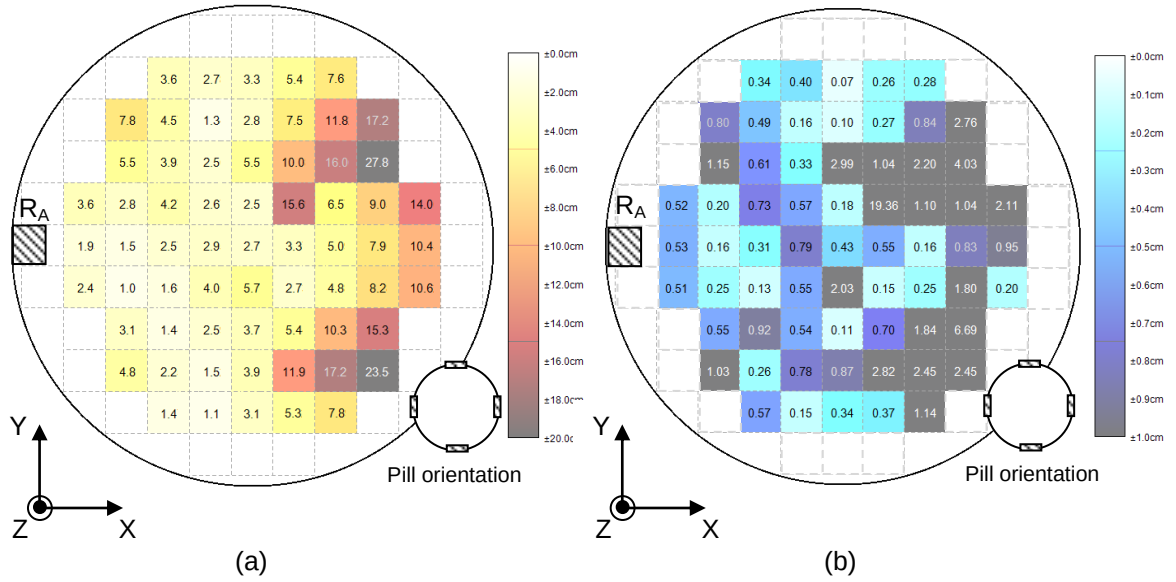

Figure 7-29: TDOA using offset knowledge, Plane C, 0° pill rotation (a) Localisation error (b) Standard deviation

Figure 7-29 (a) shows the average localisation accuracy using TDOA with offset knowledge on plane C for 0° pill rotation while Figure 7-29 (b) shows the standard deviation from three repeat

measurements. The average localisation accuracy is 6.4 cm with a worst case error of 27.8 cm and the average standard deviation is 1.23 cm with a worst case error of 19.36 cm.

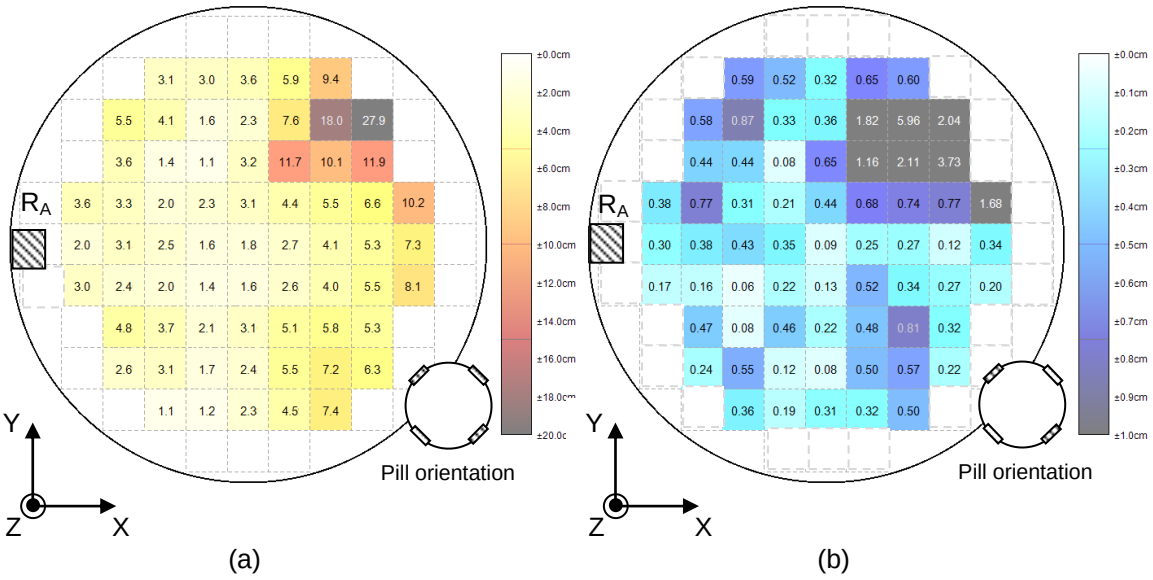

Figure 7-30: TDOA using offset knowledge, Plane C, 45° pill rotation (a) Localisation error (b) Standard deviation

Figure 7-30 (a) shows the average localisation accuracy using TDOA with offset knowledge on plane C for 45° pill rotation while Figure 7-30 (b) shows the standard deviation from three repeat measurements. The average localisation accuracy is 4.8 cm with a worst case error of 28.0 cm and the average standard deviation is 0.62 cm with a worst case error of 5.90 cm.

It has been observed that across the tested planes and pill orientations the use of TDOA offset knowledge has not reduced the localisation error in comparison to standard TDOA. Simulations in [Chapter 4.0, section 4.3.2] have shown that where an error is introduced into the localisation due to the separation of transmitters on the pill using standard TDOA, the use of offset knowledge is able to minimise this localisation error. Offset knowledge has been demonstrated to remove the error due to the separation of the transmitters.

From the experiments using TDOA it has been observed that for certain pill locations there is a large variation between the observed TDOAs and those which would be anticipated due the pill's actual location, Table 7-1. This causes the TDOA equations to tend to solutions which are inaccurate in relation to the pill's actual location. It is suggested that due to the size of the TDOA errors observed the improvements which could be made using offset knowledge are lost. The TDOA values do not represent accurately enough the actual location of the pill and therefore the refinement that offset knowledge could offer is not observed. Where the TDOA values show large error in relation to what should be expected based on the actual pill's location then offset knowledge is being used to refine TDOA values which do not represent the actual location of the centre of the pill and the results show that offset knowledge produces significant increases in the

localisation error over standard TDOA. Therefore while simulations have suggested that offset knowledge should show improved localisation accuracy the TDOA values obtained for the pill location show too much error for offset knowledge to provide any improvement.

7.4.4 Summary of Localisation Utilising TDOA Measurements with Offset Knowledge

This section has investigated the affect that using TDOA with offset knowledge has on the localisation accuracy with TDOA measurements. As the rotation angle of the pill is unknown then the offsets used are for a 0° pill orientation.

In section 7.4.1 the localisation accuracy of the system for a pill on plane A is investigated. In comparison to the results using standard TDOA equations it can be observed that the use of offset knowledge does not improve the localisation error. For results using standard TDOA where a large localisation error was observed, the use of offset knowledge can be demonstrated to cause further localisation error. The standard deviation also shows more variance in comparison to that observed using standard TDOA.

In section 7.4.2 the localisation accuracy is observed for the pill on plane B in the vessel. As was observed for standard TDOA, the localisation accuracy significantly improves on plane B in comparison to plane A however the use of offset knowledge does not improve the localisation error in comparison to the results for standard TDOA.

Section 7.4.3 details the localisation results for the pill located on plane C within the vessel. As was observed for standard TDOA, 7.3.3 plane C shows the largest localisation errors during testing. The result demonstrates that while certain pill locations within the vessel still have a localisation error of approximately 1 cm there is a section of the vessel which has significant localisation error.

7.5 Summary of Pill Localisation

This chapter has undertaken experimental localisation tests utilising localisation techniques which use TOF measurements, TDOA measurements and TDOA with offset knowledge. For each method the localisation accuracy of the system has been investigated over a number of pill locations within the vessel, considering both rotation of the pill and also the repeatability of localisation results.

In section 7.1 the implementation of the system is described. This section has covered the functional operation of the system along with detailing the localisation implementations for TOF and TDOA in practice. Experimental results have confirmed the correct operation of the modified system to detect TDOA measurements.

In section 7.2 experiments have been conducted localising the pill using TOF measurements. Three separate vertical planes have been tested with sixty five pill locations on each. Results have

demonstrated that for each of the planes the localisation accuracy is good, with average error over the three planes of approximately 2.5 cm. Results have also shown that the repeatability of measurements is very good, with millimetre variation in the error between separate tests. The section demonstrates that the use of TOF measurements for underwater localisation of the pill is a viable option for future use.

In section 7.3 experiments have utilised TDOA measurements to localise the pill. Results have demonstrated that in comparison to TOF localisation the average errors for each plane are worse, with overall average error of approximately 4.7 cm. In addition, for certain pill locations the error can be significant, in the order of tens of centimetres. There is also significantly more variation between repeat measurements, with differences in the order of centimetres. Overall the experiments have suggested that TDOA does have the possibility of implementation for underwater localisation however there is the requirement to reduce the variability in the measurements and also overcome some of the areas with large localisation error.

In section 7.4 experiments have utilised TDOA measurements using offset knowledge of the transmitter layout on the pill to improve localisation accuracy. Results have demonstrated that the use of offset knowledge in this instance does not improve the localisation accuracy of TDOA measurements. While for certain locations it can be observed that there is reduction in error, for locations within the vessel with large TDOA inaccuracies in comparison to that anticipated, the use of offset knowledge further increases those localisation errors. As such in this instance due to the TDOA errors the use of offset knowledge is not able to improve the localisation.

8.0 Conclusions and Future Work

8.1 Summary of Findings

The work in this thesis is concerned with exploring 3D localisation of a pill in underwater confined spaces, with a target environment of process vessels envisaged for future application. In process vessel applications such as mixing, there is a continual requirement to refine and improve processes to minimise waste and maximise useful product. Like most applications this refinement comes through the ability to monitor the environment and make adaptive changes to maximise the useful result. For processes such as mixing in large vessels there is a desire to be able to monitor, for example, the chemical properties in the vessel during the mixing process to ascertain the nature of the combination of materials.

Current techniques for monitoring typically involve the insertion of measuring sensors into the vessel, usually around the periphery of the vessel. While information about the environment close to the sensors can be obtained knowledge of the environment further away from these sensors, in the centre of the vessel is limited. In addition the placement of sensors into the vessel naturally changes the mixing dynamics of the vessel.

To overcome this there is a desire to be able to take real time measurements from within the vessel being able to localise a measurement reading to a specific location within the vessel. To achieve this, the development of a wireless pill has been considered, with the ability to accurately transmit its position within the vessel and relay information about the environment to an outside monitoring station. This thesis has explored the development of a wireless pill whose location can be accurately determined from an outside monitoring system.

The proposed pill described in this thesis uses low cost, low power ultrasonic transducers to achieve localisation. Transmitters are located on the surface of the pill which is 0.1 m in diameter. For this thesis the challenge has been to identify optimum strategies, for placement and excitation of transducers, and synchronisation between the pill and external system to deliver 3D localisation.

8.1.1 Investigation of Synchronisation Options

To localise the pill wirelessly from an external monitoring station there is a requirement for a synchronisation technique to allow TOF data to be obtained or alternative localisation techniques which do not require synchronisation between the pill and external receivers. Existing techniques to allow localisation of transmitters or to allow accurate synchronisation in networks primarily employ one of two methods, RTT calculations or synchronised clocks. The short ranges and confined nature of this project mean that both techniques are ineffective. Experimental research has been conducted to investigate localisation through electrical synchronisation and TDOA techniques.

Results of experiments in [Chapter 3.0, section 3.1.5] suggest that synchronisation using electrical pulses between the pill and external system is a viable technique to allow localisation measurements to be obtained in a confined vessel. Results suggest that over the ranges envisaged within the vessel it is possible to transmit an electrical pulse from an isolated pill and detect the signal at externally mounted receive electrodes. The orientation of the transmit and receive electrodes has been shown to be a crucial factor in relation to the received signal strength with results suggesting that to maintain reception of the electrical pulse signal 2 pairs of receive electrodes are required mounted perpendicular with respect to each other. For the limited vessel size and driving voltage results have shown that, while the use of electrodes with surface area of 1 cm square shows a significant increase in received signal strength in comparison to bare wires further increases in the electrode size show negligible influence of the received signal strength.

An alternative technique investigated for localisation is the use of TDOA which does not require synchronisation between the transmitter and receiver and instead utilises the relative difference in the arrival time of a transmitted signal at multiple receivers to determine the location of the transmitter. An algorithm has been constructed to compute the location of a single transmitter from 3 TDOAs obtained with 4 receivers based on a non-linear equation solver. Simulations have shown that through the use of 4 receivers it is possible to localise a single transmitter in a noiseless environment with negligible error, [Chapter 3.0, section 3.2.2].

8.1.2 TDOA Localisation with Offset Transmitters

Typical TDOA methodology involves locating a single transmitter with multiple known receivers or locating a single receiver from multiple transmitters. The single transmitter is considered a point source and the TDOA algorithms are used to determine the location of the transmitter.

In this thesis the pill is not a point source; with multiple transmitters distributed over its surface. Unlike the standard TDOA methodology, where signals arriving at different receivers originate from the same location, with multiple transmitters, signals arriving at different receivers have different points of origin. This thesis has therefore investigated the impact that offsetting the transmitters from the centre of the pill has on the localisation accuracy of the TDOA technique.

Simulations have indicated that the separation of transmitters from a single point on the pill introduces error in the TDOA localisation even for ideal TDOA values. The offset of transmitters from the centre of the pill also introduces a further localisation challenge, that of rotation. Due to the use of multiple transmitters on the pill simulations have shown that for a single centre of pill location multiple sets of TDOA values can represent the location [Chapter 4.0, section 4.2.1]. As the pill rotates the TDOA values obtained at the receivers alter. However, the centre of pill location remains constant. This rotation means that for a single pill location more than one set of TDOA values can represent the same location for the centre of the pill.

To overcome the challenges due to separation of the transmitters on the pill this thesis has explored modifying the standard TDOA equations to include offset knowledge of the transmitter locations. Through modification of the TDOA equations simulations have demonstrated that provided the origin of the signal impacting a receiver is known the centre of the pill can be localised with negligible error for ideal TDOAs, [Chapter 4.0, section 4.3.2].

The offset knowledge modifications have their limitations however when the origin of the transmission signal is unknown. As the pill moves in the vessel then the signal impacting at a receiver has been shown to switch between transmitters which mean the offsets used within the TDOA equations must be modified to maintain negligible error. With a single transmission code from the pill this is not possible. This problem is further compounded by rotation of the pill.

To overcome the problems associated with pill rotation this thesis has investigated a number of options. While the use of a two transmitter solution is a simplistic approach and has been shown to remove the problems due to rotation of the pill the limitation of beam coverage which is possible from the pill means it is an ineffective solution for the vessel. This thesis has instead investigated solving the problems due to rotation by uniquely coding the transmitters and has introduced the technique of 'double TDOA'. Simulations in [Chapter 4.0, section 4.3.3] have demonstrated that through the use of uniquely coded transmitters it is possible to obtain both the TDOA between the arrivals of signal at two receivers but also the TDOA between the arrivals of two signals from different transmitters at a single receiver. The analysis has shown that with this extra information it is possible to determine the rotation angle of the pill and in light of this update the TDOA equation offsets to accommodate rotation.

8.1.3 Influence of Receiver Location on Localisation Accuracy

Comparative simulations have been conducted to investigate the influence that the location of receivers has on the localisation accuracy of the system when noise is considered on TDOA measurements.

Through simulations, applying ranging errors due to noise to individual and multiple TDOA values, analysis has suggested that the vertical separation between receivers is a crucial factor to minimise localisation error, [Chapter 4.0, section 4.4.4]. The study investigates three receiver layouts within the vessel. While the location of receivers is limited in the *x* and *y* coordinate as the receivers must be mounted to the vessel wall, alteration of the receiver location in the vertical component is possible. Simulations have indicated that for very small vertical receiver separations the impact that small ranging errors have on the overall localisation results is considerable. With receivers mounted in close proximity the influence of noise on TDOA values causes the localisation result to converge to highly inaccurate solutions.

Improvement can be seen in the localisation result when the vertical separation between receivers is maximised, [Chapter 4.0, section 4.4.3]. For the layout with the receivers at the vessel extremities, simulations suggest that the receiver layout is able to accommodate errors on TDOA values while still maintaining excellent localisation accuracy. The advantage of the vessel extremities layout is further observed when the range error on TDOA values is increased, with simulations suggesting that for large ranging errors in individual and multiple TDOAs the overall localisation error on a single transmitter is still small.

8.1.4 Vessel Characterisation and Transmitter Interaction

To allow the detection of the acoustic localisation signal even in the presence of noise the desire to implement signal detection techniques such as cross correlation peak detection were presented. To implement these techniques the strongest received signal must correspond to the direct path signal and not reflections. Due to the highly reflective nature of the vessel surface this thesis has investigated the reflection characteristics of the vessel and the impact that reflections have at the receiver.

The impact of reflections within the vessel on the ranging accuracy of the system is investigated through experiments utilising both a single and multiple transmitter set-up. Experimental research in [Chapter 5.0, section 5.2.3] has shown that for a single transmitter in the vessel the highly reflective vessel surface causes reflection signals to be detected at the receiver with higher cross correlated amplitude than direct path signals. While the Senscomp 40KT08 transmitter has been demonstrated to have a relatively flat transmission profile, the reflective nature of the vessel causes reflection signals to arrive at the receiver with larger peak cross correlated amplitude than the direct path signal.

To overcome these problems this thesis has investigated the use of multiple transmitters on the pill in an effort to maintain signal coverage as the pill rotates and to overcome the effect of reflections within the vessel. Based on the transmission profile for a single Senscomp 40KT08 transducer two transmitter separations have been considered, that of 45° and 90°. While the use of multiple transmitters has been shown to maintain signal level at the receiver as the pill set-up is rotated it has been shown that the use of multiple transmitters does not overcome reflection issues within the vessel. In addition results have suggested that as the pill is rotated the peak received signal can be detected from either transmitter and not as would have been anticipated based on the transmission profile, [Chapter 5.0, section 5.3.3].

Experimental results have also suggested that due to the curved nature of the vessel beam focussing occurs from the vessel wall, increasing the received signal strength for reflections at the receiver. Simulations have suggested that for certain transmitter locations within the vessel multiple reflection signals from the vessel wall are effectively focussed onto the receiver. Through analysis of the range of these reflections, [Chapter 5.0, section 5.4.1] it has been observed that multiple

reflection signals arrive at the receiver with a difference in range of less than 0.01 mm. This suggests that the receiver is unable to distinguish between these arrivals and the output of the receiver is instead a single reflection signal with increased amplitude.

Through analysis of this result it has been suggested that even for an omnidirectional beam within the vessel the curved surface of the vessel wall will result in reflection amplitude signals above that of the direct path. Based on this information, even with the use of multiple transmitters on the pill peak detection methodologies within the vessel will be ineffective for accurate ranging and subsequent localisation.

Further exploration was undertaken to study the influence that the placement of transmitters in close proximity has on the received signal strength. From the experimental profile of a single transmitter separations on the pill of 90° and 45° were studied to explore how rotation of the pill alters the received signal. At a rotation angle of half the transmitter separation a large increase in received amplitude was observed. At this rotation angle the distance between each transmitter and receiver is the same which suggests either the receiver resolution is unable to distinguish between the arrivals of signals or constructive interference is observed due to the close proximity of the transmitters.

8.1.5 Optimisation of Transmitter Placement on the Pill

To ensure that the pill can be localised throughout the vessel there is the desire to ensure that regardless of the pill's location or orientation the pill is to transit acoustic signals to all the receivers within the vessel. To achieve this desire the pill implements a multiple transmitter array. The impact that transmitter location on the pill has on the received signal strength is investigated through simulations based on experimental profiling.

A feasibility study was undertaken to determine the optimum receiver for use within the project based on experimental profiling, [Chapter 6.0, section 6.3]. Through an evaluation of the both the reception profile of the receiver and also the attenuation of the signal as a function of range it was indicated that the Senscomp 40KT08 transducer offers improved performance in relation to the 5 cm receiver. The 40KT08 offers both a flatter reception profile and also due to its smaller physical size a small near field region, [Chapter 6.0, section 6.3.4].

While experimental studies have indicated that the repeatability of measurements within the vessel is good between tests an important observation is that the water composition has a significant impact on the received signal strength and reception profile within the vessel, [Chapter 6.0, section 6.3.5]. Results indicate that when the water is the tank is flushed and replaced there is an initial period of approximately 2 days where the amplitude and reception profile can be observed to differ from the long term trend. The concentration of dissolved oxygen within the vessel after the refilling

process has been attributed to this result which is a crucial result where the medium may be purged between or during mixing processes.

The influence of the transmitter layout on the received signal strength is evaluated through simulations using the experimentally determined profiles of the Senscomp 40KT08 transducers. From the work undertaken investigating the interaction of multiple transmitters and an evaluation of the transmission beam profile separation of transmitters to cope with rotation was set at 90°. Through investigating various transmitter layouts within the vessel it was determined that the limiting factor to improve received signal strength was related to the reception angle of the received signal. While the placement of transmitters on the pill is able to improve the transmission angle and therefore transmitted amplitude of the signal for the "worst case" anticipated pill locations within the vessel the reception angle at the receivers is significant which reduces the output from the receiver.

Simulations have suggested that to maximise the received signal strength the receivers within the vessel should have their mounting angles rotated, [Chapter 6.0, section 6.4.4]. This reduces the reception angle for the pill in worst case scenario locations and therefore increases the received signal strength. From simulations and consideration of the TDOA localisation accuracy due to transmitter offset from the centre of the pill, a pill layout with 8 transmitters and receivers mounted at 45° was considered. While simulations indicated that the received amplitude was better with a 6 transmitter pill and receivers mounted at 45° the location of the transmitter on the pill causes the transmitter offsets required to change as the pill moves which it was anticipated would produce larger TDOA localisation error.

8.1.6 Underwater Localisation Accuracy

The localisation accuracy of the system is considered with experimental testing for localisation techniques employing both TOF and TDOA measurements. An 8 transmitter pill has been utilised for experimental results in the 250 litre vessel. Signal generation and detected is undertaken from a system mounted external to the pill allowing both TOF measurements and TDOA measurements to be obtained. Signal detection is obtained through amplitude thresholding techniques to overcome the reflection problems observed in the target environment.

Experimental results are considered for three horizontal planes within the vessel with the pill moved in 5 cm intervals in the *x* and *y* directions to provide 65 unique pill locations per plane. The orientation of the pill is also varied to explore how the localisation accuracy alters as the pill is rotated.

Results using TOF measurements, [Chapter 7.0, section 7.2.2], demonstrate that the centre of the pill can be localised with excellent accuracy throughout the area of the vessel tested. Using TOF least minimisation techniques it can be observed that the centre of the pill can be localised within an average localisation error of approximately 2.7 cm for the 3 tests planes. Results indicate that

this localisation accuracy can be maintained as the pill is rotated and that the TOF error minimisation technique is able to cope well with rotation of the pill.

Experiments also indicate that the repeatability of measurements is excellent. Between repeat tests it has been indicated that the variation in the location of the pill calculated using TOF localisation shows mm repeatability between measurements. Overall results suggest that for a pill with 8 transmitters TOF localisation techniques are able to localise the pill within the vessel with an average error over the 3 tested planes of 2.5 cm.

TDOA localisation techniques have been considered investigating both the localisation accuracy using standard TDOA algorithms and those using the offset knowledge method as presented in this thesis.

For the standard TDOA methodology, [Chapter 7.0, section 7.3.1], results have shown a decrease in localisation accuracy in comparison to TOF localisation. For TDOA results both the average localisation error and variation between results has increased in comparison to TOF localisation. The average positional error throughout the 3 planes is 4.4 cm. While results have demonstrated that for a large number of locations within the vessel the accuracy is good there are locations where significant errors are observed. Investigations of these locations have demonstrated that in comparison to the TDOA values expected the measurements show large inaccuracies, which results in large localisation error. As for a significant number of locations the localisation error is small it is suggested that in these locations the signal detected at the receivers is below the required threshold creating the TDOA errors.

Overall while results with TDOA have demonstrated poorer localisation error in comparison to TOF localisation and more variation between repeat tests the centre of the pill can still be localised accurately to within 5 cm of the actual pill position. As such TDOA still presents a good option for localisation in a confined vessel.

When using offset knowledge in the TDOA measurements it has been observed that the average localisation error increases in comparison to that observed with standard TDOA equations. For the three tested planes the average localisation error observed is 5.0 cm, [Chapter 7.0, section 7.4.4]. While simulations have suggested that the offset knowledge method can be used to improve the localisation accuracy of TDOA measurements experiments show that due to the large TDOA inaccuracies between the expected and obtained TDOA measurements the use of offset knowledge cannot be used to refine the pill location and reduce localisation errors. As the TDOA values obtained for the pill show significant errors in relation to what should be expected for the pill's actual location then offset knowledge is being used to refine an already inaccurate position and therefore this refinement does not improve the localisation accuracy.

The work presented in this thesis indicates that both TOF and TDOA localisation techniques are a viable option for localisation of a sensor node in a confined underwater space. The use of a sensor pill with 8 transmitters has demonstrated good signal coverage within the vessel even as the pill is rotated allowing techniques which use both TOF and TDOA localisation to be able to accurately locate the pill for the majority of test locations.

8.2 Future work

8.2.1 Further Development of TOF Localisation

Experimental results with TOF localisation suggest that this method should be further pursued as an option to implement a wireless sensor pill. Results investigating the localisation accuracy of TOF measurement through the use of a wired pill have shown that the pill is able to be localised with an average error of 2.5 cm throughout the vessel. Further exploration of TOF localisation requires the development of a prototype pill with onboard signal generation for both electrical and acoustic signals along with the appropriate reception hardware to trigger acquisition of the signals on the DAQ card. Through the development of onboard signal generation a fully wireless pill can be implemented using TOF localisation.

Whilst the least mean square minimisation algorithm used to localise the pill produces good results, investigations should undertaken to determine if through the use of transmitter offset knowledge in the TOF minimisation algorithm further reductions in the localisation error can be made.

8.2.2 Further Development of TDOA Localisation

The results with TDOA localisation within this thesis have demonstrated that this technique also has potential suitability for application within the target environment. To further develop the TDOA implementation there is a requirement to develop a prototype pill with onboard acoustic signal generation.

While initial results have shown encouraging localisation accuracy there are still locations in the vessel where the TDOA methodology is shown to result in large localisation errors. Further experimental work is therefore required increasing the separation of receivers within the vessel to determine if a decrease in localisation error as predicted through simulations is observed.

In addition while initial results have suggested that the use of offset knowledge in TDOA equations has not improved the localisation accuracy of the system further work is required in this area implementing individual transmitter coding on the pill. It is anticipated that through the use of individually coded transmitters localisation accuracy can be improved, and specifically with the double TDOA method introduced in this thesis rotation of the pill can be resolved which should allow further reductions in the localisation accuracy of the TDOA implementation.

8.2.3 Improving Localisation Accuracy through Additional Measurements

While this thesis has concentrated on localisation under the most challenging conditions, with no additional measurements, future development of the pill is anticipated to contain onboard sensors such as pressure sensors to allow the depth of the pill to be varied in the target vessel.

The additional measurements from such sensors allow the localisation algorithms to be over-determined which provides two distinct advantages over the use of acoustic measurements alone. Firstly it is possible to use the vertical location of the pill to provide an “anchor” point for TDOA or TOF localisation algorithms. As the number of variables to solve for has reduced a more accurate localisation result should be possible.

The second advantage is that through the over determination of the localisation algorithms it should be possible to localise the pill when line of sight to a specific receiver is occluded due, for example, to the presence of an impeller in the vessel. Further research is therefore required in this area to investigate the localisation improvements which can be made through the inclusion of additional measurements.

8.2.4 Impact of Multiple Pills

In relation to future development, the ultimate aim is to develop a group of sensor pills for localisation in the target environment such that the environmental conditions at multiple locations within the vessel can be sampled simultaneously. The pills will be equipped with onboard sensors to take environmental readings and communication systems to transmit environmental data to an external host. In relation to localisation however the insertion of multiple pills into the target environment creates potential localisation problems due to occlusion of the localisation signal by additional pills. Therefore further work should investigate the impact that additional pills within the target environment have on the localisation accuracy and investigate potential algorithm modifications to overcome these issues.

References

Achour, M; Johlman, C; Blumer, D; 2008 "Understanding the corrosion inhibitor partitioning in oil and gas pipelines" *Society of Petroleum Engineers - 13th Abu Dhabi International Petroleum Exhibition and Conference, ADIPEC 2008*, Vol 2, pp 945-951

Adams, A.E; Acar, G; 2005 "An acoustic network protocol for subsea sensor systems*"* *Oceans 2005 - Europe*, Vol. 1, pp 172 - 176

Akyildiz, I. F; D. Pompili, Melodia, T; 2005 "Underwater acoustic sensor networks: Research challenges." *Ad Hoc Networks*, Vol. 3, pp 257-279.

Akyildiz, I.F; Su, W; Sankarasubramaniam, Y; Cayirci, E; 2002 "Wireless sensor networks: a survey" *Computer Networks* Vol. 38 Iss. 4, pp 393-422

Alkoy, S; Meyer, R.J, Jr; Hladky-Hennion, A.C; Hughes, W.J; Cochran, J.K, Jr; Newnham, R.E. 2000 "Transducer arrays from piezoelectric hollow spheres" *Proceedings of the 2000 12th IEEE International Symposium on Applications of Ferroelectrics* Vol 2 pp 737-40

Anguita, D; Brizzolara, D; Parodi, G; 2009 "Building an underwater wireless sensor network based on optical communication: research challenges and current results" *Third International Conference on Sensor Technologies and Applications (SENSORCOMM),* pp 476-9

Antoniou, M; Boon, M.C; Green, P.N; Green, P; York, T.A 2009 "Wireless sensor networks for industrial processes", *SAS 2009 - IEEE Sensors Applications Symposium Proceedings,* pp 13-18

Arnold, J; Bean, N; 2008 “Node localisation in wireless ad hoc networks using time difference of arrival” *2nd International Conference on Signal Processing and Communication Systems. ICSPCS'2008,* pp 10

Babic, S.I; Akyel, C; 2008 “Calculating mutual inductance between circular coils with inclined axes in air*” IEEE Transactions on Magnetics*, Vol. 44, Iss. 7, pp 1743-50

Baker J; Thomas H; “An integrated DGPS/acoustic system for underwater positioning” *Proceedings of the SPIE - The International Society for Optical Engineering* Vol. 3711, p. 220-228,

Bakhoum, E.G; 2006 “Closed-form solution of hyperbolic geolocation equations” *IEEE Transactions on Aerospace and Electronic Systems*, Vol. 42, Iss 4, pp 1396 – 1404

Bellin, M; Maddalena, D; Visentin, R. 1990 “The TV-trackmeter: an underwater non contact position sensor” *Autonomous Underwater Vehicle Technology, AUV '90.* pp 270 – 274

Boltryk, P; Hill, M; Keary, A; Phillips, B; Robinson, H; White, P; 2004 "An ultrasonic transducer array for velocity measurement in underwater vehicles" *Ultrasonics,* Vol. 42, Iss. 1-9, pp 473-8

Burnett-Thompson A, 2007 “A 3D Acoustic Local Positioning System to Track a Neutrally Buoyant Flow Follower”, *University of Manchester, PhD Thesis,*

Burnett-Thompson, A; York, T.A; 2007 “A 3D acoustic local positioning system to track a neutrally buoyant flow follower" *IEEE Instrumentation and Measurement Technology Conference Proceedings*, pp 266-71

Caudal, F; Glotin, H; 2008 “Multiple real-time 3D tracking of simultaneous clicking whales using hydrophone array and linear sound speed profile” *ICASSP 2008. IEEE International Conference on Acoustic, Speech and Signal Processes,* pp 2441-4

Chaczko Z; Klempous R; Nikodem J; Nikodem M; 2007 “Methods of Sensors Localization in Wireless Sensor Networks”, *Proceedings of the International Symposium and Workshop on Engineering of Computer Based Systems,* pp 145-152,

Chakraborty, U; Tewary, T; 2009 "Exploiting the loss-frequency relationship using RF communication in Underwater communication networks" *International Conference on Computers and Devices for Communication, CODEC* pp 1-4

Chandra P; Bensky A; Olexa R; Dobkin D.M; Lide D; Dowla F; 2007 "Wireless networking: know it all" *Elesevier Science & Technology, Burlington, USA* ISBN 978-0-7506-8582-5, pp 14

Chang C-C; Wang J-H; Jeng M-D; Lin; C-C; Chen K-H; 2000 "The fabrication and characterization of PZT thin film acoustic devices for application in underwater robotic systems" *Proceedings of the National Science Council, Republic of China, Part A (Physical Science and Engineering)* Vol 24, Iss 4, pp 287-292

Chen Y-M; 2006 “Recent advances in FCC technology”, *Powder Technology* pp. 2–8.

Chin R.K.Y; Wright P; York T.A; 2010 ‘Electrical Tomography Using Ad Hoc Wireless Sensors,’ *6th World Congress on Industrial Process Tomography, Beijing, China.*

Chupyra, A.G; Gusev, G.A; Kondaurov, M.N; Medvedko, A.S; Singatulin, Sh.R; 2006 "The Ultrasonic Level Sensors for Precise Alignment of Particle Accelerators and Storage Rings" *9th International Workshop on Accelerator Alignment*, pp 3

Creuze, V; Jouvencel, B; Baccou, P; 2001 "Seabed following for small autonomous underwater vehicles” OCEANS*, 2001. MTS/IEEE Conference and Exhibition 2001*, Vol.1 pp 369 - 374

De Marziani, C; Urefia, J; Hernandez, A; Mazo, M; Alvarez, F; Garcia, J.J; Villadangos, J.M; Jimenez, Al; 2005 “Simultaneous measurement of times-of-flight and communications in acoustic sensor networks”. *IEEE International Workshop on Intelligent Signal Processing,* pp 122 – 127.

Erikson, K; Stockwell, J; Hairston, A; Rich, G; Marciniec, J; Walter, L; Clark, K; White, T; 1999 "A Real-Time 3D Underwater Acoustical Camera" *Proceedings of SPIE, the International Society for Optical Engineering*, Vol. 3711, pp. 33-42

Exel, R; Gaderer, G; Loschmidt, P; 2010 "Localisation of Wireless LAN Nodes using Accurate TDoA Measurements" *Proceedings of the 2010 IEEE Wireless Communications & Networking Conference (WCNC 2010),* pp 6

Faugstadmo, J.E; Pettersen, M; Hovem, J.M; Lie, A; Reinen, T.A; 2010 "Underwater Wireless Sensor Network" *Fourth International Conference on Sensor Technologies and Applications (SENSORCOMM 2010)* pp 422 - 427

Feezor, M.D; Blankinship, P.R; Bellingham, J.G; Sorrell, F.Y, 2001 "Autonomous underwater vehicle homing/docking via electromagnetic guidance*" IEEE Journal of Oceanic Engineering,* Vol. 26, Iss: 4, pp 515

Ganeriwal S; Ganesan D; Shim H; Tsiatsis V; Srivastava B; 2005 “Estimating clock uncertainty for efficient duty-cycling in sensor networks” *Proceedings of the Third International Conference on Embedded Networked Sensor Systems (Sensys), San Diego, CA*

Ganeriwal S; Kumar R; Srivastava M.B; 2003 “Timing-sync protocol for sensor networks” *Proceedings of the Sensys’03, Los Angeles, CA*

Garcia, J.E; 2005 “Accurate positioning for underwater acoustic networks” *Oceans 2005 - Europe,* Vol. 1, pp 328 - 333

Grosicki, E.; Abed-Meraim, K; 2005 "A new trilateration method to mitigate the impact of some non-line-of-sight errors in TOA measurements for mobile localization" *IEEE International Conference on Acoustics, Speech, and Signal Processing,* Vol. 4, pp 1045 - 1048

Harput, S; Bozkurt, A; 2008 “Ultrasonic phased array device for acoustic imaging in air" *IEEE Sensors Journal* Vol 8, Iss 11, pp 1755-1762

Heidemann, J; Wei Y; Wills, J; Syed, A.; Yuan, L; 2006 “Research challenges and applications for underwater sensor networking” *IEEE Wireless Communications and Networking Conference*, pp 228 – 235

Hirata, S; Kurosawa, M.K; Katagiri, T; 2009 "Real-time ultrasonic distance measurements for autonomous mobile robots using cross correlation by single-bit signal processing" *IEEE International Conference on Robotics and Automation*, pp 3601 - 3606

Joe, J; Toh, S.H; 2007 "Digital Underwater Communication Using Electric Current Method" *OCEANS 2007 - Europe,* pp 1 - 4

Kahn, J.M; Katz, R.H; Pister, K.S.J; 1999 “Next century challenges: mobile networking for smart dust” *Proceedings of Fifth Annual ACM/IEEE International Conference on Mobile Computing and Networking,* pp. 271–278.

Kojiya, T; Sato, F; Matsuki, H; Sato, T; 2005 "Construction of non-contacting power feeding system to underwater vehicle utilizing electro magnetic induction", *Oceans 2005 - Europe*, Vol 1, pp 709 - 712

Kokal, S; Al-Ghamdi, A; 2008 "Performance appraisals of gas/oil-separation plants", *SPE Production and Operations*, Vol. 23, pp 287 - 296

Lee K.H; Yu C.H; Choi J.W; Seo Y.B; 2008 "ToA based sensor localization in underwater wireless sensor networks" *Proceedings of the SICE Annual Conference* pp 1357 - 1361

Lewin, P.A; Schafer, M.E; 1988 "Wide-band piezoelectric polymer acoustic sources", *IEEE Transactions on Ultrasonics, Ferroelectrics and Frequency Control*, Vol. 35 Iss. 2 pp 175 - 185

Lu C; Wang S; Tan M; 2009 "A time synchronization method for underwater wireless sensor networks" *Chinese Control and Decision Conference (CCDC 2009)* pp 4305 - 4310

Lygouras, J.N; Dimitriadis, C.M; Tsortanidis, M.C; Bakos, G.C; Tsalides, P.G. 1994 “Digital ultrasonic scanning system for positioning underwater remotely operated vehicles International”. *Journal of electronics* Vol. 76, no3, pp 541 - 550

Mian J.T; Ishimatsu T; Nagashima Y; 2000 "Compact underwater vehicle with acoustic link for communication and positioning" *Underwater Technology,* pp 237 – 241

Murphy S.C; Chin R.K; York T.A; 2008 “Design of an impeller-mounted electrode array for EIT imaging” *Measurement Science & Technology* Vol. 19 Iss 9, 12 pp

NagaJyothi, A; Raja Rajeswari, K; 2011 "Cross-correlation of Barker code and Long binary signals" *International Journal of Engineering Science and Technology (IJEST),* Vol. 3

Nawaz S; Hussain M; Watson S; Trigoni N; Green P.N; 2009 "An Underwater Robotic Network for Monitoring Nuclear Waste Storage Pools", *First International ICST Conference, S-CUBE,* Vol. 24, pp 236-255

Ong, K.G.; Yang, X; Mukherjee, N; Wang, H; Grimes, C.A; 2003 “Measurement of pond temperature and pH using an aqueous sensor network.” *Proceedings of the SPIE - The International Society for Optical Engineering*, Vol. 5090, pp. 225-236

Pandya, S; Engel, J; Chen, J; Fan, Z; Liu, C; 2005 "CORAL: miniature acoustic communication subsystem architecture for underwater wireless sensor networks" *IEEE Sensors* 4 pp

Parkinson, G; Boon, M; Davis J.G; Sloan, R; 2009 "3D Positioning using Spherical Location Algorithms for Networked Wireless Sensors Deployed in Grain" *IEEE MTT-S International Microwave Symposium Digest (MTT) Microwave Symposium Digest,* pp 1417 – 1420

Paul, E.L; Atiemo-Obeng, V.A; Kresta, S.M; 2004 “Handbook of Industrial Mixing: Science and Practice”, *John Wiley & Sons Inc.,* ISBN 0-471-26919-0

Preisig J; 2006 "Acoustic propagation considerations for underwater acoustic communications network development" *Proceedings of the First ACM International Workshop on Underwater Networks,* pp 1-5

Raghunathan V; Kansai A; Hse J; Friedman J; Srivastava M; 2005 “Design considerations for solar energy harvesting wireless embedded systems”, *Fourth International Symposium on Information Processing in Sensor Networks*, pp 457–462.

Rai R; Sharma P.K; Mukerjie R.K; 1991 "Multiphase long-distance pipeline transportation. An emerging technology for offshore production", *Proceedings of the SPE Production Operations Symposium*, pp 919-926

Rentel C.H; Kunz T; 2005 “A clock-sampling mutual network synchronization algorithm for wireless ad hoc networks” *IEEE Wireless Communications and Networking Conference,* Vol 1. pp 638 - 644

Rhodes M; 2007 “Electromagnetic Propagation in Sea Water and its Value in Military Systems” *Systems Engineering for Autonomous Systems Conference (SEAS)*

Shatara S; Xiaobo T; Mbemmo E; Gingery N; Henneberger S; 2008 "Experimental Investigation on Underwater Acoustic Ranging for Small Robotic Fish" *IEEE International Conference on Robotics and Automation,* pp 712-17

Sichitiu M.L; Ramadurai, V; 2004 "Localization of wireless sensor networks with a mobile beacon" *IEEE International Conference on Mobile Ad-hoc and Sensor Systems,* pp 174-83

Stephen R.A; 1998 “Ocean seismic network seafloor observatories” *Oceanus*, Vol. 41 Iss. 1, pp 33 – 37

Stojanovic M; Catipovic J.A; Proakis J.G; 1994 “Phase-coherent digital communications for underwater acoustic channels” IEEE *Journal of Oceanic Engineering,* Vol. 19 Iss 1, pp 100 – 111

Stokey R.P; Austin T.C; 1999 “Sequential long-baseline navigation for REMUS, an autonomous underwater vehicle” *Proceedings of the SPIE - The International Society for Optical Engineering,* Vol 3711, pp 212 - 219

Vardhan S; Wilczynski M; Pottie G.J; Kaiser W.J; 2000 "Wireless integrated network sensors (WINS): distributed in situ sensing for mission and flight systems” *IEEE Aerospace Conference,* Vol. 7, pp 459–463.

Vyplavin P; Melnikova E; Lukin S; 2010 "Real-time signal processing in Noise Radar" *4th Microwave and Radar Week MRW-2010 - 11th International Radar Symposium, IRS* 2010, pp 504-506

Wadke P.M; Salman A.D; Hounslow M.J, 2008 “The 'smart' temperature sphere: application in rotary drum mixers” *Powder Technology,* Vol. 185, Iss 3, pp 274 - 279

Watson S.A; Green P.N; 2011 “A De-Coupled Vertical Controller for Micro-Autonomous Underwater Vehicles (mAUV)”, I*EEE International Conference on Mechatronics and Automation (ICMA)* pp 561 - 566

Williams R.A; Beck M.S; 1995 “Process Tomography, Principles, Techniques and Applications”, *Butterworth-Heinemann, Oxford*, ISBN 0-7506-0744-0

Woosuk Chang; Daeyong Kwon; Jinoh Park; Byungdoo Jeon; 2008 "An active underwater acoustic reflection control system" *IEEE International Conference on Multisensor Fusion and Integration for Intelligent Systems,* pp 583-587

Wright P; Terzija N; Davidson J.L.; Garcia-Castillo S; Garcia-Stewart C; Pegrum S; Colbourne S; Turner P; Crossley S.D; Litt T; Murray S; Ozanyan K.B; McCann, H; 2010 "High-speed chemical species tomography in a multi-cylinder automotive engine", *Chemical Engineering Journal*, Vol. 158, pp 2-10

Wu Z; Xu J; Li B; 2010 "A high-speed digital underwater communication solution using electric current method" *2nd International Conference on Future Computer and Communication (ICFCC)*, Vol. 2, pp, 14 -16

Xu, J; Ma, M; Law, C.L; 2011 "Performance of time-difference-of-arrival ultra wideband indoor localisation", *IET Science, Measurement and Technology*, pp 46-53

Yan H; Liu W; 2010 "Design of time difference of arrival estimation system based on fast cross correlation" *Proceedings of the 2010 2nd International Conference on Future Computer and Communication (ICFCC 2010)*, pp 464 - 466,

Yick, J; Mukherjee, B; Ghosal, D; 2008 "Wireless sensor network survey" *Computer Networks* Vol. 52, Iss. 12, pp 2292 - 2330

York T.A., 2001 "Status of electrical tomography in industrial applications", *Journal of Electronic Imaging*, Vol. 10, Iss. 3, pp 608 - 619,

York, T.A; McCann, H; Ozanyan, K.B; 2011 "Agile sensing systems for tomography" *IEEE Sensors Journal,* Vol. 11, Iss. 12, pp 3086 – 3105

Zhang B-S; Kong L-J; Ge Y; 2009 "Influence of lightweight aggregate on durability of high performance concrete", *Key Engineering Materials*, Vol. 405 - 406, pp 197 - 203

Zhao T; Takei M; Masaki K; Ogiso R; Nakao K; Uchiura A, 2007 "Sensor design and image accuracy for application of capacitance CT to the petroleum refinery process", *Flow Measurement and Instrumentation*, Vol. 18, pp 268 - 276